

THE UNIVERSITY OF OKLAHOMA  
GRADUATE COLLEGE

**ELEMENTAL AND STABLE CARBON ISOTOPE  
CHEMOSTRATIGRAPHY OF THE UPPER JURASSIC  
SMACKOVER SEQUENCE OF SOUTHWEST ALABAMA BASINS,  
ALABAMA, U.S.A.**

A Dissertation  
SUBMITTED TO THE GRADUATE FACULTY  
in partial fulfillment of the requirements of the  
degree of  
Doctor of Philosophy

By

KULWADEE LAWWONGNGAM PIGOTT

Norman, Oklahoma

2004

UMI Number: 3150967

Copyright 2004 by  
Pigott, Kulwadee Lawwongngam

All rights reserved.

UMI<sup>®</sup>

---

UMI Microform 3150967

Copyright 2005 by ProQuest Information and Learning Company.  
All rights reserved. This microform edition is protected against  
unauthorized copying under Title 17, United States Code.

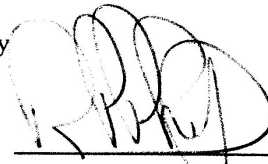
---

ProQuest Information and Learning Company  
300 North Zeeb Road  
P.O. Box 1346  
Ann Arbor, MI 48106-1346

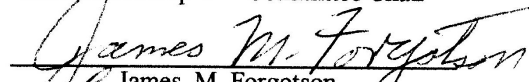
ELEMENTAL AND STABLE CARBON ISOTOPE CHEMOSTRATIGRAPHY OF  
THE UPPER JURASSIC SMACKOVER SEQUENCE OF SOUTHWEST ALABAMA  
BASINS, ALABAMA, U.S.A.

A Dissertation APPROVED FOR THE  
SCHOOL OF GEOLOGY AND GEOPHYSICS

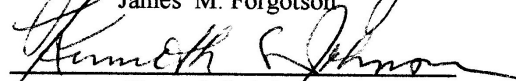
By



Richard P. Philp - Committee Chair



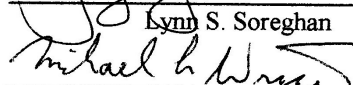
James M. Forgotson



Kenneth S. Johnson



Lynn S. Soreghan



Michael L. Wiggins



## **DEDICATION**

This dissertation is dedicated to my mother and my husband for their love and endless  
patience to this long endeavor of learning

## ACKNOWLEDGEMENTS

I would like to express my deep gratitude to God and Buddha whose teachings and knowledge have guided me to learn more about the way things are, explicitly and implicitly, throughout this mind.

I would like to extend my gratitude to my advisor Dr. R. Paul Philp, for his time, support and encouragement in helping me to be able to keep up and finally finish this thesis. I am greatly indebted to Dr. Mike Engel and Rick Maynard who helped immensely with the isotope analyses, without which this thesis would not be possible. Special thanks go to Dr. Barry Weaver who helped me to start the elemental analysis, to Dr. Mark Nanny for the use of the TOC instrument, to Dr. Neil Dickey of the Northern Illinois University who was willing to complete the elemental analysis, and to Dr. Roger Slatt for the partial support for the cost of the elemental analysis. I also wish to thank all the committee members, Dr. James Forgotson, Dr. Lynn Soreghan, Dr. Kenneth Johnson and Dr. Michael Wiggins, for their time, support and advice. My thanks also go to the Alabama Geological Survey for permission to access the cores and to Lewis Dean who kindly helped transfer the cores used in this study. In addition, I like to thank Eric Higgins for introducing me to the Smackover Formation and the fantastic core laboratory of the Alabama Geological Survey.

My sincere thanks also go to Nopawan Ratasuk for her friendship, times and thoughtful support. Many thanks are also for Jesus Maza, Mike Hsieh, Kim Dongwon, Dr. Eric Mueller, Dr. Vlad Andrus, Ron Colon, John Allen, Ahmed Alahdal, and Eshetu Gebretsadik and Lee-Kevin Acers for their assistance and friendship. I wish to thank my family for the support and encouragement. My special thanks go to Smokey, Simone, Sebastian, Sabrina, Snowbell, and Socrates for the love and companionship that they share with me. Most of all, I need to thank my husband, Dr. John Pigott, for his support, inspiration, and guidance throughout all this time.

# TABLE OF CONTENTS

|  | Page  |
|--|-------|
| <b>List of Figures</b> .....                                 | ix    |
| <b>List of Tables</b> .....                                  | xvii  |
| <b>List of Appendices</b> .....                              | xviii |
| <b>Abstract</b> .....  | xix   |
| <b>Chapter 1</b>   |       |
| 1.1 Introduction.....  | 1     |
| 1.2 Background studies.....                                  | 4     |
| 1.3 Definition of the problem.....                           | 13    |
| 1.4 Objectives.....  | 14    |
| <b>Chapter 2</b>   |       |
| 2.1 Geologic setting.....                                    | 15    |
| 2.2 Stratigraphy.....  | 16    |
| 2.3 Smackover stratigraphic sequence.....                    | 25    |
| 2.4 A depositional sequence.....                             | 27    |
| 2.5 Carbonate ramp sequence stratigraphy.....                | 33    |
| <b>Chapter 3</b>   |       |
| 3.1 Core analysis and samples.....                           | 39    |
| 3.2 Methods and Instruments.....                             | 43    |
| 3.2.1 Elemental analysis.....                                | 44    |
| 3.2.2 Stable carbon and oxygen isotopes.....                 | 44    |
| 3.2.3 Total organic carbon analysis.....                     | 46    |
| 3.2.4 Extraction and fractionation of<br>organic matter..... | 46    |
| 3.2.4 Gas chromatography.....                                | 48    |
| <b>Chapter 4</b>   |       |
| 4.1 Lithology and core observations.....                     | 49    |
| 4.2 Core analysis.....                                       | 51    |
| 4.2.1 T.R. MILLER MILLS 17-11, #1.....                       | 52    |
| 4.2.2 #1 NEAL EL AL UNIT 30-1.....                           | 55    |

|         |   |    |
|---------|---|----|
| 4.3     | Discussion.....   | 58 |
| 4.3.1   | Smackover depositional environment<br>and a stratigraphic framework ..... | 58 |
| 4.3.1.1 | Conecuh Embayment.....  | 70 |
| 4.3.1.2 | Manila Embayment.....   | 78 |
| 4.3.2   | A comparison between the Smackover<br>cores.....                          | 85 |
| 4.4     | Conclusions.....  | 86 |

## Chapter 5

|       |   |     |
|-------|---|-----|
| 5.1   | Siliciclastic and carbonate related elements..... | 90  |
| 5.2   | Carbonate diagenetic effects.....                 | 92  |
| 5.3   | Smackover elemental analysis.....                 | 96  |
| 5.4   | Results and discussion                            |     |
| 5.4.1 | Siliciclastic related elements.....               | 97  |
| 5.4.2 | Carbonate related elements.....                   | 105 |
| 5.4.3 | Redox condition.....                              | 120 |
| 5.5   | Conclusions.....                                  | 125 |
| 5.6   | Further suggested studies.....                    | 128 |

## Chapter 6

|       |  |     |
|-------|--|-----|
| 6.1   | Carbon isotope stratigraphy.....   | 129 |
| 6.2   | Carbon isotope ( $\delta^{13}\text{C}$ ).....  | 130 |
| 6.3   | Carbon isotope in a sequence stratigraphic<br>framework  |     |
| 6.3.1 | Positive $\delta^{13}\text{C}$ excursion.....  | 134 |
| 6.3.2 | Negative $\delta^{13}\text{C}$ excursion.....  | 138 |
| 6.3.3 | Sample analysis.....   | 142 |
| 6.4   | Results  |     |
| 6.4.1 | Carbon isotope composition of the<br>Smackover carbonates.....   | 144 |
| 6.4.2 | Oxygen isotopes.....   | 146 |
| 6.5   | Discussion   |     |
| 6.5.1 | Diagenetic effects.....  | 148 |
| 6.5.2 | $\delta^{13}\text{C}_{\text{carb}}$ and $\delta^{18}\text{O}_{\text{carb}}$ correlation.....                                 | 159 |
| 6.5.3 | $\delta^{13}\text{C}_{\text{carb}}$ trends of the Smackover in<br>a stratigraphic framework.....                             | 163 |
| 6.5.4 | TOC and variations between the<br>$\delta^{13}\text{C}_{\text{carb}}$ and the $\delta^{13}\text{C}_{\text{org}}$ values..... | 168 |

|                        |   |            |
|------------------------|---|------------|
| 6.5.5                  | $\delta^{13}\text{C}_{\text{org}}$ variation and the organic carbon sources.....            | 171        |
| 6.5.6                  | The $\delta^{13}\text{C}_{\text{carb}}$ stratigraphy of the global Oxfordian sequences..... | 178        |
| 6.6                    | Conclusions.....  | 180        |
| 6.7                    | Further suggested studies.....  | 183        |
| <b>Chapter 7</b>       |   |            |
| 7.1                    | Synthesis: the Smackover depositional model.....  | 185        |
| 7.2                    | Oxfordian sea level variation and tectonic activity.....                                    | 198        |
| 7.3                    | Late Jurassic paleoclimates .....   | 200        |
| 7.4                    | Conclusions.....  | 201        |
| <b>References.....</b> |   | <b>206</b> |

# LIST OF FIGURES

|   | Page |
|---|------|
| <b>Figure 1-1.</b> Paleogeographic map during the Late Oxfordian illustrating sediment deposits where mostly limestone and shales and the oolite bars distributions represent the Smackover Formation (from Salvador, 1987).....  | 2    |
| <b>Figure 1-2.</b> Location map of the Smackover trend along the states of the northern US Gulf Coast rim (from Moore, 1984).....   | 3    |
| <b>Figure 1-3.</b> Sedimentary basins in southwest Alabama where Smackover depositions occurred; the Mississippi Interior Salt Basin, the Conecuh Embayment, and the Manila Embayment.....  | 5    |
| <b>Figure 1-4.</b> Sequence stratigraphic framework of the Smackover Formation in southwest Alabama proposed by Prather (1992).....   | 7    |
| <b>Figure 1-5.</b> The Late Triassic-Jurassic stratigraphic column of the northern Gulf of Mexico showing dark organic source rock correlation with the other Upper Jurassic sedimentation of different areas. The Smackover Formation consists of three upward shoal cycles from lower to upper called C, B, A cycles (from Heydari et al., 1995)..... | 12   |
| <b>Figure 2-1.</b> The regional tectonic features and basins of the southeastern Gulf Coast area (from Prather, 1992).....  | 17   |
| <b>Figure 2-2.</b> Generalized Mesozoic stratigraphy from the northern US Gulf Coast (from Prather, 1992).....  | 19   |
| <b>Figure 2-3.</b> Isopach map of the Smackover Formation of southwest Alabama, showing major depocenter and basinal areas (from Kopaska-Merkel and Mann, 1992).....  | 21   |
| <b>Figure 2-4.</b> The regional structural map of the Smackover Formation top in southwest Alabama, showing slope gradient on the depositional carbonate platform (from Kopaska-Merkel and Mann, 1992).....   | 22   |
| <b>Figure 2-5.</b> Typical log characteristic (gamma ray and neutron/density logs) of the lower, middle and upper member of the Smackover Formation in southwest Alabama (from Benson, 1988).....   | 23   |
| <b>Figure 2-6.</b> A comparison of sequence stratigraphic frameworks of the Upper Jurassic strata of the Gulf of Mexico basins which includes the Smackover Formation proposed by Vail et al.(1984), Haq et al.(1988) and Mancini et al.(1990).....   | 28   |

|  |    |
|--|----|
| <b>Figure 2-7.</b> Depositional system tracts and lithological records of the Upper Jurassic sequences characterized by Manicini et al. (1990).....  | 29 |
| <b>Figure 2-8.</b> The hierarchy and different time-scale of the stratigraphic depositional sequences related to eustatic sea level cycles, showing with different key features (from Duval, 1992).....  | 31 |
| <b>Figure 2-9.</b> The influence of tectonic and climatic processes on the relative sea level changes and sediment supply (from Church and Coe, 2003).....   | 32 |
| <b>Figure 2-10.</b> Homoclinal carbonate ramp showing main sedimentary facies. Inner ramp (A) peritidal and sabkha facies with stromatolitic algae and evaporites; (B) bioturbated and variably bedded lagoonal lime mudstone, packstone, and wackestone; (C) shoreface or shoal cross-laminated oolitic or bioclastic grainstones and packstones. Midramp: (D) amalgamated coarse, graded tempestites, commonly with hummocky cross-stratification. Outer ramp: (E) fine-grained, graded tempestites interbedded with bioturbated or laminated lime or terrigenous mudstone; (F) laminated or sparsely rippled silt-grade carbonate sediment or quartz silt in a predominantly terrigenous mudstone succession. All these boundaries are gradational (from Burchette and Wright, 1992)..... | 35 |
| <b>Figure 2-11.</b> Sequence stratigraphic components of a homoclinal carbonate ramp of a grainstone-dominated system with outer-ramp buildups and a well-developed lowstand system tract (from Burchette and Wright, 1992).....   | 36 |
| <b>Figure 2-12.</b> The influences of pore water circulation systems for ramp platform during relative sea level highstand and lowstand (from Burchette and Wright, 1992).....   | 38 |
| <b>Figure 3-1.</b> Locations of two Smackover cores examined in this study.....  | 40 |
| <b>Figure 3-2.</b> A sequence depositional framework of the Smackover of southwest Alabama proposed by the Smackover core, the T.R. MILLER MILLS 17-11, #1, similar to the core of this study.....   | 41 |
| <b>Figure 3-3.</b> The Smackover depositional system tracts during relative changes sea level, interpreted by Mancini (1993) from the #1 NEAL ET AL UNIT 30-1 well of the Manila Embayment.....  | 42 |
| <b>Figure 4-1.</b> (a) Algal boundstone (microreefs) incorporated oncoids, packstone, wackestone and anhydrite nodules during the Smackover reported by Kopaska-Merkel (1994) and, (b)The sketched structure proposed by Kopaska-Merkel (1994) and (c) Algal boundstone incorporated with oncoids, wackestone, anhydrite and terrestrial sediment observed in the Smackover from the T.R. MILLER MILLS 17-11, #1 core of the Conecuh Embayment of this study.....  | 53 |
| <b>Figure 4-2.</b> Approximated paleowater-depth interpretation of the T.R. MILLER MILLS 17-11, #1 and the #1 NEAL ET AL UNIT 30-1 cores from the Conecuh Embayment and Manila Embayment. Lithologic columns are based upon core descriptions in Table 4-1 and Table 4-2.....  | 83 |

|   |     |
|---|-----|
| <b>Figure 4-3.</b> Depositional cycles, recorded by relative water depth variation of the Corallian Oxfordian sequence from the Dorset Coast, England (Sun, 1989).The sediment sequence is of equivalent age to the Smackover Formation on the United States and variation of paleowater-depth related to third-order relative sea level changes..... | 84  |
| <b>Figure 5-1.</b> Cluster analysis illustrating relationship of different elements on chemical composition of recent sediments collected from the Gulf of Paria (Calvert, 1976 ).....  | 93  |
| <b>Figure 5-2.</b> Ternary diagrams illustrating relative content of the Ca, Si and Al in the Smackover samples from the Conecuh and the Manila Embayments.....   | 98  |
| <b>Figure 5-3a.</b> The vertical distributions of siliciclastic related elements compared to Ca of the Smackover samples from the Conecuh Embayment. Data are listed in Appendix E.....   | 99  |
| <b>Figure 5-3b.</b> The vertical distributions of siliciclastic related elements compared to Ca of the Smackover samples from the Manila Embayment. Data are listed in Appendix F.....  | 100 |
| <b>Figure 5-4a.</b> Al and Al-normalized siliciclastic major elements in comparison with Al-normalized Ca for eliminating siliciclastic influence on the Smackover samples from the Conecuh Embayment. Data are listed in Appendix E.....   | 102 |
| <b>Figure 5-4b.</b> Al and Al-normalized siliciclastic major elements in comparison with Al-normalized Ca for eliminating siliciclastic influence on Smackover samples from the Manila Embayment. Data are listed in Appendix F.....  | 103 |
| <b>Figure 5-5.</b> Ternary diagrams illustrating relative content of carbonate related elements, Ca, Mg and Sr, for the Smackover samples from the Conecuh and the Manila Embayments. The arbitrary numbers are applied in order to balance data on the diagrams.....   | 106 |
| <b>Figure 5-6a.</b> Major and minor carbonate related elements of the Smackover samples from the Conecuh Embayment. Na and P plotted in this group to compare their distributions in a carbonate environment. Data are listed in Appendix E.....  | 108 |
| <b>Figure 5-6b.</b> Major and minor carbonate related elements of the Smackover samples from the Manila Embayment. Na and P plotted in this group to compare their distributions in a carbonate environment. Data are listed in Appendix F.....   | 109 |
| <b>Figure 5-7a.</b> Al-normalized and Ca-normalized major and minor of carbonate related elements for carbonate and diagenesis in the Smackover samples from the Conecuh Embayment. Data are listed in Appendix E.....  | 110 |

|   |     |
|---|-----|
| <b>Figure 5-7b.</b> Al-normalized and Ca-normalized of major and minor carbonate related elements for carbonate and diagenesis in the Smackover samples from the Manila Embayment. Data are listed in Appendix F.....   | 111 |
| <b>Figure 5-8.</b> Cross-plots between (a) Al and Sr/Sr+Al, (b) Ca/Ca+Al and Sr/Sr+Al and (c) Sr/Sr+Ca (x1000) and $\delta^{18}\text{O}_{\text{carb}}$ of the Smackover samples from the Conecuh and the Manila Embayments. Data including $\delta^{18}\text{O}_{\text{carb}}$ values are listed in Appendix E and F.....   | 114 |
| <b>Figure 5-9.</b> Cross-plots between (a) Ca/Ca+Al and Mn/Mn+Al, (b) Al and Mn/Mn+Ca to investigate the variation of Mn to Ca and Al. Diagenetic effect on Mn concentration (c) is examined by plotting with the $\delta^{18}\text{O}_{\text{carb}}$ . Data including $\delta^{18}\text{O}_{\text{carb}}$ values are listed in Appendix E and F.....   | 117 |
| <b>Figure 5-10.</b> Mn content evolution curve in the pelagic limestones during a third-order sequence (from De Refelis et al., 2001).....  | 119 |
| <b>Figure 5-11a.</b> Normalized ratios with respect to Al of the Smackover samples from the Conecuh Embayment. Data including the TOC values are listed in Appendix E.....  | 122 |
| <b>Figure 5-11b.</b> Normalized ratios with respect to Al of the Smackover samples from the Manila Embayment. Data including the TOC values are listed in Appendix F.....   | 124 |
| <b>Figure 6-1.</b> A diagram illustrating the global carbon cycle with the major carbon reservoirs and related processes. The estimated amount of carbon mass in each reservoirs, the rate of the mass transferring and the carbon isotope compositions are reported in Table 6-1 (from Anderson and Arthur, 1980).....   | 132 |
| <b>Figure 6-2.</b> Schematic of major sedimentary and chemical carbon components and their average range of $\delta^{13}\text{C}$ values (from Anderson and Arthur, 1980).....  | 135 |
| <b>Figure 6-3.</b> Components of nonmarine carbon cycle and their inter-relationships of the $\delta^{13}\text{C}$ values (from Anderson and Arthur, 1980).....   | 136 |
| <b>Figure 6-4.</b> Diagram illustrating effect of meteoric water diagenesis on $\delta^{13}\text{C}$ composition of limestone sediments that results from mixing of carbon from metastable marine sediments with carbon from soil-gas carbon dioxides ( $\text{CO}_2$ ). The $\delta^{13}\text{C}$ composition of carbonates depend on the molar ratio $C_L/C_{SG}$ ( $C_L$ = No. of moles carbon derived from limestone sediment; $C_{SG}$ = No. of moles carbon derived from soil-gas $\text{CO}_2$ ). Increase in ratio results in production of isotopically heavier carbonates; decrease results in isotopically lighter carbonates (from Allan and Matthews, 1982)..... | 140 |
| <b>Figure 6-5.</b> Diagram illustrating potential patterns of $\delta^{18}\text{O}$ and $\delta^{13}\text{C}$ variations in the ancient carbonate rocks which can be useful for interpreting diagenetic depositional environments on the vertical trends in a time-stratigraphic framework that possibly are relative to changes of sea level (from Allan and Matthews, 1982).....  | 144 |

**Figure 6-6.** Carbon isotope variation ( $\delta^{13}\text{C}_{\text{carb}}$ ) from the whole rock samples of Smackover Formation from the T.R. MILLER MILLS 17-11, #1 well of the Conecuh Embayment and from the #1 NEAL ET AL UNIT 30-1 well of the Manila Embayment. The dashed lines exhibit a similar positive trend from the lower to the upper Smackover..... 145

**Figure 6-7.** Oxygen isotope variation ( $\delta^{18}\text{O}_{\text{carb}}$ ) from the whole rock samples of the Smackover Formation from the T.R. MILLER MILLS 17-11, #1 well of the Conecuh Embayment and from the #1 NEAL ET AL UNIT 30-1 well of the Manila Embayment. The dashed lines illustrate an average oxygen isotopic composition of the today sea water..... 147

**Figure 6-8.** Diagrams illustrating diagenetic influence on multi-component in carbonate systems. According to Brand and Veizer (1980 and 1981), geochemical reactions affect the shifting of concentration of these components into equilibrium in diagenetic environment. It is noted that the schematic examples are given only the common diagenetic trends in decreasing or increasing concentrations during meteoric and burial environments. The actual geochemical changes in an individual carbonate or component are dependent on the diagenetic history of the sediment and the availability of specific ions or isotopes (from Marshall, 1992)..... 151

**Figure 6-9.** Cross-plots illustrating the distribution between (a) the  $\delta^{13}\text{C}_{\text{carb}}$  values and the carbonate content (including dolomite) analyzed by acid dissolution (HCl) and (b) the  $\delta^{13}\text{C}_{\text{carb}}$  values and the Mg/Ca ratio for dolomite presented in these two cores..... 155

**Figure 6-10.** Cross-plots between (a) the  $\delta^{18}\text{O}_{\text{carb}}$  values of the Smackover samples and the Mg/Ca ratios illustrating different diagenetic environment on dolomitization between the two embayments and (b) the Sr and the Mg concentration for the effect from diagenesis where both elements would be reduced. The negative correlation between Sr and Mg suggests to variation of original calcite mineral in the sediment (high-Mg and low-Mg calcite) and the variation of dolomitization effect between the two depositional areas..... 157

**Figure 6-11.** Cross-plots between (a) the Sr and Mn concentrations, (b) the Sr concentration and  $\delta^{18}\text{O}_{\text{carb}}$  values, and (c) the Mn concentration and  $\delta^{18}\text{O}$  values illustrating diagenetic variation on chemical composition of the Smackover depositions in southwest Alabama. It is noted for the similar range of the  $\delta^{18}\text{O}_{\text{carb}}$  values for diagenetic alteration. The greater concentrations of the Sr and Mn in the T. R. MILLER MILLS 17-11, #1 samples are interpreted as a possible influence from changes of seawater composition as the Conecuh Embayment was probably more connected to open marine condition during relative sea level rise and highstand. Mn and  $\delta^{18}\text{O}_{\text{carb}}$  correlation indicates separate trends of diagenetic effect on samples with different range of Mn concentrations..... 160

**Figure 6-12.** Cross-plots between the  $\delta^{13}\text{C}_{\text{carb}}$  and  $\delta^{18}\text{O}_{\text{carb}}$  values from whole rock samples of the Smackover Formation in the Conecuh Embayment and the Manila Embayment. Except in a few samples, the  $\delta^{13}\text{C}_{\text{carb}}$  and  $\delta^{18}\text{O}_{\text{carb}}$  values of samples fall in almost similar ranges. Two distinctive trends are recognized; the first trend illustrates diagenetic alteration of both  $\delta^{13}\text{C}_{\text{carb}}$  and  $\delta^{18}\text{O}_{\text{carb}}$  values and the second trend illustrates diagenetic effect mostly on the  $\delta^{18}\text{O}_{\text{carb}}$  values..... 161

**Figure 6-13.** The correlation between the  $\delta^{13}\text{C}_{\text{carb}}$  and  $\delta^{18}\text{O}_{\text{carb}}$  values of the Smackover Formation from the Conecuh Embayment and the Manila Embayments. The different variation between dark solid line on the  $\delta^{18}\text{O}_{\text{carb}}$  values indicates different diagenetic environments. The similar variation pattern between the  $\delta^{13}\text{C}_{\text{carb}}$  trends suggests the same time-stratigraphic controls which occurred on both local scale (diagenetic alteration) and the regional/global scale (changes in relative sea level)..... 165

**Figure 6-14.** Cross-plots illustrating the correlations between (a) the TOC and the  $\text{CaCO}_3$  concentrations and (b) the TOC and the  $\delta^{13}\text{C}_{\text{carb}}$  values. Negative correlation between the TOC and the  $\text{CaCO}_3$  values is observed in both cores but with a different relationship. The variation of the TOC content in the Smackover samples illustrates indistinct correlation with the  $\delta^{13}\text{C}_{\text{carb}}$  values..... 169

**Figure 6-15.** The cross-plots between (a) the TOC and  $\delta^{13}\text{C}_{\text{org}}$  values and (b) the  $\delta^{13}\text{C}_{\text{carb}}$  and the  $\delta^{13}\text{C}_{\text{org}}$  values. Different correlations between the TOC and  $\delta^{13}\text{C}_{\text{org}}$  values suggest a possible variation in the original organic carbon sources between the two Smackover depositional environments. In the Conecuh Embayment, data plotted between the  $\delta^{13}\text{C}_{\text{carb}}$  and  $\delta^{13}\text{C}_{\text{org}}$  values are separated into two groups; the first group illustrating a positive correlation which is interpreted to be affected by increasing terrigenous organic source material and the second group illustrating a negative correlation which possibly due to an increase in marine organic input..... 170

**Figure 6-16.** Gas chromatograms of the saturate fraction from the extracted organic matter of the Smackover samples from the two depositional areas. The T.R. MILLER MILLS 17-11, #1 samples from the Conecuh Embayment characterize major marine organic matter (n-C<sub>22</sub>) with mixed algal (n-C<sub>17</sub>) and terrigenous (n-C<sub>26-30</sub>) materials. The #1 NEAL ET AL UNIT 30-1 samples from the Manila Embayment illustrate the dominant algal source (n-C<sub>17</sub>) and the terrigenous organic material (n-C<sub>26-30</sub>)..... 173

**Figure 6-17.** Vertical distribution of saturate fractions of the organic carbon component and the  $\delta^{13}\text{C}_{\text{org}}$  values of the Smackover samples from the two study cores..... 174

**Figure 6-18.** The vertical variations of the TOC,  $\delta^{13}\text{C}_{\text{org}}$  and  $\delta^{13}\text{C}_{\text{carb}}$  values of the Smackover carbonate depositions in the Conecuh Embayment and in the Manila Embayment. The variations of the  $\delta^{13}\text{C}_{\text{org}}$  in the Smackover sedimentary organic matter in these Smackover samples illustrate the mixing in the primary organic input and probably reworking processes during organic matter burial rather than changes by global increased of TOC accumulation. The  $\delta^{13}\text{C}_{\text{org}}$  shifts to heavier values are caused by increasing algal and terrigenous material during shallower paleowater-depth and relative low sea level where the  $\delta^{13}\text{C}_{\text{carb}}$  values become depleted due to diagenetic alteration..... 177

**Figure 6-19.** Carbon isotope stratigraphy of the Callovian to the Oxfordian sequences from (a) the Rovere Veronese, north Italy, (b) the Camposilvano, north Italy, (c) the Chabrieres, southern France (from Jenkyns, 1996) and, (d) the Smackover Sequence (the Conecuh Embayment, southwest Alabama, USA; this study)..... 179

**Figure 7-1.** Carbon isotope and elemental stratigraphic correlations used for synthesizing the Smackover depositional models corresponded to relative sea level changes; (a)  $\delta^{18}\text{C}_{\text{carb}}$  for local and global variation of relative sea level rise and fall (transgressive-refractive) due to changes of global carbon budgets, (b) Mn for a sequence framework caused by a global hydrothermal activity and, (c) Sr for local and global variation of Sr in the seawater..... 186

**Figure 7-2.** Elemental and oxygen isotope correlations between the Smackover sequences during local variations used for synthesizing depositional model for the Conecuh and the Manila Embayments, (a) and (b) carbonate and siliciclastic components (Ca and Al) for depositional environments and, (c)  $\delta^{18}\text{O}_{\text{carb}}$  for diagenetic environments..... 187

**Figure 7-3.** Elemental, organic carbon content and  $\delta^{13}\text{C}_{\text{org}}$  correlations between Smackover sequences from the Conecuh and the Manila Embayments (a) K/K+Al ratios for siliciclastic variation of different related minerals because of local (and global?) chemical weathering cycle, (b) TOC for organic carbon accumulation associated with source input and/or depositional condition, (c)  $\delta^{13}\text{C}_{\text{org}}$  for local effect caused from mixed organic source input during relative sea level variation..... 188

**Figure 7-4.** Schematic depositional model related to relative sea level changes proposed for the Smackover deposition in the Conecuh Embayment. The lowest sequence, the Sm-S1, formed during the major flooding for Smackover carbonates may include the upper siliciclastic Norphlet as the lowstand deposit. The Sm-S2 sequence earlier occurred in a partially restricted condition but became more normal marine during the later stage of high sea level. The Sm-S2 and the Sm-S3 sequences were interrupted by falling sea level period showing increasing siliciclastic influx. The Sm-S4 deposit formed on top of the lowstand cycle occurred during long-term Smackover progradation where depositional energy became high. At the top of the Smackover Formation of the Sm-S4 Sequence, relative sea level fell illustrated by an erosional surface and increased dolomite and evaporite precipitation..... 189

**Figure 7-5.** Schematic depositional model related to relative sea level changes proposed for the Smackover deposition in the Manila Embayment. The lowest sequence, the Sm-S1, formed during the major flooding for Smackover carbonates but consists mostly the massive, marine reworked siliciclastic sandstone in the uppermost Norphlet Formation. The next two sequences, the Sm-S2 and the Sm-S3, illustrate shallowing-upward cycles in a peritidal environment where the sediments in the uppermost intervals were affected from meteoric diagenesis and subaerial exposure. The Sm-S4 sequence formed during the high energy sea level condition of the long term progradational Smackover sequence. Coastal/shoreface mixed siliciclastic-carbonate intercalation occurred near the shoreline. Because of the high structural setting condition, Smackover depositional sequences experience strong diagenetic alteration and dolomitization. Similar parameters can be recognized during variation of sea level and sediment deposition of different system tracts..... 193

**Figure 7-6.** A diagram illustrating the possible relationship between the fluctuation of sea level and the short-term peritidal cycles observed during the long-term Smackover sequence in the #1 NEAL ET AL UNIT 30-1 of the Manila Embayment. In this sequence, a stacking of the small cycles formed during the higher order eustatic sea level cycles can be observed but it is interpreted that this only occurred during the major relative sea level fall (third-order) which interrupted the continuous carbonate production and resulted in subaerial exposure and diagenesis (from Pratt et al., 1992)..... 195

**Figure 7-7.** A diagram illustrating the hypothetical stratigraphy of meter-scale, peritidal, successions which could possibly have occurred between the two sequence boundaries in the #1 NEAL ET AL UNIT 30-1 core of the Manila Embayment. Each succession, formed by sediment progradation, was most likely associated with the higher frequency sea level fluctuation. The balance between sea level changes, sedimentation and subsidence rate affected the stacking pattern of the tidal flat sediment succession (Pratt et al., 1992)..... 195

**Figure 7-8.** Depositional model proposed for the Smackover upward-shoaling sequence in the Mississippi Interior Salt Basin, central Mississippi described and as the lower, middle and upper Smackover by Shew (1991). It is noted that the Smackover carbonates were interrupted by several episodes of siliciclastic sediment influx which probably contributed to siliciclastic observed in the Smackover deposition of the Manila Embayment..... 197

**Figure 7-9.** The global plaeoclimate model proposed by Weissert and Mohr (1996) and illustrated the link between different components during the Late Jurassic global water and carbon recycling due an increased atmospheric CO<sub>2</sub>..... 202

## LIST OF TABLES

|  | Page |
|--|------|
| <b>Table 4-1.</b> Core observations and thin section description from the sediment samples of the T.R. MILLER MILLS 17-11, #1 well of the Conecuh Embayment and paleo-environment and paleowater-depth interpretations.....  | 59   |
| <b>Table 4-2.</b> Core observations and thin section description from the sediment samples of the #1 NEAL ET AL UNIT 30-1 well of the Manila Embayment and paleoenvironment and paleowater-depth interpretations.....  | 63   |
| <b>Table 5-1.</b> Chemical compositions of major and minor elements in seawater and freshwater stream (from Veizer, 1986).....   | 95   |
| <b>Table 6-1.</b> The estimated mass of carbon (organic and inorganic) in various Earth's reservoirs and the transferred fluxes of carbons between the different reservoirs and their average $\delta^{13}\text{C}$ compositions (from Anderson and Arthur, 1980)..... | 133  |

## LIST OF APPENDICES

|  | Page |
|--|------|
| <b>Appendix A</b> Photographs of the T.R. MILLER MILL 17-11, #1 core from the Conecuh Embayment.....   | 222  |
| <b>Appendix B</b> Photographs of the #1 NEAL ET AL UNIT 30-1 core from the Manila Embayment.....   | 232  |
| <b>Appendix C</b> Photomicrographs of thin sections of Smackover samples at variable depths in the T.R. MILLER MILLS 17-11, #1core.....  | 242  |
| <b>Appendix D</b> Photomicrographs of thin sections of Smackover samples at variable depths in the #1 NEAL ET AL UNIT 30-1 core.....   | 246  |
| <b>Appendix E</b> Tables for concentrations of major, minor and trace elements, isotopic compositions of carbonate and organic materials, TOC in Smackover samples from the T.R. MILLER MILLS 17-11, #1 well of the Conecuh Embayment..... | 251  |
| <b>Appendix F</b> Tables for concentrations of major, minor and trace elements, isotopic compositions of carbonate and organic materials, TOC in Smackover samples from the #1 NEAL ET AL UNIT 30-1 well of the Manila Embayment.....      | 263  |

## ABSTRACT

The sequence stratigraphy of the Upper Jurassic (Oxfordian) Smackover marine carbonate sequence was investigated from a chemostratigraphic analysis of samples of the Conecuh Embayment and the Manila Embayment of southwest Alabama, Gulf Coast of the United States. The analytical approaches were based upon an integration of core descriptions, petrography of thin sections, elemental compositions, oxygen and stable carbon isotopes from carbonate and organic materials. The results demonstrate the effectiveness of using stable carbon isotope chemostratigraphy for a ramp sequence stratigraphic model which allows possible local and global stratigraphic correlations.

During the Oxfordian, core and petrographic data indicated that the Smackover depositions in the southwest Alabama basins occurred in different depositional environments and diagenetic conditions related to the structural setting and paleotopography. Early carbonate deposition took place in the Conecuh Embayment, although in partially restricted conditions owing to basement highs, as low-energy, restricted lagoonal to shallow marine conditions. The mudstone, algal mudstone and peloidal, pelletoid wackestones are dominant from the lower to middle Smackover and show small relative diagenetic changes into stable diagenetic calcite. In the upper Smackover, increasing depositional energy and an open less restricted connection to normal marine waters permitted the deposition of high energy oolitic packstone and grainstones of a barrier-shoal environment. Changes of the original carbonate phase associated with changing subsurface environmental conditions increased diagenesis. The shallower structural setting of the Manila Embayment affected pervasive dolomitization of sediment deposited under a tidal shallow water environment. The shallowing-upward cycles are dominated by intertidal mudstone and wackestone “ribbon rock”. Dark organic-rich subtidal sediments commonly overlie the anhydritic dolostone of the previous cycle. In the upper Smackover, intercalation between siliciclastic

sandstone and carbonate intervals revealed similar increasing depositional energy. During the Smackover sequence, siliciclastic sediment interruptions occurred, but are only distinctive in the sediment from Conecuh Embayment owing to a higher siliciclastic background which was present in the Manila Embayment. However, subaerial exposure superimposed on the dolomitized upper intertidal to supratidal sediments is detectable. Based upon a carbonate ramp stratigraphic model, the variation between carbonate-siliciclastic sedimentation and variable Smackover facies are interpreted to record the variations of relative sea level cycles, depositional environment and paleowater-depth conditions.

Elemental compositions of the Smackover sediments from the two areas are variable, but support the differences in the two embayments which can be shown by the normalized ratios and the cross-plot correlation among the elements. Local variations such as higher siliciclastic background and dolomitization in carbonates of the Manila Embayment are clearly manifested. The depositional environment, as interpreted from redox elements and Sr, suggests that the Manila Embayment occurred under oxic conditions. Sedimentary cycles are recognized only in the Smackover sequence from the Conecuh Embayment and were likely related to both local and regional/global controls. A long-term regressive cycle with an increase in depositional energy is illustrated in four shorter cycles. The variation of unusual high Mn and Sr contents observed in Smackover in the Conecuh Embayment suggests possible global events which affected a variation of seawater elemental concentrations. In the lower Smackover, the depositional environment which formed during a marine transgression was probably not anoxic but possibly became restricted during the periods of falling relative sea level.

Oxygen isotopes ( $\delta^{18}\text{O}_{\text{carb}}$ ) of the Smackover sediments illustrated variations which are interpreted to be controlled by differing diagenetic environments. Stronger diagenetic effects observed in the Smackover of the Manila Embayment are interpreted to be affected by shallower conditions which were subjected to subsequent subsurface meteoric diagenesis. In contrast, similar variations in carbon isotopes ( $\delta^{13}\text{C}_{\text{carb}}$ ) suggests that local diagenetic environments and

sedimentary facies were not the exclusive factors but instead, regional and, probably, global sea level changes were most important. During the falling of relative sea level, recycling of the organic carbon materials from land into the ocean affected a global scale shift which increased the abundance of the lighter carbon isotope ( $^{12}\text{C}$ ) in the ocean and caused a negative carbon isotope excursion to be observed. For the Smackover carbonate, organic carbon isotopes appear to be locally affected by the mixed organic carbon sources between marine, terrestrial and algal materials during the sea level fluctuation and vary with distance from land.

Correlation between the  $\delta^{13}\text{C}_{\text{carb}}$  variations of the two Smackover cores suggests that regardless of the effect of variable depositional environments and diagenetic alteration,  $\delta^{13}\text{C}_{\text{carb}}$  stratigraphy is a strong signal that can be applied to the Smackover carbonate sequences. Short-term depositional cycles are detected and correlated by the fluctuation of the  $\delta^{13}\text{C}_{\text{carb}}$  values. During the Smackover long-term sequence (second order?), carbon isotope stratigraphy indicates there were four smaller and third-order eustatic sea level cycles superimposed. Owing to different local variations on sedimentary facies and elemental composition, cyclicity might not be always clearly manifested. However, using multiple techniques, it may be possible to correlate short-term depositional cycles and their boundaries. Chemostratigraphy and lithological observation suggest that the lowest Smackover carbonate sequence was possibly formed and cut across the lithostratigraphic boundary between the Norphlet and Smackover Formations of the two study areas. The lower Smackover occurred in the Conecuh Embayment was time-correlative with the reworked siliciclastic marine sandstone of the Norphlet Formation interpreted as regressive sandstone in the Manila Embayment. During a lowstand sea level associated with a disconformable sequence boundary, a combination of both local and global effects caused a negative  $\delta^{13}\text{C}_{\text{carb}}$  excursion. In the transgression and relative sea level highstand, low to absent siliciclastic contamination increased carbonate sedimentation and resulted in heavier  $\delta^{13}\text{C}_{\text{carb}}$  values. During the third-order shorter Smackover sequences, transitional surfaces, such as a marine flooding surface and a maximum flooding surface, were not clearly visible due to a low

slope gradient on a ramp structural setting where rising sea level was laterally more effective than vertically effective in determining facies trends. While lateral paleoenvironment changes during the Smackover sequence were recorded by lithological and elemental composition variations, the sequence stratigraphy of the Smackover can be vertically revealed by applying a  $\delta^{13}\text{C}_{\text{carb}}$  stratigraphic approach, which is shown by a global correlation of the Smackover with other Oxfordian rock sequences and to the third-order eustatic cycles.

Chemostratigraphy is a powerful tool for helping to decipher global effects from local effects in carbonate sequence analysis, providing correlative insight into the timing of intrabasinal depositional events, and in discriminating the original from the overprinted diagenetic signal. Carbonate ramp platforms such as the Smackover, owing to gradational facies changes which can occur laterally under small vertical changes in relative sea level, make ideal proxies for testing hypotheses of global versus local effects of sea level upon carbonate sequence development.

# CHAPTER 1

## 1.1 INTRODUCTION

The Upper Jurassic Smackover Formation is a limestone unit which occurs extensively in the subsurface around the rim of the Gulf of Mexico (**Figure 1-1**). It is well known not only for its hydrocarbon productivity but also for serving as a template for the classic carbonate ramp platform model (Ahr, 1973; Read, 1985). According to Salvador (1987), Smackover deposition occurred during the major flooding event related to the opening of the future Gulf of Mexico basin from the Late Triassic-Jurassic breakup of Pangea. Imlay and Herman (1984) interpreted the age of the Smackover sedimentation to be between 144 to 151 Ma from the Middle to the Late Oxfordian. In the northern Gulf of the United States, the Smackover deposit is only found in the subsurface but extends from central Texas, Arkansas, through Louisiana and central Mississippi, and continues into southwest Alabama and terminates in the panhandle of northwest Florida (**Figure 1-2**).

Early regional studies which described the Smackover include those by Imlay (1943), Swain (1949) and Dickinson (1968). Within the U.S. Gulf Coast, the spatial geometry of Smackover deposition has been redefined numerous times by different authors (e.g. Mancini and Benson, 1980; Moore, 1984, Wade and Moore, 1993; Heydari, 2002). Owing to the importance of the Smackover relative to hydrocarbon generation, many more local investigations on the field level have also been conducted. For example, the Smackover has been studied in Texas (e.g. Barrett, 1998), south Arkansas and north Louisiana (e.g. Troell and Robinson, 1987), Mississippi (e.g. Meendsen et al., 1987; Rhode and Maxwell, 1993; Shew, 1991), southwest Alabama (e.g. Sigsby, 1976; Bradford, 1984; Benson and Mancini, 1984; Wade et al., 1987; King and Hargrove, 1991) and Florida (e.g. Vinet, 1984; Lloyd et al., 1986).

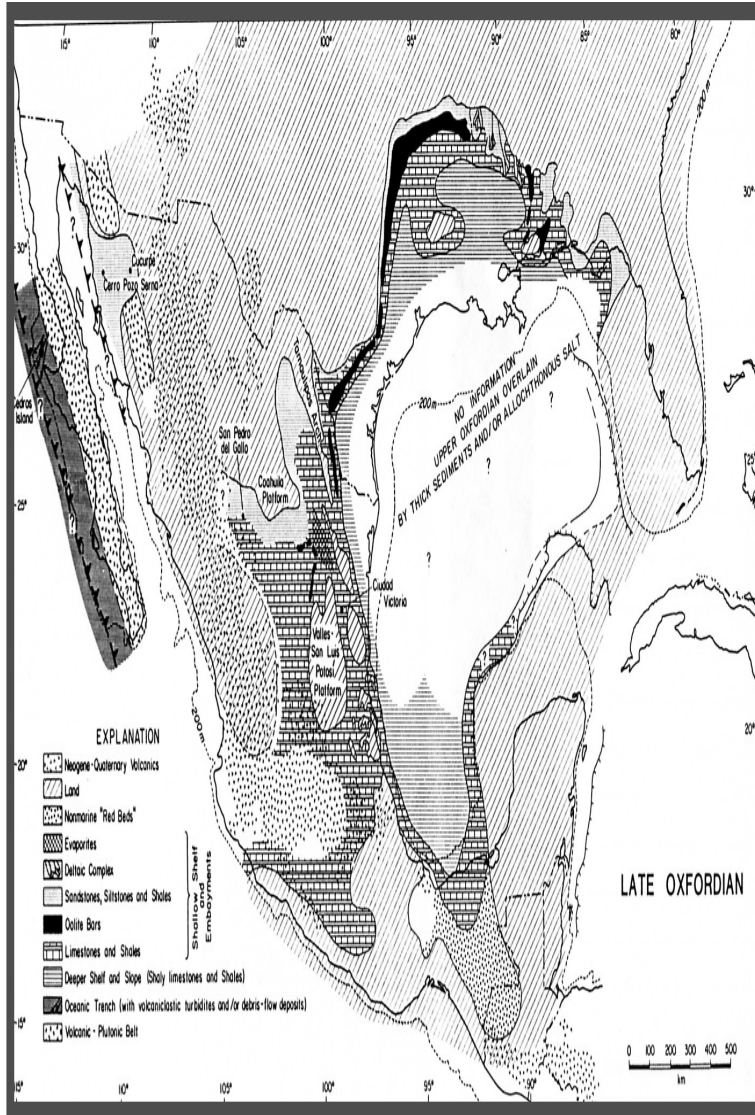
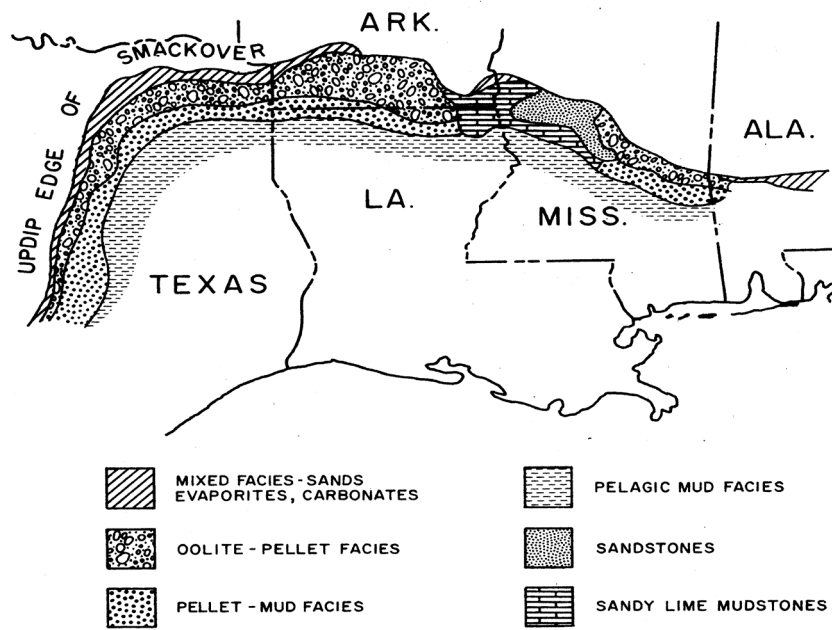


Figure 1-1. Paleogeographic map during the Late Oxfordian illustrating sediment deposits where mostly limestone and shales and the oolite bars distributions represent the Smackover Formation (from Salvador, 1987).



**Figure 1-2.** Location map of the Smackover trend along the states of the northern US Gulf Coast rim (from Moore, 1984).

## 1.2 BACKGROUND STUDIES

General hypotheses based on a study which contains limited data can be at risk unless comparable results have been presented elsewhere. In contrast, conclusions can be drawn from the results of many studies by determining the differences between those studies. Numerous reports of Smackover Formation from individual interior basins along the U.S. Gulf rim have presented variable conclusions for the effects of sea level changes on the Smackover depositional system. In southwest Alabama, the results of sequence stratigraphic studies of the Smackover Formation are rather different from those proposed for the Upper Jurassic Oxfordian sequence in the Gulf of Mexico Basin and in the nearby interior basin (i.e. the Mississippi Interior Salt basin) under the control of eustatic sea level cycles. A brief review of some of these studies is necessary in order to understand the purpose of this research.

Deposition of the Smackover Formation in southwest Alabama occurred in three separate basins which are now called the Conecuh Embayment, the Manila Embayment and the Mississippi Interior Salt Basin (**Figure 1-3**). Depositional environment and sedimentary facies were believed to be principally controlled by the third order eustatic sea level cycle but were also modified by paleotopography related to structural low and high in the area and the local movement of the Louann Salt (Benson, 1988).

Starting from the Conecuh embayment, sedimentary facies of the Smackover Formation were analyzed and mapped by Sigsby (1976) into a time-slice basis using a large number of core samples. A long term transgressive-regressive sequence was proposed and during the lower Smackover a paleoenvironment of deposition was suggested to occur under restricted marine conditions. A change of paleowater-depth was believed to be associated with a variation in siliciclastic sediment influx and a short term sea level fluctuation during the Smackover long-term event (Sigsby, 1976). Later, a local study by Bradford (1984) characterized the Smackover Formation from lower to middle and upper into ten different facies and also suggested a long-

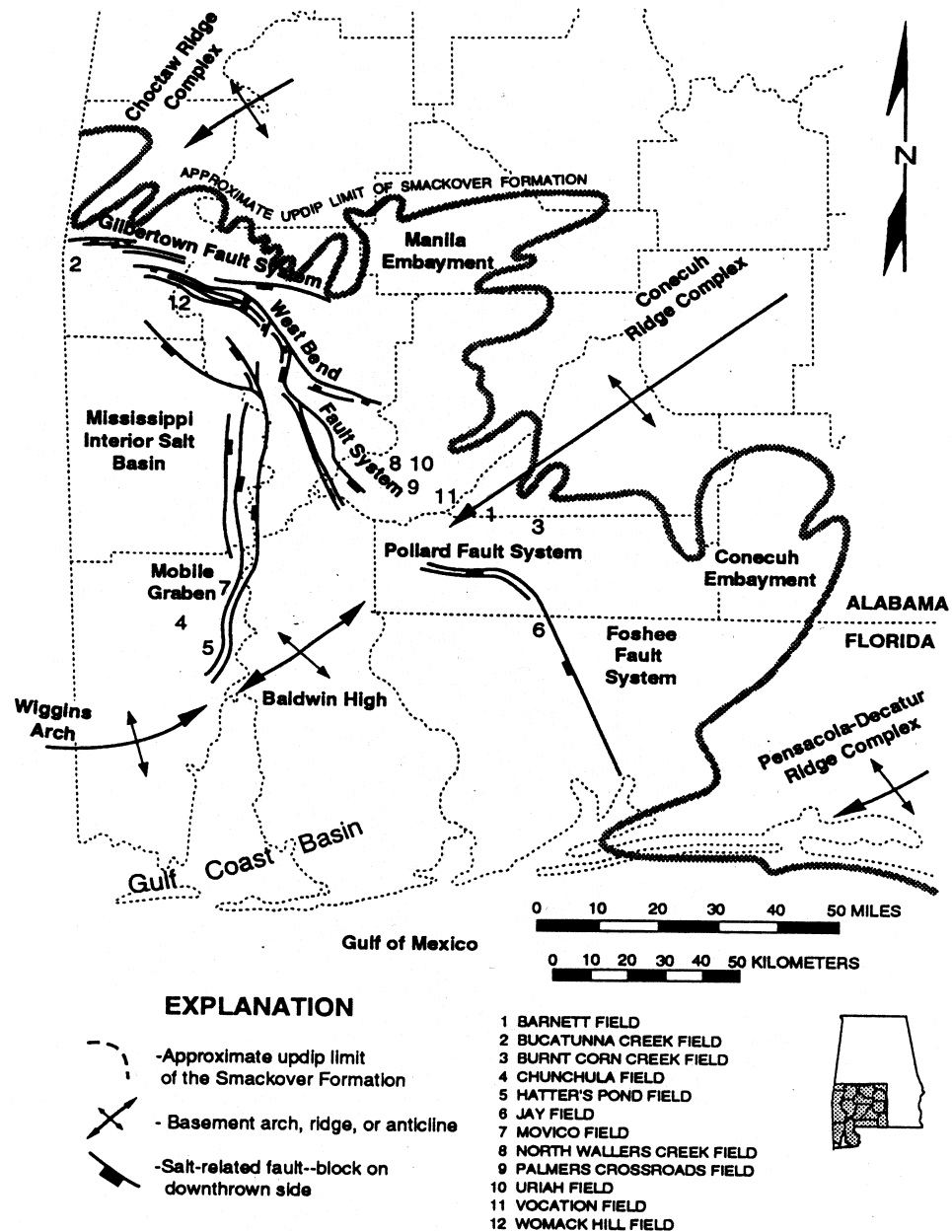


**Figure 1-3.** Sedimentary basins in southwest Alabama where Smackover depositions occurred; the Mississippi Interior Salt Basin, the Conecuh Embayment, and the Manila Embayment (from Kopaska-Merkel and Mann, 1992).

term transgressive-regressive sequence. According to Bradford (1984), the lower Smackover, dominated by laminated mudstone and packstone, was deposited during the transgressive cycle under an open-marine environment. The middle Smackover, characterized by fossiliferous mudstone and intercalated with black laminated mudstone, was interpreted to record deposition restricted marine conditions. The upper Smackover was suggested to represent a regressive sequence comprised of ooid shoal, lagoonal and sabkha facies. In 1987, Esposito and King reported the same interpretation but observed six major sedimentary facies. Comparing with the early global eustatic sea level cycle, which had just been proposed for the Upper Jurassic sequence in the Gulf Coast basins by Vail et al. (1984) (later revised by Haq et al., 1988), a eustatic J3.1 cycle was believed to be a major control for Smackover deposition of southwest Alabama. The lower and upper Smackover depositions were affected by a long-term sea level rise of two different increasing rates. The sequence stratigraphic model of the Smackover deposition in the Conecuh Embayment and the adjacent areas was proposed again by the work of Prather (1992; **Figure 1-4**). In this study, the Buckner Anhydrite, the Smackover and the upper Norphlet Formation were related under the single eustatic sea level control. Sequence boundaries and important bounding surfaces were interpreted from the lithological marker units observed on the time-slice facies map which had been created from electrical well-log correlations and core observations. The uppermost Norphlet sandstone was interpreted to result from a reworking process during the initial Smackover rapid sea transgression. The Smackover Formation was deposited during a transgressive system tract and a highstand system tract which were separated from each other by a maximum flooding surface or a condensed section of the middle Smackover interval. The Buckner Anhydrite was part of the Smackover regressive sequence during the highstand system tract and the Smackover carbonate was separated from the main part of the Norphlet Formation by a type 2 sequence boundary. It is necessary to note that the Vail et al., (1984) global sea level cycles were modified and corrected to the Haq et al., (1988) global sea level model. The single third-order Oxfordian eustatic sea level J3.1 cycle was divided into four

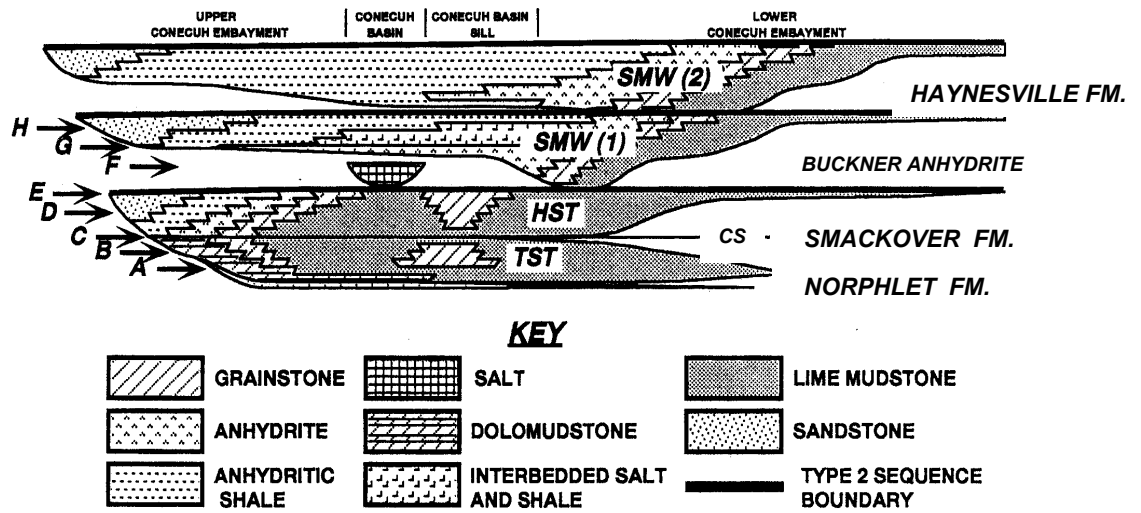


**Figure 1-4.** Sequence stratigraphic framework of the Smackover Formation in southwest Alabama proposed by Prather (1992). The alphabets A to H are represented the lithological key markers that were used to define the chronostratigraphic surfaces for the model (from Prather, 1992).

smaller third-order cycles, the LZA 4.1 to LZA 4.4, according to later and additional coastal onlap data.

In the Manila Embayment, Smackover lithofacies correlations were also used for interpreting the Smackover depositional framework and relating to its eustatic sea level cycle. In 1987, Wade et al. interpreted the sedimentary facies of the Smackover deposition from east to west and north to south in the Manila Embayment, starting as a shelf facies in the lower Smackover and passing into ramp facies in the upper Smackover with some modification from basin topography. In their study, it was also suggested that the Manila Embayment, which is now a separate basin, was once connected to the Mississippi Interior Salt Basin during the Smackover time. Similarly, a Smackover deposition of the northern part of the Manila Embayment was reported by King and Hardgrove (1991) to start as carbonate shelf system and later became a ramp platform. The Smackover carbonate sequence formed under a single sea level cycle but contained two different genetic packages which were controlled by two different rates of sea level rise. The Late Jurassic third-order eustatic cycle expanded from the early Oxfordian to early Kimmeridgian was suggested as the Smackover primary control. The lower and upper Smackover packages were interpreted as a transgressive system tract and a highstand system tract separated by a maximum flooding surface, or a condensed section. A similar interpretation was from the Smackover study of southern part of the Manila Embayment reported by King and Moore (1992). Two depositional packages were termed a parasequence set and were described for the Smackover sequence as being controlled by a single third-order eustatic sea level cycle. The depositional systems were affected by different rates of sea level rise which started as a lower carbonate shelf and changed into a ramp carbonate facies. The two packages were separated by the second flooding surface, or a maximum flooding surface, in the middle of the Smackover Formation.

A sequence stratigraphic model for the Upper Jurassic Smackover deposition of southwest Alabama was proposed primarily by Wade and Moore (1993). An example of a

reference well showing sequence boundaries and bounding surfaces was taken from the Manila Embayment. Within a sequence framework, the lower Smackover was defined as a transgressive system tract (TST) and the upper Smackover was defined as a highstand system tract (HST). The uppermost reworked sandstone of the Norphlet Formation was part of the Smackover sequence during initial transgression. According to Wade and Moore (1993), the siliciclastic Norphlet Formation was not a separate sequence from the Smackover Formation but was instead a lowstand system tract (LST) of a long-term Smackover sequence. However, they concluded that the different interpretation for the sequence framework and depositional system tract of the Smackover sequence in southwest Alabama from those interpretations in the other basins of the central and western Gulf of Mexico resulted from a strong local lithofacies variation caused from paleotopography and salt tectonics. Furthermore the depositional bounding surfaces and sequence boundaries might not generally coincide with the formation boundaries. Lithofacies interpretations alone might not be sufficient to constrain a sequence framework in southwest Alabama compared to other sequence interpretation from broader areas owing to sediment modification resulting from variable local controls.

So far, most Smackover sequence-stratigraphic models based on sedimentation in the Conecuh and in the Manila Embayments have not been significantly different from each other. Other regional sequence models of the Smackover Formation in southwest Alabama which were characterized from the sediment deposited in the Mississippi Interior Salt Basin located in southwest Alabama and Mississippi included examples from Mancini and Benson (1980) and Mancini et al., (1991; 1992; 1993). Based upon these studies, the stratigraphic framework of Smackover sequence in the Mississippi Interior Salt Basin appeared to be similar to that applied to the sequence in the Conecuh and the Manila Embayments. Mancini et al., (1990 and 1993) also proposed their model for the Smackover deposition for the entire Gulf area. Hydrocarbons found in the upper Smackover grainstone and packstone of the highstand system tract were derived from the source rocks which were believed to be the condensed section occurring in the middle

Smackover during the maximum flooding surface. The sea level cycle model of Mancini et al. (1990 and 1993) assumed the Upper Jurassic strata along the Gulf rim were controlled by eustatic sea level changes similar to the model proposed earlier by Vail et al. (1984). The Smackover Formation was characterized as a transgressive system tract and highstand system tract formed under a single third-order eustatic sea level cycle during the Oxfordian period. It appears that this Smackover model has also been similar to the sequence concept applied to the Smackover depositions in both the Conecuh and the Manila Embayments in most studies reported thus far.

However, not all studies of the Smackover stratigraphic framework of the Mississippi Interior Salt Basin are in agreement. One study from Shew (1991) compared and interpreted continuous Smackover cores from central Mississippi and from the eastern part of Louisiana. Shew (1991) proposed a long-term regressive sequence for the Smackover stratigraphic model related to relative sea level changes. The upper part of the Smackover core characterized the upwardly shoaling carbonate cycles of carbonate packstone and grainstone. During the Smackover period, siliciclastic influxes influenced and caused interruption of carbonate sedimentation several times. In his report, it was proposed that an ancestral Mississippi river could have played a significant role in delivering terrigenous material from the continent during fluctuations of relative sea level. The interfingering between the sandstone and carbonate lithofacies might also be recorded in both the basin and in the nearshore environment due to the influence from longshore currents and storm processes. Another sequence model was reported from many subsequent studies (Heydari and Moore, 1994; Heydari et al., 1995 and 1997; Heydari, 2002; Heydari and Wade, 2002), where several core samples from the Mississippi, Louisiana and Arkansas were used for correlations. According to Heydari et al. (1995 and 1997), a time-stratigraphic model interpreted from Smackover lithofacies and petrographic observations suggested the Smackover Formation is comprised of three upwardly shoaling cycles controlled by changes in relative sea level and paleoclimates. These three cycles from lower to upper called C, B and A occurred during an evolution of the Smackover platform from an early ramp to a shelf

carbonate system (**Figure 1-5**). During an early period, the paleoenvironment of the lower Smackover was anoxic and marked by high organic matter accumulation in the laminated and thin bedded lime mudstones and wackestone. The major hydrocarbons found in the upper Smackover reservoir rocks were believed to be derived from the organic source in this lowest Smackover cycle source rock. The middle and the upper Smackover cycles are mainly packstone and grainstone formed during progradation of the barrier shoal complex after the end of the lowest cycle shelf margin deposit. Relative sea level fall occurred by the end of these separated cycles but an exposure surface could only be observed by the end of the uppermost cycle. High organic accumulation observed in the lowest cycle was suggested as a result from increased productivity of algal blooming cycles controlled by paleoclimate and paleoceanography variation. An increased nutrient was associated with a freshwater influx from the ancestral Mississippi river. Meteoric diagenesis occurred during upper Smackover time, evident from carbon and oxygen isotopes values and elemental data of the ooid grainstones. Lately, a sequence-stratigraphic model for the Smackover Formation of the north and central U.S. Gulf Coast basins, proposed by Heydari (2002), consisted of three separate depositional sequences which were controlled by three third-order relative sea level cycles, paleoclimate, and carbonate production rate.

Clearly, there is discrepancy in the sequence stratigraphy of the Upper Jurassic sequence, especially the Smackover of the southwest Alabama basins. This study is therefore proposed to address and analyze such issues by reinvestigating the stratigraphic framework of the Smackover sequence in this area. It is believed that in order for the Oxfordian Smackover sequence to be correlated with the other global Oxfordian sequences, such as the Corallian group from the Dorset Coast of southern England (Sun, 1989) or the deep-shelf carbonate from southern Germany and southern Spain (Pittet et al., 2000), a better understanding about controls and variations observed in the Smackover sequence of this particular area can be very useful.

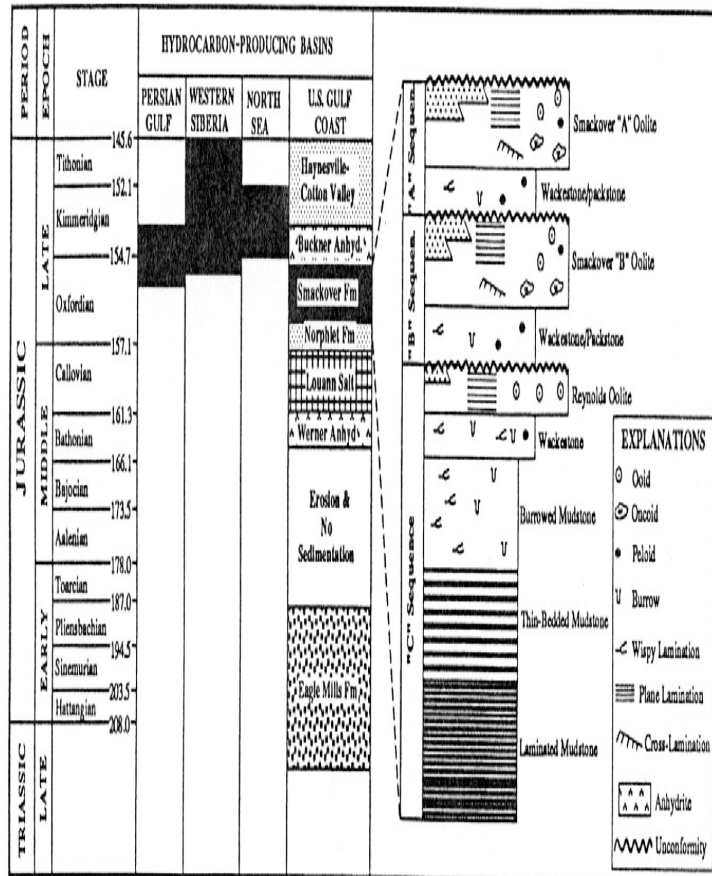


Figure 1-5. The Late Triassic-Jurassic stratigraphic column of the northern Gulf of Mexico showing showing dark organic source rock correlation with the other Upper Jurassic sedimentation of different areas. According to Heydari et al. (1995), the Smackover Formation consists of three shoaling upward cycles from lower to upper called C, B, A cycles (from Heydari et al., 1997).

### 1.3 DEFINITION OF THE PROBLEM

From the preceding paragraphs, the variation in the sequence stratigraphic interpretation model proposed for Smackover deposition in southwest Alabama can be summarized into the following questions. 1) Is the Smackover a long term regressive sequence (third order sea level cycle) or controlled by shorter term sea level fluctuations? 2) Were relative sea level changes of the Smackover controlled by global eustasy and/or local tectonic activity and/or palaeoclimate/paleoceanography? 3) Can a sequence framework of a modified Smackover deposition by paleotopography of different basins be possibly compared? 4) Is there different approach beside lithofacies that can be used to correlate the Smackover depositional framework? 5) If Smackover depositional system in southwest Alabama and in the northern Gulf basins were primarily controlled by eustatic sea level changes, why are the depositional models of the Smackover in these adjacent basins variable? 6) Is there any stratigraphic approach which would allow the depositional system of the Smackover from the Conecuh and/or the Manila Embayment to be correlated with the other Oxfordian sequences? It is assumed that the answers to these questions probably hinge upon lithofacies and depositional environments that varied through time and space and were related to their local paleotopographic variation and/or different subsidence rate.

The interpretation of the Smackover depositional sequences can be problematic for other reasons. First, it could be due to a lack of well defined absolute age biostratigraphic data which could help to refine any correlation. Second, a non-coincidence between sequence boundary and lithological formation has possibly leads to difficulties in interpretation. Third, a lithological modification by a pre-Jurassic paleotopography and a gradational boundary and facies change on a carbonate ramp platform setting also affected the interpretation for the depositional system tract boundary. Therefore, a solely stratigraphic correlation based upon sedimentary facies analysis may not be sufficient to provide constraint under variable local effects on a conformable

boundary-based sedimentary sequence between different basins in this area. This dissertation attempts to investigate the sequence stratigraphy of the Smackover Formation in southwest Alabama by using lithostratigraphic and chemostratigraphic approaches based upon elemental and stable carbon isotopic analyses.

#### **1.4 OBJECTIVES**

Initially, the purpose of this study was to examine, in detail, the organic matter in a defined depositional framework of the Smackover sequence of southwest Alabama (i.e. Mancini et al., 1990 and 1993; Prather, 1992). The preliminary results from organic geochemical and elemental analysis, however, did not appear to be consistent with the established sequence framework. Biomarkers in the sediment derived from a condensed section were not representative of a maximum sea transgression and results indicated mixing of terrestrial material input with marine organism. A subsequent literature survey indicated that the Smackover framework in southwest Alabama basins did not appear to be in accord with the framework proposed from the nearby Mississippi Interior Salt Basin and the global sea level cycle model for the Gulf of Mexico basin. Therefore, the objective of this study changed to characterizing the sequence framework of the Smackover deposition in southwest Alabama, i.e. the Conecuh and the Manila Embayment, by using multi-stratigraphic approaches and combining lithological observations, elemental analyses, stable carbon isotope stratigraphy and organic geochemistry. The premise is that, under the same major control (i.e. sea level changes), even though sedimentary facies were altered by paleotopography and depositional conditions (i.e. diagenesis), it should be possible to correlate the time-stratigraphic framework for a depositional sequence such as the Smackover Formation in the southwest Alabama basins using various chemical parameters.

## CHAPTER 2

### 2.1 GEOLOGIC SETTING

The geologic setting of the northern U.S. Gulf Coast region was primarily controlled by tectonic activities during the opening of the Gulf of Mexico from the Late Triassic to Middle Jurassic (Wood and Walper, 1974; Martin, 1978; Buffler, 1980; Walper, 1980). Different continental blocks combined with the horst and graben system were created in response to the tensional stresses associated with supercontinent riftings. The Jurassic sedimentation and depositional environments were affected by differential basement subsidence and paleotopography of the pre-Jurassic and mid-Jurassic structures (Wilson, 1975). On the eastern Gulf Coast region, the Jurassic strata were significantly influenced by the inherited framework that resulted from the combined effects of the earlier continental collision and suturing during the Late Paleozoic and subsequent extension during continental rifting in the later Late Triassic-Jurassic (Martin, 1978; Salvador, 1987). Major positive and negative structures were created generally normal to the axis of the main Gulf basin. Some of these structures which were particularly important in the northern Gulf Coast basins were the San Marcos, Sabine and Monroe Uplifts. Halokinetic effects created by local Louann Salt movements increased lithologic complication by adding the formation of salt diapirs, pillows, anticlines, grabens and several peripheral en echelon extensional faults. In general, most basins and sedimentation along the northern Gulf Coast are commonly associated with the salt-related fault systems and/or high-rise salt structures. The major fault system caused by local salt movement, and which extended from Mississippi to southwest Alabama, is the Pickens-Gilbertown, the West Bend, Pollard, and Forshee Fault. Moore (1984) indicated that most fault movement activities probable occurred after Smackover Oxfordian stage but during the Late Jurassic Haynesville-Cotton Valle deposition and the development of the Cretaceous deposits.

On the southeastern Gulf Coast area of Mississippi and southwest Alabama, the three sedimentary basins, the Mississippi Interior Salt Basin, the Conecuh Embayment, and the Manila Embayment, were formed and associated with the local major positive basement features; the Wiggins Arch Complex, the Wiggins Arch, the Baldwin High, the Choctaw Ridge complex, the Conecuh Ridge complex, and the Pensacola-Decatur Ridge complex (**Figure 2-1**). The positive structure which separated the Mississippi Interior Salt Basin from the Manila Embayment on the east was the Mobile Graben. According to Wade (1987), during the Late Jurassic, a depositional area in Mississippi was probably connected to southwest Alabama as a main a large, active, subsided depocenter caused by a prominent depression of the basement surface. The Manila Embayment was probably not separate from the Mississippi Interior Salt Basin during the Smackover time but instead affected by a slower subsidence rate. The very thick sediment sequence in Mississippi was also associated with thick local salt diapirs especially in the central part of the basin. To the south of the Wiggins and on the east side of the Mississippi Interior Salt Basin, the Conecuh Basin and embayment was another depocenter for sedimentation. This embayment is separated from the Manila Embayment by the Paleozoic Conecuh-Wiggins Arch, a positive structure.

## **2.2 STRATIGRAPHY**

Sedimentary strata in the central and eastern Gulf Coast, including southwest Alabama, consist of pre-Mesozoic basement rocks, the Triassic-Early Jurassic Eagle Mills Formation, the Jurassic Werner Formation, the Louann Salt (including Pine Hill Anhydrite Member), the Norphlet Formation, the Smackover Formation, the Haynesville Formation (including the Buckner Anhydrite Member), and the Jurassic Cotton Valley Group (**Figure 2-2**). The pre-Mesozoic basement that provided the surface upon the Mesozoic and Cenozoic sedimentation was comprised of the Proterozoic and Paleozoic igneous, metamorphic and some sedimentary rocks of the Wiggins basement complexes (Mink et al., 1990). The Eagle Mills Formation, the

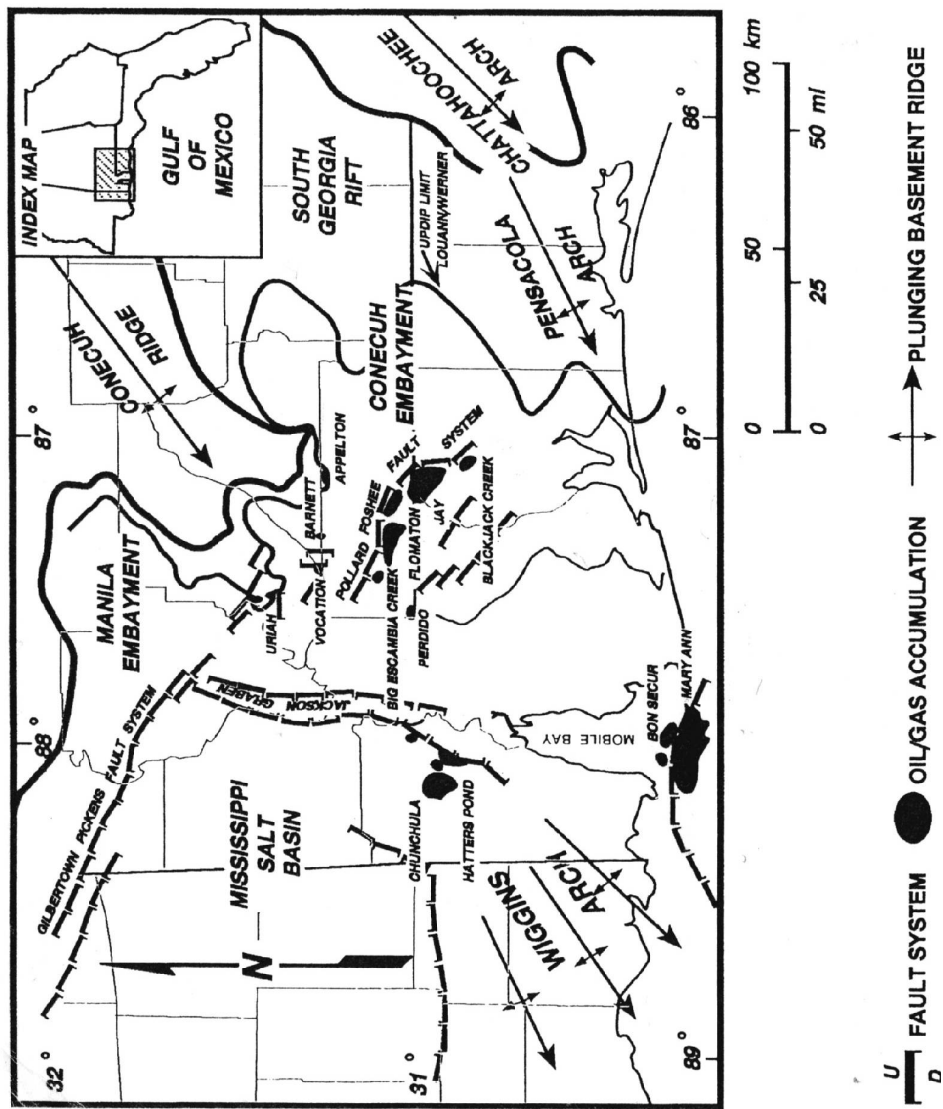


Figure 2-1. The regional tectonic features and basins of the southeastern Gulf Coast area (from Prather, 1992)

oldest Mesozoic non-marine strata present, is represented by a red bed siliciclastic sequence which was interpreted to be an eroded graben-fill sediment associated with diabase and basalt dikes and sills (Salvador, 1987). Disconformably overlying either the Eagle Mill Formation or the basement rock is the Werner Formation which consists of mainly anhydrite with some minor shale, sandstone, and conglomerate at its base. Tolson et al. (1983) interpreted the Werner sediment to be the result of the initial incursion of marine water into the nascent Gulf of Mexico basin. The major marine inundation occurred later and allowed the development of the Louann Salt on top of the Werner Formation, or the Eagle Mill Formation, or the basement rock. The Louann Salt thickness varies locally depending upon the related structures and topography but generally to consist of silty, sandy, massive halite and anhydrite (Tolson et al., 1983). According to Bishop (1973), the updip limit of thick Louann Salt might be coincidence with the peripheral fault complex along the Gulf margin. The Norphlet Formation overlying the Louann Salt, or the Werner Formation, or the Eagle Mill Formation or basement rocks is dominated by the siliciclastic alluvial, redbed wadi deposits, eolian dune and interdune subarkose sedimentation (Benson, 1988). In southwest Alabama, the thickness of the Norphlet Formation can vary greatly from less than 1 ft to over 800 ft (Mancini et al., 1985). The uppermost Norphlet sedimentation is found locally to consist of the massive and clean sandstone which has been interpreted to result from the marine reworking process during an initial marine transgression during the Oxfordian period.

The Smackover Formation, which overlies the Norphlet Formation, was named by Bingham (1937) for the carbonate strata of the Smackover field in south Arkansas. The Smackover carbonate sedimentation occurred extensively across the northern rim of the Gulf of Mexico basins continuing from south Texas through Florida. It represents the sedimentary record formed during the complete marine invasion throughout the northern Gulf Coast region (Moore, 1984, Salvador, 1987). According to Ahr (1973), the Smackover was deposited as a carbonate

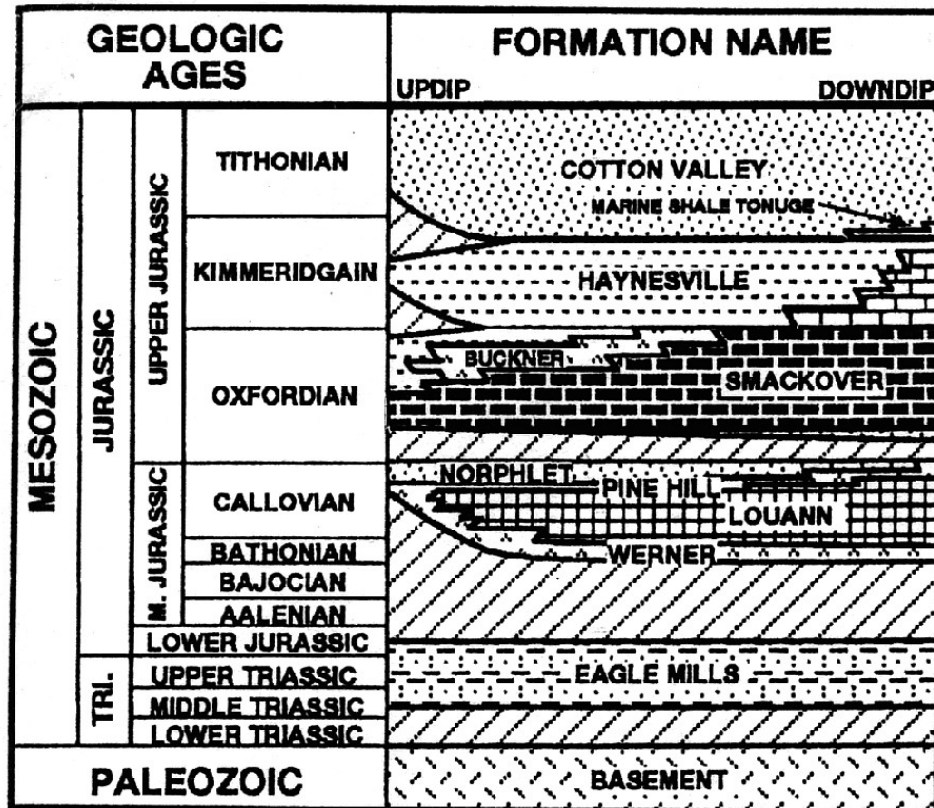
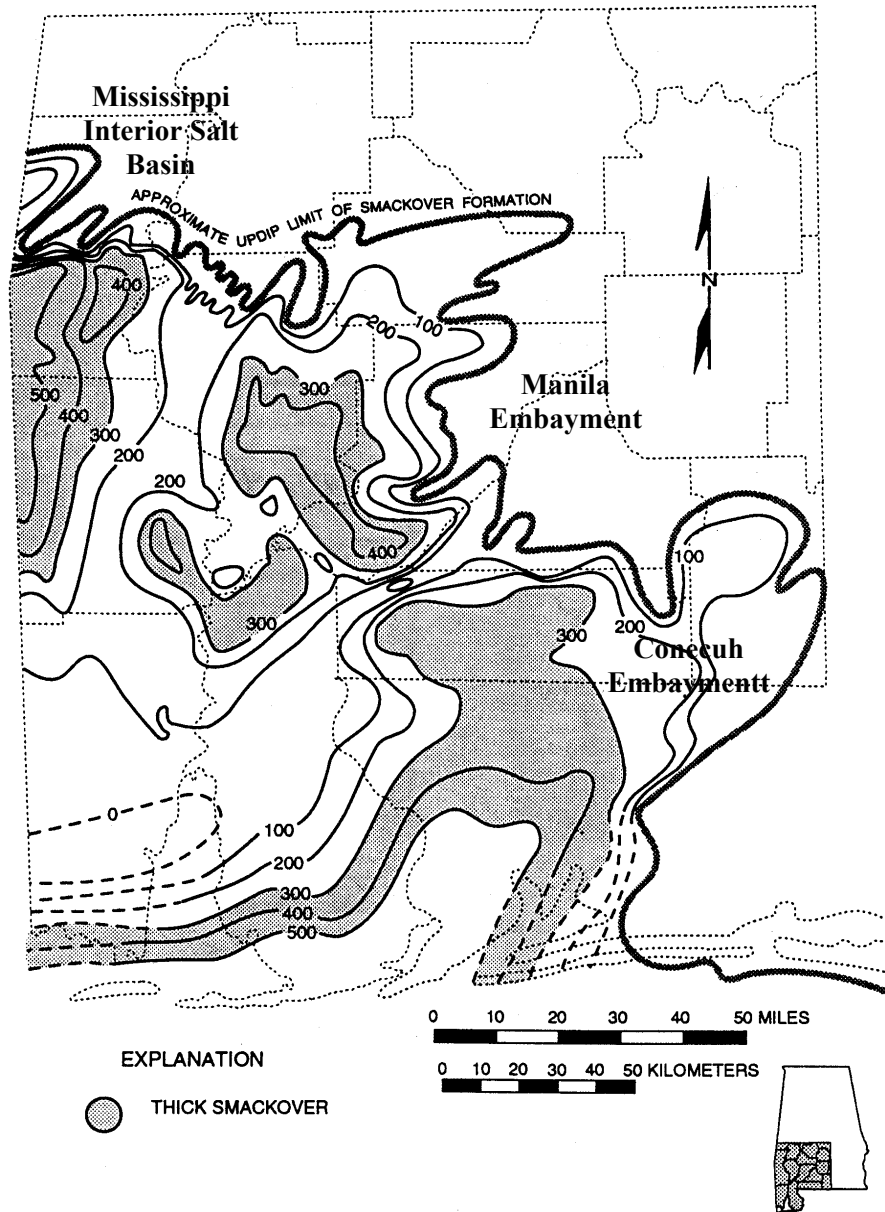


Figure 2-2. Generalized Mesozoic stratigraphy from the United States northeastern Gulf Coast (from Prather, 1992).

ramp platform along the gentle slope of the Gulf of Mexico passive margin. The variation of Smackover sediment thickness in different basins characterizes the influence and/or the modification from the pre-Jurassic paleostructure (Benson, 1988). The carbonate lithofacies, including those deposited in southwest Alabama, were interpreted to be primarily controlled by depositional environments which were altered, either alone, or in combination, by the inherited basement structures and the Louann salt movements. In southwest Alabama, the thickness of the Smackover locally exceeds 550 ft in the Mississippi Interior Salt Basin (Mancini et al., 1990) but are between 300 ft to 500 ft in both the Conecuh and the Manila Embayments (Wade and Moore, 1993). In the Manila Embayment, sediments are thicker near the flank where is the depocenter located and become thinner along the paleostructural highs (**Figure 2-3**). Tew et al. (1993) has suggested the Smackover deposition of southwest Alabama occurred in the inner ramp facies which were highly modified. The outer ramp sedimentary facies were interpreted for sediment deposited on the south of Pensacola-Decatur Ridge Complex which are in the offshore areas of southwest Alabama and the Florida Panhandle (**Figure 2-4**).

Conventionally, the Smackover is divided into three members, the lower, the middle and the upper Smackover (Benson, 1988; **Figure 2-5**). The lower Smackover, either gradationally or abruptly adjacent next to the siliciclastic Norphlet sandstone (Mancini et al., 1990), characterizes an intertidal to subtidal, microbial laminated mudstone and intraclastic, peloidal, oncoidal wackestone and packstone sediments which are partially dolomitized (Mancini and Benson, 1980; Benson, 1985; Claypool and Mancini, 1989). Some carbonate organic-rich laminated mudstone and/or organic-rich microbial layers alternately occur forming planar to wavy wackestone and packstone facies of this member contain tabular intraclasts of light gray to tan color microbial laminated mudstone. The peloidal, oncoidal packstone and wackestone facies can be bioturbated and abundant of allochems and skeletal materials. The middle Smackover were interpreted as subtidal laminated mudstone interbedded with peloidal, skeletal wackestone and packstone



**Figure 2-3.** Isopach map of the Smackover Formation of southwest Alabama, showing major depocenters and basinal areas (from Kopaska-Merkel and Mann, 1992).

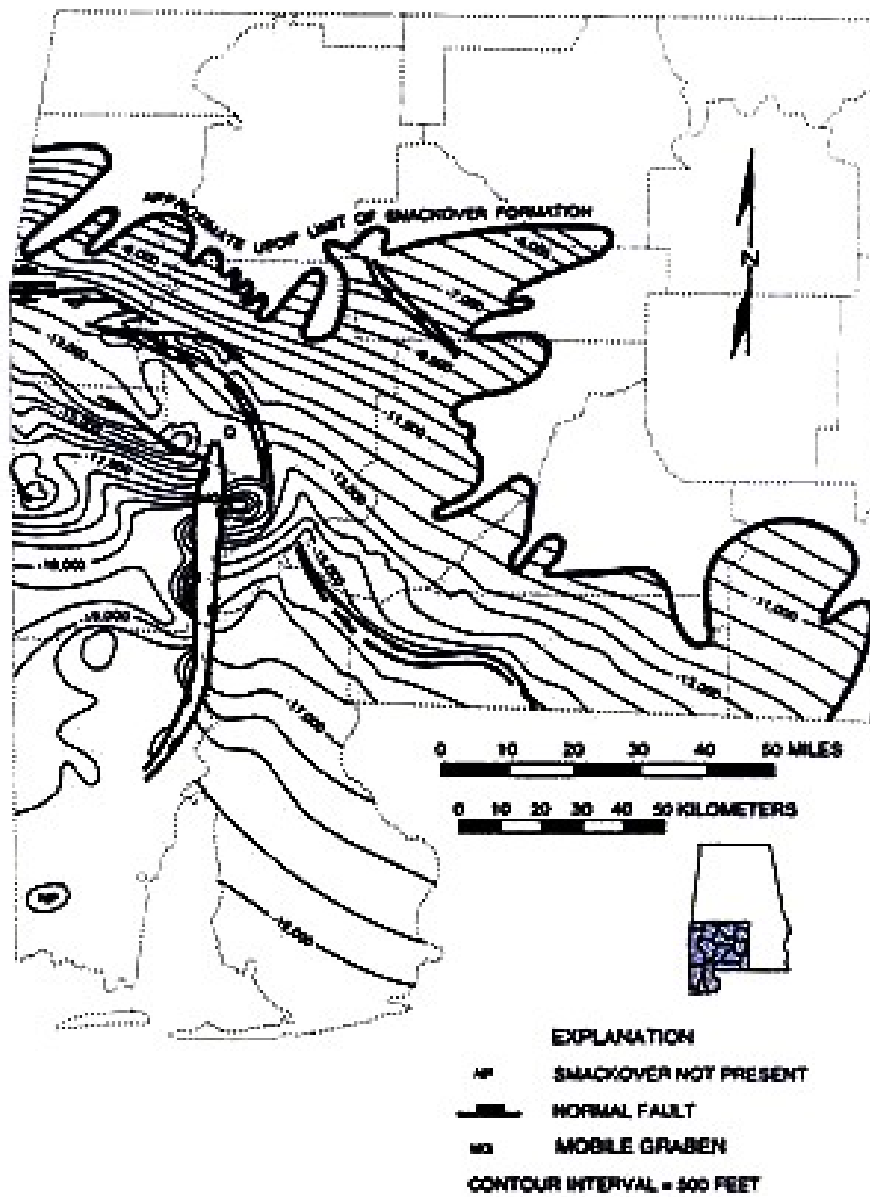


**Figure 2-4.** The regional structural map of the Smackover Formation top in southwest Alabama, showing slope gradient on the depositional carbonate platform (from Kopaska-Merkel and Mann, 1992).

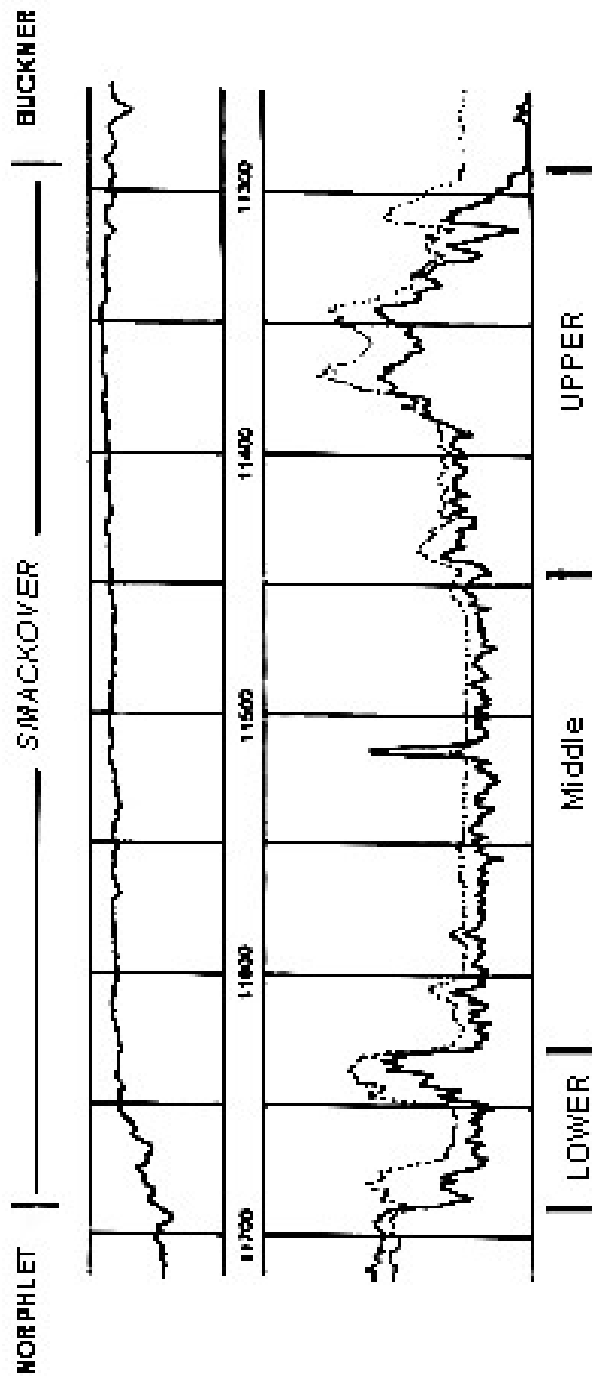


**Figure 2-5.** Typical log characteristic (gamma ray and neutron/density logs) of the lower, middle and upper member of the Smackover Formation in southwest Alabama described by Benson (1988).

(Mancini and Benson, 1980; Benson, 1985; Claypool and Mancini, 1989). The sediment color varies from light- to medium-brown showing signs of pervasive to absent bioturbation (Benson, 1988) and also argillaceous and locally silty. According to Benson (1988) and Sassen and Moore (1988), a nonfossiliferous laminated mudstone was observed and exhibits dark-gray to black with slight bioturbated sedimentary structure. Mancini and Benson (1980), Claypool and Mancini (1989), and Sassen (1989) interpreted the microbial and amorphous organic matter in this middle unit as the major source rock for Smackover hydrocarbons in the Gulf Coast basins. The upper Smackover, extensively dolomitized throughout southwest Alabama, primarily consists of oolitic, oncolitic, peloidal grainstone, packstone, interbedded supratidal laminated mudstone and some anhydritic dolostone in the uppermost part of the unit (Mancini and Benson, 1980; Benson, 1985; 1988; Claypool and Mancini, 1989; Sassen, 1989). On the paleohigh structures such as the areas around the Wiggins Arch complex and across the Conecuh Ridge complex, microbial boundstones can be abundant (Baria et al., 1982; Benson, 1988). Depositional environments of the upper Smackover are interpreted to vary from subtidal to supratidal characterizing the multiple shallowing-upward cycles (Benson, 1988; Mancini et al., 1990; Mann and Kopaska-Merkel, 1992). The nodular to massive anhydrite observed in the uppermost part was conformably beneath the Buckner Anhydrite (Benson, 1988; Mann and Kopaska-Merkel, 1992). Several investigations, e.g. Barrett (1987), Benson (1988), Mancini et al. (1990) reported the presence of subaerial exposure features such as mudcracks, fenestra and dissolution fabrics, vadose pisoids and gravitational cements.

Conformably overlying the upper Smackover is the Buckner Anhydrite and the Haynesville Formation (Tolson 1983). Salvador (1987) interpreted this sedimentary unit to be Kimmeridgian in age. The Buckner Anhydrite at the base of the Haynesville Formation consists of massive anhydrite, intercalated with dolomite, shale or anhydritic shale and anhydritic sandstone. On the onshore location, where the Buckner Anhydrite is absent, the basal part of the

Haynesville is dominated by the anhydritic shale and sandstone and/or thin anhydrite beds and salt stringers (Tolson et al., 1983). The upper part of the Haynesville Formation includes interbedded fine and coarse siliciclastic rocks associated with anhydrite imbedded or containing clastic materials. On the flank of Wiggin Arch complex, in the Mississippi Interior Salt Basin and in the Conecuh Embayment, thin beds of carbonate deposition are associated with the Haynesville sedimentation (Tolson et al., 1983)

### **2.3 SMACKOVER STRATIGRAPHIC SEQUENCE**

Along the Gulf Coast basins, the eustatic sea level cycles were interpreted to affect the distinctive changes in coastal onlap and sequence stratigraphic records throughout the Phanerozoic time including the post-Triassic period (Todd and Mitchum, 1977; Vail et al., 1984; Haq et al., 1988). The Jurassic strata from the Lower to the Upper in this region were characterized by Todd and Mitchum (1977) as four sequences. The Upper Jurassic sequence included the Werner, Louann Salt, Norphlet, Smackover and Haynesville Formations were grouped into three unconformity-bound depositional sequences, which was later proposed by Vail et al. (1984) to be controlled by the third eustatic sea level cycles designated as the J2.4, (from 155-151ma), the J3.1 (from 151-144ma), and the J3.2 (from 144-141.5ma). Later, with additional global data and greater resolution, Haq et al. (1988) modified the Vail et al. (1984) global sea level cycles and updated the Upper Jurassic sediments into six depositional sequences and the long J3.1 cycles were divided into small four third-order sea level cycles of shorter time periods. Based upon Haq's global eustatic cycles, the Upper Jurassic strata thus consist of six depositional sequences. These sequences were redesignated as the Lower Zuni A or the LZA-3.2 (155.5-150.5ma), the LZA-4.1 (150.5-149.5ma), the LZA-4.2 (149.5-148.5ma), LZA-4.3 (148.5-146.5), the LZA-4.4 (146.5-144) and the LZA-4.5 (144-142ma). The Smackover Formation which is

Oxfordian in age and was equivalent to the long-term third-order J.1 sequence under the Vail et al. (1984) model would possible consist of four depositional sequences controlled by third-order relative sea level changes . However, in southwest Alabama, the shorter third-order cycles during Smackover deposition were not recognizable. Therefore, most sequence stratigraphic interpretations of Smackover deposition in southwest Alabama have proposed that the Smackover deposition was controlled by a single long term third-order relative sea level cycle equivalent to the J3.1 cycle (e.g. Esposito and King, 1987; Mancini et al., 1990; King and Moore, 1992; Prather, 1992).

The early regional stratigraphy of the Smackover along the Gulf rim has also been proposed by Budd and Loucks (1981) from south Texas into three Smackover members of progradational sedimentation which characterized the stacking of regressive cycles. Later, Moore (1984) added that relative sea level changes should have increased at different rates because of the varying sedimentary thickness of each interval. He suggested that rapid sea level rise must have occurred during earliest Smackover deposit and the evidence was the presence of deep and anoxic pelagic laminated carbonated mudstone. This initial rapid sea transgression likely bypassed some sediment into basinal area and formed a non-deposition on the upslope due to the very quick migration of high-energy up-ramp sedimentary facies. In the next stage, sea level rise slowed and after the normal oxic environment had terminated, moderate biological activities for carbonate sedimentation became dominant. Later, when relative sea level reached a standstill, the development of a high energy shoal deposit took place at the sediment- water interface under the high-energy wave base condition. According to Moore (1984), the upper Smackover sediment, although not entirely progradational, was accommodated during a period of time when subsidence and sedimentation rate were in equilibrium which was supported by the coarsening-upward stacking packages. In southwest Alabama, Mancini et al. (1990) also proposed a stratigraphic framework of the Smackover sequence to be controlled by eustatic sea

level cycles into three sequences called as the Lower Zuni A Gulf Coast (LZAGC). Based upon their report, the Upper Jurassic strata model consists of three unconformity-bounded depositional sequences controlled by third-order eustatic sea level cycles and were called the LZAGC-3.1, the LZAGC-4.1 and the LZAGC-4.2. The Smackover Formation and the upper Norphlet sedimentation were interpreted to have been deposited during the LZAGC-4.1 sequence which is equivalent to the J3.1 under the Vail et al. (1984) model (**Figure 2-6**). Under the Mancini et al. (1990) model, the long-term Smackover sequence was controlled by a single third-order eustatic sea level cycle and comprised the transgressive and the highstand system tracts. The boundary between the transgressive and the highstand system tract was the condensed section or the maximum flooding surface which represented the middle Smackover and a high organic accumulation interval (**Figure 2-7**). This Smackover stratigraphic model which has been accepted in the southwest Alabama basins was also proposed by Mancini et al. (1993) for the Smackover sequence for the entire Gulf Coast area.

## **2.4 A DEPOSITIONAL SEQUENCE**

In order to learn more about the stratigraphic sequences of Smackover Formation, at first, it is helpful to introduce the general concept of a depositional sequence and a eustatic sea level cycle. A depositional sequence is interpreted as rock sequence deposited during a cycle of relative sea level changes from a starting to an ending inflection point on the sea level curve. It is usually defined as a succession of genetically related strata, bound at the top and bottom by unconformable or conformable surfaces termed a sequence boundary (van Wagoner et al., 1988 and 1990). There can be two different types of sequence boundaries within a depositional sequence called as type 1 and type 2. A type 1 sequence boundary is formed when the rate of eustatic fall exceeds the rate of basin subsidence at the bank or platform margin. It is usually characterized by subaerial exposure and erosion of the platform, concurrent submarine erosion on

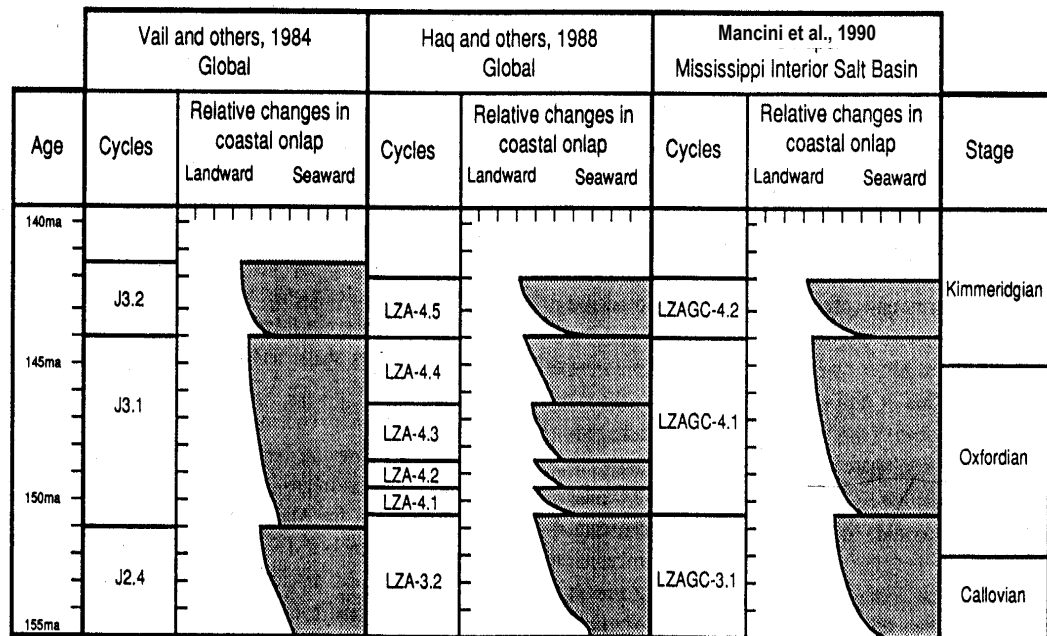


**Figure 2-6.** A comparison of sequence stratigraphic frameworks of the Upper Jurassic strata of the Gulf of Mexico basins which includes the Smackover Formation proposed by Vail et al.(1984), Haq et al.(1988) and Mancini et al.(1990) (from Mancini et al.,1990).

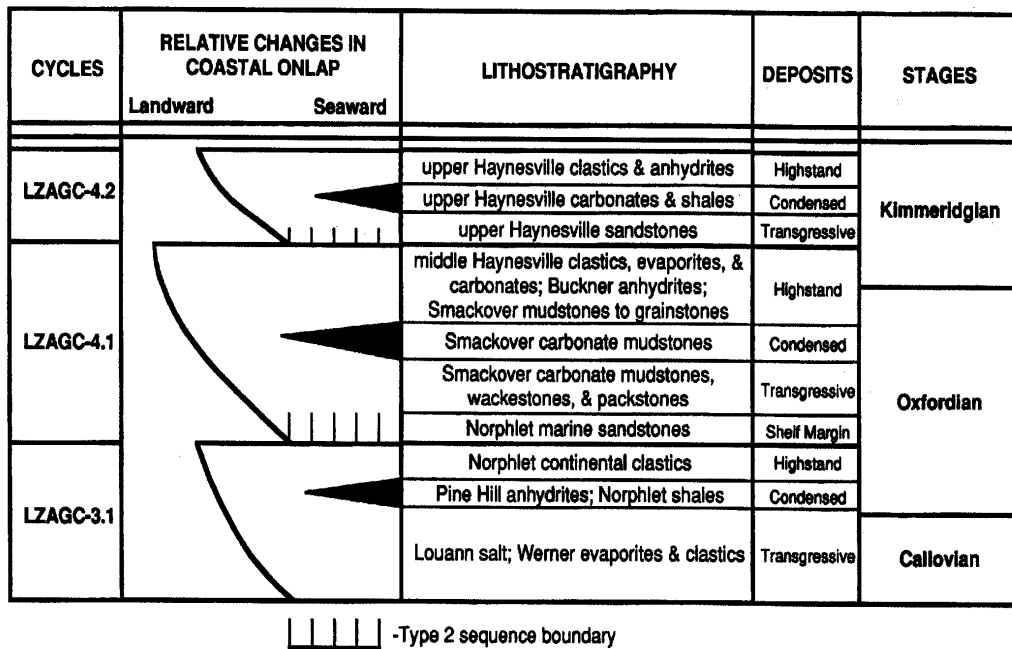


**Figure 2-7.** Depositional system tracts and lithological records of the Upper Jurassic sequences characterized by Mancini et al. (1990).

the foreslope and a downward shift of the coastal onlap. Unlike type 1, the type 2 sequence boundary is formed when the rate of eustatic fall is less than or equal to the rate of basin subsidence. It is commonly marked by subaerial exposure of the inner platform peritidal and shoal areas. There are five orders of relative sea level changes that could occur depending upon time intervals and the processes which control them (**Figure 2-8**). Two major controls upon sea level changes (i.e. recorded changes in vertical accommodation space which are termed “relative” when used within an intrabasinal perspective, but with the term “global” when used within a correlative interbasinal or global perspective), the tectonic activities and climate, can be very sensitive to the third-order eustatic sea level changes and sediment supply by different processes and different magnitudes (**Figure 2-9**). While the orders might not be rigidly defined owing to the wide range of conditions, the basic building block for the depositional system in a sequence which may be recognized especially in the high frequency sequence (the 4<sup>th</sup> and the 5<sup>th</sup> order) are defined as a parasequence. A stacking of parasequences is called a parasequence set which is equivalent to a depositional system which is the building block system for a sequence and is called a system tract (van Wagoner et al., 1988). A system tract is a linkage of contemporaneous depositional systems or a parasequence set which is defined by the types of bounding surfaces, stratal geometry, and position or time interval during the relative changes in sea level cycle. There are four types of system tracts that occur in a sequence and these are the lowstand system tract (LST), the transgressive system tract (TST), the highstand system tract (HST) and/or the shelf margin wedge system tracts (SMW). In a sequence, a lowstand system tract deposits basinward above the preceding platform/bank margin. It is separated from a preceding highstand system tract or a shelf margin wedge of the earlier sequence the type 1 or type 2 sequence boundary. The transgressive system tract represents a rising of relative sea level and is separated from the lowstand system tract by the first transgressive surface or what is known as the first flooding surface. The transgressive system tract consists set of sedimentations occurring during the rise of relative sea level (i.e. backstepping or retrogradational units) which is usually thicker

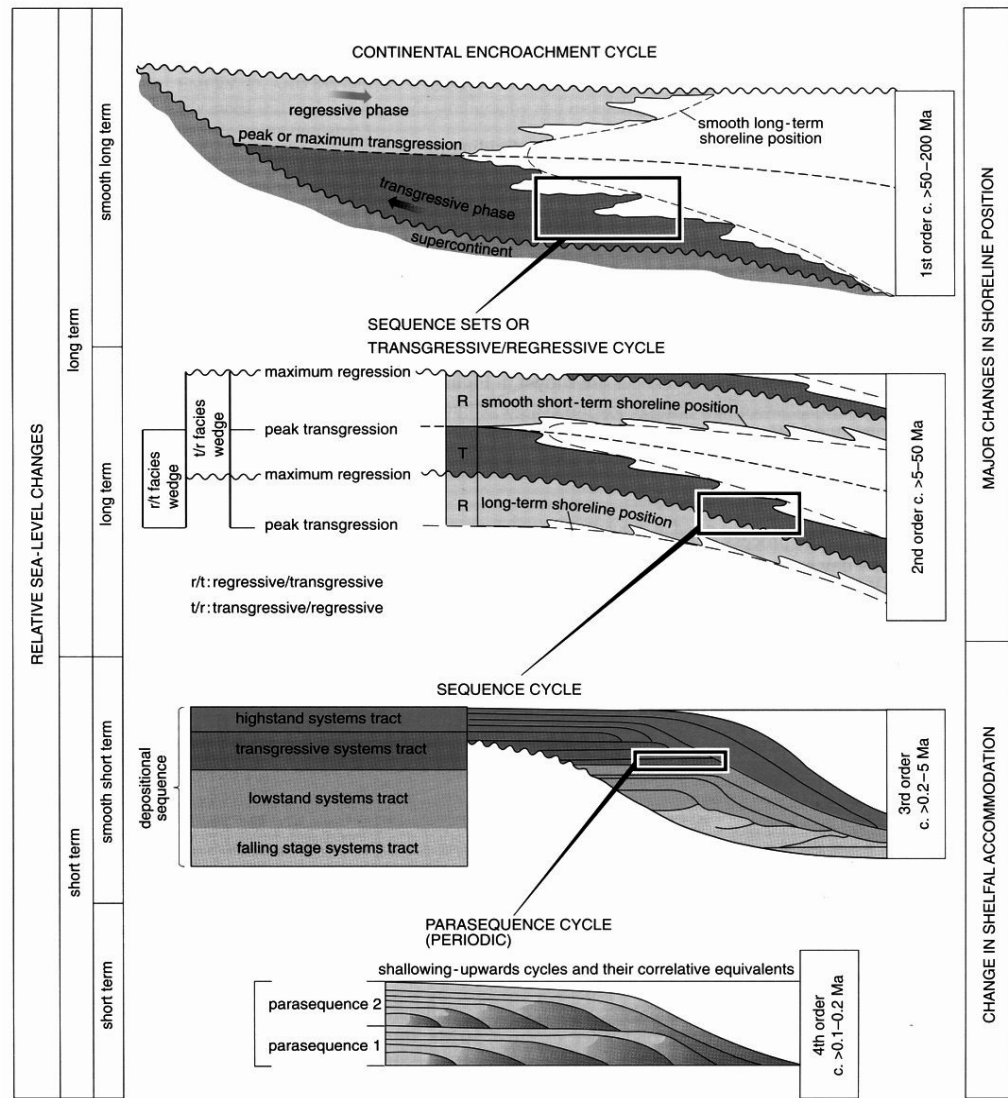


**Figure 2-8.** The hierarchy and different time-scale of the stratigraphic depositional sequences related to eustatic sea level cycles, showing with different key features (from Duval, 1992).

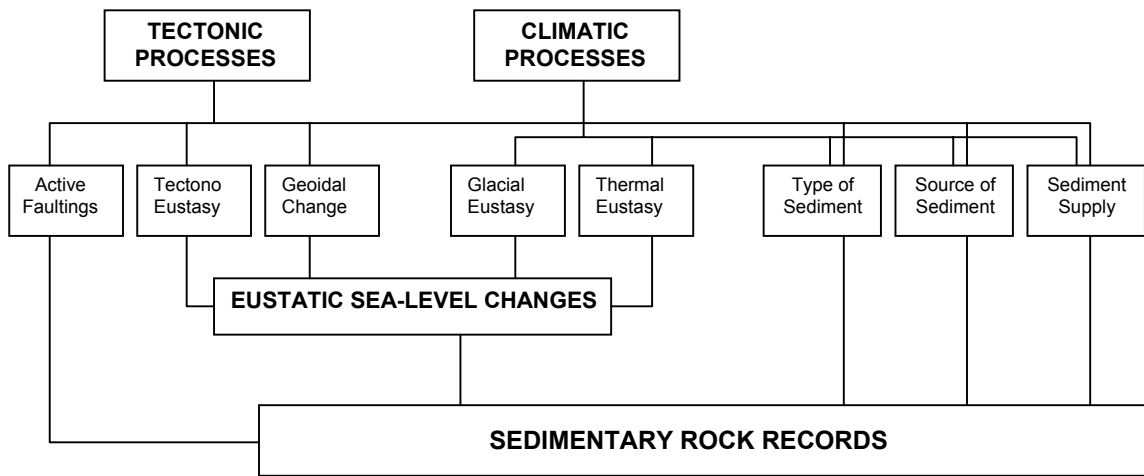


**Figure 2-9.** The influence of tectonic and climatic processes on the relative sea level changes and sediment supply (from Church and Coe, 2003).

shelfwardly and thin basinwardly. The highstand system tract is separated from the transgressive system tract by the maximum flooding surface or a condensed section zone. The condensed section typically characterized period of high organic accumulation and low sediment from the shelf. A very slow sedimentation rate in the deep basin affects the formation of the deep marine hemipelagic or pelagic deposition (Loutit et al., 1988). The shelf margin wedge system tract is formed above the highstand system tract if sea level fall is not beyond the major slope break point. The formation of the sequence boundary either type 1 or type 2 is dependent upon the rate of eustatic fall and the rate of sediment subsidence (e.g. van Wagoner et al., 1988).

## **2.5 CARBONATE RAMP STRATIGRAPHIC SEQUENCE**

A carbonate ramp depositional setting was first introduced by Ahr (1973) using the Upper Jurassic Smackover carbonate platform of the Gulf of Mexico as an example. In this concept, a carbonate ramp is simply a carbonate platform with a low gradient slope ( $<1^\circ$ ) from shoreline to basin. There are two ramp platform categories depending upon the slope gradient from the shoreline to the deeper basin which are a homoclinal ramp and a distal steepened ramp (Read, 1982 and 1985). Burchette and Wright (1992) reported carbonate ramps are formed in all types of sedimentary basins, but are best developed where subsidence is flexural and local gradients are slight over large stable areas. Due to a low platform gradient, a major slope break is not commonly recognizable in the shallow water depth environments. Sedimentary facies on the ramp platform simply vary gently downdip from proximal shallow-, high-energy water facies to a distal-, low-energy facies. Depositional boundaries are controlled by two critical interfaces which are the products of the wave energy conditions (Markello and Read, 1981; Aigner, 1984; Calvert and Tucker, 1988; Burchette and Wright, 1992) known as the fair weather wave base (FWWB) and the storm wave base (SWB). From these boundaries the carbonate ramp depositional profile is subdivided into the inner ramp, mid-ramp, outer-ramp and basinal settings. The water-depth

conditions of these settings are related to the distance between these two interfaces and the slope gradient of the platform (**Figure 2-10**). Sedimentary facies in the depositional zone are variable depending upon controlling factors related to carbonate sediment factory and water energy along the platform slope. Burchette and Wright (1992) also indicated that tectonic activity proximal to where carbonate ramp platforms develop can be very important as it can amplify or diminish environmental conditions that are favorable to carbonate production and deposition (e.g. high rate of clastic input, hypersalinity, or cool climate).

The depositional sequence of carbonate platforms consists of variable carbonates depositing during different system tracts which are controlled by changes in relative sea level or between the accommodation space and the sedimentation rate. For a carbonate ramp system, the simple platform geometry creates a simple and relatively straightforward concept when compared to the siliciclastic and the shelfal or rimmed type carbonate platform (Burchette and Wright, 1992; Tucker et al., 1993; **Figure 2-11**). Because of the gentle and slight gradient on a platform slope with no major break, sedimentary facies which are usually formed parallel to the platform strike (Imlay, 1973) can be sensitive primarily to even a small change of relative sea level. During a major sea level change, sedimentary facies along the stable platform will, in principle, be correlative for a wide horizontal scale. Tucker et al. (1993) suggested depositional conditions of simple carbonate ramp platforms can be used to diagnose sea level changes due to the control of the facies belts which move up and down along the low slope gradient. The internal sequence architecture and sequence stacking patterns usually reflect a frequent change of small cyclic scale due to base-level excursion that responds to the change of slope accommodation space (Burchette and Wright, 1992). The sequence boundary on the carbonate ramp system is different from that which occurs in other carbonate systems and is affected by its small slope gradient. The sequence boundary on a ramp system can be associated with fluvial incision and/or siliciclastic influx rather than expressed by typical exposure surfaces and/or karstification which observed on a rimmed or shelf system (Tucker et al., 1993). The other transitional surfaces occurred between

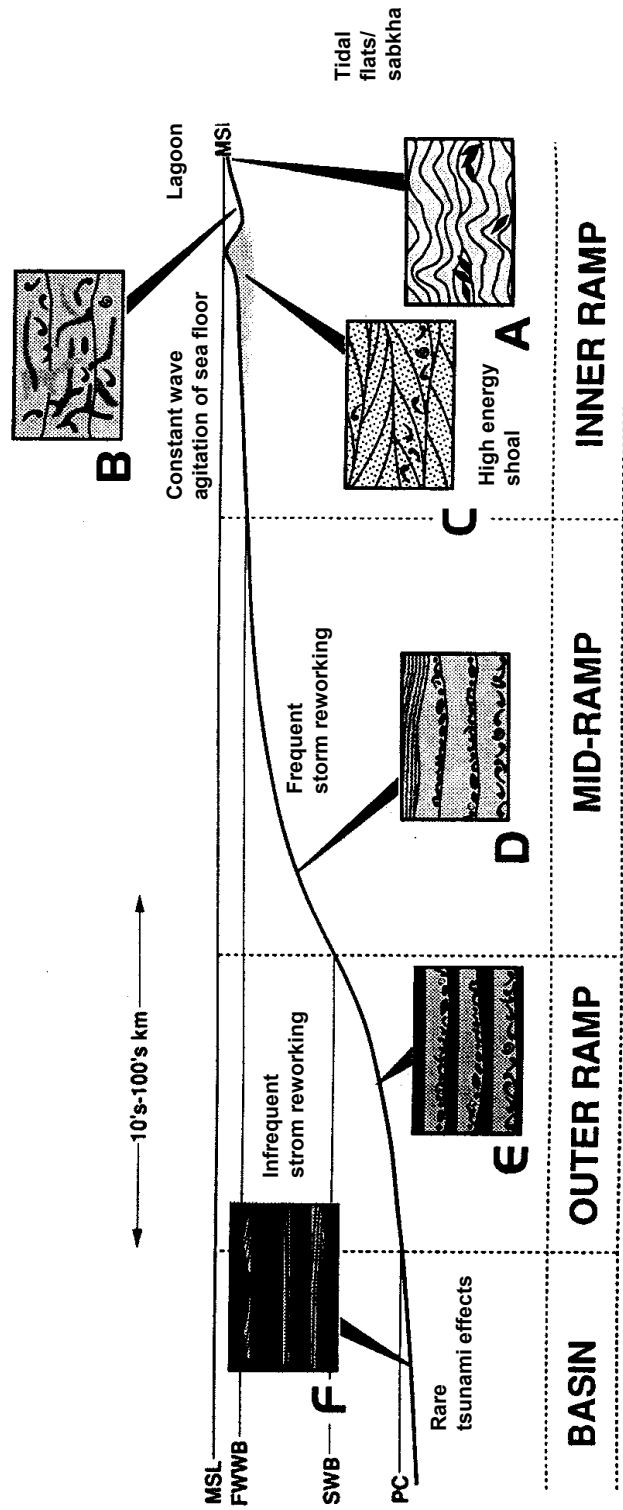


**Figure 2-10.** Homoclinal carbonate ramp showing main sedimentary facies. Inner ramp: (A) peritidal and sabkha facies with stromatolitic algae and evaporites; (B) bioturbated and variably bedded lagoonal lime mudstone, packstone, and wackestone; (C) shoreface or shoal cross-laminated oolitic or bioclastic grainstones and packstones. Midramp: (D) amalgamated coarse, graded tempestites, commonly with hummocky cross-stratification. Outer ramp: (E) fine-grained, rippled tempestites interbedded with bioturbated or laminated lime or terrigenous mudstone; (F) laminated or sparsely rippled silt-grade carbonate sediment or quartz silt in a predominantly terrigenous mudstone succession. All these boundaries are gradational (from Burchette and Wright, 1992).

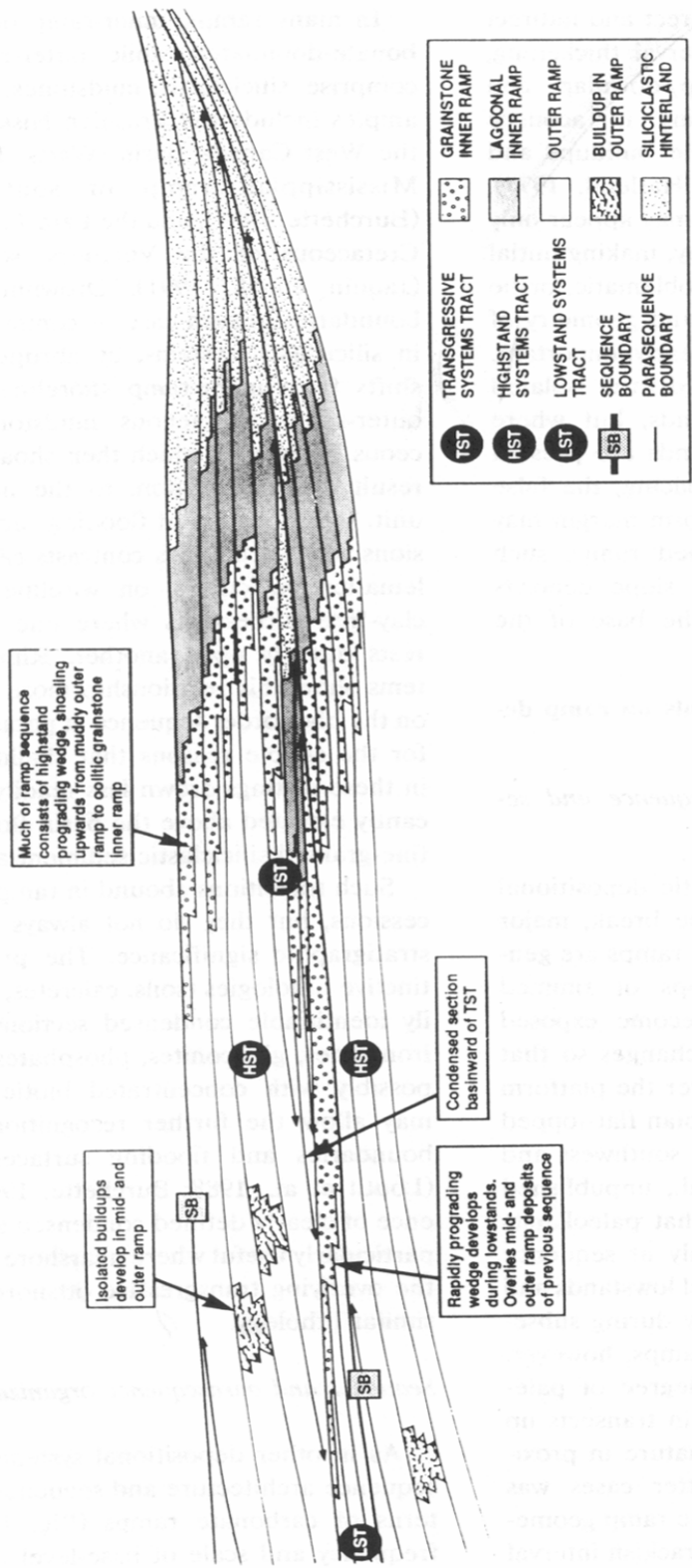


**Figure 2-11.** Sequence stratigraphic components of a homoclinal carbonate ramp of a grainstone-dominated system with outer-ramp buildups and a well-developed lowstand system tract. It is noted that the lowstand inner-ramp grainstones rest abruptly upon outer-ramp mudstones (although erosion may be slight), and well-developed backstepping shorelines in the transgressive system tract. These may comprise barrier or beach grainstones on a high-energy ramp or be packstone-dominated on a low-energy ramp. The location of the outer ramp and mid-ramp buildups may be influenced by the slope-crest morphology of the underlying sequence or by extrinsic factors such as halokinesis or tectonism. In the mid-ramp zone, the vertical succession generated by ramp progradation

different system tracts are the maximum flooding surface and the first transgressive surface.

Because carbonate production is highly sensitive to sea level changes, for most carbonate sequences, the TST and HST are more important depositional systems than the LST. During the lowstand sea level, carbonate production can be highly affected by siliciclastic sediment dilution showing low carbonate sedimentation. In the TST which deposited during a following sea transgression, variable sediment geometries (i.e. retrogradation, aggradation or progradation) can be produced depending upon the rates of relative sea level changes which are controlled by the accommodation space and carbonate sedimentation rate. For the HST, the high and stable sea level promotes thicker carbonate sedimentation of aggradation and progradation. Because of a very small slope platform angle, Burchette and Wright (1992) suggested that a dramatic change in sediment characteristics between the ramp HST and LST might not be recognizable and a distinct transitional surface for the change on vertical lithofacies may not be observed. Unless the sea level fall is substantial, a distinctive marked exposure surface on the inner ramp facies and a downward shift of a shallower sedimentary facies can represent the carbonate ramp sequence boundary. During the LST, an evaporite deposition, a meteoric diagenesis, and/or high amount of siliciclastic influx can be very common due to a basinal restriction, a mixing zone between meteoric-marine water and/or an increase of the continental river discharge that approaches the ocean (**Figure 2-12**). Because of the lower solubility of evaporites in seawater, some LST evaporites may have a greater chance of being preserved when buried by an ensuing rapidly advancing TST. For a ramp HST evaporite, with the ensuing LST, it will eventually be exposed to meteoric waters and thus can be subjected to stronger early meteoric diagenesis. Burchette and Wright (1992) reported that preserved evaporites, especially if subaqueous, may be a potential indicator of a ramp LST, while increased carbonate production rate is correlated with the TST and definitely with the HST. Thus for a ramp there are lithofacies occurrences which can potentially be diagnostic indicators of sea level excursions.

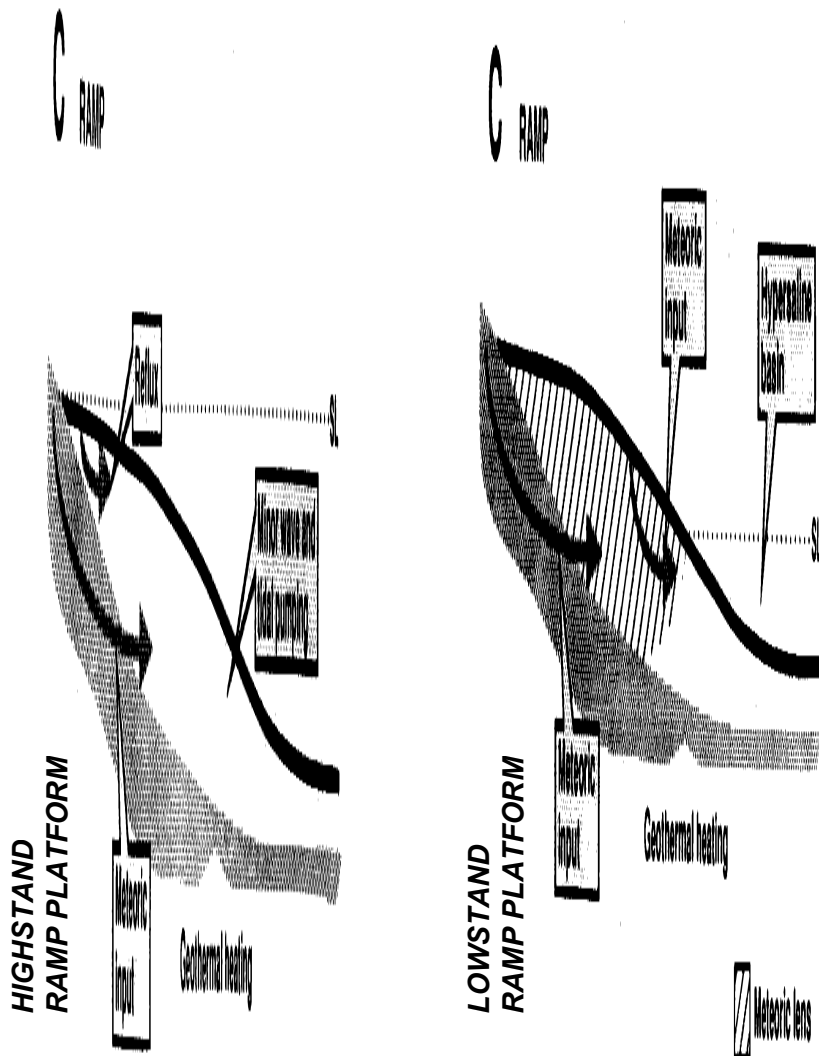


**Figure 2-12.** The influences of pore water circulation systems for ramp platform during relative sea level highstand and lowstand. In general, the ramp platform is suggested to have less influence from the marine pore water circulation if compared to the other types of platform (i.e. isolated buildup, rimmed shelf), but is highly susceptible to more meteoric influence from the attached land masses. Therefore, early marine cementation and sea-water dolomitization are less prominent even during relative sea-level highstand. During sea-level lowstand, the distribution of meteoric lenses and the development of buoyant circulation systems promote seawater mixing environment where the meteoric water circulation, driven by hydrostatic head, can extend downwind beyond the shoreline and can even discharge at the sea floor (from Burchette and Wright, 1992).

## CHAPTER 3

### 3.1 CORE ANALYSIS AND SAMPLES

The core samples that were used for investigating the Smackover depositional framework were collected from single wells in the Conecuh Embayment and in the Manila Embayment (**Figure 3-1**). These two cores have been used elsewhere as a reference well for framework of the Smackover deposition in the two basins. From the Conecuh Embayment, the Smackover core for study is from the T.R. MILLER MILLS 17-11, #1 well (17-2N-11E, Escambia County, permit 2465) which was earlier described by Esposito and King (1987) and Prather (1992; **Figure 3-2**). From the Manila Embayment, the Smackover core is from the #1 NEAL ET AL UNIT 30-1 well (30-7N-4E, Clark County, permit 3648) which has been investigated by Manicini et al. (1990) and Wade and Moore (1993; **Figure 3-3**). The vertical distribution of organic content has been characterized on the depositional system tract for the Smackover sequence. By correlating these two cores on a sequence framework, both lateral and vertical variations can also be examined. Both cores contain almost the complete Smackover carbonate interval and include the Norphlet Formation and the Buckner Anhydrite at the bottom and the top, respectively. Therefore these cores are ideal for providing data to compare the Smackover between the two study areas.

Cores were drilled and collected by different oil companies and were stored in part as the permanent core collection of the Alabama Geological Survey in Tuscaloosa, Alabama. Core description and photos were undertaken at the core facility unit and then small pieces of core samples were taken back to the University of Oklahoma for petrographic and geochemical analyses. Core derived from the T.R. MILLER MILLS 17-11, #1 well are from depths labeled as 13504 ft to 13863 ft and contain the total thickness of Smackover carbonate sediment of about 1335.8 ft. The other core from the #1 NEAL ET AL UNIT 30-1 well is from depths labeled as 13093 to 13596.3 ft and the total thickness of the Smackover carbonate was about 442.8 ft.

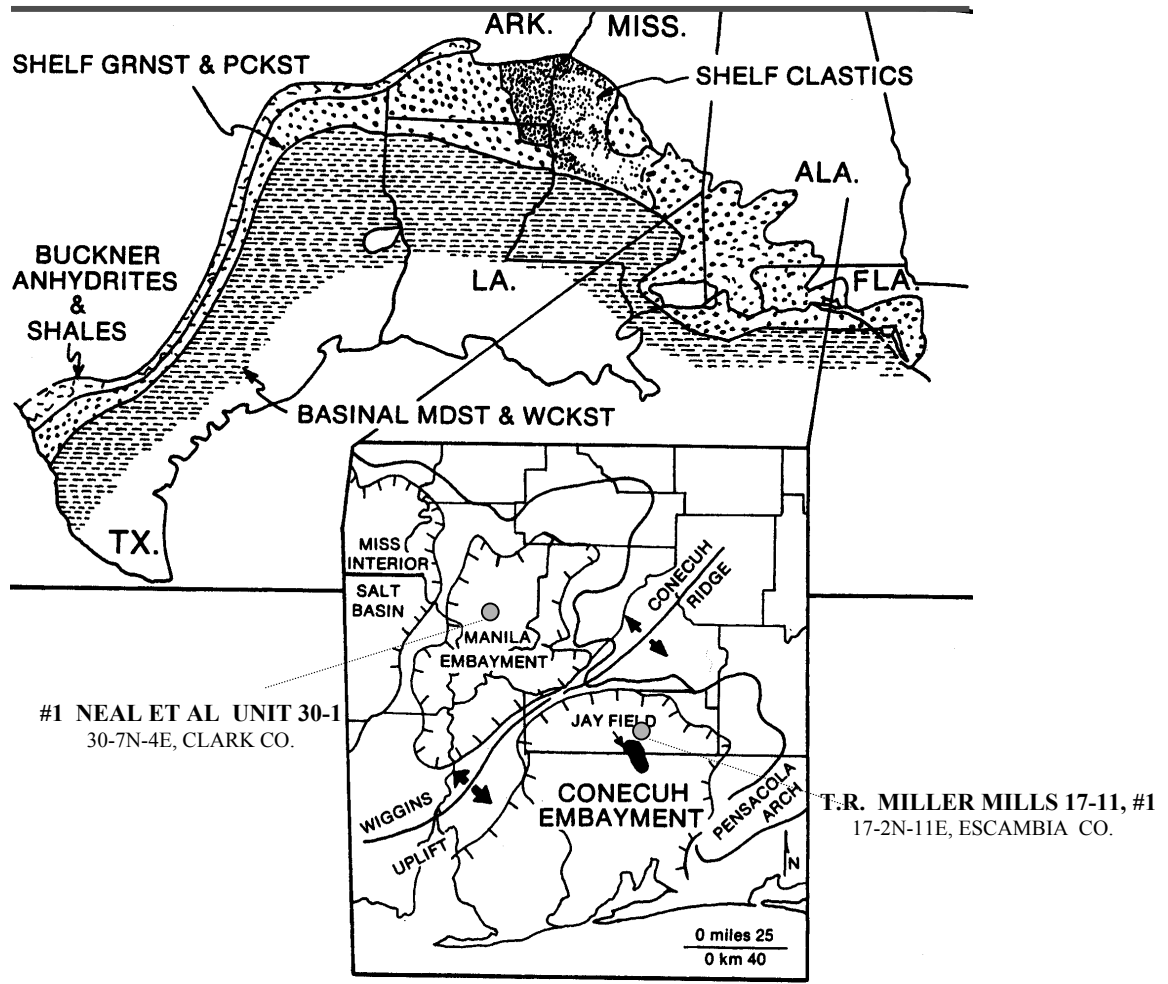


**Figure 3-1** Locations of two Smackover cores examined in this study.

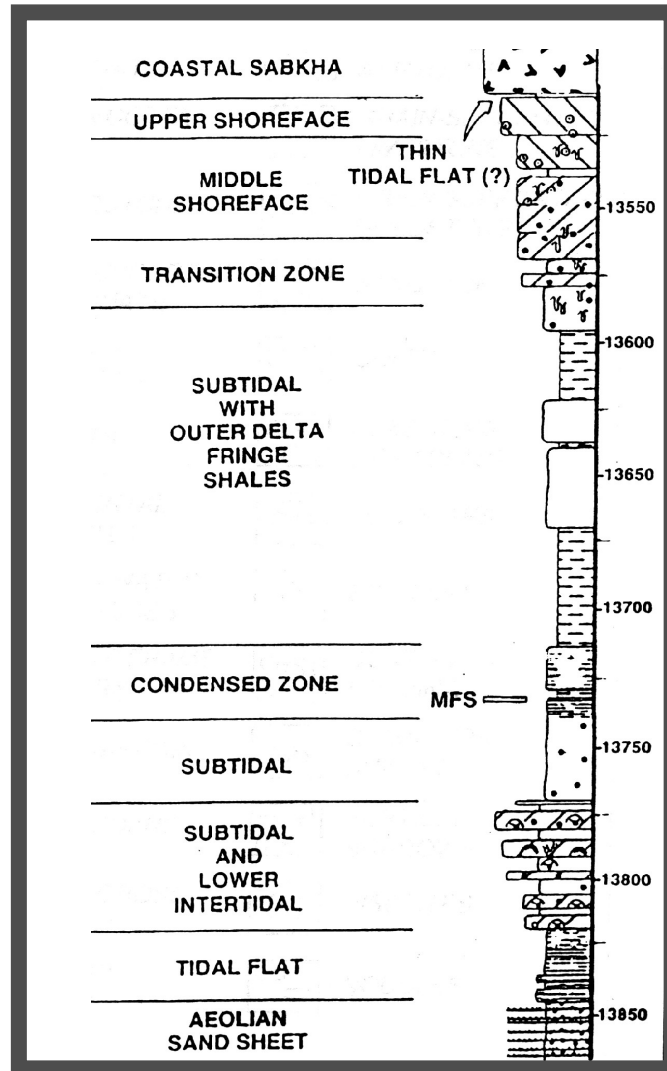


**Figure 3-2.** A sequence depositional framework of the Smackover Formation from southwest Alabama based on the Smackover core of the T.R. MILLER MILLS17-11, #1 well similar to the core used in this study (Prather, 1992).

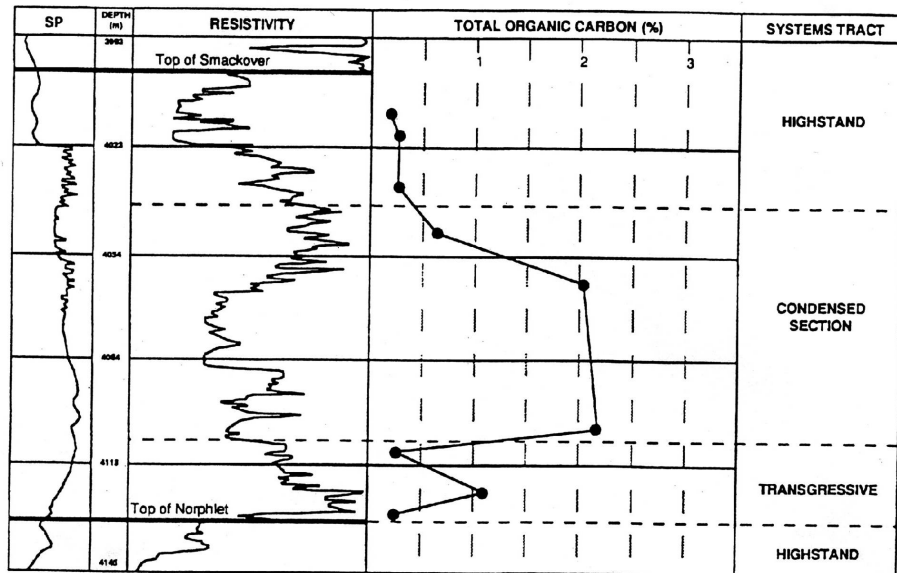


**Figure 3-3.** The Smackover depositional system tracts during relative sea level changes interpreted by Mancini et al. (1993) from the #1 NEAL ET AL UNIT 30-1 well in the Manila Embayment. Well log characteristics and the TOC were suggested to correspond to changes of the third-order relative sea level.

Photomicrographs of thin sections from samples of both cores were taken to compare lithofacies and paleoenvironment and paleowater-depth interpretations.

### **3.2 METHODS AND INSTRUMENTS**

For chemical, isotopic, and organic geochemical analysis, whole rock samples from different Smackover lithofacies and variable core depth were selected randomly. Seventy-five samples were taken from the T.R. MILLER MILLS 17-11, #1 well and eighty-three samples were from the #1 NEAL ET AL UNIT 30-1 well. A few samples were also derived from the Norphlet sandstone and the Buckner Anhydrite. Small pieces of individual samples, after cleaning with water and methanol were dried and subsequently crushed into powder (grain size 200 mesh) using a shatter box (SPEX Industries, 2-3 min, at ca. 900 rpm). Between each crushing process, the shatter box was thoroughly cleaned by detergent, rinsed with water and distilled water, and dried by methanol or acetone in order to prevent cross-mixing and contamination.

Prior to the subsequent analyses, each crushed rock sample was also analyzed for carbonate (and dolomite) minerals using acid dissolution technique (HCl). Approximately 2 gm of sample (duplicated) was weighed and placed into individual porous crucibles which were in a glass tray in order to allow acid dissolution reaction to proceed. Ten percent hydrochloric acid (10% HCl) was used to fill each crucible. Each crucible frequently refilled for period of at least 72 hours or longer until no more CO<sub>2</sub> from carbonate or dolomite dissolution was observed. The samples were removed from the tray and the insoluble residue, or a non-carbonate fraction, left in the crucible was washed and rinsed by distilled water several times using a vacuum suction until acid was completely removed (checked by a listmus paper for neutral). The samples were subsequently dried in the oven and weighed after cooling to room temperature. The insoluble residue (if any) was weighed. The exact weight loss of each sample caused by acid dissolution is assumed as the carbonate and/or dolomite fractions. Finally, the percentages of dissolved

carbonate minerals and the non-carbonate fraction were calculated and averaged between the two analyses using precision no greater than +/- 0.5 %. These insoluble residues were later used for total organic carbon and organic carbon isotope analysis.

### **3.2.1 ELEMENTAL ANALYSIS**

All of the whole crushed rock samples were analyzed for carbonate and siliciclastic minerals and related elements using X-ray Fluorescence Spectrometry. Before analysis, whole rock powder samples were prepared into pressed borate powder pellets of approximate 0.5 cm thick. The measurement was later performed at the Laboratory of the Geological Department at the Northern Illinois University, Illinois through the operation and assistance of Dr. Neil Dickey. The spectrometer X-ray fluorescence instrument was a Siemen (Bruker) SRS300 with a Rhodium end-window tube detector. The intensity of a characteristic line of a specific element of interest in each samples was measured after samples were loaded into the instrument. The intensity value was corrected by subtracting the peak intensity from that of the background measurement taken nearby but away from the influence of the peak. Each element intensity was then calibrated with the standard curve created from several known standards and converted into percent (for the major elements) and parts per million (ppm). For the major elements (Al, Si, Ca, Mg, Mn, Ti, P, Na and K), the percentages of each elements were first derived as the oxide mineral contents using a program developed by Dr. Barry Weaver (personal comm., 2004). However, the data reported in the Appendices of this thesis are percentages of individual elements after a recalculation from the element weight percent in each oxide minerals.

### **3.2.2 STABLE CARBON AND OXYGEN ISOTOPES**

Carbon isotope analyses were performed for both inorganic carbonate ( $\delta^{13}\text{C}_{\text{carb}}$ ) and organic carbon ( $\delta^{13}\text{C}_{\text{org}}$ ). Oxygen isotopes ( $\delta^{18}\text{O}_{\text{carb}}$ ) were measured on the same sample that was

analyzed for carbonate carbon isotopes. Carbonate carbon and oxygen isotopes were analyzed on the whole crushed rock samples while organic carbon isotopes were analyzed on the non-carbonate fraction. All of the isotope analyzes were determined in the isotope laboratory of the School of Geology and Geophysics, University of Oklahoma by Rick Maynard with permission from Professor Michael Engel.

For carbonate carbon and oxygen isotope analyses, approximately 2-3 mg of the crushed sediment were placed in the hand-made Pyrex glass sample boat. The sample boat was then dropped into a Pyrex tubes (22cm x 7 mm i.d) for the reaction with the 100% H<sub>3</sub>PO<sub>4</sub> at 90°C for 1.5 to 2 hours. For all samples, the temperature was set at 90° C by using the online-automated system in order to ensure that all of the CO<sub>2</sub> would be released from the calcite and/or dolomite minerals (in general, 50°C is usually assigned if only calcite mineral is presented). The resulting CO<sub>2</sub> gas was isolated and purified cryogenically in a vacuum line before continuing to the inlet of the Finnigan Mat Delta E Isotope Ratio Mass Spectrometer. Both inorganic carbon and oxygen isotope compositions were detected and calculated using the following equations.

$$\delta^{13}\text{C} = [ (R_{\text{sample}} / R_{\text{standard}}) - 1 ] \times 1000 \quad \text{as} \quad R = \text{C}^{13} / \text{C}^{12}$$

$$\delta^{18}\text{O} = [ (R_{\text{sample}} / R_{\text{standard}}) - 1 ] \times 1000 \quad \text{as} \quad R = \text{O}^{18} / \text{O}^{16}$$

For the organic carbon isotopes, unlike the carbonate carbon, the non-carbonate component from the decarbonization process of approximately 1 mg was used. Initially, this sample was placed into the Pyrex glass in a similar manner to the inorganic carbon process, but with the temperature of the preheated tube at 550°C. Fired cupric oxide (3 gm-CuO, 850 °C) was loaded into the tube as a catalyst to insure complete combustion of organic carbon combustion that occurs at 550 °C for two and a half hours. The CO<sub>2</sub> gas from the combusted organic material was subsequently analyzed in steps similar to those described for carbonate carbon above. The composition of the organic carbon isotope was calculated using a similar equation applied for the carbonate carbon. All the carbon and oxygen isotope compositions of samples were reported in

the delta notation ( $\delta$ ) in parts per thousand unit (‰) relative to the PeeDee Belemnite (PDB) standard after being corrected for  $O^{17}$  contribution to mass 45 and  $C^{13}$  contribution to mass 46 (Craig, 1957). Oxygen isotopes were also corrected to a temperature of 25 °C reaction through the fractionation factors of calcite or dolomite with 100 %  $H_3PO_4$  at 25 °C and 50 °C (Swart et al., 1991).

### **3.2.3 TOTAL ORGANIC CARBON (TOC) ANALYSIS**

Total organic carbon (TOC) analyses were performed at the laboratory of the Environmental Science Department of the University of Oklahoma with a permission of Associate Professor Mark Nanny. The TOC instrument was a Shimadzu TOC 5050 Total Organic Carbon Analyzer. Residual fractions from decarbonized samples from acid dissolution step were used. Some of these samples were subsequently used for organic carbon isotope analysis. In the first step, each sample was precisely weighed on a pre-cleaned (heated) ceramic boat. The sample was then pushed into a combustion chamber to combust at 900 °C using oxygen gas and a platinum catalyst. The yield of organic carbon materials in the sample as  $CO_2$  was subsequently detected by the combined IR spectrometer. For each measurement, the released  $CO_2$  was converted into organic carbon percent on the calibration curve using glucose as standard ( $C_6H_{12}O_{6(solid)}$  of 40% C by wt.). During the analysis, the accuracy of the glucose standard curve was also repeatedly checked with the carbonate standard ( $CaCO_3$  of 12% C by wt.). Each sample was measured in duplicate with a precision of +/- 0.05 % wt.

### **3.2.4 EXTRACTION AND FRACTIONATION OF ORGANIC MATTER**

In addition, a few whole crushed rock samples selected from both cores were analyzed for biomarkers and determine their organic geochemical characteristics. Sample preparation and

analysis were conducted at organic geochemical laboratory of Professor Richard P. Philp, the supervisor of this dissertation, at School of Geology and Geophysics, the University of Oklahoma. Before extraction, the powdered rock sample was weighed. Although the recommended weight is typically 50 to 100 gm, for this study it was dependent upon sample availability (sample size ranged between 20 to 70 gm). The sample was placed in the extract thimble in the Soxhlet apparatus which had been previously cleaned. Solvent extraction was performed for 48 hours using approximate 350 ml of mixed 1: 1 (v/v) solvent of methylene chloride ( $\text{CHCl}_3$ ) and methanol ( $\text{CH}_3\text{OH}$ ). After finishing, the solvent was removed using a rotoevaporator under low pressure and temperature ( $\sim 40^\circ\text{C}$ ). The whole extract was transferred into a small vial by small amount of solvent, dried under nitrogen ( $\text{N}_2$ ) gas, and weighed. In the next step, a known weight of organic extract was treated by addition of a 40 fold volume of pentane ( $\text{C}_5\text{H}_{10}$ ) solvent. The mixture agitated using an ultrasonic shaker and allowed to stand for at least 12 hours to permit the asphaltene to precipitate in a glass centrifuge tube. The non-dissolved asphaltene component was separated from the dissolved component (called maltene) by centrifuging. The pentane/maltene solution after centrifugation was transferred into the flask and was evaporated using a rotoevaporator. The asphaltene precipitate in the centrifuge tube was washed with pentane at least two times for complete maltene separation. After pentane evaporation, the maltene was transferred into small vial using a small amount of pentane and dried under  $\text{N}_2$  gas before weighing. At the same time, the asphaltene fraction was transferred into small vial using a small amount of methylene chloride, dried and then weighed.

After removal of asphaltenes, the maltene fraction was separated into saturates, aromatics and polar (NSOs) compounds. The fractionation was performed using high performance liquid chromatography (HPLC, Eldex Model 9600, equipped with Whatman Partisil 5Pac Column, 25cm). The maltenes were dissolved in hexane (50mg/20ml) prior to injection in the HPLC system. The fractionation process was achieved with a timed program using different mixtures of hexane, methylene chloride, and ethylacetate as eluents at designated time periods (McDonald

and Kennicutt, 1992). The eluent containing each fraction was evaporated using low temperature and low pressure rotoevaporator. After drying under N<sub>2</sub> gas, each fraction was weighed. The saturate fraction was analyzed by gas chromatography as described below.

### **3.2.5 GAS CHROMATOGRAPHY (GC)**

The saturate and aromatic fractions of each rock sample were analyzed by gas chromatography using a Hewlett Packard 5890A GC and Varian 3300 GC, respectively. For the saturates, the HPLC-5890A-GC with a split/splitless capillary injection system was equipped with a 30m x 0.32 mm (i.d.) J&W Scientific DB-1HT fused silica capillary column of 0.1µm film thickness of dimethylene polysiloxane. The injector temperature was fixed at 300 °C. The temperature program for saturates was from 40 to 360 °C, with 1.5min initial holding time and then increased with the rate of 4°C/min to final temperature of 360 °C, and held 37.5min for a total running time 120 min. In the GC analysis, helium gas (He) was used for a carrier gas. For identification and quantification, the fully deuterated C<sub>24</sub> alkane ( n-C<sub>24</sub>D<sub>50</sub>) was used as an internal standard for saturate fraction.

## CHAPTER 4

### 4.1 LITHOLOGY AND CORE OBSERVATIONS

In the first instance, the two Smackover cores were examined for their lithology and sedimentary facies. The paleoenvironments and paleowater-depths are interpreted from core descriptions and photomicrographs of thin sections. Because of the distinct intervals marked by an increase in slioclastic influx and/or dolomitization observed in both cores, sedimentary facies of the Smackover were combined into facies associations recorded by depth unit. The general criteria for the paleoenvironment and paleowater-depth interpretations were taken from published literature (i.e. Wilson, 1975; Read 1980; Tucker, 2001). The specific lithofacies concepts which will be used within a carbonate environment setting are summarized as follows:

| <b>Observed Sedimentary Facies</b>   | <b>Interpreted Paleoenvironment and Water-depth Interpretation</b> |
|--|--|
| Texturally supermature quartz sand displaying cross –stratification                | Terrestrial (eolian)/proximal to shoreface                         |
| Sediment grading (fining-upward)   | Terrestrial-fluvial/ tidal channel                                 |
| Anhydrite nodules and/or gypsum ghosts   | Supratidal/ tidal flat environment or back barrier lagoon          |
| Planar stratification, submature sandstones  | Lower supratidal/ strandplain/ shoreface (beach)                   |
| Finely wavy laminated algal boundstones and mudstones “ribbon rock” characteristic | Low energy lower intertidal to subtidal, tidal environment         |

|  |   |
|--|---|
| Pelloidal grainstones  | Moderate energy intertidal  |
| Ooid grainstones   | High energy intertidal  |
| Limpid dolomite  | Schizohaline intertidal<br>(intermittent fresh/saline water zone)   |
| Textural inversion or<br>mixed grain size (bimodal )   | Low energy subtidal behind barrier<br>(lagoon) with washovered sediment<br>from high energy (storm surge) |
| Green/gray calcareous algal packstones   | Shallow subtidal  |
| Bioturbated pack/wackestones   | Moderate depth subtidal   |
| Mixed carbonate siltstone and mudstone,<br>(clastic inputs such as metamorphic<br>rock fragments, quartz, etc) | Moderate depth subtidal proximal<br>to distal deltaic sediment input                                      |
| Sparse silty quartz wacke/mudstone   | Moderate depth subtidal<br>with windblown quartz detritus   |
| Spiculiferous calcarenite  | Moderate to deep subtidal of<br>low energy sponge community   |
| Brachipod pack/wackestone  | Open marine (normal saline water)   |
| Mudstone (micrite)   | Restricted peritidal (lagoon) or<br>subtidal  |
| Sparse fossil mudstone/wackestone  | Stressed environment (restricted)<br>e.g. hypersaline water   |
| Bioturbated and<br>massive carbonate   | Destruction from biogenic action<br>during primary deposition   |

|                           |   |
|---------------------------|---|
| Euhedral limpid dolomite  | Primary dolomite, mixed salinity waters                                   |
| Massive dolomite          | Post depositional diagenetic replacive dolomite                           |
| Massive/nodular evaporite | Likely subtidal in restricted basin associated with high evaporation rate |

## 4.2 CORE ANALYSIS

The Smackover Formation from the Conecuh and the Manila Embayment consists of different thicknesses at different depth intervals. Sedimentary facies exhibit variations between the two depositional environments which were probably affected by paleotopography and relative sea level. The photographs of both cores are shown in **Appendix A** and **Appendix B** and the photomicrographs of thin sections are shown in **Appendix C** and **Appendix D**.

In both cores, the Smackover carbonates overly the siliciclastic sandstone of the Norphlet Formation. In the Conecuh Embayment, although some samples were missing, a distinct boundary contact is observed and illustrates a sharp change from sandstone to carbonate sedimentation (from 13845-13847 ft). In the Manila Embayment, a thin bed of carbonate lies above the oxidized red bed sandstone. The major part of the Smackover carbonate however overlies the top of the clean massive sandstone interval which marks the upper boundary of earlier sedimentation of a thin carbonate bed (13557.5 ft). Between these two cores, there were different sedimentary facies that occurred during the Norphlet deposition. In the Conecuh Embayment, the sediments from 13860 ft (bottom of core) to 13845 ft exhibit graded bed of fining- upward structure, heavy mineral partings, tabular cross beds and changes from grayish pink to light gray color. The heavy mineral partings are abundant along the stratifications. In the Manila Embayment, sediments from (13596.3 ft) (bottom of core) to (13557.5 ft) exhibit the mixed siltstone and sandstone with different sedimentary structures. Underlying the carbonate the

massive, white sandstone is observed. Under thin sections, metamorphic rock fragments are noticeable in the Norphlet sediments deposited in both areas.

#### 4.2.1 T. R. MILLER MILLS 17-11, #1 (17-2N-11E, ESCAMBIA CO.)

During the Smackover period, carbonate deposition in the Conecuh and the Manila Embayment exhibited similar and variable carbonate facies. Mudstone, algal laminated mudstone and fecal pellet materials, peloidal mudstone/wackestone are dominant in the lower Smackover sediment. Esposito (1987) and Moore (1991) had also reported that 60 to 80 percent of sedimentary facies of the Smackover carbonates in the Conecuh and the Manila Embayment are comprised of carbonate mud.

From the core depth 13845 ft to 13740 ft, carbonate sediments illustrate small sedimentary cycle (meter scale and smaller) changes from algal laminated mudstone to massive carbonate mudstones/ wackestones. A thin section from the base of the Smackover of this core (13845 ft) illustrates an abundance of fossils but with diagenetic calcitization the sediments were unable to identify thoroughly. Between 13800 ft and 13797 ft, a biogenic bounded structure consists of oncoidal wackestone/mudstone and peloidal wackestone, anhydrite nodules, algal and microbial components and terrestrial materials was occurred and mixed with the gray mudstone. Kopaska-Merkel (1994) identified this type of biogenic structure in the Smackover and called organic microreef (**Figure 4-1**). The abundance of the microreef in the lower Smackover sedimentation in the southwest Alabama, including the Conecuh and the Manila Embayments, was also previously reported by many others (Baria et al., 1982; Bradford, 1984; Cunningham, 1984; Markland, 1992; Kopaska-Merkel, 1994). For the non-structural mudstone, horsetail stylolites and pressure solutions are very common and some also exhibit layering organic accumulation. At about 13787.5 ft, the thin section shows pelletoid mudstone with broken spicules, scattered medium to fine silty quartz and abundant fenestra. During this interval,

(a)

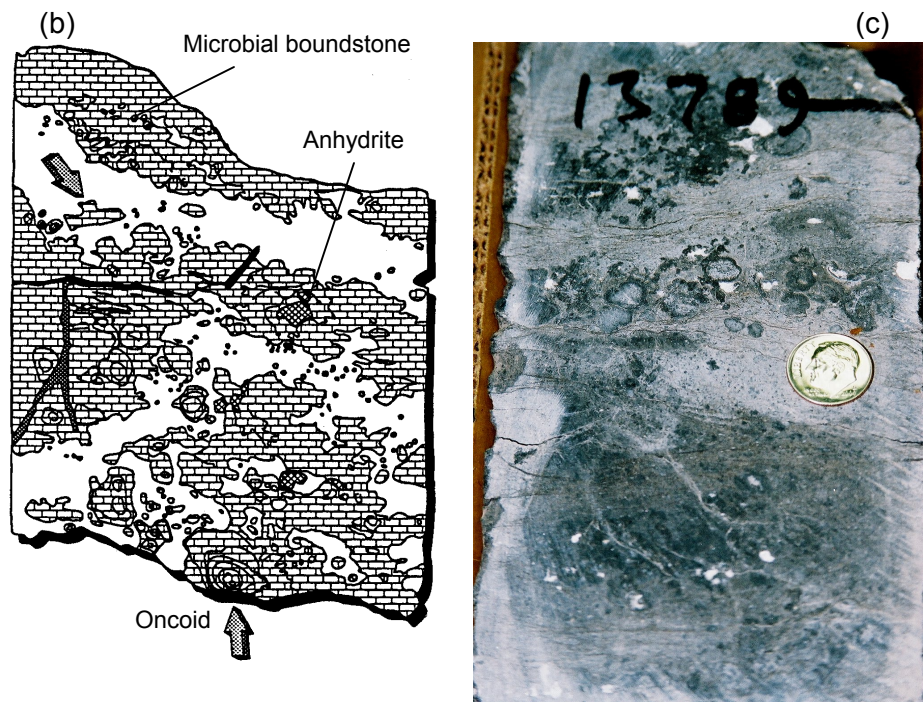
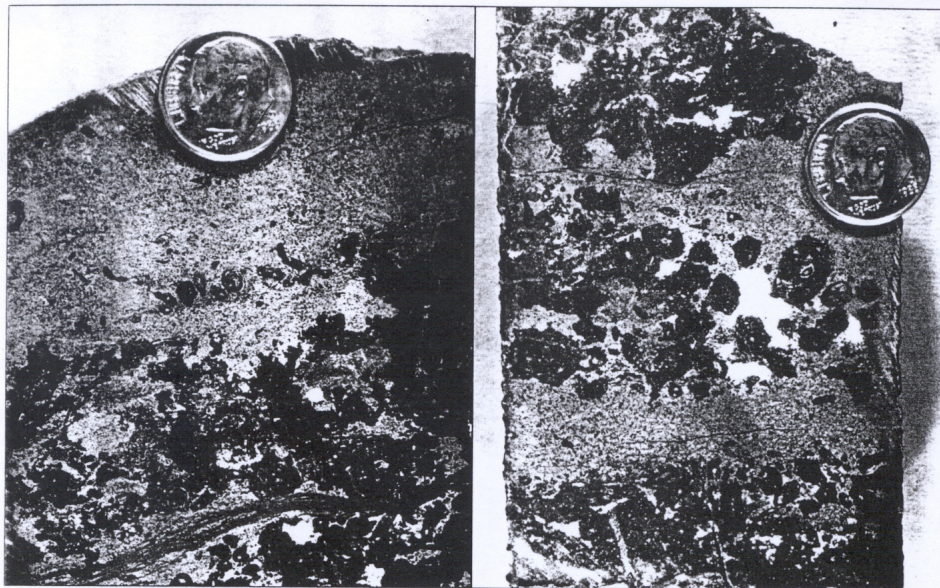


**Figure 4-1.**

(a) Algal boundstone (microreefs) incorporated oncoids, packstone, wackestone and anhydrite nodules, (b) The sketched structures of microreefs. Arrows indicate oncoids that formed as the nucleus part of the microreefs which grew on top of the previous one (Kopaska-Merkel, 1994), (c). Algal boundstone incorporated with oncoids, wackestone, anhydrite and terrestrial sediment observed in the Smackover deposition in the T. R. MILLER MILLS 17-11, #1 core (this study)

some fossils, bioturbation and small abundant of terrigenous materials are observed in the core. Most of the silt size quartz appears to be associated with algal laminations but become more visible at the end of this interval.

From 13740 ft to 13675 ft, the sediment deposition of the T.R. MILLER MILLS 17-11, #1 well exhibits significantly increased fine grain terrigenous clay fraction. Carbonate sediments show fissility and become contorted or split apart along these terrigenous bedding planes. Thin sections from sediments at 13737 ft, 13712 ft, and 13703 ft, illustrate mudstone mixed with claystone, scattered organic material and pyrite. Beside gray bluish mudstone and argillaceous shale alternation there is no organic-rich black shale that can be observed in this part of the core.

From 13675 ft to 13622 ft, the carbonates consist of massive wackestone/mudstone and packstone/wackestone with very low or no terrigenous input. At the base of this interval there is little terrigenous material observed, large coated grains (e.g. oncolites) are visible. In the core, some marine fossils (e.g. brachiopod) can be observed on the dark bluish gray to black brownish gray sediment. Microstylolites with concentrated organic material are common. Near the top of this interval, in the packstone and wackestone facies, small anhydrite nodules and terrigenous material become visible. Photomicrograph of a thin section at 13622.5 ft exhibits a sparse peloidal microcrystalline wackestone of dissolved grains filled with precipitated calcite.

From 13622 ft to 13589 ft, the carbonates of the Smackover Formation received an increase in terrigenous sediment influx similar to that observed between 13740 ft to 13675 ft. The sediments become increasingly fissile with contorted structures or even broken. The thin section at 13600.7 ft illustrates sediments of mixed siltstone and wackestone with coarse to fine silty quartz grains and scatter micaceous phyllarenite. Some carbonate grains (e.g. peloids, *Favreina* pellet), fossils (ostracods) and shell fragments are also observed.

From 13589 ft to 13510.2 ft, the Smackover sediment is mainly dominated by carbonate deposition and terrigenous materials are rare. In the lower part of this core interval, sediments are dominated by wackestone and mudstone but at shallower depths, packstones and grainstones

are abundant and dominated by oolitic and peloidal carbonate grains. Sediment colors vary from bluish gray in the wackestone and mudstone to light gray and tan in the packstone and grainstone facies. The carbonates and dolomitized carbonates of this interval illustrate some grading sediment structures and show fining upward grainstone. Photomicrographs of thin sections show dolomitized algal laminated mudstone (13555 ft), porous peloidal/ oolitic packstone (13526 ft), and nonporous dolomitized oolitic grainstone (13516 ft). At the end of this interval, a sharp boundary occurred separating an overlying anhydrite from carbonate sedimentation. The Buckner anhydrite overlying the Smackover exhibit mixed anhydritic mudstone and anhydrite (thin section at 13505.8 ft).

#### **4.2.2 #1 NEAL ET AL UNIT 30-1 ( 30-7N-4E, CLARK CO.)**

At the base of the Smackover Formation of this core, some flaser lens of carbonate sedimentation are present lying next to the white and massive sandstones of the Norphlet Formation. Under these sandstones and above the poorly cemented siliciclastic red bed sands, the thin carbonate bed is also observed intercalating between the sandstones. The Smackover carbonates of the #1 NEAL ET AL UNIT 30-1 illustrate different sedimentary facies when compared to those occurring in the Conecuh Embayment. In this core, the carbonates generally exhibit a higher abundance of terrigenous sediments and are dolomitized. Large and small anhydrite nodules are abundant throughout the core. The centimeter small carbonate cyclicity is observed alternating between the wackestone and mudstone of a ribbon rock characteristic. Within this core, dark organic-rich layers (millimeters) and sediments (centimeters) occur. Shallowing upward cycles are noticeable. Each cycle consists of interbedded dark organic-rich mudstone interval at base, alternating mudstone and wackestone small centimeter cyclicity, which could be dolomitized in the middle, and dolomitic wackestone mixed with evaporite and siliciclastic sediments at the top. Between these cycles, a sharp transition may or may not be

recognizable. In the upper part of this Smackover sedimentation, carbonates exhibit strong dolomitization and obscured original carbonate grains and sedimentary structures. There is a major difference between the upper Smackover sediments in the Manila Embayment and the Conecuh Embayment. In the #1 NEAL ET AL UNIT, 30-1, the oolitic packstone and grainstone sediments which predominate in the T.R. MILLER MILLS 17-11, #1 are absent. Instead, the dolomitized carbonates alternate with several sandstone beds. In the following description, the carbonate sedimentation of the #1 NEAL ET AL UNIT 30-1 well is examined and separated into core depth intervals.

The first interval starts from the lower Smackover next to the white and massive sands of the Norphlet Formation and is from 13557.5 ft to about 13435.5 ft. At least two sedimentary cycles of different thickness occur. The sedimentary facies of these cycles consist of alternating planar laminated organic rich intervals and mudstone near the base, alternating wackestone and mudstone centimeters scale cycles contain ribbon rocks characteristic in the middle and dolomitic limestone to dolostone in the top. A sharp contact can be observed between the cycles which the dolomitic carbonate is overlain by the dark organic rich sediment (13460 ft). Within these sediments, terrigenous components are readily observable (thin section at 13516 ft) compared to the lower Smackover from the Conecuh Embayment area. Photomicrographs of the other thin sections illustrate spiculiculous dolomitic mudstone/wackestone (13532.2 ft and 13515.5 ft). Sparse peloid and pyrite are also observable (13592 ft and 13532 ft).

From 13435.5 ft to 13339 ft, the carbonate sediments illustrate pervasive dolomitization. Sedimentary structures although are obscure but are comparable to which observed in the previous section. Organic rich sediments are less abundant and are thinner. Sediments become dolomitized and many evaporite nodules are observable. Photomicrographs of thin sections illustrate the organic rich layer in the mudstone (13434 ft), the variable detrital quartz in a dolomitic wackestone (13407 ft and 13388.5 ft), the fine crystalline anhydritic and evaporitic ghost dolospar in dolosparite (13372.5 ft). In the upper dolostone, probably originally

wackestone/packstone, thin sections exhibit medium crystalline dolosparite with abundant limpid dolomite crystals (13345 ft).

From 13339 ft to 13213 ft, the carbonate sediments illustrate a sharp contact concentrated with thin dark organic material at the base at 13339 ft. Overlying this contact, sediment is missing from 13332 ft to 13313 ft. At least two sedimentary cycles of variable thickness occur. Within each cycle, dark organic-rich layers mixed with mudstone and wackestone are present at the base. The top of the lower cycle consists mostly of bioturbated dolomitic wackestone. Sediment near the base of the shallower cycle (thin section at 13302 ft) characterizes silty dolomitic algal boundstone/mudstone with an abundance of mica flakes. In the upper part of this cycle, bioturbated dolomitic wackestone and mudstone display the partially preserved ribbon rock characteristic. A photomicrograph of a thin section (13275 ft) shows a fine crystalline dolosparite. Within this interval, biogenic structures interpreted as root casts and burrows and small evaporite filled fenestral pores are observed. At the top from 13215 ft to 13213 ft, two sandstone intervals are interbedded with the carbonate sediments.

In the upper Smackover of this core from 13213 ft to 13117 ft, the carbonates illustrate an increase of siliciclastics. Sediments are mixed dolomitic carbonate mudstone, wackestone and siliciclastic sandstone. Sedimentary structures are primarily bioturbation. In the sandstone, planar lamination may be observable. Dark organic-rich sediments are apparent and alternate with dolomitic carbonate, and dolostone. Thin section photomicrograph of sandstone (13143 ft) illustrates medium subarkose with silica cements and sparse chert metamorphic rock fragments. The contact between grains shows compaction. Another photomicrograph (13130 ft) indicates fossiliferous/spiculitic wackestone with sparse organic materials and abundant coarse to fine silty detrital quartz.

At the top of this Smackover sequence, a sharp boundary is recognizable. Evaporitic sedimentation becomes dominant mixing carbonate mud and then turns into nodular anhydrite with abundant terrigenous input.

### **4.3 DISCUSSION**

The sedimentary description of the Smackover deposition from the Conecuh Embayment and the Manila Embayment, represented by the T.R. MILLER MILLS 17-11, #1 well and the #1 NEAL ET AL UNIT 30-1 well, and their paleoenvironment and paleowater-depth interpretations are summarized in **Table 4-1** and **Table 4-2**. For the stratigraphic model, the interpretation was based upon sedimentary facies formed and discussed on a ramp stratigraphic sequence proposed by Burchette and Wright (1992) and Tucker et al. (1993). There is a significant limitation to the stratigraphic interpretation based on a limited number of core samples. Paleoenvironment and paleowater depth indications vary due to lateral sedimentary facies variation which is very common in a carbonate depositional system. Relative sea level changes, nevertheless, are believed to be one of the main factors controlling the sedimentation pattern on carbonate ramp platform in addition to climate and tectonic controls. For the Smackover Formation, carbonate deposition was believed to form during a stable tectonic activity period (Salvador, 1987). Even though the local factors such as a pre-Jurassic paleotopography or the Louann salt movements could be associated, it was possible that relative sea level variation would still have the major effect among the other parameters. It is assumed that a Smackover stratigraphic framework which was observed in the two cores may be comparable based on similar relative sea-level control. The interpretation will be constrained later by an elemental analysis and carbon isotope stratigraphy.

#### **4.3.1 SMACKOVER DEPOSITIONAL ENVIRONMENT AND A STRATIGRAPHIC FRAMEWORK**

Sedimentary facies and paleoenvironment interpretation for the Smackover deposition that occurred in the Conecuh Embayment and the Manila Embayment suggest lateral and vertical variations due to different structural settings on the carbonate platform. At the base of the

**Table 4-1** Core and thin section description and paleoenvironment and paleowater-depth interpretation of the Smackover well T.R. MILLER MILLS 17-11, #1 of the Conecuh Embayment.

| Core Interval (ft) | Thinsection (ts) Core photos(cp)   | Sediment-structure and color   | Macro-lithology (Dunham Name)  | Micro-lithology and description (Folk Name)*   | Paleo-environment   | Inferred paleo-water depth           |
|--------------------|--|--|--|--|---|--------------------------------------|
| 13500-13510.2      | 13505.8 ft (ts)<br>13506 ft (cp)<br><br>13508.8 ft (ts)                  | Nodular;<br>gray/white   | Anhydrite<br><br>Dolomicro-sparite<br><br>Anhydrite Nodules Pellets, | Calclutite: nodular anhydritic sandy quartz dolomicrosparite<br><br>Siltstone: nodular anhydritic immature micaceous litharenite   | Sabkha  | Supra-tidal                          |
| 13510.2 - 13522    | 13516.7 ft (ts)  | Massive and occasional lamination;<br>Tan, gray                        | Ooid grainstone (dolomitized)  | Calcarenite : sparse quartz silty oodolomicrosparite (fitted ooids ghosts, coatings unaltered) with some anhydritic replacement  | Beach, high energy  | Intertidal                           |
| 13522-13538.5      | 13526 ft (ts)<br><br><br>13535 ft (ts)<br>13537 ft (cp)<br>13538 ft (cp) | Light tan, gray<br><br><br>Textural inversion;<br>Light to medium gray | Packstone<br><br><br>Occasional gastropods, ooids<br><br>Wackstone   | Calcarenite: oomicrodolospaite (most ooids are now vugs; originally oomicrite) textural inversion<br>Oolitic packstone<br><br>Calcarenite: foram, peloidal (ooids?) microsparite | High energy shoal<br><br><br>Lower shoreface                      | Shallow subtidal                     |
| 13538.5-13540.5    | 13553.5 ft (ts)  | Massive;<br>dark gray  | Packstone  | Calcarenite: green calcareous algal peloidal (ooids?) foram, microdolospaite   | Intermediate energy marine, lower shoreface                       | Lower intertidal to shallow subtidal |
| 13540.5-13569      | 13555 ft (ts)  | Massive and occasional stylolites;<br>Tan gray                         | Laminated algal Boundstone-Wackestone                                | Calcarenite: peloidal (ooids?) blue-green algal intraclasts, limpid dolomite biolithite  | Tidal mudflat proximal to tidal channel;<br>Low to moderate enegy | Upper intertidal to supratidal       |
| 13569-13589        |  | Massive;<br>Gray   | Mudstone   |  |   | Subtidal                             |
| 13589-13615        | 13600.7 ft (ts)<br>13601 ft (cp)<br>13615 ft (cp)                        | Fissile with muddy clastic layers (~2-3cm);<br>Gray, brown             | Mudstone   | Siltstone: immature ostracods, micaceous phyllarenite  | Marine  | Subtidal                             |

| Core Interval (ft) | Thin section(ts)<br>Core photos(cp) | Sediment-structure and color                                 | Macro-lithology (Dunham Name)       | Micro-lithology and description (Folk Name)*              | Paleo environment   | Inferred paleo-water depth        |
|--------------------|-------------------------------------|--|-------------------------------------|---|---|-----------------------------------|
| 13615-13622        |                                     | Massive; Gray  | Wackestone                          |   |   | Shallow Subtidal                  |
| 13622-13675        | 13622.5 ft (ts)                     | Massive; Dark gray   | Wackestone                          | Calcarenite : sparse peloid calcareous algae microsparite | Shallow marine  | Shallow Subtidal                  |
|                    | 13646 ft (ts)<br>13674 ft (cp)      | Sparse algal laminae, brachiopods                            | Mudstone                            | Calcilutite: algal laminae in micrite                     | Normal marine   | subtidal (open marine?)           |
| 13675-13700        |                                     | Interbedded terrigenous mudstone, contorted beds; Dark brown | Mudstone                            |   | Carbonate marine with intermittent (deltaic?) clastic input | Subtidal                          |
| 13700-13730        | 13703.5 ft (ts)<br>13707 ft (cp)    | Fissile, silty lenses (1cm); Alternated dark gray and brown  | Mudstone (Claystone)                | Claystone: laminated calcite cemented micaceous clay      | Marine  | Subtidal                          |
|                    | 13712 ft (ts)                       | Algal laminae  | Algal Boundstone/<br>Mudstone       | Calcilutite: peloidal, pelletoid intramicrudite           | Lower shore face  | Shallow subtidal                  |
| 13730-13773        | 13737.5 ft (ts)                     | Massive with sparse algal laminae; Dark gray                 | Mudstone                            | Calcilutite: pelmicrite                                   | Low energy shallow marine                                   | Shallow subtidal                  |
|                    | 13765 ft (ts)                       | Occasional gypsum ghosts, peloid                             |                                     | Calcilutite: mottled micrite                              | Restricted marine   | Supra-tidal                       |
| 13773-13774        |                                     | Clastic interbedded with carbonate, contorted layers; Gray   | Silty Mudstone<br><br>Gypsum ghosts |   | Distal clastic input into carbonate marine                  | Subtidal<br><br>Inter-supra-tidal |
| 13774-13787        |                                     | Brachiopod, sparse algal laminae                             | Peloidal Mudstone/<br>Wackestone    |   | Moderated energy, carbonate marine                          | Subtidal                          |
|                    | 13787.5 ft (ts)                     | Dark gray  |                                     | Calcarenite: algal peloidal micrite                       |   |                                   |

| Core Interval (ft) | Thin section(ts) Core photos(cp)     | Sedimentary structure and color   | Macro-lithology (Dunham Name)                    | Micro-lithology and description (Folk Name)*   | Paleo environment                             | Inferred paleo-water depth   |
|--------------------|--------------------------------------|---|--|--|---|--|
| 13787-13789        |                                      | Oncolites, pellets, <i>Tubiphytes</i> algal; Dark gary  | Boundstone/<br>Mudstone                          |  |   | Intertidal   |
| 13789-13791        | 13789 ft (cp)                        | Tubiphytes and blue-green algal oncolites in planar, deformed laminae, Parallel algal laminated             | Sparse<br><br>Algal Boundstone                   |  | Sabkha<br><br>Upper tidal mudflat, low energy | Inter-supratidal   |
| 13791-13793        |                                      | Massive; Gary   | Mudstone   |  |   | Shallow subtidal (?)   |
| 13793-13796.5      | 13795 ft (cp)                        | Gray  | Agal Boundstone                                  |  | Low energy, tidal mudflat                     | Upper intertidal   |
| 13796.5-13801      | 13797 ft (cp)                        | Massive, anhydrite nodules, Anhydritic nodules in massive to sparsely coarse laminae; Gary and white        | Mudstone/<br>Wackestone<br><br>Mudstone          |  | Restricted marine, low energy                 | Shallow subtidal<br><br>Intertidal to supra-tidal                            |
| 13801-13805        | 13804.9 ft (ts)                      | Planar to slight wavy, algal laminae; Gray  | Algal Boundstone/<br>Mudstone                    | Mixed siltstone: immature micaceous litharenite and calcilitite; algal laminated pelleted microspar biolithite | Low energy                                    | Upper intertidal   |
| 13805-13816        |                                      | Massive, horsetail stylolites, organic layers; Gray   | Mudstone/<br>Wackestone                          |  | Moderate energy                               | Lower intertidal   |
| 13816-13827        | 13820.5 ft (ts)<br><br>13826 ft (cp) | Wavy lanminated; Gray<br><br>Massive at the top and coarsely laminated at the base with sparse bioturbation | Foram Wackestone<br><br>Algal laminated mudstone | Calcilitite; sparse foram dolomitic biomicrite   | Shallow marine<br><br>Shallow marine          | Shallow subtidal to lower intertidal<br>Shallow Subtidal to lower intertidal |
| 13827-13834        | 13830 ft (cp)                        | Pallarel to slight wavy, bioturbated and burrow filled  | Algal laminated mudstone/<br>Wackestone          |  | Shallow marine                                | Lower intertidal   |

| Core Interval (ft) | Thin section(ts) Core photos(cp)   | Sedimentary structure and color   | Macro-lithology (Dunham Name)              | Micro-lithology and description (Folk Name)*   | Paleo environment  | Inferred paleo-water depth            |
|--------------------|--|---|--|--|--|---------------------------------------|
| 13834 - 13834.5    | 13834 ft (cp)  | Oncolites, algal fragments; Gray  | Wackestone                                 |  | Shallow marine   | Shallow subtidal to lower intertidal  |
| 13834.5- 13840     | 13838 ft (cp)  | Parallel to slightly wavy fine laminae  | Algal Boundstone/ Mudstone                 |  |  | Lower intertidal                      |
| 13840- 13843.5     | 13843 ft (ts)  | Planar fine settle out laminae; Gray  | Parallel bedded dolomitic algal Boundstone | Calcilutite: blue green algal dolomitic biolithite   | Tidal mudflat  | Upper intertidal                      |
| 13843.5 - 13844    |  | Massive, intraclasts; Gray  | Wackestone                                 |  | Low to moderate energy   | Lower intertidal                      |
| 13844- 13845.2     | 13845.5 ft (ts)  | Planar fine algal laminae<br><br>Gray   | Dolomitic Boundstone                       | Calcilutite: Sparse ostracod mollusk bearing blue-green algal biolithite   | Low energy tidal flat  | Upper intertidal                      |
| 13845.2 - 13860    | 13847.2 ft (ts)<br>13845-7 ft (cp)<br><br>13851 ft (cp)<br>13856.5 ft (ts) | Tabular cross bedded; Light gray<br><br>Gravel to sand to silt tabular bedsets with heavy minerals concentrated along laminae; Grayish pink to pink | Sandstone                                  | Sandstone: submature metamorphic litharenite<br><br>Sandstone: submature metamorphic rock fragment, micaceous bearing phyllarenite | High enery beach to eolian dune<br><br>Alluvial braided stream | Upper supra-tidal<br><br>Terres-trail |

Note: \* Microlithology and Folk classification was based upon microscopic picture of thin section when there is available

**Table 4-2.** Core and thin section description and paleoenvironment and paleowater-depth interpretation of the Smackover well #1 NEAL ET AL UNIT 30-1 of the Manila Embayment.

| Core Interval (ft) | Thinsection (ts) Core photos(cp)                    | Sedimentary structure and color   | Macro-lithology (Dunham Name)  | Micro-lithology and Description (Folk Name)*  | Paleoenvironment Interpretation                     | Inferred Paleo-Water Depth |
|--------------------|---|---|--------------------------------|---|---|----------------------------|
| 13100-13101        |   | Massive; Gray   | Anhydrite with sand lens       |   | Sabkha  | Supratidal                 |
| 13101-13104        |   | Faint bedding; Gray (broken core)   | Sandstone/ Anhydrite           |   | Sabkha to intertidal                                | Supratidal                 |
| 13105-13116        | 13110 ft (cp)<br>13114.5 ft (ts)<br>13114.5 ft (cp) | Nodular to Massive; Gray  | Anhydrite                      |   | Sabkha  | Supratidal                 |
| 13116-13117        | 131117 ft (cp)                                      | Finely laminated  | Sandstone                      |   | Sabkha  | Intertidal                 |
| 13117-13124        |   | Coarsely laminated; Light to medium pink                                      | Mudstone                       |   | Low energy marine carbonate                         | Lower intertidal           |
| 13124-13135        | 13130 ft (ts)<br>13130 ft (cp)                      | Massive; Light pink   | Mudstone/ Wackestone           | Silty quartz spiciferous wackestone   | Low energy marine                                   | Subtidal                   |
| 13135-13139        |   | Alternating coarse and fine laminated; Light pink to brown, organic materials | Mudstone                       |   | Low energy marine                                   | Low to upper intertidal    |
| 13139-13140        | 13140 ft (ts)                                       | Interbedded; Dark gray to black   | Black organic rich mudstone    | Sparse spicule silty quartz micrite   | Low energy marine                                   | Subtidal                   |
| 13140-13152        | 13143 ft (ts)<br>13143 ft (cp)                      | Massive; White to light pink  | Sandstone                      | Medium sandstone: silica cemented, sparse chert metamorphic rock fragment subarkose | High energy beach to eolian dune                    | Supratidal                 |
| 13152-13165        | 13153 ft (cp)<br><br>13159 ft (ts)                  | Coarsely laminated with sand interbeds  | Algal boundstone and sandstone | Quartz medium sandy algal biolithite  | Low energy carbonate ramp proximal to clastic input | Intertidal                 |
| 13165-13174        |   | Faint cross-stratification to massive; White and brown stains                 | Sandstone                      |   | Beach   | Supratidal                 |

| Core Interval (ft) | Thinsection (ts) Core photos(cp) | Sedimentary structure and color                                  | Macro-lithology (Dunham Name) | Micro-lithology and Description (Folk Name)*      | Paleoenvironment Interpretation  | Inferred Paleo-Water Depth     |
|--------------------|----------------------------------|--|-------------------------------|---|----------------------------------|--------------------------------|
| 13174-13179        | 13175 ft (cp)                    | Massive with occasional fine laminations                         | Mudstone/Wackestone           |   | Low energy marine carbonate      | Shallow subtidal to intertidal |
| 13179-13180        |                                  | Massive; White   | Sandstone                     |   | Beach sand                       | Supratidal                     |
| 13180-13185        | 13181 ft (ts)<br>13181 ft (cp)   | Massive Gray   | Wackestone                    | Silty quartz spiculiferous micrite                | Low energy marine carbonate      | Subtidal                       |
| 13185-13186        |                                  | Massive; Very light gray to white                                | Sandstone                     |   | Beach                            | Supratidal                     |
| 13186-13188.5      |                                  | Discontinuous algal mass, bioturbated; Gray                      | Mudstone                      |   | Low energy marine carbonate ramp | Subtidal                       |
| 13188.5-13196.5    | 13191.5 ft (ts)                  | Coal Interbeds, bioturbated; Gray                                | Mudstone                      | Dolomicrite with evaporitic ghosts, faint laminae | Sabkha                           | Supratidal                     |
| 13196.5-13213      | 13208 ft (cp)                    | Interbedded to massive, bioturbated                              | Mudstone/Wackestone           |   | Low energy                       | Intertidal                     |
| 13213 - 13215      |                                  | Interbedded, planar laminated, dark organic layer; Brown to gray | Sandstone/Mudstone            |   | Low Energy upper shore           | Intertidal                     |
| 13215-13216        |                                  | Coal interbeds; Gray to dark gray                                | Mudstone                      |   | Low energy marsh and swamp       | Subtidal                       |
| 13216 - 13224      |                                  | Massive; Gray  | Mudstone                      |   | Low energy marine                | Intertidal to subtidal         |
| 13224-13240        | 13230 ft (ts)<br>13230 ft (cp)   | Coal interbeds, sparse evaporite; Gray to dark gray              | Mudstone                      | Dolospar with evaporate ghosts                    | Sabkha or low energy marsh       | Supratidal to intertidal       |

| Core Interval (ft)                          | Thinsection (ts) Core photos(cp)   | Sedimentary structure and color   | Macro-lithology (Dunham Name)                            | Micro-lithology and Description (Folk Name)*   | Paleoenvironment Interpretation  | Inferred Paleo-Water Depth  |
|---|--|---|--|--|--|---|
| 13240-13293                                 | 13240 ft (cp)<br>13256 ft (ts)<br><br>13275 ft (ts)<br><br>13280.2 ft (ts) | Coarsely wavy interbedded, dessicated cracks, burrows, bioturbated, sparse evaporite; Gray  | Wackestone<br><br>Wackestone<br><br>Mudstone             | Sparse silty quartz, algal laminated microdolospar biolithite;<br><br>Sparse silty quartz algal laminated peolidal micrite;<br><br>Dolosparite | Low energy carbonate ramp proximal to clastic input (windblown quartz?)<br><br>Moderate energy shallow marine<br><br>Low energy marine | Intertidal<br><br>Intertidal<br><br>Subtidal if replacive dolomite supratidal |
| 13293-13303                                 | 13298 ft (ts)<br><br>13302 ft (ts)<br>13302 ft (cp)                        | Finely laminated; Dark organic patches alternating with white patches increasing vertically; Quartz diminishing vertically<br>Gray to dark gray | Algal laminated Mudstone<br><br>Algal laminated Mudstone | Algal laminated muddy biolithite, sparse quartz;<br><br>Silty quartz, algal laminated dolospar biolithite                                      | Low energy carbonate ramp proximal to clastic input (windblown quartz?)  | Subtidal<br><br>Subtidal to Intertidal  |
| 13303-13310                                 | 13305 ft (ts)  | Massive; Pinkish gray   | Algal boundstone   | Silty quartz, slightly algal laminated biolithite  | Low energy carbonate ramp proximal to clastic input  | Intertidal  |
| 13310-13339 (missing core from 13313-13332) |  | planar laminated, Interbedded coal layers, pyrite; Green, Gray  | Rich-organic Mudstone                                    |  | Low energy, reducing environment   | Subtidal  |
| 13339-13365                                 | 13339 ft (cp)  | Coarse, wavy interbedded, evaporites, anhydrite filled vugs   | Dolostone  |  | Moderate energy shallow marine   | Subtidal origin, and later subkha to subaerial                                |

| Core Interval (ft) | Thinsection (ts) Core photos(cp)   | Sedimentary structure and color  | Macro-lithology (Dunham Name)       | Micro-lithology and Description (Folk Name)*   | Paleoenvironment Interpretation                        | Inferred Paleo-water depth                                  |
|--------------------|--|--|-------------------------------------|--|--|---|
|                    | 13345 ft (ts)<br>13345 ft (cp)<br><br>13353 ft (ts)<br><br>13364.5 ft (ts) | Pink to pinkish brown, dark brown stain next and along horizontal cracks                                     |                                     | Silty quartz, slightly muddy evaporitic ghost dolospar<br><br>Quartz silt dolomitic microspar;<br><br>Fine sandy quartz, evaporitic ghost dolospar | Low energy carbonate ramp proximal to clastic input    |   |
| 13365-13388        | 13372.5 ft (ts)<br>13372.5 ft (cp)   | Coarsely interbedded with occasional large anhydrite nodules, faint "ribbon rock"; brown and gray alternated | Dolostone                           | Evaporite ghost dolospar, dolomitic wackestone/packstone   | Low energy   | Intertidal  |
| 13388-13412.51     | 13388.5 ft (ts)<br>13398 ft (cp)<br>13407 ft (ts)<br>13410 ft (cp)         | Coarsely laminated, discontinuous algal mass, occasionally anhydrite nodules; brownish gray                  | Silty dolomitic Boundstone/Mudstone | Quartz silt dolomitic slight clay parting microspar  | Low energy carbonate ramp with distal clastic influx   | Intertidal to moderate subtidal                             |
| 13412.5-13432      | 13422.5 ft (cp)  | Intraclasts of algal fragments, burrows, anhydrite nodules, grain texural inversion                          | Mudstone/Wackestone                 | Quartz silt dolomitic microspar  | moderate energy marine with occasionally high energy   | lower Intertidal to subtidal                                |
| 13432-13435        | 13434 ft (ts)  | Finely laminated, dark organic-rich layers; Gray to dark gray  | Algal laminated Mudstone            | Quartz silt algal laminated biolithite   | Low energy   | Subtidal  |
| 13435-13439        | 13435 ft (cp)  | Interbedded; Alternated brown and dark gray  | Mudstone/Wackestone                 |  | Low to moderate energy (alternated)                    | Subtidal to Intertidal and then subkha                      |
| 13439-13445        | 13443 ft   | Large evaporite/anhydrite nodules, <i>Tubiphytes</i> algal, Pinkish brown with dark stain layers             | Evaporite/Wackestone                | Quartz sand, spiculiferous, intraclast peloidal dolospar   | Moderate energy in origin and then to low energy later | Shallow subtidal then sabkha or close to subaerial exposure |

| Core Interval (ft)                     | Thinsection (ts) Core photos(cp)  | Sedimentary structure and color  | Macro-lithology (Dunham Name)                | Micro-lithology and Description (Folk Name)*                       | Paleoenvironment Interpretation          | Inferred paleo-water depth           |
|--|-----------------------------------|--|--|--|--|--------------------------------------|
| 13445-13453                            | 13452 ft (cp)                     | Massive and Interbedded algal mass, finely laminated mud; Alternated brown and gray and dark gray                            | Algal boundstone/<br>Wackestone/<br>Mudstone |  | Low energy shallow marine                | Upper Intertidal to shallow subtidal |
| 13453-13460                            | 13460 ft (ts)<br>13460 ft (cp)    | Fine, planar, laminated, peloids, silty quartz, organic rich layers; Brownish gray to dark gray                              | Mudstone/<br>Wackestone                      | Calcilutite: silty pelmicrite                                      | Low energy                               | Subtidal                             |
| 13460-13481                            | 13461 ft (ts),<br>13472.5 ft (ts) | Faintly interbedded to massive, abundant small anhydrite filled vugs; Pinkish gray to gray                                   | Dolomitic mudstone                           | Sparse quartz silt and sparse spicule dolospar;                    | Low energy shallow marine carbonate ramp | Shallow subtidal to intertidal       |
| 13481-13498 (missing core 13481-13482) | 13492 ft (ts)<br>13492 ft (cp)    | Coarse wavy interbedded "ribbon rock", algal layers, peloids, burrows, sparse small anhydrite; Alternated dark gray and gray | Algal boundstone/<br>Mudstone                | Interbedded quartz silt blue green algal biolithite and pelmicrite | Low energy mudflat                       | Shallow subtidal to lower intertidal |
| 13498-13499                            |                                   | Massive; Gray  | Mudstone                                     | Micrite  | Low energy shallow marine                | Shallow subtidal                     |
| 13499-13512                            |                                   | Massive to fine, planar interbedded to wavy "ribbon rock", burrows, sparse anhydrite filled vugs; Light brown to gray        | Algal boundstone/<br>Mudstone/<br>wackestone | Micro biolithite   | Low energy mudflat                       | Upper intertidal to lower intertidal |
| 13512-13513                            | 13513 ft (cp)                     | Nodular anhydrite, algal mass; Gray  | Algal boundstone                             |  | Low to moderate energy                   | Intertidal                           |

| Core Interval (ft) | Thinsection (ts) Core photos(cp)   | Sedimentary structure and color   | Macro-lithology (Dunham Name)       | Micro-lithology and Description (Folk Name)*                              | Paleoenvironment Interpretation                     | Inferred paleo-water depth           |
|--------------------|------------------------------------|---|-------------------------------------|---|---|--------------------------------------|
| 13513-13515        | 13515 ft (ts)<br>13515 ft (cp)     | Massive to faintly laminated;<br>Brownish gray  | Silty Mudstone                      | Calcilutite: Quartz silt, spiculiferous laminated micrite                 | Low energy shallow marine ramp                      | Shallow subtidal to lower intertidal |
| 13515-13516        | 13516 ft (ts)                      | Mixed grain size, intraclasts, organic material, algal fragments, anhydrite;<br>Gray  | Mudstone/Wackestone                 | Anhydrite nodules in micrite  | moderate energy intertidal, high energy storm surge | Shallow subtidal                     |
| 13516-13524        | 13522 ft (cp)                      | Massive to coarse to fine interbedded, wavy to planar laminae, interbedded dark organic layers, anhydrite;<br>Pinkish gray to dark gray | Sandy Mudstone/Wackestone           | Calcarenite: quartz sand dolomitic microsparite-micrite                   | Low energy to moderate                              | Lower intertidal                     |
| 13524-13544        | 13532.2 ft (ts)<br>13532 ft (cp)   | Massive to fainted coarse interbedded, bioturbated, burrows, sparse dark organic layers;<br>Brownish gray to gray                       | Silty Mudstone                      | Mixed quartz silty calcilutite: spicule micrite                           | Low energy mixed clastic-carbonate marine           | Upper to Lower intertidal            |
| 13544-13552.5      | 13545.5 ft (ts)<br>13545.5 ft (cp) | Fine laminated to thin interbedded, organic silt layers;<br>Brown and gray  | Algal boundstone/Mudstone           | Calcilutite: quartz silt algal biolithite interbedded with micrite        | low energy  | Lower intertidal                     |
| 13552.5 - 13554    | 13554 ft (ts)<br>13554 ft (cp)     | Finely laminated and bioturbated;<br>Gray   | Algal boundstone                    | Calcilutite: quartz silt green calcareous and blue green algae biolithite | Low energy mudflat                                  | Shallow subtidal                     |
| 13554-13557.5      |                                    | Laminated to massive, ripped up clasts at lower;<br>Gray to medium gray   | Peoloidal algal boundstone/Mudstone | Calcilutite: sparse peoloid and algal laminated micrite                   | Moderate energy                                     | Lower intertidal                     |
| 13557.5-13568.5    | 13558 ft (ts)<br>13558 ft (cp)     | Massive,<br>White to very light gray  | Sandstone                           | Bimodal medium and fine sandstone: mica and chert bearing subarkose       | High energy beach                                   | Supratidal                           |

| Core Interval (ft)  | Thinsection (ts) Core photos(cp)                    | Sedimentary structure and color   | Macro-lithology (Dunham Name) | Micro-lithology and Description (Folk Name)*   | Paleoenvironment Interpretation                             | Inferred paleo-water depth |
|---------------------|---|---|-------------------------------|--|---|----------------------------|
| 13568.5 (~2.5 inch) | 13568.5 (ts)  | White sand lens, layers, interbedded with medium gray                         | Sandstone/Mudstone            |  | High energy beach   | Shallow intertidal         |
| 13568.5-13577       |   | Massive with clay partings, Pinkish to light brown                            | Sandstone                     | Fine sandstone: immature mica bearing phyllarenite   | Low energy lagoonal   | Supratidal                 |
| 13577-13587         | 13587 ft (ts)                                       | Massive bioturbated to laminated with evaporite nodule; Dark brown to brown   | Sandstone-siltstone           | Medium sandstone: poorly sorted immature mica bearing phyllarenite (metamorphic quartz, mica flakes, feldspar) | Restricted shallow sabkha lagoonal or interdistributary bay | Supratidal                 |
| 13587-13590.5       |   | Low angle cross stratification to massive; Gray                               | Sandstone                     | Medium coarse sandstone: quartz cemented mature chloritic subarkose  | Eolian  | Supratidal                 |
| 13590.5-13596.3     | 13591 ft (cp)<br><br>13594 ft (ts)<br>13594 ft (cp) | Poorly cemented; Light gray<br><br>Low angle cross stratification to massive, | Sandstone                     | <br><br>Fine sandstone: submature mica-bearing subarkose   | Alluvial  | Supratidal                 |

**Note:** \* Microlithology and Folk classification was based upon microscopic picture of thin section when there is available

Smackover Formation in the Conecuh Embayment, a sharp discontinuity surface and abrupt change from siliciclastic Norphlet sandstone to dominant carbonate mudstone indicates a rapid rise of relative sea level permitting a full marine carbonate condition. This interpretation is supported by an abundance of marine fossils observed in the carbonate at the base just above the erosional contact. The low angle tabular cross-bedded sandstone with a heavy mineral parting suggests an eolian environment. According to Wilkerson (1981), the Norphlet Formation in southwest Alabama started updip in an alluvial-braided stream environment and continued downdip through subsequently sediment reworking process to deposit in a desert dune and interdune environments. In different local areas, the massive, clean and structureless sandstone exists just below the contact of the Smackover and the Norphlet Formations. The contact between the Norphlet and the Smackover Formations was interpreted by Wade and Moore (1993) as a ravinement surface representing a coarse transgressive lag during initial Smackover deposition. In the T.R. MILLER MILLS 17-11, #1, at this contact, coarse and unconsolidated sediments suggest a possible an erosional surface. However with missing core sample the interpretation is uncertain.

#### **4.3.1.1 Conecuh Embayment**

For the Conecuh Embayment, low fossil diversity, a dominant mudstone with an abundance of algal lamination, a variety of peloid, pellet and oncolitic coated grains associated in the mudstone, and a presence of microbial boundstone or microreef observed in the lower and middle part of the Smackover core, are interpreted to represent a restricted and probably a high salinity lagoonal environment of the shallow inner ramp facies. During Smackover deposition, paleowater depth in the Conecuh Embayment probably fluctuated between subtidal and intertidal but never became a supratidal environment. Compared to the ramp geometry and facies dynamics of the Middle Jurassic carbonate ramp system from the west central Portugal reported by Aceredo (1998), sedimentary facies of an inner ramp lagoon are comprised of mudstone, wackestone and

floatstone associated with oncoids and algal-cyanobacteria nodules with diverse benthic foraminifera, ostracods but restricted in macrofauna.

The presence and abundance of algal lamination in the lower Smackover of the T.R. MILLER MILLS 17-11, #1 core indicates that initial Smackover sedimentation occurred in a tidal-flat environment adjacent to the carbonate lagoon behind a beach barrier or some locally high structures. The majority of carbonate mud associated with peloidal and pelletal grains and a low diversity of normal marine fauna observed in this core and the restricted environment interpretation are similar to the other Smackover investigations reported from this area (e.g. Sigsby, 1976; Bradford, 1982; Esposito and King, 1987). The structural high features which are believed to partially restrict the Conecuh Embayment during Smackover deposition were indicated by Bradford (1982) to be the igneous and metamorphic Paleozoic structural highs to the north and east and probable the eolian dune to the west. From the basal Smackover (13845 ft to 13740 ft), vertical facies variation suggests a possible lateral facies changes that formed along the platform slope in the inner ramp setting. These sediments were probably deposited above the fair-weather wave base (FWWB) of the intertidal to subtidal conditions during shallow marine lagoonal - tidal flat environments. An absence of supratidal mud flat facies, however, suggests carbonate production rate was outstripped by rate of sea level rise. Because of a restriction by the adjacent structure highs, the embayment was probably less open to the normal marine ramp condition. The embayment would probably not be effectively connected to open marine conditions until sea level rise continued at a later time. A partial restriction means that during the relative sea level lowstand, high evaporation and no marine water circulation would increase water salinity. Carbonate sediments at this time could be affected by some episodically fresh-water diagenesis and increase the small fenestral pores which were filled later with evaporite from the ensuing marine water.

The two tidal cycles of algal laminated mudstone mixed with wackestone/mudstone and anhydritic micritic oncoidal-peloidal wackestone/packestone facies at the top observed from

13805 ft to 13785 ft suggest a possible stillstand or decreasing rate of relative sea level rise.

According to Tucker and Wright (1990), oncoids occurring as biogenic forming structures can be formed by trapping and binding of sediment by the filaments of algal mats (Tucker and Wright, 1990, references therein). The oncoidal structures occurred as cyanobacteria bioherms and were prominent in many Paleozoic and Mesozoic limestones of shallow marine peritidal environment (Tucker, 2001) are the micritic and a spongy fabric oncoids (Riding, 1983), which could be similar to those observed in the lower Smackover. Kopaska-Merkel (1994) reported the small reef structures in the Smackover are a combination of microbial boundstones incorporating the oncoids and peloids and their cavities are subsequently filled with fossils, oncoidal *Favriena* pelletoid packstone (Figure 4-1). Many of these reefs, but of larger sizes and higher abundance and diversity of organisms, are also observed in the lower Smackover of Arkansas and Louisiana. The different characteristics of the reefs that occurred in southwest Alabama was suggested to be due to the restricted condition in the area which affected the salinity, circulation and turbidity of the marine water (Baria et al., 1982). The formation of the organic reef was suggested by Kopaska-Merkel (1994) to be affected by two different water energy conditions; the low energy for the algal boundstone formation and high energy for the oncoid transportation during its structural growth. Relative to sea level changes, these microreefs could have formed during a highstand to stillstand sea level and with subsequently brief falling sea level. The presence of evaporite filled pores and evaporite nodules infer that the embayment could possibly become hypersaline condition. On a carbonate ramp sequence model, Tucker (1993) had indicated that small organic structures or isolated reefs could be found on the ramp platform during highstand sea level and continue to lowstand. The example was from the Silurian Michigan basin where small patch reefs were observed along a dipping ramp during a falling sea level and associated with the type 2 sequence boundary (Sarg, 1982 and 1983). Sarg (1983) also commented that during a relative sea level lowstand, hypersaline environment could have been initiated and associated with evaporitic replacement and dolomitization. Therefore, the presence of the organic

reefs observed in the T.R. MILLER MILLS 17-11, #1 is interpreted to form during the late relative sea level highstand continued to the small relative sea level falling. The lacking of a distinct contact or sequence boundary surface was affected by insignificant change in sedimentary facies on a lateral variation as a relative sea level fall might have occurred in a small magnitude. A non-deposition or subaqueous omission condition probably occurred during this first relative falling of sea level in the lower Smackover. This relative sea level fall interpretation will later be compared with different observations. In Sigsby (1976), the short-term regression occurred during the long-term Smackover sequence in the Escambia County of southwest Alabama had also been interpreted by the presence of the partial to complete dolomitized micritic-pelletal-oncoidal limestones (which vary from mudstone to packstone) which appeared to be the microreefs observed in this study. Sigsby (1976) had noted that during this brief regressive period in the lower Smackover, a subaerial exposure and leaching occurred in the other area caused the collapse of breccias on some stable positive areas.

The prominent peloidal mudstone/wackestone facies with normal marine fossils that occurs between 13785 ft to about 13740 ft are interpreted as a transgressive to a highstand sea level deposit when the normal marine water had reached into the embayment. Large fossils of normal marine water i.e. brachiopods, are observed in the core. Terrigenous sediments are minimal. The absence of major packstone and grainstone sediments and variable bioclasts or sediments with hummocky cross-stratification, or graded tempestite structures, which usually are indicators of the open mid-ramp facies (Burchette and Wright, 1992) suggests that these sediments were still deposited in a partially protected, low energy environment. The protection described by Sigsby (1976) was due to a deeply embayed shoreline of the Conecuh Embayment. An open lateral marine current circulation was interpreted to be still partially impeded by the Pensacola arch to the southeast and by the other local topographic highs to the northwest. Although high-energy waves could have occurred next to the ridge areas, where packstone and

grainstone would have developed, most wave energy was dissipated over the large restricted area in the embayment where only most non-skeletal carbonate grains were productive.

The presence of terrigenous sediments intercalated with mudstone between 13740 ft to 13675 ft is interpreted to result from an incoming and increasing terrigenous influx during the late highstand to relative sea level fall. Due to a very low slope angle on the ramp platform, a major exposure or sequence boundary and flooding surface can be unusually diachronous (Burchette and Wright, 1992). A drowning of sequence boundary could have occurred and exhibits an abrupt upward facies changes from inner ramp carbonates to outer ramp terrigenous mudstones or argillaceous limestones that then shoal or prograde upward to the inner ramp facies of another sea level cycle. It is proposed that during this relative sea level falling period, the carbonate mud of Smackover was still continuously delivered from the tidal flats of the restricted inner ramp to the northeast of the embayment. Terrigenous sediments, however, were transported to the distal area by the prograding delta front and rivers. Falling relative sea level resulted in decreased accommodation space forming a restricted inner ramp of low energy depositional condition in the entire embayment. Because of the partial stagnation of water circulation and effect of periodical siliciclastic contamination, carbonate production rate and accumulation became very low marked by thin sediment intercalated with siliciclastics. It is suggested that falling relative sea level did not affect a simple shift of sedimentary facies on this low gradient platform condition but instead affected the depositional environment by increased siliciclastic input which has been reported in the Smackover elsewhere (Chimene, 1976; Ahr and Palko, 1981; Judice and Mazzullo, 1982). An increased siliciclastic sediment during falling relative sea level is not uncommon on a carbonate ramp platform. An example in a field study was reported from the Northern Sinai Cretaceous ramp by Bachmann and Kuss (1998). During relative sea level fall, an offlapping delta progradational process increases the amount of siliciclastic sediments to mix with carbonate sedimentation. For the Smackover, evidence for subaerial exposure was probably restricted to areas over which the inner ramp prograded,

suggesting the Smackover ramp may be responding to only relatively minor changes in relative sea level which forced strong progradation followed by abrupt deepening rather than extensive ramp exposure. The interpretation that falling relative sea level occurred during the middle Smackover has also been observed and was reported from the Appleton Field of the Escambia County, the Conecuh Embayment (Benson et al., 1996).

An increasing mudstone/wackestone facies and coated grain components in the Smackover from 13675 ft to 13622 ft are interpreted to reflect a subsequent rise of relative sea level. A transgressive event with increasing water energy is marked by an abrupt facies change from mixed argillaceous mudstone to the onciodal wackestone/packstone facies (13675 ft). In rising sea level, the distal inner ramp become open to normal marine conditions and left the siliciclastic delta front and rivers behind. A decrease terrigenous input thus gave way to a carbonate factory to become productive. Open marine fossils are more abundant and can be observed macroscopically in the core. However, a partial enclosure setting of the embayment probably did not permit enough wave action for a shoal sediment formation, thus only wackestone and mudstone are observed. No sedimentation (e.g. tempestite) and/or sedimentary structure (e.g. hummocky stratification) could be recognized as an indication of a storm or strong wave action. A sedimentary cycle or parasequence and the transgressive/ highstand boundary are not distinguishable. A maximum flooding surface, or condensed section, is not detectable as the Smackover deposition in this particular area occurred mainly on a shallow carbonate condition where the carbonate precipitation rate was rather high and environment of deposition was likely an oxic. However, a gradational transition from inner ramp mudstone to wackestone suggests an increased carbonate production which kept-up with accommodation space under more open marine environment during maximum relative sea level rise. The upper part, where wackestone diminished and sediment mixed with terrigenous material, is interpreted to be the time when the embayment was approached again by prograding delta and rivers from the north. Depositional environment from 13675 ft to 13589 ft is interpreted as an inner ramp facies that occurred during

late highstand to falling sea level. Most carbonate sediment formed in an earlier condition became mixed mudstone, siltstone/wackestone and argillaceous shale with abundant shallow environment grains and fossils such as pellet, peloid, ostracods, some shell fragments.

Wackestone to packstone facies lying above the siliciclastic influx at 13589.5 ft is interpreted to be an early transgressive sedimentation. Oolitic packstone and grainstone had formed as sea level continued rising adding accommodation space and increasing wave energy during the transgressive and highstand deposition. The interrelationship between accommodation space and the formation of ooids has been mentioned by Jenkyns and Strasser (1995) and Pittet et al. (1995) and also by Bachmann and Kuss (1998). These studies suggested that a favorable ooid formation to skeletal grains deposition occur during the transgression where there were an increasing accommodation space and increasing extension of flat, high energy areas. In this upper Smackover interval, a minimal siliciclastic sediment suggests a shallow inner ramp depositional environment of lagoon which received higher terrigenous influx probably occurred farther or more landward side behind the ooid shoal bar or barrier. The isopach map of oolitic grainstone formed in the Conecuh Embayment (Bradford, 1982) illustrates an oolite shoal complex which is thicker to the west of the basin area and becomes thinner to absent when it moved further to the east. During the upper Smackover, the packstone/grainstone deposit characterizes a regressive shoaling sequence where accommodation space and strong wave energy were available. In this interval, oolitic packstone and grainstone exhibit more carbonate diagenetic alteration including dolomitization. Thin section photomicrographs show aragonite, which is most common mineral of ooid grains, was dissolved away and/or altered to calcite. The calcite and their pore vugs or have been replaced by dolomite precipitation. Diagenesis and dolomitization of grainstone in the upper Smackover were interpreted by several studies to be associated with meteoric or mixed-meteoric water system. Based upon Smackover deposition from Louisiana, Humphrey et al. (1986) suggested early mineralogical stabilization of the non-porous interval occurred in a high flow, near-surface, meteoric phreatic lens. From the Jay Field in Escambia County, Vinet (1984)

indicated that dolomitization of the Smackover Formation occurred as a result of mixed marine-meteoric water influence during subaerial exposure near the end of Smackover depositional period. Another Smackover dolomite study by Haywick et al. (2000) discovered four different textural types of dolomites formed in the Smackover Formation of the Appleton Field, Escambia County. They suggested that three types out of four were formed during early relative diagenesis conditions varied from meteoric to hypersaline process. Two types, which are mostly observed dolomite in the Smackover, occurred in a mixed condition between meteoric and hypersaline water (Figure 4 in Haywick et al., 2000). In this Smackover core, dolomite is observed to be abundant in the upper part of the core near the end of the Smackover deposition where the mudstone content is low. At the transition between the Smackover and the Buckner, a sharp interface also shows an abrupt facies changes between sediments below and above the contact which is possible a subaerial exposure during a drop of sea level or sequence boundary.

The interpretation of the boundary between the upper Smackover and the lower Buckner is also controversial. For example, from the Mississippi Interior Salt Basin, Badon (1973) and Ottman et al. (1973) interpreted the lower Buckner anhydrite as a supratidal environment which continued shallowing during falling sea level and was equivalent to the upper Smackover. However, Oglesby (1976) concluded, from the same study area, that either marine regression or salt tectonic must have previously occurred and elevated the oolitic sediment in the upper Smackover into meteoric diagenetic environment before another sea transgression cycle was resumed. From Moore (1984), the Buckner/Haynesville Formation was interpreted as a separate sedimentological package from the Smackover Formation which occurred during the next sea level cycle. Prather (1992) suggested that the anhydrite of the Buckner Member to prograde basinward on top of the Smackover shoreface and tidal-flat units and took place as an subaqueous anhydrite deposition within a salinas on a coastal sabkha environment. However, Prather (1992) noticed that an apparent absence of shoreface and tidal mud units at the top of the Smackover grainstone could be an indicator to a drop of relative sea level and erosion of shoreline sediments.

Nevertheless, because there is no evidence of preserved sedimentary structures in a conventional core along the edge of the Conecuh basin, Prather (1992) summarized that a relative sea level fall by the end of the Smackover period could not be confirmed.

#### **4.3.1.2 Manila Embayment**

The variable sedimentary structures and carbonate facies observed from the #1NEAL ET AL UNIT 30-1 well suggest that the Smackover deposition in the Manila Embayment probably occurred in a shallow marine peritidal and shoreline environment.

In the Manila Embayment, the transition from the Norphlet siliciclastic to the basal Smackover carbonate in the #1NEAL ET AL UNIT 30-1 characterize sediments which are produced of initial marine transgression overlying the eolian sandstone sedimentation of the Norphlet Formation. The initial marine transgression for carbonate deposit is evident at 13568.5 ft shown by a formation of thin carbonate bed associated with some flaser sand lens. The boundary between the lowest Smackover and the previous sequence, however, is interpreted to occur at about 13587 ft. As part of the Smackover sequence, the red bed sandstone of the Norphlet formation is interpreted as supratidal wadi deposit. This sediment then graded into the first sedimentation of marine carbonates, which was previously mentioned, before sharply changing into a clean and massive marine reworked sandstone. At the top, this massive marine sand is overlain by a continuous carbonate deposit of the lower Smackover. The intercalation of the marine reworked sandstone between the first carbonate deposit and the carbonate of the lower Smackover indicates that the formation boundary is not coincident with the sequence boundary in this area. This incidence supports an earlier reported from Wade and Moore (1993) which noted that, in southwest Alabama, the Smackover sequence boundary may not necessary coincide with the formation boundary. During an initial sea transgression, sedimentary characteristics suggests sea level rise fluctuated and its height was probably not sufficient or stable enough for a

carbonate factory to be established and continually produce carbonate in this area.

In this well, initial carbonate sedimentation with the sedimentary structure of flaser sand lens, earlier mentioned at 13557.5 ft, indicates possible isolated ripples caused by increased marine wave energy (Tucker, 2001) during the major Smackover transgression. This earlier carbonate deposition probably occurred in a shallow marine carbonate tidal environment. The abundance of algae, sponge spicules, and peloids, in the sediments suggests the carbonate environment was still shallow and low energy. The sedimentary structure of ribbon rock suggests depositional occurred under subtidal to intertidal environment. Alternation between the peloidal mudstone to wackestone and algal boundstone/mudstone represent a fluctuation of sea level which could be additionally affected from climate variation. Interlaminated algal mats formed during shallow intertidal trapped more silt size quartz through windblown process during the low sea level period. The stacking of smaller (centimeters scale) shallowing cycles may be recognizable. Within these shallowing cycles, sedimentation began with peloidal mudstone to wackestone interpreted to occur in a lower intertidal to subtidal and then changed to probable wackestone which was highly dolomitized and was interpreted to occur during shallowing condition where meteoric water zone could become effective. The dark organic-rich sediments, occurred mostly at the base of these cycles and characterized as algal-laminated mudstone, are interpreted as the transgressive deposit formed during a stagnant, euxinic to anoxic condition. Algal boundstones (*Tuiphytes*; Moore, 1991) were later built up above this mudstone after sea level continued to rise. During the late relative sea level highstand, a shallowing conditions and an influence from meteoric water environment caused pervasive dolomitization. Increasing siliciclastic input was probably transported from the Mississippi Interior Salt basin or from the landward to the north while relative sea level was low. Under shallow water conditions, the formation of evaporite nodules occurred and was associated with the algal fragments or the microreef structures due to the effect from freshwater dissolution which had been subsequently filled by evaporite precipitation probably during increasing evaporation. The shallowing trend

toward the end of the lower Smackover was also recorded in the in Smackover Formation from the southeast part of Mississippi Interior Salt Basin (Meendsen et al., 1987) and from the Conecuh Embayment (Sigsby, 1987). On ramp stratigraphy, Burchette and Wright (1992) has pointed out that the sedimentary characteristic of sequence boundary (i.e. karst, calcretization or zone of meteoric diagenesis) or during the transition between the highstand to the lowstand sediment deposits might not be distinguishable as the very low slope angle of the platform unless sea level drop is significant. A study report from Hillgartner (1998) revealed the characteristic of the discontinuity surfaces on the ancient shallow carbonate ramp platform in France and Switzerland during the falling sea level of the third order eustatic cycle. From his observation, the sequence boundary surface which commonly influenced by topographic variations and lateral facies changes does not necessary to be a one widespread single zone; rather it appears to be expressed by zone of small-scale discontinuities or repeated environment changes due to the superposition of high frequency, low-amplitude sea-level fluctuation. Based upon Hillgartner's observation, the Smackover sedimentation occurred between 13534.5 ft to 13545 ft is interpreted as the transitional sediment deposit occurred during the relative lowstand sea level associated with a sequence boundary.

After a brief period of falling sea level, an increase in sea level resumed from 13435.5 ft to 13339. Rising sea level was interpreted by the deposition of the tidal-flat ribbon rock dolomitic wackestone/packstone to dolostone. On this Smackover sequence, tidal ribbon characteristic is less distinctive; bioturbation and carbonate diagenesis especially dolomitization appeared to be pervasive. An abundance of intraclast algal fragments also suggests that sedimentation likely occurred above the fair weather wave base (FWWB) where wave actions can be common. The presence of anhydrite nodules, mixed of fine to coarse siliciclastic grains associated with prism crack sedimentary structure suggest to a shallow flat deposition. The subtidal environment probably occurred briefly at the beginning after sea level rise and then become shallower into upper intertidal as carbonate sediment caught up and kept up with sea level. Haywick et al. (2000)

has reported the majority of dolomites which observed spanning during Smackover deposition were the types which occurred under mixing water conditions during the meteoric diagenesis exposure and the marine water zone. The presence of dolostone associated with large pore vugs filled by evaporite precipitation is interpreted as the influence of mixed meteoric-marine water which could have occurred during the late highstand to lowstand sea level. Meteoric diagenesis was possible occurred and overprinted the earlier marine diagenesis.

A sharp contact observed at 13339 ft in the #1 NEAL ET AL UNIT 30-1 core is interpreted as a transgressive surface overlying the highstand deposit of the previous sequence which probably had been overprinted by meteoric diagenesis during subaerial exposure because of falling relative sea level. The stacking pattern of small sediment cycles observed from 13339 ft to 13213 ft is interpreted to have resulted from resuming of relative sea level rise. There is no distinguishable maximum flooding surface or a condensed section because of shallow carbonate deposition, but it could have been characterized by the intercalation between subtidal dark laminated mudstone intervals and peloidal mudstone/wackestone facies mixed with glauconite minerals. During this interval, biogenic structures exhibit bioturbation with the abundance of borings and horizontal burrows, rhizoliths and dark organic material sediment layers filled with evaporites. Increasing of mixed terrestrial materials suggest a shallow deposition proximal to a coastal environment. The first presence of planar laminated siliciclastic sandstone bed (13213 ft) observed in the upper Smackover of the #1 NEAL ET AL UNIT 30-1 is interpreted as the strand plain barrier deposition. The multiple sandstone intervals interbedded with the bioturbated mudstone to wackestone carbonate sediments suggests the middle and upper shoreface deposition. Although the upper Smackover occurred in the Conecuh Embayment was mostly carbonate shoal sediments (packstone and grainstone), the intercalation between carbonate and sandstone sediments has been earlier recognized in the Mississippi Interior Salt Basin (Shew, 1991). According to Shew (1991), in the Mississippi Interior Salt Basin, the siliciclastic influx become decreasing along the north-south trend or the distant from its proximal source provenance

of the deltas (Dinkins et al., 1968), ancestral Mississippi rivers, (Mann and Thomas, 1968) or the failed rifting arm formed during an opening of the Gulf of Mexico (Ervin and McGinnis, 1975). The lateral effect of the longshore current and storm processes could have transported the finer grains of the siliciclastic sediment eastwardly and deposited in the Manila Embayment area. Shew (1991) reported the absence of finer grains and clay component in the large sandstone influx in the Mississippi Interior Salt Basin was due to the extreme current reworking and/or sediment bypassing to the distal and probably the nearby basin.

At the top the Smackover Formation, a sharp contact illustrates abrupt facies changes from the upper Smackover carbonate to the Buckner Member of the Haynesville Formation and is interpreted as possible sequence boundary. Mixed carbonate-evaporite sedimentation with some lenticular structures indicates a transgressive surface next to the erosional surface at the end of the long term Smackover sequence.

The estimated paleowater-depth variations during the Smackover depositions in the Conecuh and in the Manila Embayments are approximately sketched and shown in **Figure 4-2**. Because of a tidal environment and likely a strong effect exerted by a tidal current, sediment deposition of the Smackover carbonate in the Manila Embayment occurred on a shallower and high-frequent fluctuated-water conditions. Nevertheless, a comparison can still be made with the sedimentation occurred in the Conecuh Embayment. The label spaces on the diagrams are recognized from the core intervals which were used to describe both cores in this study.

The short-term third-order sea level cycles during the Oxfordian period affected the regressive-transgressive cycles has been reported and illustrated by the paleowater-depth recorded in the sediments. Reported from the Corallian Group of the Coast, England, four depositional sequences of regressive-transgressive cycles occurred on the three different lithological units, the limestone, argillaceous, and the sandstone, and started from the lower Oxfordian to middle and upper Oxfordian-Kimeridgian times (Sun, 1989; **Figure 4-3**). A regressive cycle was characterized by a shallowing-upward succession and was separated from a transgressive cycle, or a deepening upward

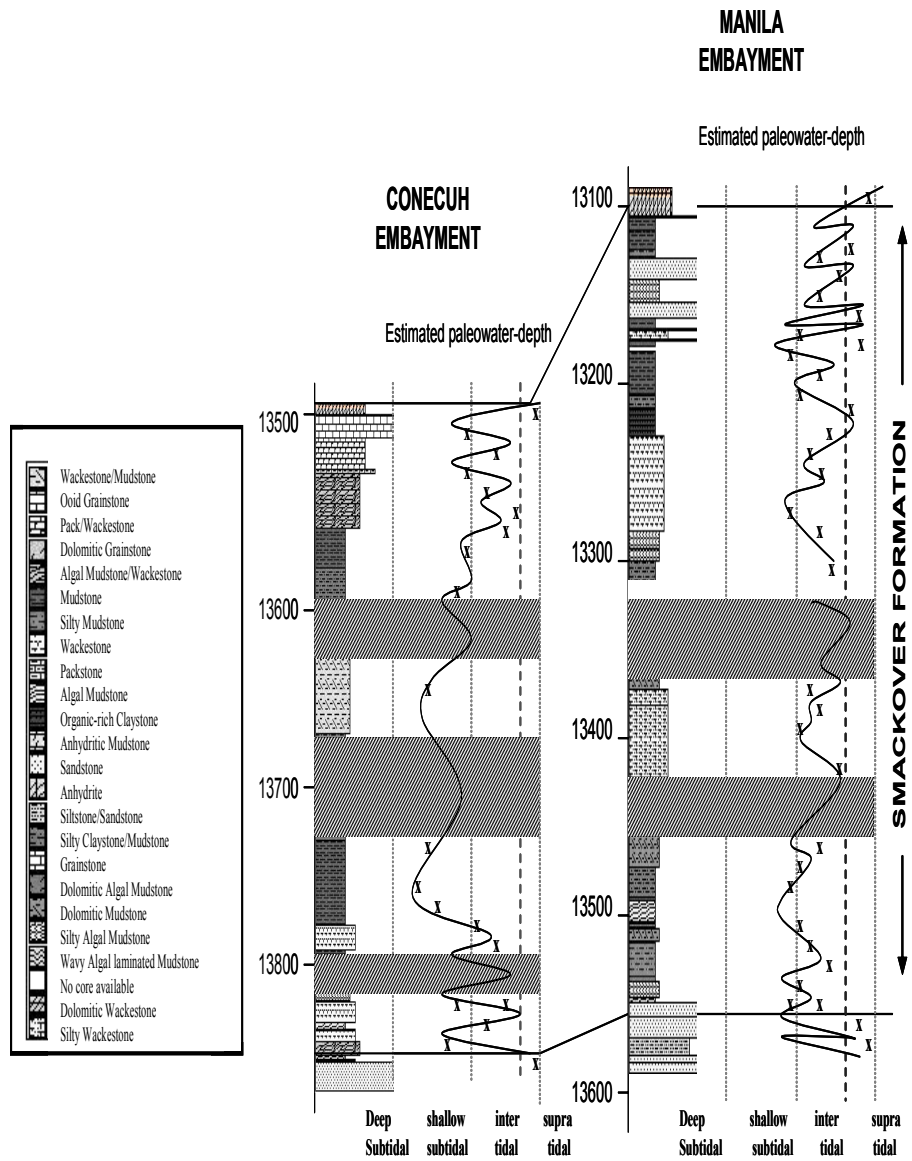


**Figure 4.2.** Approximated paleowater-depth interpretation of the #1 T.R. MILLER MILL 17-11 core and the #1 NEAL ET AL. 30-1 core from the Conecuh Embayment and the Manila Embayment. Lithologic column was based upon core description presented in Table 4-1 and Table 4-2.

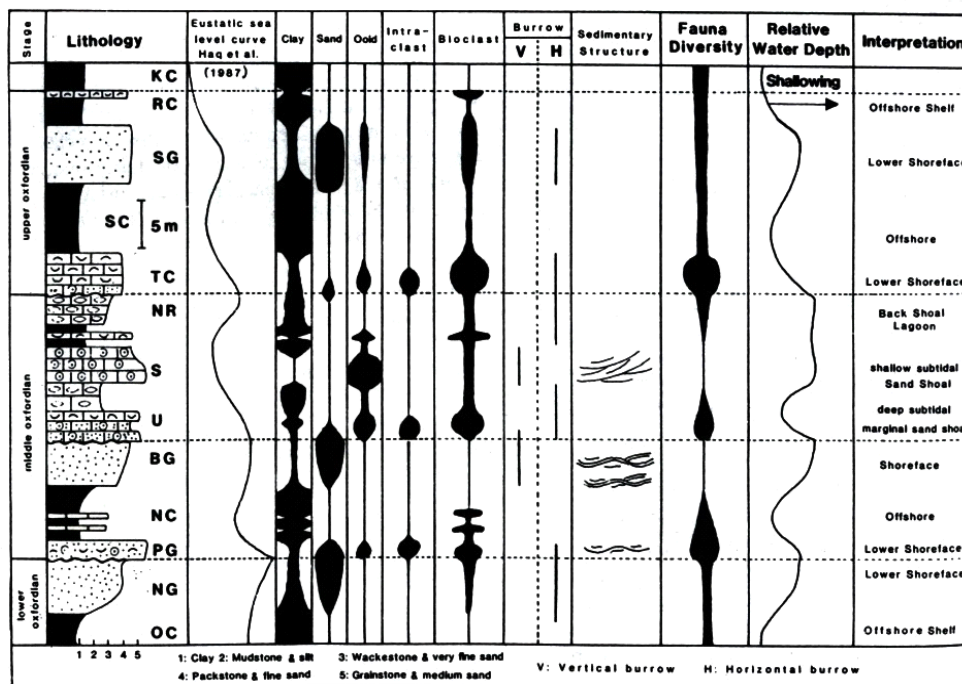


**Figure 4-3.** Depositional cycles recorded by relative water depth variation of the Corallian Oxfordian sequence from the Dorset Coast, England (Sun, 1989). The sediment sequence is equivalent age to the Smackover Formation on the United States and illustrated variation of paleowater-depth related to third-order relative sea level changes.

sequence, by a sharp-erosional surface. Compared to the Corallian Group, although the Smackover deposition was possibly controlled by the same eustatic sea level cycles, a different depositional environment and a setting of the Smackover carbonate on a ramp platform would make the carbonate and siliciclastic variation during the Smackover to be different pattern. Nevertheless, the similarity of sedimentary cycles that occurred on this large scale between sediments of different continents seems to support that the global relative sea level changes could be their major control in addition to local variation of depositional condition.

#### 4.3.2 A COMPARISON BETWEEN THE SMACKOVER CORES

A summary of the core lithofacies observations made from macroscopic and thin section analysis for the two locations is:

|                                     | <b>T.R. MILLER MILLS 17-11, #1<br/>(Conecuh Embayment)</b>   | <b>#1 NEAL ET AL UNIT 30-1<br/>(Manila Embayment)</b>   |
|-------------------------------------|--|---|
| <b>Predominant carbonate facies</b> | Algal laminate mudstone, mudstone, peloidal wackestone; ooid packstone and grainstone  | Mudstone and wackestone ribbon rocks; laminated to massive sandstones   |
| <b>Depositional environment</b>     | Partial restricted lagoonal-shoal barrier, open marine   | Shallow marine peritidal, coastal/shoreline   |
| <b>Diagenesis</b>                   | Cementation, micritization in the lower smackover; dissolution and dolomitization in the upper ooid packstone and grainstone | Cementation, micritization and dolomitization throughout the core but were intense in particular depth interval associated with evaporite replacement nodules |
| <b>Interpreted</b>                  | Subtidal lagoonal mudstone/wacke-  | Lower intertidal  |

|   |   |  |
|---|---|--|
| <b>highstand deposit</b>                                      | stone with normal marine fossils; shoaling packstone/grainstone   | mudstone/wackestone; shoreface siliciclastic sandstones  |
| <b>Interpreted lowstand deposit</b>                           | Adjacent to late highstand carbonate sedimentation, intercalation between carbonates and siliciclastic intervals, algal laminate mudstone, small fenestral pores filled with evaporite minerals | Intense diagenesis of dolomitization superimposed of previous highstand deposit; increase siliciclastic input; abundance of large evaporite, anhydrite nodules |
| <b>Interpreted transgressive or flooding surface</b>          | Subtidal planar laminate mudstone or normal marine carbonate on top mixed carbonate and siliciclastic interbedded   | Subtidal laminate mudstone on top of partial structureless dolomitized wackestone to packstone   |
| <b>Interpreted discontinuity contact or sequence boundary</b> | Undifferentiated; amalgamated between late highstand to lowstand deposit; repetitive carbonate and siliciclastic intercalation  | Sharp contact of deeper facies overlying intensive dolomitized shallow facies; multiple cycles   |

#### 4.4 CONCLUSIONS

Core observations suggest that depositions of the Smackover in the T.R. MILLER MILLS 17-11, #1 well of the Conecuh Embayment and the #1 NEAL ET AL UNIT 30-1 of the Manila Embayment of southwest Alabama occur under different depositional environments and paleowater-depth. In the Conecuh Embayment the Smackover carbonate abruptly overlies the eolian sandstone of the Norphlet Formation. The sharp contact is interpreted as a possible sequence boundary and the missing sediment could probably result from a weathering process during subaerial exposure. During the Smackover period, the Conecuh Embayment was probable

partially restricted to a normal marine environment by the paleostructural highs of the Paleozoic basement. The depositional environment during the lower Smackover was mostly restricted to the lagoonal-tidal flat system where carbonate sediments were dominated by algal laminated mudstone, peloidal mudstone/ wackestone and micritic pelletoid-oncoidal wackestone to packstone. Diversity of marine fossils was very low but a few normal marine fossils could be observed during a high relative sea level cycles. Dolomitization is limited in the lower Smackover mudstone and the uppermost Smackover grainstone and packstone. The evaporite anhydrite nodules were mainly associated with the algal boundstone and micritic, pelletoid-oncoidal wackestone to packstone of a microreef. The presence of microbial boundstone or microreef in the lower Smackover of the T.R. MILLER MILLS 17-11, #1 core is found to be similar to other Smackover reports which were interpreted as a brief relative sea level falling period near the end of the lower Smackover deposition. Ensuing sea level rises in the next period affected the restricted condition in the Conecuh Embayment and permitted a better condition to normal marine environment.

In the Conecuh Embayment, the periods of relative sea level falling exhibit an abundance of siliciclastic sediment influx interrupting carbonate deposition. The incoming of siliciclastic influx was initially observed during the late highstand sea level and increased during the lowstand as sea level also regressed. A sequence boundary is not distinguishable in this embayment area as the sea level falling was probable not substantial due to a lack of the subaerial exposure. Organic-rich sediments deposited during the transgression period deposited adjacent to the mixed siliciclastic-carbonate lowstand sediment with or without the distinct transgressive surface. In the middle Smackover, in the vicinity of the T.R. MILLER MILLS 17-11, #1 well, the relative sea level fall allowed argillaceous clays and fine grain siliciclastic components from the river systems in the area to be transported farther onto the exposed platform and into the ocean. Because of lowstand sea level, a partial restriction affected from structural high would decrease water energy and water level in the embayment. Water evaporation without or small normal marine water

recharge could promote hypersaline condition during the late highstand and the falling period of relative sea level. After sea level was rising again, the increased paleowater depth and decreasing siliciclastic input gave way to carbonate sediment to catch up and keep up illustrating an abundance of more carbonate grains in sediments. The shallowing carbonate cycles are not really recognizable but the presence of scattered fenestral features filled with evaporite minerals might be indicative a shallowing condition or warmer climates. The next relative sea level falling cycle characterized an interruption of this carbonate sedimentation with an increase of fine grained siliciclastic and clay influx which appeared to occur periodically during river discharges cycles. A lowstand deposit of mixed siliciclastic/carbonate or a siltstone and wackestone exhibit bioturbation and abundant fossils from shallow and low energy conditions. In the upper Smackover, when sea level was relatively high, high energy and normal marine environments prevailed and allowed a shoal barrier to be established. Diagenetic alterations are distinctive as carbonate mineral in most grains (aragonite) was highly unstable and subject to dissolution showing ooid vugs where reprecipitation occurred. The mixing between seawater and freshwater became prominent as dolomite formation occurred.

In the Manila Embayment, the Smackover depositional environment was significantly different from that in the Conecuh Embayment due to a geographic separation caused by a paleohigh structure of the Conecuh Ridge. During the Smackover period, the partial connection between the Manila Embayment and the Mississippi Interior Salt Basin (Wade et al., 1987) could affect larger distant for wave and current transporting siliciclastic influx from the Mississippi Interior Salt Basin to the Manila Embayment. Carbonate sedimentation in the Manila Embayment, thus, illustrates higher content of the terrigenous component. Core observation from the #1 NEAL ET AL UNIT 30-1 suggests the Smackover deposition in the Manila Embayment occurred in a shallow marine tidal environment. Carbonate deposits illustrate sedimentary structures of shallow tidal-flat from upper to lower intertidal which dominated by ribbon rocks, biogenic structures, pore vugs filled with evaporites, and prism cracks. Subtidal

sedimentation with a dark laminated mudstone occurred during the repeated transgressive events adjacent to the lowstand deposit of the previous sea level cycle. The pervasive dolomitization in this core suggests the diagenetic environment could be influenced by meteoric water during falling relative sea level in the late highstand and lowstand. In the #1 NEAL ET AL UNIT 30-1 Smackover core, two sediment intervals illustrated a highstand deposit which probably had been overprinted by meteoric diagenesis during the period of relative sea level fall. The disconformable surface, or possibly a sequence boundary, did not exhibit a single surface but instead comprised of repeated smaller cycles which were probably influenced by a higher frequency of sea level fluctuation. In the upper Smackover, the interbedded siliciclastic sandstone intervals with carbonate sedimentation characterized the shoreface deposition during a long-term regressive Smackover sequence.

Core observations of the Smackover sequence from the Conecuh Embayment and the Manila Embayment suggest the lower Smackover sequence boundary is not necessarily coincident with the formation contact. The sharp contact and abrupt facies changes from shallow to a deeper facies in the upper Smackover next to the Buckner anhydrite in both cores, however, suggest to possible fall of relative sea level where erosion probably also involved

Although the paleoenvironments between the Smackover deposition in the Conecuh Embayment and in the Manila Embayment differed because of paleotopography, geological settings, diagenetic environments, and siliciclastic distribution and influx, core observations suggests the sequence stratigraphic framework between the two depositional areas can be correlated. The Smackover Formation in both cores illustrate three possible shorter regressive-transgressive cycles superimposed on single long-term regressive sequence. During these three shorter cycles, a time span for each sea level cycle and the rate of rise and fall sea level were probably the major controls for carbonate sediment accumulation and sedimentary facies component between the two areas.

## CHAPTER 5

### 5.1 SILICICLASTIC AND CARBONATE RELATED ELEMENTS

Sedimentary rocks deposited in an ocean basin consist of a number of different components and minerals derived from different sources which are detrital, authigenic and biogenic (Kastner, 1999). Evidence for the origin and subsequent recycling processes of these materials in the ocean can be examined either directly or indirectly from the rock fragments and from disassociated minerals or chemical elements. In general, the detrital components are rock fragments of aluminosilicates primarily derived from the continent by weathering, and supplied to the ocean by rivers, ice or wind. The original source rocks of the continent may include exposed metamorphic, igneous and/or older sedimentary rocks. The inorganic authigenic components are comprised of different types of precipitates formed in the nearshore or offshore areas and materials which formed after deposition of the bulk sediment. The biogenic components are commonly derived from the inorganic skeletal remains of marine organisms or come from dispersed organic materials produced by degradation of organic tissues. In marine carbonate environments, although the sediment accumulations are primarily of a biogenic and authigenic origin, the proportion of non-carbonate detrital grains (terrigenous clastics) can be present depending upon the geological setting and conditions which affected the transportation and depositional processes. In this chapter, variations of carbonate and siliciclastic elements in the Smackover deposition from the Conecuh and the Manila Embayments will be investigated for the information related to their sources, existing environment and post-depositional diagenetic environments.

Major, minor, and trace elements are basic constituents in minerals which in turn become basic constituents of sedimentary rocks. Different types of sedimentary rock consist of variable concentrations of major and minor elements which are governed by their relative proportions in

minerals. Siliciclastic sediments usually results from physical and chemical rock weathering where the weathered grains are transported by different processes to sedimentary basins with different types of depositional environments. With increasing transportation distant, the grains from the original rocks generally become enriched in aluminosilicate and feldspar minerals such as  $\text{Al}_2\text{O}_3$ ,  $\text{Fe}_2\text{O}$  and  $\text{K}_2\text{O}$  and depleted in  $\text{SiO}_2$ ,  $\text{FeO}$ ,  $\text{CaO}$ , and  $\text{Na}_2\text{O}$ . The detrital grains which are abundant in the clastic sediments and predominate in silt-size, sand-size, or larger, are quartz, feldspar, rock fragment and heavy minerals. Smaller size fractions which can be transported for longer distances are the detrital clay size particles consisting primarily of different clay minerals. In carbonate sediments which are products of biogenic and inorganic processes, the major minerals (more than 50%) are carbonate minerals such as calcite (high and low magnesium  $\text{CaCO}_3$ ), dolomite ( $\text{CaMg}(\text{CO}_3)_2$ ) and aragonite ( $\text{CaCO}_3$ ). The constituent elements in these minerals are Ca, Mg and C. Other minor and trace elements can be incorporated with carbonates during and after burial depending upon their distribution coefficient relative to the Ca ions (Veizer, 1983). For example, with larger crystal lattices (e.g orthorhombic) such as aragonite, the larger elements such as Sr, Na, Ba and U are more readily incorporated while smaller crystal lattices (e.g. rhombic) of calcite prefer to accommodate the smaller elements such as Mg, Fe, Mn, Zn, Cu and Cd (Brand and Veizer, 1980).

In carbonate deposition, factors important to carbonate production and sedimentation are sea level changes, climate, light, temperature, and nutrients (Wilson, 1975; Tucker and Wright, 1990). An interruption of carbonate production can be affected by an increase in terrigenous sediment input which can cause water turbidity. In addition, if the amount of light that can reach the sea floor is diminished, photosynthesis, which is necessary for growth of calcareous algae and sea grasses and other marine organisms, is discouraged and affects the overall carbonate precipitation. Therefore, it is not uncommon to observe a reverse correlation between carbonate and siliciclastic sediments or elements which are associated with them. A number of studies of recent and ancient sediments grouped major and minor elements and used them as indicators for

provenance and transport processes. The element groups are Al, K, Na, Rb, Ga, Cr, Li, B, Ba, Pb for aluminosilicate minerals, Ca, Sr, Mg, CO<sub>2</sub> for carbonate, Fe, Co, Mn, V, P for the dispersed oxide minerals, Na, B, Ba, Be for clay minerals and glauconite, and Ti and Zr for heavy mineral input (Hirst, 1962a and b; Spencer, 1968; Price and Wright, 1971; Calvert, 1976). Some of those elements may also reflect conditions of paleoenvironment deposition, i.e. oxic and anoxic environment and these are Cu, Cd, Ni, Zn, V, Cr, Pb, Re, and U (Calvert and Pedersen, 1993). The relation among many of these elements in the recent sediment has been illustrated by Calvert (1976) on a cluster analysis (data from Hirst, 1962a and b; **Figure 5-1**).

## **5.2 CARBONATE DIAGENETIC EFFECTS**

During and after deposition, sedimentary rocks undergo diagenetic alteration affected by pore water chemistry and burial conditions associated with elevated temperature and pressure. For carbonates, diagenetic processes include micritization, cementation, neomorphism, dissolution, compaction and dolomitization (Tucker and Wright, 1990; Chapter 7). Diagenesis in carbonate sediments usually starts at the seafloor during sedimentation and continues with increasing burial depth. Upon diagenesis, concentrations of major and minor elements incorporated in the carbonate minerals also change from their original concentrations. The chemical composition of ancient carbonate rocks can be used as a parameter for evaluating the diagenetic effect and deducing the stabilization of the original carbonate minerals. Stabilization of metastable carbonate assemblages during diagenesis is also achieved through complimentary textural, mineralogical and chemical changes. The original carbonate precipitation will usually incorporate major and trace elements from the ambient seawater conditions. The initial precipitated inorganic components are therefore in equilibrium with those in the sea water (Brand and Veizer, 1980). Under diagenetic conditions, the three original carbonate minerals: a low-Mg calcite, high-Mg calcite and aragonite, can be dissolved partially or fully, exchange, and/or mix

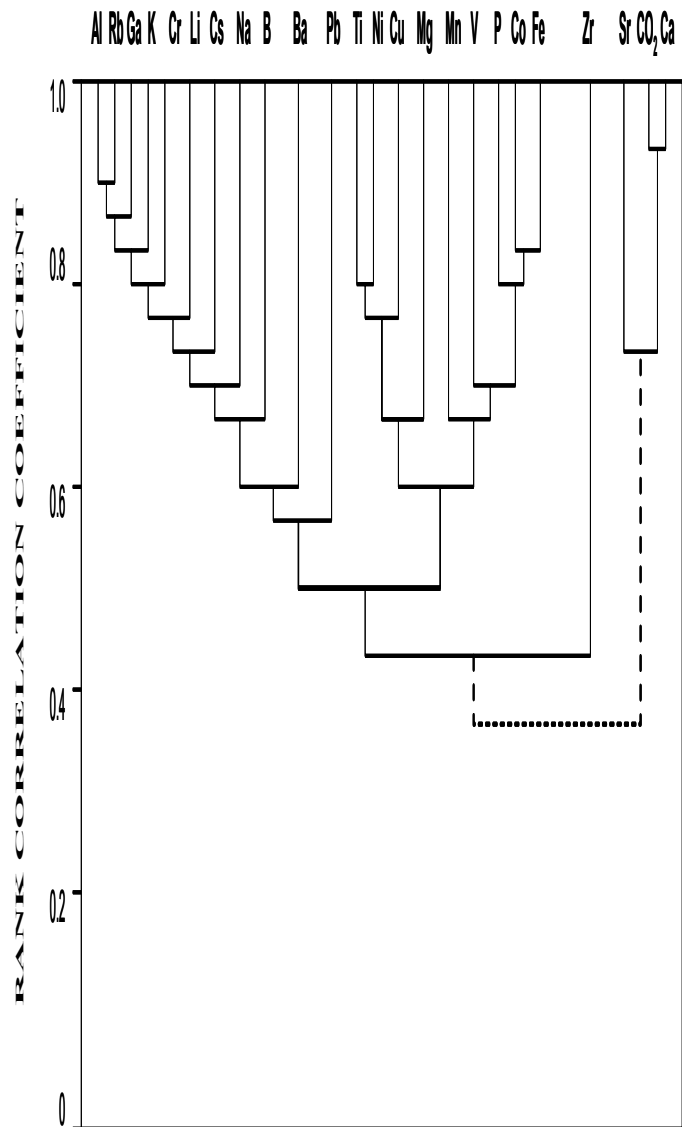


Figure 5-1. Cluster analysis illustrating relationship of different elements on chemical compositions of recent sediments from the gulf of Paria (from Calvert, 1976, with original data from Hirst, 1962).

with trace elements and stable isotopes of those in the interstitial water. The stabilized calcite mineral, which is the diagenetic low magnesium calcite, usually accompanies some changes in variable element concentrations. If exposed under meteoric water, diagenetic low-Mg calcite can consist of trace elements and stable carbon isotope values which are comparable in their ratios to the compositions of interstitial meteoric water. The carbonate-related elements which could be affected under this condition are Sr, Na, Mg, Mn, Fe, and Zn (Brand and Veizer, 1980). Due to the concentration differences between seawater and meteoric water elements (**Table 5-1**), carbonate sediments of diagenetic low-Mg calcite generally become depleted in Sr and Na (and lighter  $\delta^{18}\text{O}$  and  $\delta^{13}\text{C}$ ) but enriched in Mn, Fe and Zn concentrations (Veizer 1983). These altered concentrations, however, can still be used to infer the depositional environments and, to some degree, the changes of chemical composition during relative sea level fluctuation. It was recommended by Veizer (1983) that an alteration of the carbonate trace elements by diagenesis would usually occur below or would not exceed the concentration limits which existed in the primary rocks. This is because the sediment pore volumes are relatively smaller compared to the larger volume of the bulk rocks. Therefore, the relative differences between the original concentrations of individual elements during variable mineralogical phase can still be preserved, to some degree, even though the absolute concentrations have been changed. Examples of diagenetic studies of ancient carbonate rocks can be found by Rachold and Brumsack (2001) and Dolenec et al. (2001). In this study, chemical compositions of Smackover sedimentation from the two study areas have been investigated. The purpose of the study is to clarify differences and similarities between sediments of the two depositional locations in term of depositional environments and diagenetic effects which may lead to an understanding of the controlling factors on the Smackover sedimentary sequence.

**Table 5.1** Chemical compositions of major and minor elements in the sea water and freshwater streams (from Veizer, 1983).

|  | Seawater             | Freshwater (Stream) |
|--|----------------------|---------------------|
| <b>Major elements (mg/kg or ppm)</b>         |                      |                     |
| Chloride (Cl)                                | 19,350               |                     |
| Sodium (Na)                                  | 10,760               | 5.1                 |
| Sulfate (SO <sub>4</sub> <sup>2-</sup> )     | 2,710                |                     |
| Magnesium (Mg)                               | 1,290                | 3.8                 |
| Calcium (Ca)                                 | 411                  | 14.6                |
| Potassium (K)                                | 399                  |                     |
| Bicarbonate (HCO <sub>3</sub> <sup>-</sup> ) | 142                  |                     |
| Strontium (Sr)                               | 8                    | 60                  |
| Silica (Si)                                  | 0.5-10               |                     |
| Oxygen (O <sub>2</sub> )                     | 0.1-6                |                     |
| Nitrate (NO <sub>3</sub> <sup>2-</sup> )     | 0.005-2              |                     |
| Phosphate (PO <sub>4</sub> <sup>3-</sup> )   | 0.001-0.05           |                     |
| Dissolved organic matter (as C)              | 0.3-2                |                     |
| <b>Minor elements (µg/kg or ppb)</b>         |                      |                     |
| Lithium (Li)                                 | 180                  | 10                  |
| Beryllium (B)                                | 6 x 10 <sup>-4</sup> | 20                  |
| Aluminium (Al)                               | 2                    | 50                  |
| Titanium (Ti)                                | 1                    | 10                  |
| Vanadium (V)                                 | 2                    | 1                   |
| Chromium (Cr)                                | 0.3                  | 1                   |
| Manganese (Mn)                               | 0.2                  | 8                   |
| Iron (Fe)                                    | 2                    | 40                  |
| Copper (Cu)                                  | 0.5                  | 7                   |
| Cobalt (Co)                                  | 0.05                 | 0.2                 |
| Zinc (Zn)                                    | 2                    | 30                  |
| Nickel (Ni)                                  | 0.5                  | 2                   |
| Zirconium (Zr)                               | 0.03                 |                     |
| Barium (Ba)                                  | 2                    | 50                  |
| Lead (Pb)                                    | 0.03                 | 1                   |
| Molybdenum (Mo)                              | 10                   | 0.5                 |
| Cadmium (Cd)                                 | 0.05                 |                     |
| Iodine (I)                                   | 60                   |                     |
| Gold (Au)                                    | 4 x 10 <sup>-3</sup> | 0.002               |
| Silver (Ag)                                  | 0.04                 | 0.3                 |
| Mercury (Hg)                                 | 0.03                 |                     |
| Radium (Ra)                                  | 1 x 10 <sup>-7</sup> |                     |
| Uranium (U)                                  | 3.3                  | 0.1                 |
| Thallium (Th)                                | 0.01                 | 0.1                 |

### 5.3 SMACKOVER ELEMENTAL ANALYSIS

Whole rock samples of the Smackover carbonate, including the Norphlet sandstone and the Buckner anhydrite, are used for the analysis of their major, minor and trace elements by X-ray fluorescence (XRF) techniques. A total of sixty five samples from the T.R. MILLER MILLS 17-11, #1 well of the Conecuh Embayment and seventy five samples are from the #1 NEAL ET AL UNIT 30-1 well of the Manila Embayment were characterized in this study. Twenty-three samples from the total sixty-five samples of the Conecuh Embayment were also analyzed by X-ray diffraction (XRD) for carbonate and evaporite minerals for confirmation. Techniques and instrumentation have been previously described in Chapter 3. The elements which are associated with carbonate and/or siliciclastic origins investigated in this study are Al, Si, Ti, Fe, Mn, Mg, Ca, Na, K, P, Sr, Pb, Ba, Zn, Cu, Ni, Cr and V. Most major and minor elements are measured as a percentages of oxide minerals which are subsequently recalculated and converted into percentages of each element based on their atomic weights. In this study, the concentration of an element which is less than the instrument detection limits (2 ppm) is approximated to 0.5 ppm in order to permit normalization with respect to major elements. For terrigenous components, aluminium (Al) is used as proxy for additional input from the current background (Calvert, 1990; Murray and Leinen, 1996). Although Al can also have authigenic origin, from the early X-ray diffraction (XRD) and scanning electron microscopy (SEM) analysis of Amy et al. (1995), it was been shown that the authigenic clay content in the Smackover carbonates (from the Manila Embayment) is relatively low and insignificant. In order to eliminate the effects from sediment dilution and the mixed influence from either carbonates or siliciclastics, most of analyzed elements are normalized and reported as ratios with respected either to Al or Ca. The siliciclastic elements normalized to Al are Ti, Si, Fe, K, Na, Mn and P. The carbonate minor, and trace elements Mg and Sr and Mn will be normalized with respected to Ca. For Mn, its presence will be

discussed separately as Mn concentration in sediments were used not only for indicating the redox conditions of depositional environments (Calvert and Pedersen, 1993; 1996) but it has been recently related to the changes of eustatic sea level cycles (third order) associated with the hydrothermal activities during the oceanic ridge spreadings (Corbin et al., 2000; De Rafelis et al., 2001). The presence of the Na and P are also reported as ratios normalized to Ca so that diagenetic effects of these elements are constrained with trends of oxygen isotope variation. The results from elemental analysis from samples derived from the two Smackover cores are presented in **Appendix 5-1** and **Appendix 5-2**.

## **5.4 RESULTS AND DISCUSSION**

### **5.4.1 Siliciclastic related elements**

The carbonate and siliciclastic distributions for the Smackover carbonates of the Conecuh and the Manila Embayments are compared in the ternary diagrams of the three elements, Ca, Al and Si (**Figure 5-2**). These diagrams exhibit the sedimentation in the two embayments consisted of similar relative proportions of carbonate (Ca) and aluminosilicate (Al), although the measured concentrations of these three elements are variable. An inverse relationship between Al and Ca is observed in samples from both Smackover core sequences. In the Manila Embayment, samples with increased silica (Si) content and presented near the axis point correspond to multiple sandstone units interbedded with carbonate sediments in the upper Smackover.

The negative vertical covariations between siliciclastic related elements, Al, Ti, Si, Fe, K and Ca (**Figure 5-3a and b**) suggested that Smackover sedimentation related to the presence of these elements was controlled by a simple two-component mixing model. With increasing siliciclastic influx, carbonate production became interrupted along with carbonate content in the samples. However, other factors such as depositional energy, redox conditions and weathering

CONECUH EMBAYMENT  
(T.R. MILLER MILLS 17-11,#1)

MANILA EMBAYMENT  
(#1 NEAL ET AL UNIT 30-1)

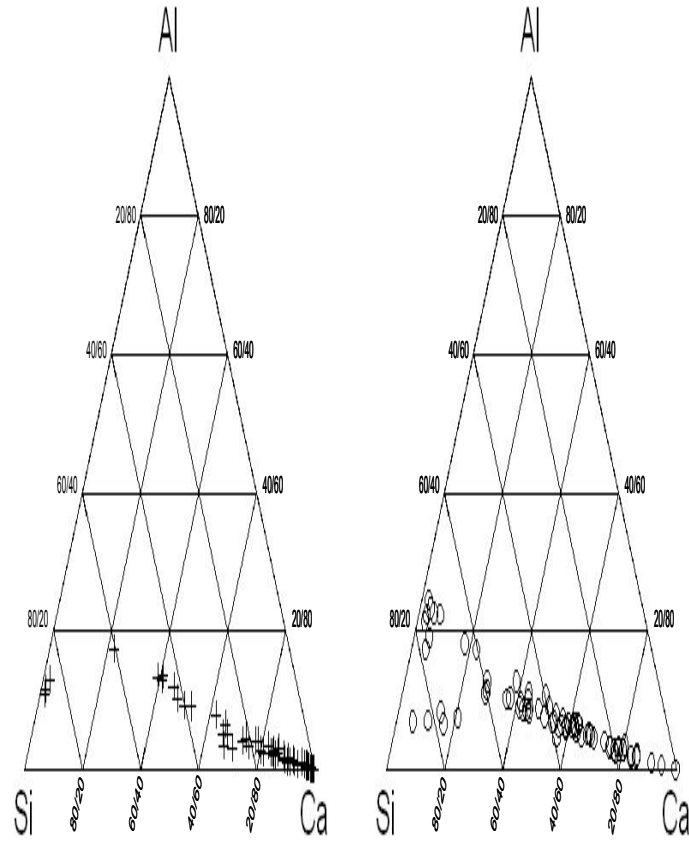
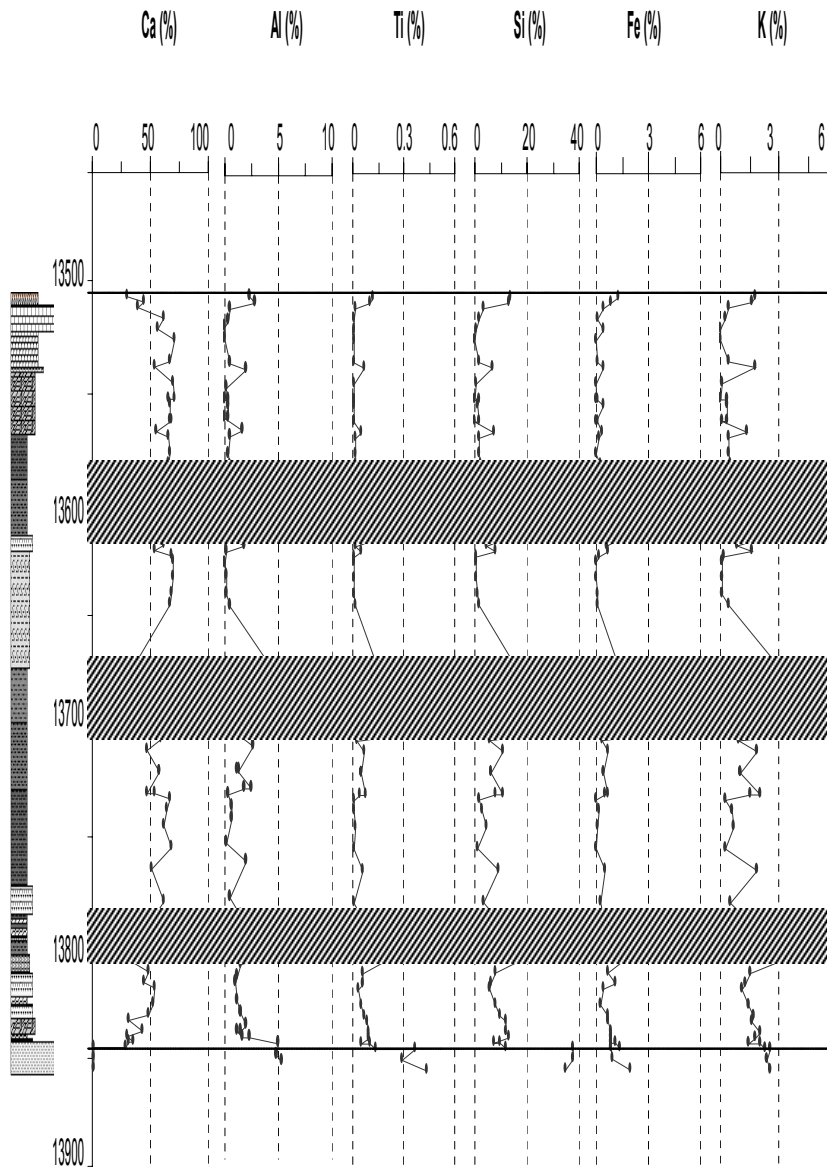


Figure 5-2 Ternary diagrams illustrating relative content of the Ca, Si and Al elements in the Smackover samples from the Conecuh and the Manila Embayments.

# CONECUH EMBAYMENT - T.R. MILLER MILLS 17-11, #1 WELL



**Figure 5-3a.** The vertical distributions of siliciclastic related elements compared to Ca of the Smackover samples from the Conecuh Embayment. Data are listed in Appendix E.

# MANILA EMBAYMENT - #1 NEAL ET AL UNIT 30-1 WELL

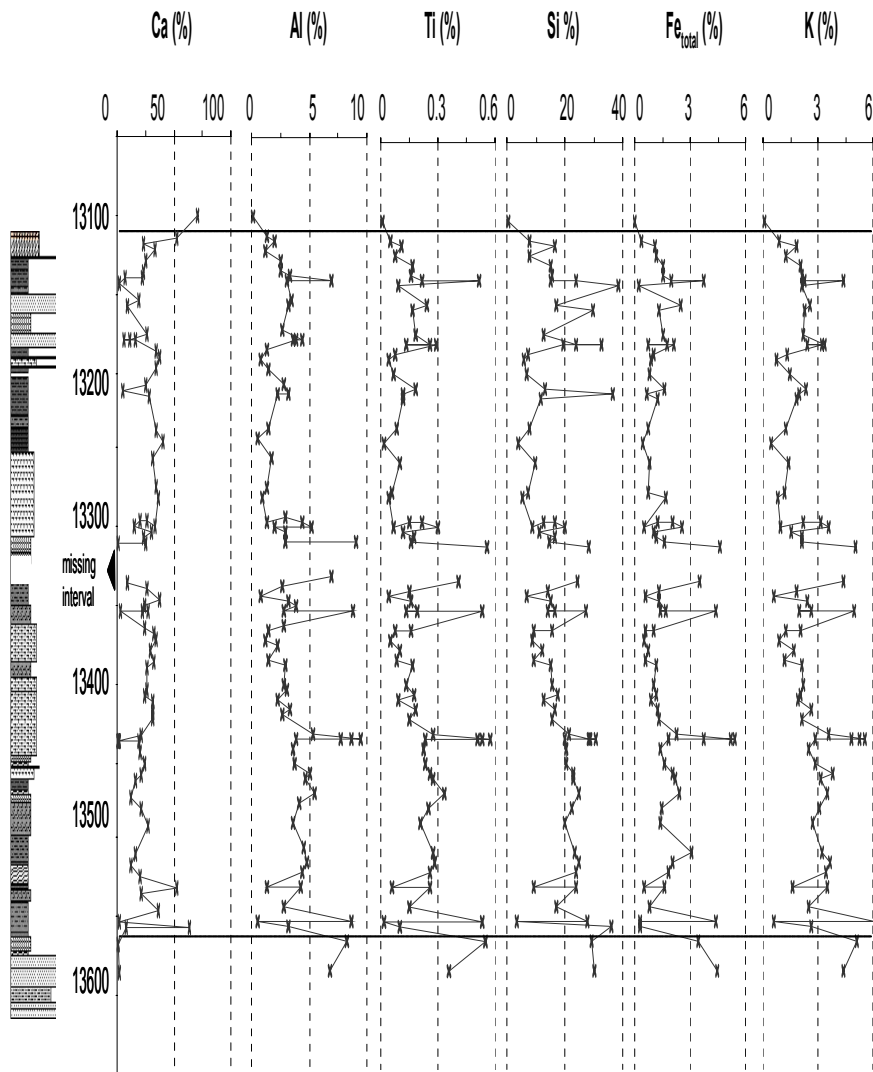


Figure 5-3b. The vertical distribution of siliciclastic related elements compared to Ca content of the Smackover samples from the Manila Embayment. Data are listed in Appendix F.

etc. may also involved with individual elements as discussed later. In the Conecuh Embayment, the inverse correlation between siliciclastic input based upon Al content and carbonate sedimentation is clearly observed (Ca/Ca+Al ratios are used for carbonate component in order to minimize Ca from CaO from the siliciclastic fraction). Although some positive covariation of Al is observable between the two Smackover cores, the concentrations of Al are variable between these two Smackover cores. The higher Al content in the Smackover sedimentation of the Manila Embayment suggests a proximal geological setting to terrigenous sources as compared to the Conecuh Embayment. During lower Smackover deposition, shallow and adjacent coastal conditions of the Manila Embayment, interpreted as tidal-flat environment in the previous chapter, continued to receive an abundant siliciclastic input from land compared to the Conecuh Embayment which was probably located farther seaward and under deeper conditions. Less contamination from siliciclastic sediments in the Conecuh Embayment therefore permitted higher carbonate growth and accumulation. During Smackover deposition in the Conecuh Embayment, carbonate sedimentation illustrates distinct intervals of increasing siliciclastic influx (13740 ft to 13765 ft; 13622 ft to 13589 ft). This increasing siliciclastic influx also occurred during Smackover sedimentation in the Manila Embayment, but because of a larger siliciclastic content in the background, this variation was less distinguishable in the #1 NEAL ET AL UNIT 30-1 core sequence. The variation in siliciclastics between Smackover deposited in the Manila and the Conecuh Embayments could be influenced by different structural settings which affected a transportation and availability of siliciclastic sediment source on these inner ramp depositional environments.

For each individual element, additional influences may also be recognized when the normalized ratios with Al are considered (**Figure 5-4a and b**). Because of a stronger variation between the carbonate and siliciclastic components, these other influences can be better recognized from the element variation that occurred in the T.R. MILLER MILLS 17-11, #1 core from the Conecuh Embayment than the #1 NEAL ET AL UNIT 30-1 from the Manila

# CONECUH EMBAYMENT - T.R. MILLER MILLS 17-11, #1 WELL

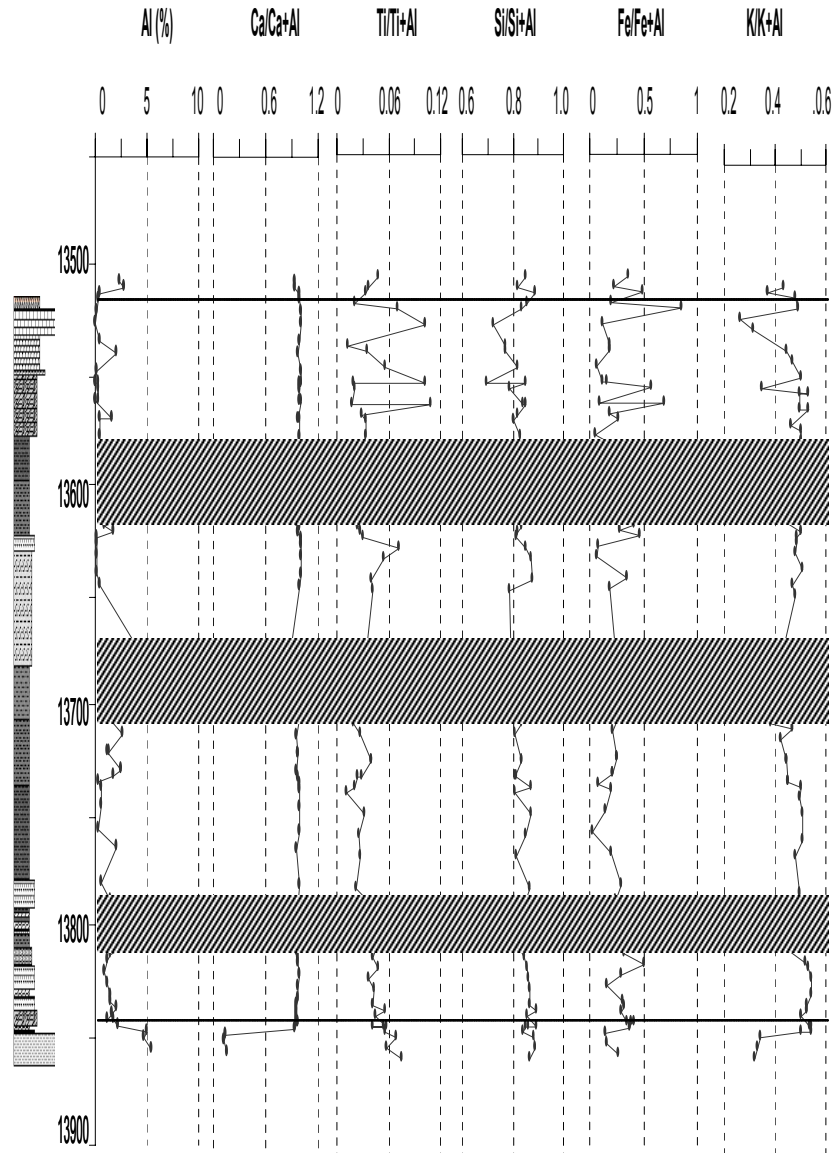


Figure 5-4a. Al and Al-normalized siliciclastic major elements in comparison with Al-normalized Ca for eliminating siliciclastic influence on the Smackover samples from the Conecuh Embayment. Data are listed in Appendix E.

# MANILA EMBAYMENT - #1 NEAL ET AL UNIT 30-1 WELL

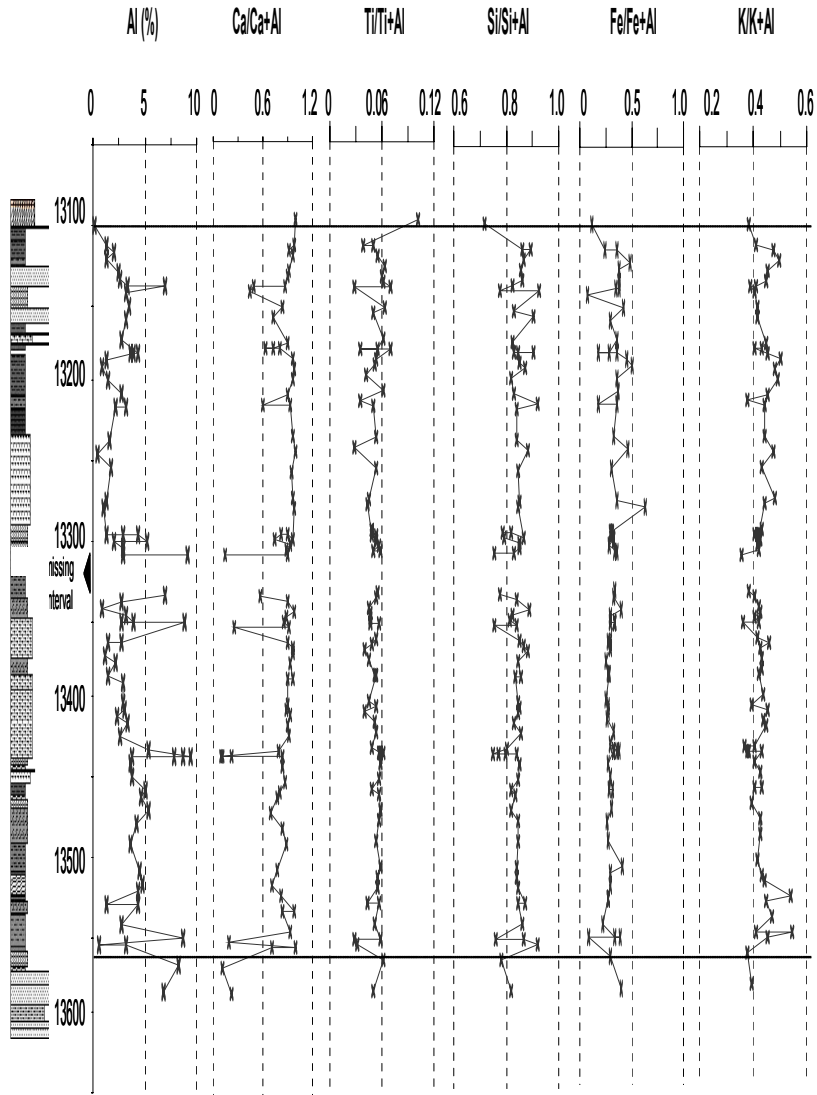


Figure 5-4 b. Al and Al-normalized siliciclastic major elements in comparison with Al-normalized Ca on eliminated siliciclastic influence on the Smackover samples from the Manila Embayment. Data are listed in Appendix F.

Embayment. Except for a higher fluctuation in the upper Smackover, samples of the Manila Embayment illustrate a trend which is rather uniform that suggests a primary siliciclastic control of these elements under variable depositional conditions. In the Conecuh Embayment, higher normalized ratios of Ti to Al indicate an increased depositional energy in the carbonate environment from the lower to upper Smackover period. This interpretation is in agreement with the formation of the shoaling environment observed in the upper Smackover in the Conecuh Embayment. An almost uniform Si to Al trend (interpreted as Al increasing, Si also increasing correlatively) with some slightly higher values in the lower Smackover (probably affected by different larger grain size) suggests the Si content was primarily associated with siliciclastic component. For the Fe/Fe+Al ratio, the long-term fluctuation trend and the variation in correlation with Al and Ca/Ca+Al suggest Fe was probably not entirely bound to aluminosilicate minerals but instead may have been associated with pyrite or oxyhydroxide minerals that were affected by the depositional environment. An almost inverse correlation between the K/K+Al and Al indicates most siliciclastic inputs in the Smackover sediment of the Conecuh Embayment are likely silt or clay size particles dominated by clay minerals instead of feldspar minerals which are higher in K element. This observation could be interpreted by saying that siliciclastic influx during Smackover deposition in the Conecuh Embayment area represented the distal sediment from the river discharge or deltaic system. The smaller size particles were transported farther away from the original source location. This event could be interpreted to occur during falling relative sea level by seaward migration of these rivers of the deltaic system. The other possibility was it occurred due an enhanced chemical weathering on the continent area without relative sea level changes, or by the combination of both effects. Reinhardt and Ricken (2000) suggested K/Al ratio, in comparing with Ti/Al and Si/Al ratios, as an indicator for siliciclastic input due to weathering process. With increasing chemical weathering the K/Al ratio in the rock could become different. Higher weathering would lower the K/Al (or K/K+Al) ratio as increasing Al content. In reverse, when low to absence weathering processes, siliciclastic fraction could have

higher K/Al values. Therefore it is possible that variation of K/Al ratio observed in the Smackover sedimentation, especially the Conecuh Embayment, may refer to the changing conditions during sea level fluctuation and/or variation in chemical weathering processes. Because the variation of the K/K+Al values is not distinctive in the Smackover in the Manila Embayment which received higher siliciclastic influx, this enhanced chemical weathering effect, although possible, needs more investigation.

#### **5.4.2 Carbonate related elements**

The ternary diagrams for Ca, Sr and Mg illustrate variable carbonate chemical compositions between the Smackover deposition in the Conecuh and Manila Embayments (**Figure 5-5**). Arbitrary multipliers are applied to the Sr and Mg concentrations in order to relocate the data for better display. In the Conecuh Embayment, Smackover samples are dominated by samples with relative high Ca content which have a low to moderate Sr and Mg content. In contrast, the Smackover of the Manila Embayment is comprised of samples which are much higher in Mg, but low and variable in Ca and Sr. The variation of the Ca and Mg concentrations between the two Smackover wells are believed to be affected by different diagenetic conditions especially for dolomitization. In general, the diagenetic conversion of the original mixed carbonate phases (high-Mg calcite, low-Mg calcite and aragonite) to the stable low-Mg calcite phase generally leads to a decrease in Sr, Mg and Na concentrations in the sediment sample (Brand and Veizer, 1980). Except for dolomitization, Mg contents can increase by the replacement of Ca by Mg element during reprecipitation. In the Manila Embayment, evidence from core observations suggest dolomitization effects would be the cause for high Mg and low Ca concentrations in the samples due to a replacement of  $Mg^{2+}$  to  $Ca^{2+}$  molecules. The higher Mg/Mg+Ca in the #1 NEAL ET AL UNIT 30-1 samples confirm this interpretation.

CONECUH EMBAYMENT  
(T.R. MILLER MILL 17-11, #1)

MANILA EMBAYMENT  
(#1 NEAL ET AL UNIT 30-1)

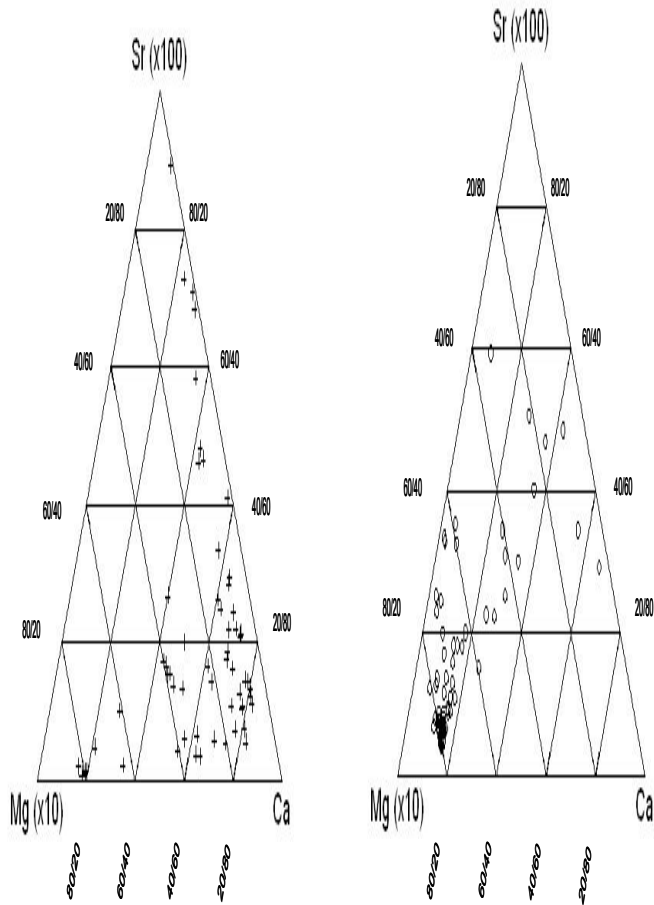


Figure 5-5. Ternary diagrams illustrating relative content of carbonate related elements, Ca, Mg and Sr, in the Smackover samples from the Conecuh and the Manila Embayments. The arbitrary numbers are applied in order to balance data on the diagrams.

On the vertical trend, the Ca, Mg, Sr, Mn, Na and P elements exhibit different variations that suggest variable depositional environments from the lower to the upper Smackover (**Figure 5-6 a and b; Figure 5-7 a and b**). In the Conecuh Embayment, the Mg/Mg+Ca values, used as indicator for dolomitization, were high in the lower and upper Smackover adjacent to the Norphlet and the Buckner anhydrite and during the intervals with increased siliciclastic influx. It is assumed that Mg content in the Smackover carbonate was mainly controlled by carbonate phase, therefore this observation suggests the increased dolomitization during the high siliciclastic influx could form during the falling relative sea level period when the freshwater mixing zone became closer. Under marine-fresh water mixing conditions, dolomites can form as the Mg/Ca in the mixed water increased by adding fresh-water which consists, relatively, of a much lower Mg/Ca ratio (between 0.1 to 0.3) compared to marine water (about 3) (Folk and Land, 1975). However, another possible interpretation is dolomite formed in this Smackover area occurred under the restricted to hypersaline conditions during relative sea level lowstand. Folk and Land (1975) explained that under a shallow marine, hypersaline environment, the precipitation of evaporite minerals (e.g. CaSO<sub>4</sub>) and a consequence loss of Ca would increase Mg/Ca values to above the normal values in the sea water (5 to 10 times) and dolomite precipitation could thus form. For the #1 NEAL ET AL UNIT 30-1 in the Manila Embayment, the high Mg and Mg/Mg+Ca values on the long trends support pervasive dolomitization. The smaller dolomitization in the lower Smackover in the #1 NEAL ET AL UNIT 30-1 sequence could be interpreted as lesser effect from the freshwater mixing zone due to more seaward (and probable deeper) location during the earlier Smackover deposition in this embayment. As sea level continued rising and fluctuating, shallowing carbonate condition on a long-term Smackover regressive sequence promoted higher dolomitization in the area.

Sodium and phosphorous contents in the Smackover sediments of both cores illustrate negative covariation with Ca and suggest their primary influence was not associated with

## CONECUH EMBAYMENT - T.R. MILLER MILLS 17-11, #1 WELL

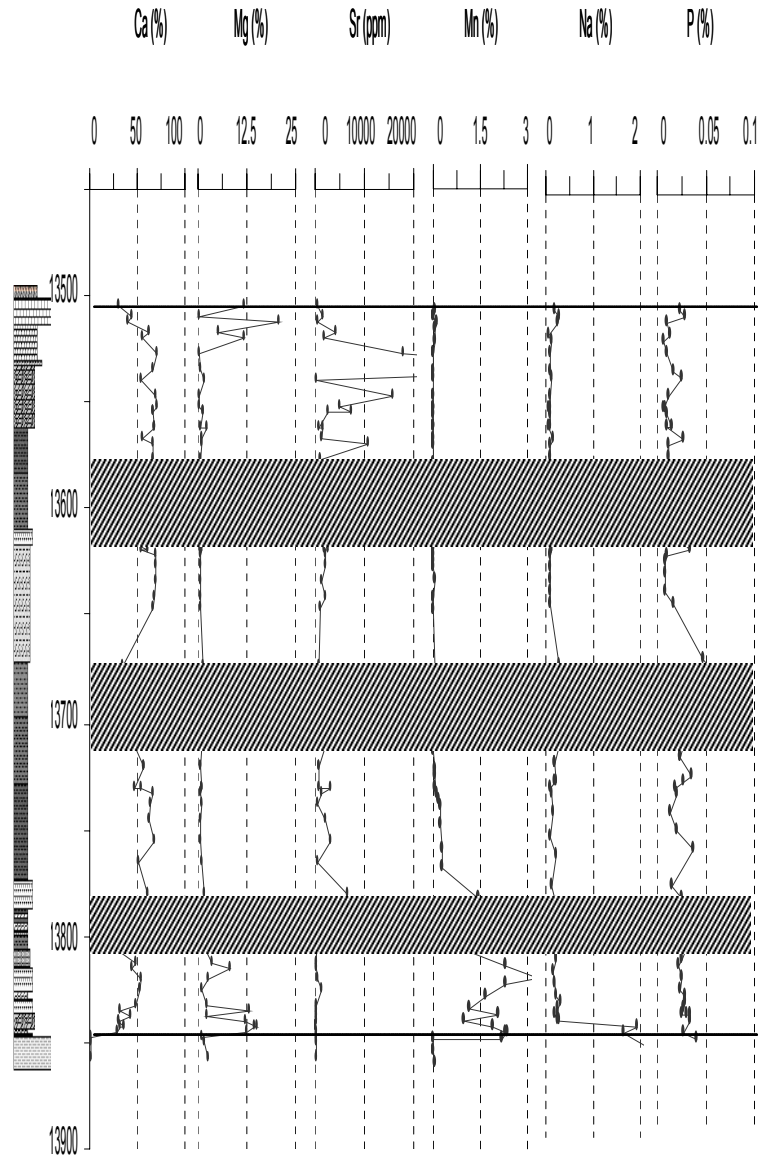


Figure 5-6a. Major and minor carbonate related elements of the Smaekover samples from the Conecuh Embayment. Na and P plotted in this group to compare their distributions in a carbonate environment. Data are listed in Appendix E.

# MANILA EMBAYMENT - #1 NEAL ET AL UNIT 30-1 WELL

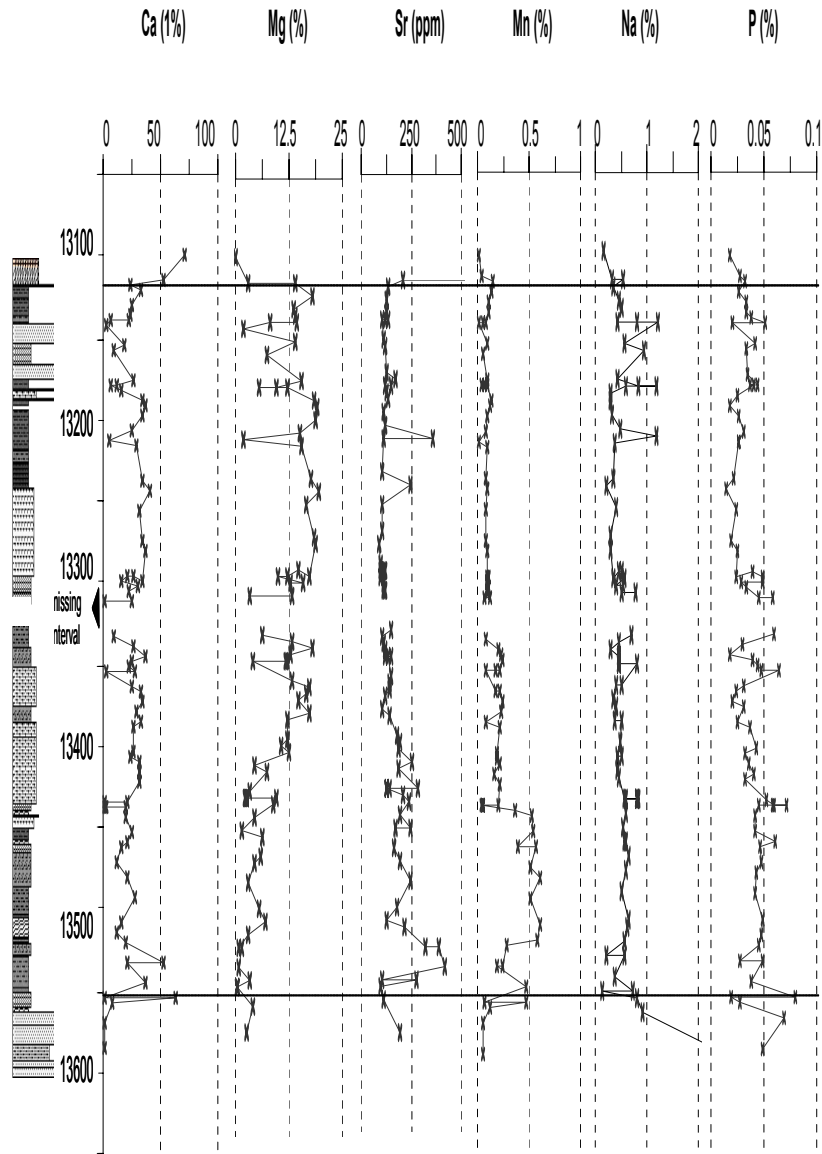


Figure 5-6b. Major and minor carbonate related elements of the Smackover samples from the Manila Embayment. Na and P plotted in this group to compare their distributions in a carbonate environment. Data are listed in Appendix F.

# CONECUH EMBAYMENT - T.R. MILLER MILLS 17-11, #1 WELL

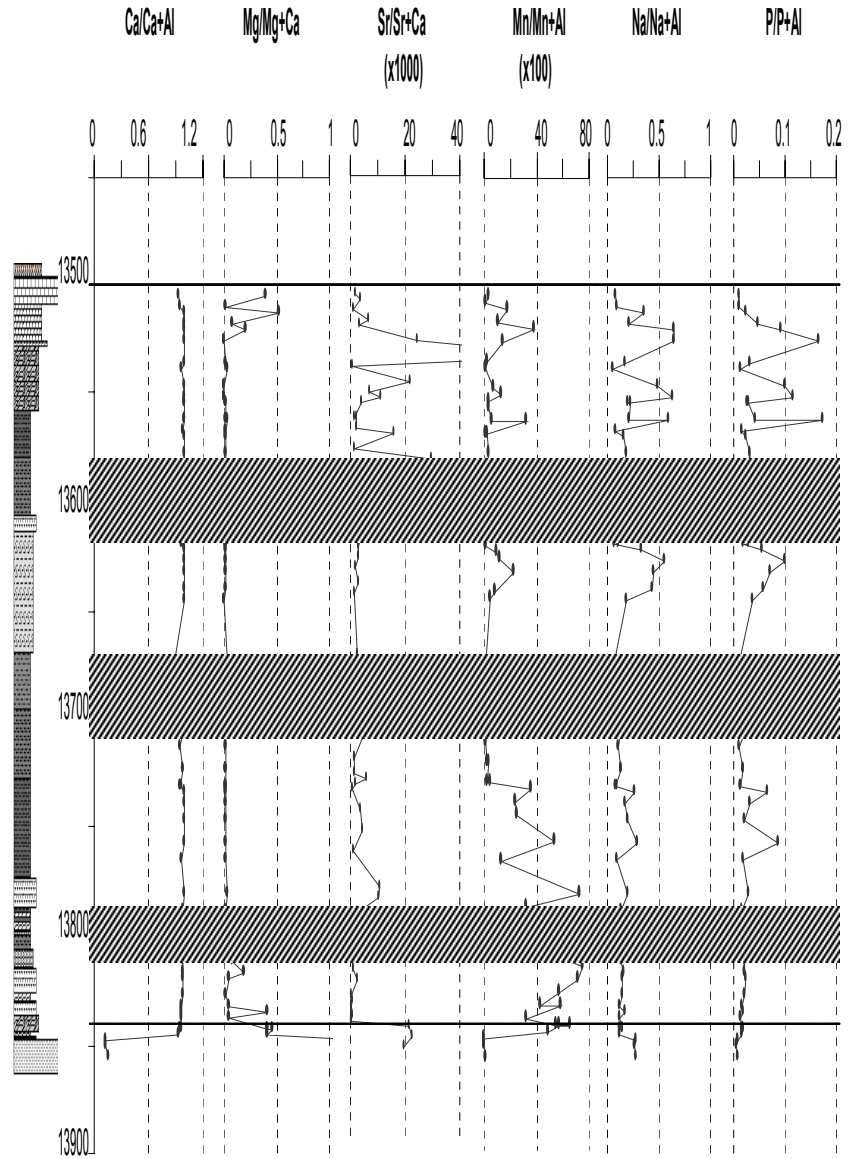


Figure 5-7a. Al-normalized and Ca-normalized major and minor of carbonate related elements for carbonate and diagenesis in the Smackover samples from the Conecuh Embayment. Data are listed in Appendix E.

MANILA EMBAYMENT - #1 NEAL ET AL UNIT 30-1 WELL

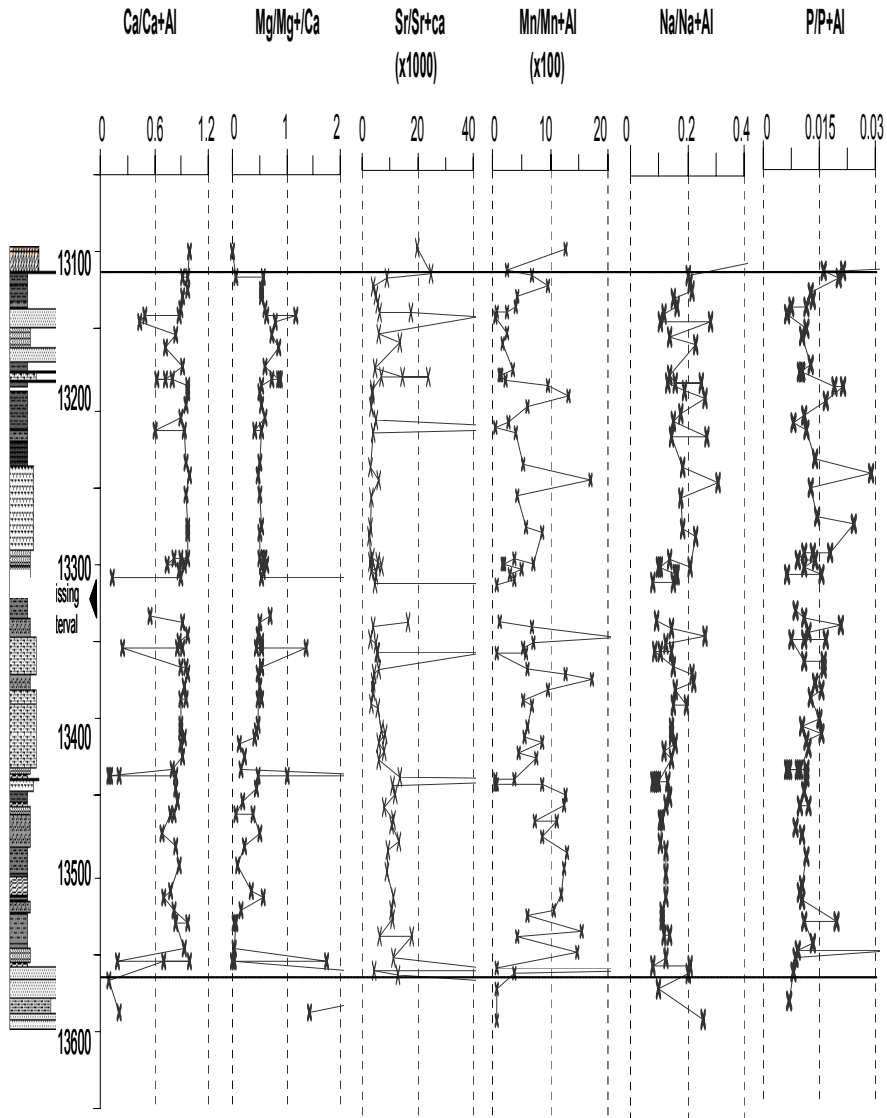


Figure 5-7b. Al-normalized and Ca-normalized major and minor of carbonate related elements for carbonate and diagenesis in the Smackover samples from the Manila Embayment. Data are listed in Appendix F.

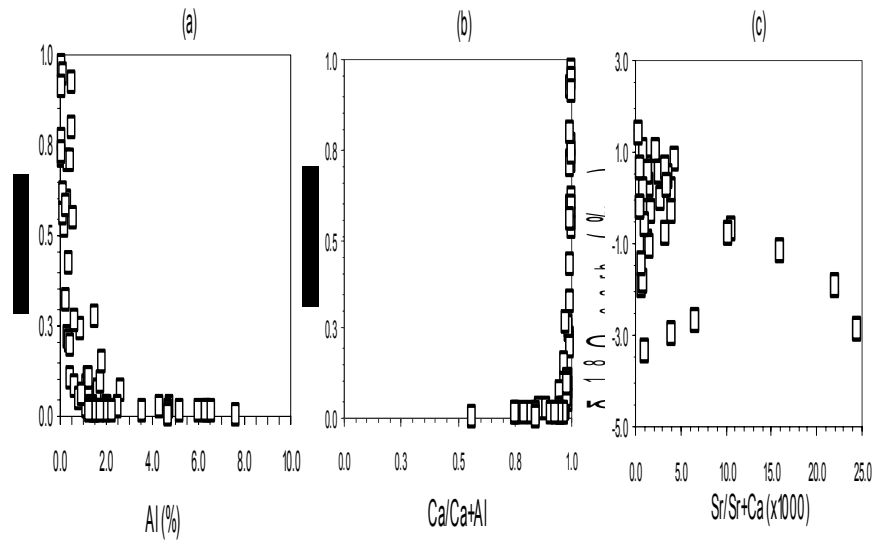
carbonate depositional conditions, but rather siliciclastic control. In the terrigenous component, Na can be associated with the illite and glauconite minerals (Spencer et al., 1968). P can come from the terrigenous apatite grains which were delivered into the Embayment by river discharges during deltaic progradation. Because Na and P elements were also present in the seawater, the positive covariation of the  $\text{Na}/\text{Na}+\text{Al}$  and  $\text{P}/\text{P}+\text{Al}$  with the  $\text{Ca}/\text{Ca}+\text{Al}$  values in Smackover samples from the Conecuh Embayment support the shorter-cyclicality of the Smackover depositional sequence in the Conecuh Embayment. Under these shorter cycles, both Na and P elements illustrate a long term increasing trend from lower to the upper Smackover. A diagenetic effect can be excluded for Na content as Na should decrease as carbonate mineral (aragonite) in the upper Smackover grainstone and packstone were more subjected to higher diagenetic alteration. The possible explanation for higher Na and P in the upper Smackover could be related to increased evaporation on the seawater surface as the climate became more arid which was evident by increasing evaporite formation of the Buckner anhydrite on top of the Smackover.

### **Strontium (Sr)**

During carbonate deposition, the original strontium (Sr) concentrations in carbonate sediments can decrease from several diagenetic reactions including dolomitization. Thus, Sr can be used as an indicator for carbonate diagenesis study (e.g. Baker et al., 1982; Veizer, 1983). Based upon the information published by Rachold and Brumsack (2001), calculated Sr concentrations of the pure carbonate materials were about 500 ppm for diagenetically recrystallized carbonate chalks (diagenetic low-Mg calcite; Scholle, 1977), 1100 ppm for low-Mg calcite (Morse and Mackenzie, 1990), 1600 ppm for recent marine carbonate (Scholle, 1977) and more than 2500 ppm up to 10,000 ppm for aragonite (Morse and Mackenzie, 1990). In the Conecuh Embayment, Smackover samples illustrate Sr variations from less than 500 ppm to higher than 10000 ppm. Most samples with Sr contents less than 500 ppm and between 500 ppm to 1000 ppm are observed in the lower Smackover and in sediment intervals where there is an increased siliciclastic input. The high Sr concentrations (>1500 ppm) occurred in samples which

are high in Ca or low in Al content. Carbonate samples which contain > 10,000 ppm Sr occur in the upper Smackover where the carbonate packstone and grainstone are dominant. For this interval, the Sr content was unlikely influenced by siliciclastic components as they were relatively low compared to the carbonate component. Diagenetic alteration which could be significant in the upper Smackover oolitic packstone and grainstone already decreased the Sr from its original content. However, as these packstone and grainstone ooids were likely dominated by aragonite which generally consists of high Sr content, suggesting high Sr in the upper Smackover can also be related to the original carbonate phase. Nevertheless, the Sr values in the upper Smackover sediments are too high as most of the original aragonite in these sediment grains have been converted into the stable diagenetic low-Mg calcite. Therefore, the unusually high Sr in this upper Smackover interval could reflect an increased Sr content in the seawater during late highstand sea level near the end of a long-term Smackover regressive cycle caused by an increased Sr delivery from an exposed or a shallow aragonitic platform drowning. For the Smackover deposition in the Manila Embayment, most samples from the #1 NEAL ET AL UNIT 30-1 core contains less than 500 ppm Sr. Diagenetic effects including dolomitization are interpreted to decrease Sr contents in the stabilized carbonate phase in the Smackover samples of this core. The relationships of Sr (as Sr/Sr+Ca) with Al (siliciclastic control), Ca (carbonate control) and  $\delta^{18}\text{O}_{\text{carb}}$  values (diagenetic effect) are illustrated in **Figure 5-8**. The cross-plot correlations between Sr/Sr+Ca and Al content and between Sr/Sr+Ca and the  $\delta^{18}\text{O}_{\text{carb}}$  values are slightly different between the two Smackover units. In the Conecuh Embayment, a stronger negative correlation between Sr/Sr+Ca and Al content and a weaker positive correlation between Sr/Sr+Ca and the  $\delta^{18}\text{O}_{\text{carb}}$  support the concept that Sr concentrations were not principally affected only from siliciclastic influx and diagenetic effect. Instead, the covariation between Sr/Sr+Ca and Ca/Ca+Al ratios indicates high Sr could have coprecipitated with carbonate precipitation. In the Manila Embayment, although similar correlations occurred between Sr/Sr+Ca and Al and between Sr/Sr+Ca and Ca/Ca+Al ratios, the cross-plots between Sr/Sr+Ca and  $\delta^{18}\text{O}_{\text{carb}}$  show distributions which suggest a different diagenetic

CONECUH EMBAYMENT (T.R. MILLER MILLS 17-11, #1 WELL)



MANILA EMBAYMENT (#1 NEAL ET AL UNIT 30-1 WELL)

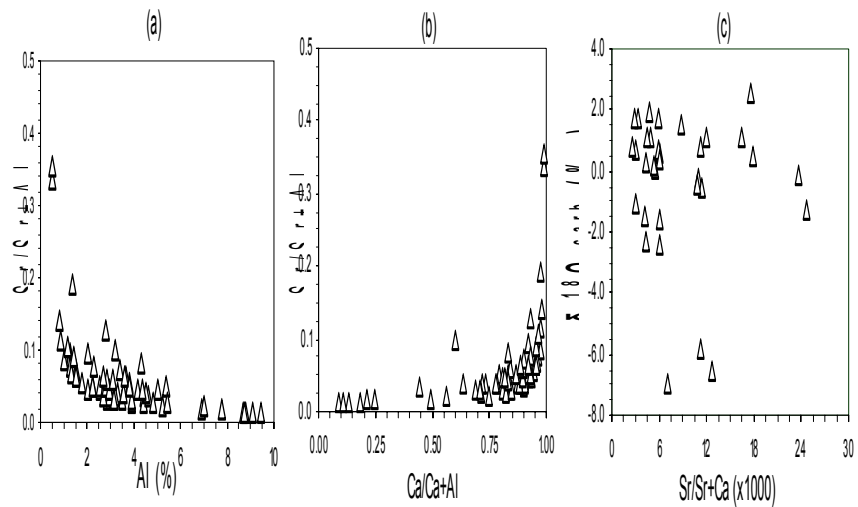


Figure 5-8. Cross-plots between (a) Al and Sr/Sr+Al, (b) Ca/Ca+Al and Sr/Sr+Al and (c) Sr/Sr+Ca (x1000) and  $\delta^{18}O_{carb}$  of the Smackover samples from the Conecuh and the Manila Embayments. Data including  $\delta^{18}O_{carb}$  are listed in Appendix E and F.

environment from the Conecuh Embayment.

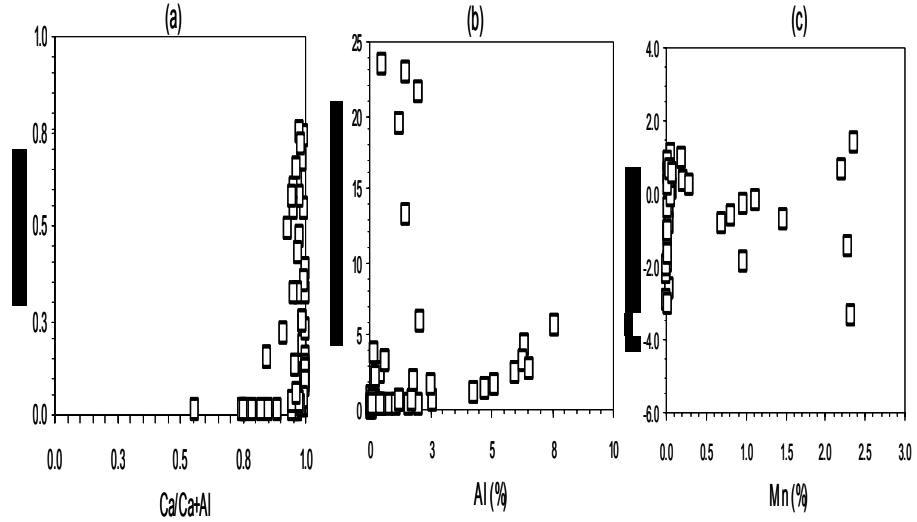
### **Manganese (Mn)**

Although varying in the measured concentrations, Mn distributions from both Smackover core sequences exhibit similar decreasing-upward concentrations on their long-term vertical trends (Figure 5-7a and b). In the Conecuh Embayment, the cyclicity of Mn variation is also observable. The Mn contents (Mn/Mn+Al) are relatively higher in Smackover deposited in the Conecuh Embayment than in the Manila Embayment. Although Mn can increase due to diagenesis (Brand and Veizer, 1980), diagenetic alteration cannot be the sole explanation for the higher Mn in the T.R. MILLER MILLS 17-11, #1 well samples. If diagenesis was primarily responsible for an enrichment of Mn in the Smackover sediment, one would expect that the higher Mn concentration should present in samples from the #1 NEAL ET AL UNIT 30-1 well instead from the T.R. MILLER MILLS 17-11, #1 well. Siliciclastic factor (as MnO; Spencer, 1968) could not be able to explain this high Mn in the Conecuh Embayment Smackover either as higher siliciclastic component also occurred in samples from the #1 NEAL ET AL UNIT 30-1 well. In addition, the reducing depositional environment during the lower Smackover probably was not applied to these high Mn concentrations. Based upon Arther and Dean (1991); Calvert and Pederson (1993 and 1996), high Mn content in sediment sample also occurs in oxic conditions. An enrichment of Mn in marine carbonates can be influenced by increasing terrestrial input or by direct precipitation as authigenic Mn from sea water during carbonate precipitation (Krishnaswami, 1976). According to Calvert and Pederson (1993), solid phase Mn in marine carbonate can occur not only as manganese oxide (MnO<sub>2</sub>) but also as manganese oxyhydroxide (MnOOH) phase. Mn<sup>2+</sup> which is observed to be related with a reducing or anoxic condition was due to the diffusion of the Mn<sup>2+</sup> from the MnOOH in the sediment into the suboxic water zone as the sediment/water interface became anoxic but not necessarily in the water column as a result of high organic productivity (Calvert and Pederson, 1993).

From the study of Rachold and Brumsack (2001), Mn concentration was reported in an average shale sediment to be around 0.09 %. In this study, Mn contents in the lower Smackover especially for the T.R. MILLER MILLS 17-11, #1 core are up to 3.3 % and around 0.6 % for the #1 NEAL ET AL UNIT 30-1 core. As previously mentioned, siliciclastic contribution and diagenetic alteration are not effective to explain the high Mn observed in the Conecuh Embayment Smackover. The relationship between Mn (Mn/Mn+Ca and Mn/Mn+Al) and Ca (Ca/Ca+Al), or Al or  $\delta^{18}\text{O}_{\text{carb}}$  values are also illustrated by cross-plots in **Figure 5-9**. Mn/Mn+Al values plotted with Ca/Ca+Al values illustrate that Mn contents in samples of the Conecuh Embayment show a different correlation with carbonates compared to samples from the Manila Embayment and have less variation with the Ca content. The correlation between the Mn/Mn+Ca and Al suggests that Mn in samples from the Manila Embayment was more or less influenced by siliciclastic component than Mn recorded in samples from the Conecuh Embayment. A poor correlation between Mn and  $\delta^{18}\text{O}_{\text{carb}}$  values in both cores suggests that Mn was not only affected by diagenetic alteration. Different distributions between Mn and  $\delta^{18}\text{O}_{\text{carb}}$  values between the two sample set confirm different diagenetic depositional environments. Because Mn variation in the Smackover samples was not principally controlled by siliciclastic and/or diagenetic effect, it is possible that these high Mn samples were directly influenced by an increased Mn content in the seawater during the Oxfordian ocean conditions. In that case, separation of the Mn content observed on both vertical scale with depth and on the cross-plot with the  $\delta^{18}\text{O}_{\text{carb}}$  values indicate there were at least three shorter cycles of the Mn fluctuation which related to sea level variation during the long-term Smackover sequence.

Dissolved Mn in seawater is primarily of hydrothermal origin. According to von Damm (1995), a hydrothermal event can increase the input of Mn to 30 times higher than that contributed from a terrigenous supply alone. In general, the average Mn concentration under normal marine conditions is quite low, varying between 0.5 to 5 nmol/kg or about 3 to 30 ( $\times 10^{-5}$ ) mg/kg (ppm) (Chester, 1990). With increasing hydrothermal activity, Mn in the seawater can

CONECUH EMBAYMENT (T.R. MILLER MILLS 17-11, #1 WELL)



MANILA EMBAYMENT (#1 NEAL ET AL UNIT 30-1 WELL)

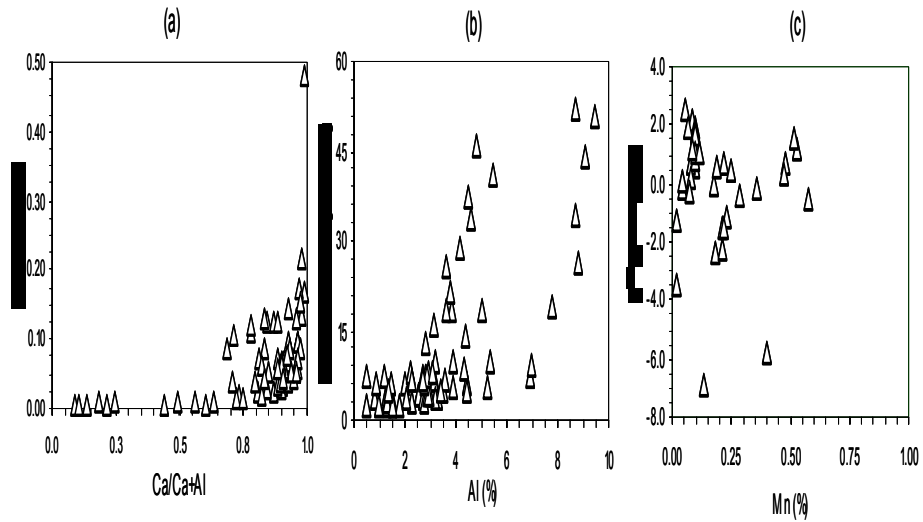


**Figure 5-9.** Cross-plots between (a) Ca/Ca+Al and Mn/Mn+Al, (b) Al and Mn/Mn+Ca to investigate the variation of Mn to Ca and Al. Diagenetic effect on Mn concentration (c) is examined by plotting with  $\delta^{18}\text{O}_{\text{carb}}$ . Data including  $\delta^{18}\text{O}_{\text{carb}}$  values are listed in Appendix E and F.

increase up to 33-41 mg/kg (Klinkhammer et al., 1986; Lyle et al., 1986; Edmond et al., 1990). This Mn increase can still be observed in sediments which are located more than 2000 km from the spreading ridge source (Lyle 1976; Klinkhammer et al., 1980) and vertically more than 1500 m above the sea floor with a factor of 3 per 1000 m above the hydrothermal plumes (Gordeev and Demina, 1979). For the Smackover deposition, it was possible then that an initial sea level transgression which was rapid and pervasive throughout the US Gulf margin in the Early Oxfordian period was a result of an event related to an increasing spreading ridge accretion which not only raised the relative sea level but also increased Mn content in the seawater during this period of time. An increase of Mn content in the Oxfordian carbonates has been recorded in pelagic sediments from basins in France (Corbin et al., 2000; De Rafelis et al., 2001). According to Corbin et al. (2000), there was a long-term variation of Mn concentrations which were related to the second-order sea-level changes and controlled by mid-oceanic activities from the Late Toarcian to the Oxfordian period. A decreasing Mn trend was recorded under the Oxfordian regressive phase of the second-order eustatic sea cycle. A major event of the very sharp increase of Mn content (above 1000 mg/kg), which was recognized in the Late Callovian and continued to the Early Oxfordian, could be equivalent to the high Mn which occurred at the base of the Smackover carbonates. Corbin et al. (2000) interpreted the increased Mn as corresponding to the first occurrence of oceanic crust (in Corbin et al., 2000; Figure 4). In De Rafelis et al. (2001), where the sediment sequence from Upper Oxfordian to Lower Kimmeridgian was investigated, the concentrations of Mn detected at the Upper Oxfordian were also lower (between 170 to 866 ppm or mg/kg) compared to the Mn in lower Oxfordian (Corbin et al., 2000) which then suggests to decreasing trend from the Lower Oxfordian to the Upper Oxfordian and then Kimmeridgian period. De Rafelis et al. (2001) illustrated the general trend of Mn variation relative to the changes in the third-order eustatic sea level cycle (**Figure 5-10**). During a lowstand system tract, Mn contents in the sediments are relatively constant with lowest values. With a rise in relative sea level during the transgressive system tract, Mn increases in concentration and then becomes

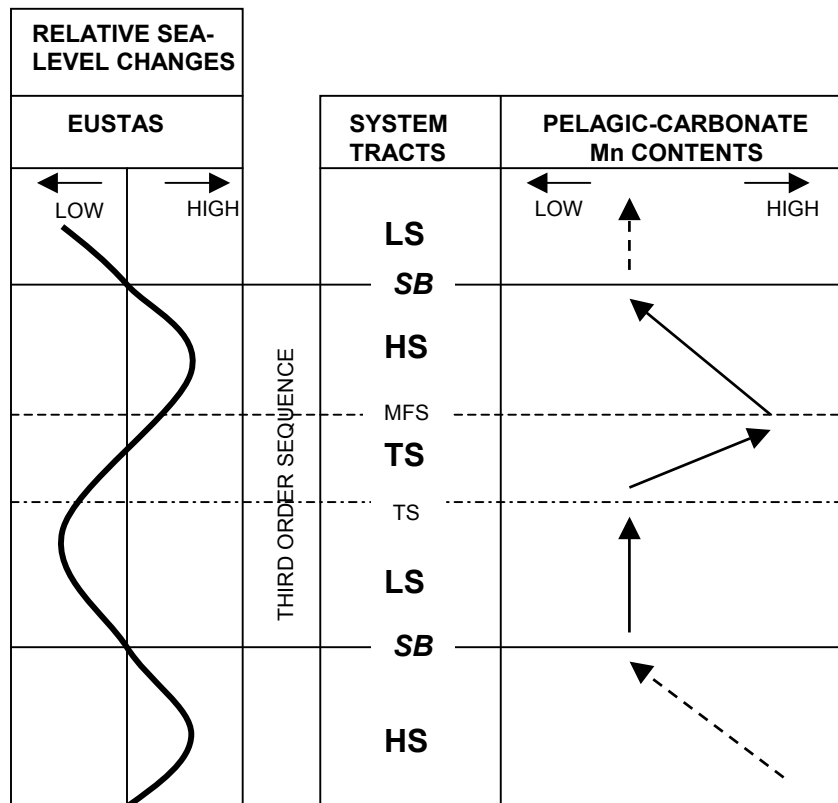


**Figure 5-10.** Mn content evolution curve in the pelagic limestones during a third-order sequence (from De Refelis et al., 2001).

highest at the maximum flooding surface or the condensed section. From the maximum flooding and up to a sea level highstand, Mn concentrations exhibit a decreasing trend and low values are typically observed at the sequence boundary between the highstand and the lowstand system tracts

In order to support the correlation with the hydrothermal event during the Oxfordian period, the strontium isotopic composition ( $^{87}\text{Sr}/^{86}\text{Sr}$ ) of the Smackover sample of the Conecuh Embayment has been analyzed by a commercial laboratory (Geochron Inc.). The  $^{87}\text{Sr}/^{86}\text{Sr}$  value of the Smackover samples at depth 13712 ft is reported of 0.706983. This number agrees with the values of the  $^{87}\text{Sr}/^{86}\text{Sr}$  ratios which have been recorded between 0.7068 and 0.7070 in the Oxfordian sediments and used to represent the worldwide Oxfordian seawater strontium isotopes (Koepnick et al., 1990; Jones et al., 1994). The average and unusual low  $^{87}\text{Sr}/^{86}\text{Sr}$  values of the oceanic water during the Oxfordian period were suggested by Jones et al. (1994) as possibly representing the major pulse of hydrothermalism caused by the spreading ridges of the Atlantic ocean. The changing intensity of the mid-ocean ridge hydrothermal fluxes lead to a decreased  $^{87}\text{Sr}/^{86}\text{Sr}$  isotope ratios in the ocean. Therefore it might be possible that the high Mn concentrations in the sediments during this period, including in the Smackover sequence, were also associated with the increased Mn content in the seawater affected by those events. It can probably be reasonable to assume that the sharp increase of Mn in the lower Smackover and the variation of Mn concentration during Smackover deposition were primarily controlled by the global hydrothermal events relative sea level changes on the third-order scale.

### **5.4.3 Redox Conditions**

Information concerning the redox state during and after deposition of sedimentary sequences may be obtained from selected trace elements and their abundances, such as Ba, Zn, Cu, Ni, Cr, V and Pb. According to Calvert and Pedersen (1993), these elements can occur by

precipitation, where the surface sediments are in contact with the anoxic or sulphidic water, and/or by the diffusion from sea water into anoxic sediments that lie below the surface oxic horizons. However, for continental margin sediments, these metals can also increase significantly with increasing local fluxes of detrital components. The ambiguity for the presence of these elements is caused by the tendency of these elements to become enriched in the anoxic surface sediments and in the subsurface anoxic deposits underlying the surface oxic zone. Therefore it is probably more reliable for this study to use the presence and absence of these elements as a guide for sediment conditions. The absence of enrichments of these metals strongly suggests that sedimentation occurred under oxygenated bottom water conditions. The concentrations of the individual elements normalized to Al are used in order to subtract their contributions from, and during, the large siliciclastic sediment influxes and to indicate their contents which likely occurred during the Smackover carbonate precipitation.

In the Smackover of the Conech Embayment, the vertical distributions of the normalized concentrations of these elements with respect to Al, except Zn/Zn+Al ratios, illustrate a similar fluctuation showing a long-term increasing trend (**Figure 5-11a**). The fluctuations of these elements are assumed to probably occur during carbonate precipitation. Usually, intervals of high concentrations were interpreted to represent conditions underlying the sediment-water interface becoming anoxic and diffusion of these elements from the seawater into the sediment occurred. If bottom sediment or the sediment-water contact was anoxic during Smackover deposition, the high ratios in these elements normalizing with Al would be expected and might not be covariant with increased siliciclastic sediments. However, increasing values shown in the upper Smackover might possibly suggest an increased concentration of these element due to changing seawater chemistry as changing depositional environment and/or paleoclimate conditions. However, for Cr and V, although they are eventually removed from the ocean into anoxic sediments, the propensity for the reduced species of both elements to precipitate as sparingly soluble oxides/hydroxides or to be absorbed on particle surfaces, also allow them to

# CONECUH EMBAYMENT - T.R. MILLER MILLS 17-11, #1 WELL

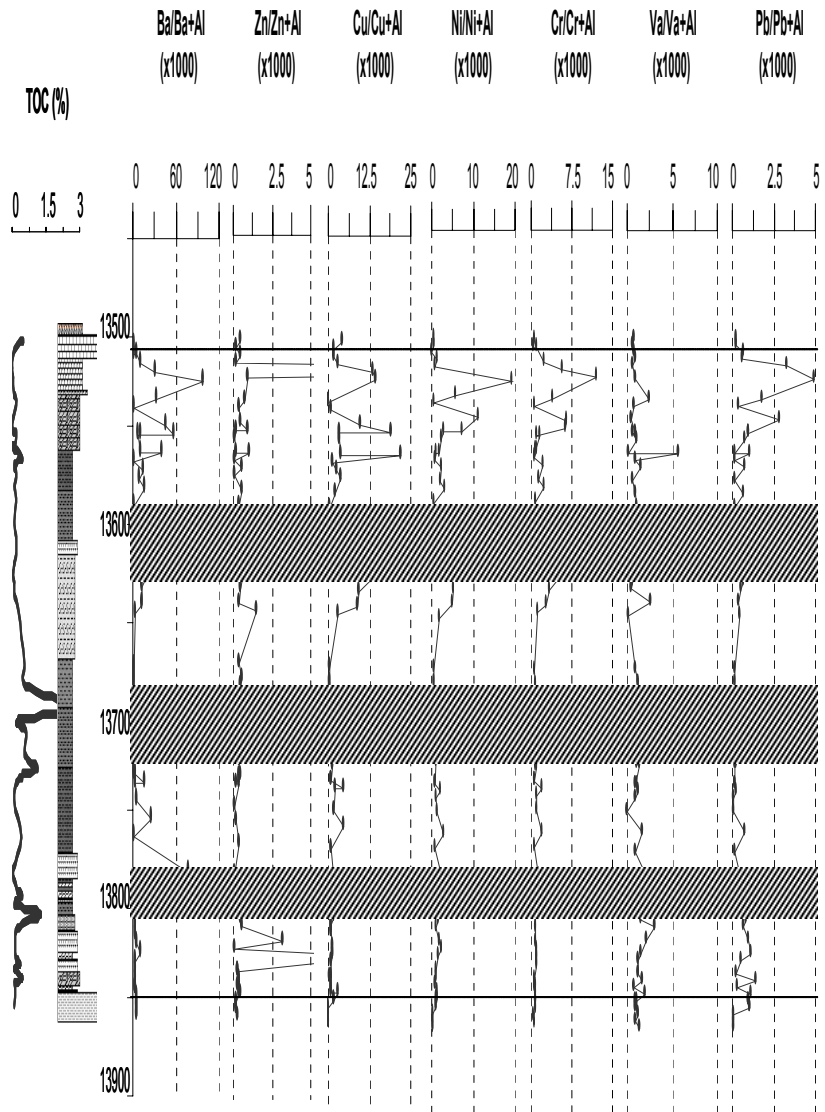


Figure 3-11a. Normalized ratios of trace elements with respect to Al of Smackover samples from the Conecuh Embayment. Data including TOC values are listed in Appendix E.

exist under oxic sea water conditions (Calvert and Pedersen, 1993). In contrast, the low contents of Cu, Ni, Cr, in the lower Smackover suggest that the depositional environments were not anoxic but could have been less oxygenated when compared to the upper Smackover sediment. When compared with the vertical distribution of total organic carbon (TOC), it was noted that intervals where these elements were absent in the lower and middle Smackover still correspond to those intervals of higher TOC content. This observation suggests that high TOC accumulation in samples did not occur under anoxic or reduced conditions, but were probably influenced instead by high terrigenous input. However, it must also be noted that the absence of these elements was not always characterized by the high TOC samples either such as in the upper Smackover where the packstone and grainstone predominated. The different trend of the  $Zn/Zn+Al$  suggests that high values in the lower and upper Smackover near the Norphlet and the Buckner anhydrite sedimentation were probably caused by other factors. From Calvert and Pedersen (1993), an increasing Zn concentration can be influenced not only by the anoxic condition of the bottom sedimentation but may also be supplied by the settling out of the particulate organic matter, or by the diffusion of the dissolved metals from the overlying oxygenated water, or the pore water from the adjacent intervals into the subsurface anoxic horizons.

Because enrichments of these elements are not only affected by the magnitude of the precipitation from the oxic water column into the deep anoxic condition at the water-sediment contact but are also strongly controlled by the balance with the detrital aluminosilicates which are supplied in to the ocean (Jacob et al., 1987), the variation of these elements under different depositional environments and siliciclastic inputs can be different. This explanation might explain the different distributions of these elements observed in the Smackover sedimentation of the Manila Embayment (**Figure 5-11b**). The relatively low concentrations of these metals suggest that the environment in this embayment area was probably oxic. The small scale fluctuations of individual elements are not significantly different and are interpreted to be partially affected by the variable compositions of the aluminosilicate detrital supply during the Smackover in this

# MANILA EMBAYMENT - #1 NEAL ET AL UNIT 30-1 WELL

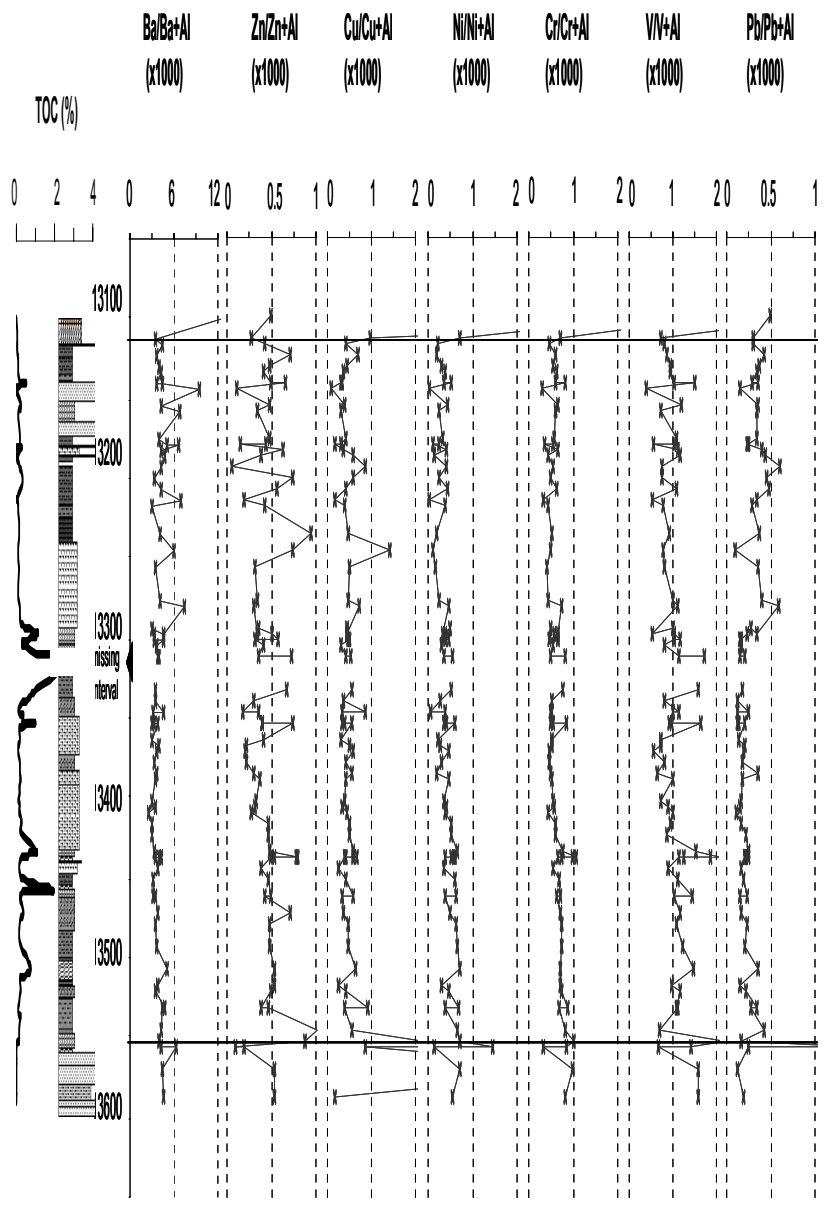


Figure 5-11b. Normalized ratios of trace elements with respect to Al of Smackover samples from the Manila Embayment. Data including the TOC values are listed in Appendix F.

embayment and there was also possibility that some of these elements (i.e. Cr and V) existed under oxic condition (Calvert and Pedersen, 1993). The low concentrations of Cr and V elements in Smackover sedimentation of the Manila Embayment can be interpreted by saying that these elements were not efficiently removed from the seawater as it would have been under anoxic conditions. Usually, V and Ni can accumulate with organic molecules such as porphyrins, and the presence of a high concentration of organic matter which probably occurred under anoxic conditions will also lead to high V or Ni in the sediments. For the Manila Embayment deposits, the fluctuations and positive covariation of the V and Ni and with the TOC content suggest these two elements could be associated with the accumulation of organic matter. However, the lack of positive variation between the Cr and V in the lower Smackover samples of this core also supports that the depositional environment was not anoxic. A stronger variation of the  $Zn/Zn+Al$  values is interpreted to be influenced variable grain sizes of the siliciclastic sediments and different sediment particle settling processes.

## 5.5 CONCLUSIONS

The bulk chemical composition of Smackover sedimentation in the Conecuh Embayment and the Manila Embayment from southwest Alabama was controlled by the variation of carbonate sedimentation which was affected by episodes of siliciclastic influx. In the Conecuh Embayment, the predominant carbonate deposition was interrupted by at least three major pulses of siliciclastic influx which are revealed by increases in several major siliciclastic component major elements. (i.e. Al, Ti, Si, Fe, K). The normalized ratios with Al of these elements suggest to changes in deposition condition during the long term from the lower to the upper Smackover. The variation of the elemental compositions suggested Smackover deposition, especially the lower Smackover, occurred generally under oxic conditions. The depositional energy became higher toward the end of the Smackover Formation and it is possible that, during the Smackover deposition, the

fluctuation of chemical weathering processes could be involved. The less distinctive patterns of these elements in Smackover sedimentation of the Manila Embayment resulted from a higher siliciclastic background content within the carbonate sedimentation which were controlled by the depositional environment and structural setting. The constant and high siliciclastic fraction supply lead to lower carbonate production and sedimentation in this area when compared to the Conecuh Embayment. The normalized siliciclastic ratios (with respect to Al) in samples from the Manila Embayment became less effective in illustrating a shorter-cyclicality during Smackover deposition as compared to what observed in the Conecuh Embayment.

Except in the upper Smackover, diagenetic alteration on the element concentrations is interpreted to be small in samples from the Conecuh Embayment owing to their more stable original carbonate phase in the mudstone (low-Mg calcite). Dolomitization indicated by Mg/Mg+Ca values could be distinguished in the lower and upper Smackover near the Norphlet Formation and the Buckner Anhydrite and was partially observed during intervals associated with increasing siliciclastic sediment influx. The increasing upward trend of the Sr elements and decreasing upward of the Mn element suggested a long-term Smackover regressive trend. While an increasing Sr content in the upper Smackover was probably affected by aragonite phase of the grainstones and increasing Sr in the seawater from shallow aragonite platform erosion during regressive trend of the Smackover, the high Mn observed in the lower Smackover is interpreted to be probably controlled by a direct increase of Mn in the seawater due to hydrothermal activities. The presence of cyclicality on the carbonate (Ca), siliciclastic (Al) and minor (Si, K, Na, P, Ti) and trace elements that occurred in the Smackover deposition in the Conecuh Embayment indicate that there were at least three short-term variations during the long term Smackover sequence.

For the Smackover deposition of the Manila Embayment, high structural setting and nearshore location of this area permitted higher siliciclastic sediment input and promoted dolomitization by the approaching of the meteoric water zone. Siliciclastic elements are high and illustrate a very distinctive shorter-trend compared to the Smackover of the Conecuh Embayment.

Pervasive dolomitization is supported by high Mg and shows an increase towards the end of the Smackover. Sr and Mn concentrations can be partially affected by diagenesis but were probably also related to relative sea level variation conditions. Even though expressing relative lower concentration, Smackover samples from the Manila Embayment also present a decreasing-upward trend of the Mn which is similar to that observed in the Conecuh Embayment. The small scale fluctuations of some elements in these Smackover core samples are interpreted to be affected from diagenesis, especially dolomitization.

The major and minor elemental chemical composition of Smackover sedimentation of the Conecuh Embayment and the Manila Embayment indicate slightly differing redox conditions during deposition. In the Conecuh Embayment, low concentrations of Ba, Cu, Ni, Cr, V, and Pb elements suggest the environment was probably not anoxic. The low content of TOC and V in the oxic condition during upper Smackover and the different variation between Cr and V suggest that the Cr content could possibly affect by additional environment factor. Higher Zn contents observed near the upper and lower boundary were affected from the meteoric diagenesis from which additional Zn could have been derived. The fluctuations and increasing trend introduce the possibility that the bottom water at the water-sediment contact and/or subsurface deposit under the oxic sediment horizons did not entirely remain under oxic conditions. Increasing concentrations of these elements occurred during high carbonate production (high Ca content) which became dominant during relative sea level rise and highstand. It is also possible that during the rise in relative sea level, local rapid sedimentation rates could have caused the bottom water or subsurface sediment under the oxic sediment horizon to become anoxic. However, such conditions were unlikely to occur in the Manila Embayment where these elements illustrate much lower concentrations. The fluctuation of V also partially correlates with fluctuations in the TOC accumulation in the Smackover. The high variability of Zn might have been affected by diagenetic effects including dolomitization. The redox conditions of both Smackover areas show no anoxic conditions.

The variation of the elemental component of the Smackover depositions in the Conecuh Embayment and in the Manila embayment indicate that the structural setting and depositional environment and diagenesis have significant impact on the distribution of these elements both laterally and vertically. However, the information about the possible original sediment and the conditions of their depositional environment during Smackover deposition from the lower to the upper Smackover can still be obtained. The effect from relative sea level changes can be speculated by comparing with related information from the literature. The key elements which could be very useful for relative sea level cycles and other related processes (weathering) are Mn, K and Sr.

## **5. 6 FURTHER SUGGESTED STUDIES**

These results suggest the Smackover depositional sequence was affected by both long term and a short term sea level fluctuations and modified by diagenetic alteration and mixing with siliciclastic influxes. Increasing chemical weathering and changes in paleoclimate are possibly involved. In order to investigate the short term and long term sea level effect and their other parameters on the Smackover stratigraphy, an additional study is warranted. Such a study would investigate Smackover sedimentation in different locations such as in an updip and/or downdip areas of the same basin and from the nearby basin especially the Mississippi Interior Salt Basin. Such studies could be related to 1) siliciclastic and carbonate minor and trace element analysis especially the Sr values and Mn concentration; 2) oxygen and carbon isotope composition of the Smackover as well as the TOC content in a finer scale sampling; and 3) siliciclastic grain size analysis and different clay mineral analysis and K variation.

## CHAPTER 6

### 6.1 CARBON ISOTOPE STRATIGRAPHY

Carbon isotope stratigraphy concept is based upon time-equivalent changes in  $^{13}\text{C}/^{12}\text{C}$  ratios that serve as an additional powerful tool for stratigraphic correlation of carbonate sequences (e.g. Scholle and Arthur, 1980; Varenkamp, 1996; Ferreri et al., 1997; Jarvis et al., 2001; Buggisch et al., 2003). The basic theory is that the carbon isotope signal of a particular carbon-containing material can be recorded during a global event which has been driven by large-scale changes of the carbon cycle. The variation of carbon isotope composition in the rock record may possibly provide an analysis for the local and/or regional controls which occur in a time-stratigraphic framework. Studies have indicated carbon isotope stratigraphy of carbonate sediments could be comparable in stratigraphic resolution to biostratigraphy or magnetostratigraphy (Scholle and Arthur, 1980; Weissert et al., 1985; Margaritz, 1989; Weissert and Lini, 1991; Lini et al., 1992; Follmi et al., 1994; Jenkyns., 1994).

In marine carbonate environments, carbonate sediments precipitate in depositional conditions which are directly associated with seawater composition. Any changes which affect the carbonate sediment environment and composition of seawater, including carbon isotopic equilibrium of carbon in seawater, will affect basic carbonate minerals which are precipitated as well as the carbon isotopic composition of carbonate secreting organisms which live in the seawater and then eventually become carbonate sediments. For long-time scale variations, the change of the carbon isotope value of seawater occurs on a time scale of  $> 10^5$  years due to long-term variations of carbon burial, continental weathering, sea surface temperature and oceanic water condition, i.e. pH and compositions (Kump and Arthur, 1999). On short time scales, the effect may come from changes in primary productivity, seawater composition, the release of methane gas hydrates, or changes in oceanic water circulation. In this chapter, carbon isotope

variations of the Smackover sequences in the Conecuh Embayment and the Manila Embayment of southwest Alabama are investigated and correlated in a time-stratigraphic framework. Many shallow water carbonate studies also show that carbon isotope variations caused by changes in local and global events are recorded in shallow-water carbonates on the platform and in the bulk carbonate sediments (Varenkamp, 1996; Ferreri et al., 1997). Oxygen isotope compositions of the carbonate samples were also analyzed but due to the instability from temperature effects and diagenetic alteration during and after sedimentation were not used for stratigraphic correlation.

## 6.2 CARBON ISOTOPES ( $\delta^{13}\text{C}$ )

Carbon isotope studies make use of the natural variation of stable isotopes of carbon elements ( $^{12}\text{C}$  and  $^{13}\text{C}$ ) within carbon containing materials (both organic and inorganic) in the bio- and geochemical carbon cycles of the Earth's environment. The lighter  $^{12}\text{C}$  isotope is preferentially utilized by primary producers during photosynthesis, leaving the hydrosphere-atmosphere relatively depleted in  $^{12}\text{C}$  and enriched in  $^{13}\text{C}$ . Variations in the level of primary productivity in oceanic surface waters and sedimentation rates or in the level of burial of organic materials affected by anoxia and/or accumulation rates can lead to temporal fluctuations in carbon isotope ratios. Temporal and spatial variations can be reconstructed from the carbon isotope analysis of carbonates and/or organic matter.

The carbon isotope compositions ( $\delta^{13}\text{C}$ ) of inorganic carbon in carbonate sediments are derived from a variety of pathways and operate on different temporal scales. According to Anderson and Arthur (1983), fractionation of carbon isotopes starts on a molecular or crystal level in sediments where partial separation of different isotopes related to the physio-chemical properties occurs during physical or chemical processes. This isotopic separation process is also known as "isotope fractionation". Two types of isotope fractionations are kinetic isotope fractionation and thermodynamic fractionation. The kinetic fractionation occurs when the rate of

chemical reactions, or physical processes of isotope fractionation (e.g. evaporation), of isotope species differ from one another. Thermodynamic fractionation occurs as the thermodynamic equilibrium between components and phases of substance approach a state of minimum free energy in a natural system (Anderson and Arthur, 1983). For example, the isotope values (both  $\delta^{13}\text{C}$  and  $\delta^{18}\text{O}$ ) of calcareous marine organisms which are basic constituents of carbonate sediment are a function of the equilibrium carbon and oxygen isotope compositions (thermodynamic) and temperature (kinetic rates of precipitation) of the ambient waters where organisms reside. With respect to kinetic process, the effect from temperature variation on the carbon isotope fractionation in stabilized calcite mineral in sediment is usually very small (0.035 ‰ per °C or 1‰ for every 27 °C) compared to alterations which occur to oxygen isotope compositions (Emrich et al., 1970). This reason thus underscores the potential utility of carbon isotopes for stratigraphic purposes.

Equilibrium carbon isotope fractionations among the important carbonate species have been summarized by Denies et al. (1974). The general relationships predict the following order of  $^{13}\text{C}$  enrichment from higher to lower:  $\text{CaCO}_3 > \text{HCO}_3^- > \text{CO}_3^{2-} > \text{H}_2\text{CO}_3 = \text{CO}_2$ . In seawater at normal tropical surface water pH's (~8) and temperatures (~28 °C) (Morse and Mackenzie, 1990), the dominant carbon component is dissolved bicarbonate ion. Carbonate precipitated from the marine environment can then be +1 to +3 ‰ enriched in  $^{13}\text{C}$  relative to dissolved  $\text{CO}_2$  in the seawater. The effect that may cause variable  $\delta^{13}\text{C}$  values in biogenic carbonates may come from different precipitation rates (Turner, 1982) and the vital effects of different organisms (Urey et al., 1951).

The larger scale carbon isotope fluctuation is dependent upon variation in the Earth's major carbon reservoirs from different environments. The carbon stored in these reservoirs consists of different average  $\delta^{13}\text{C}$  values (**Figure 6-1** and **Table 6-1**). Any global events that could cause major carbon mass storage shifts will therefore change the global thermodynamic carbon isotope equilibrium of the Earth system. In nature, two significant carbon reservoirs

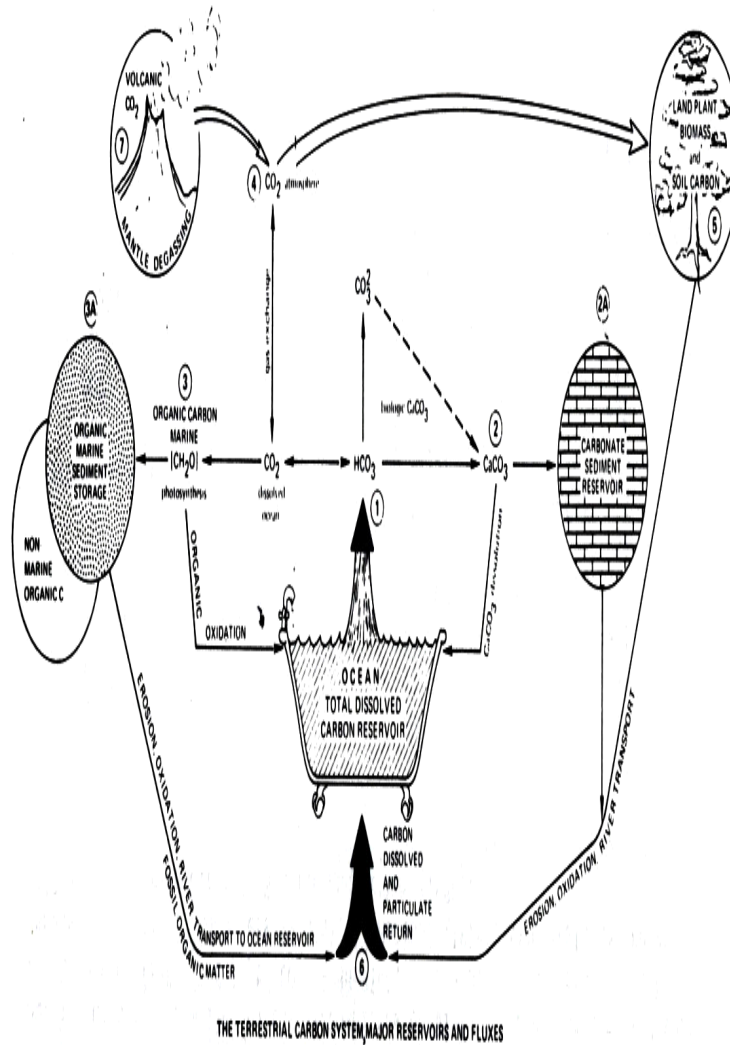


Figure 6-1. A diagram illustrating the global carbon cycle with the major carbon reservoirs and the related processes. The estimated amount of carbon mass in each reservoirs, the rate of the mass transferring and the carbon isotope compositions are reported in Table 6-1 (from Anderson and Arthur, 1980 with the original of Scholle and Arthur, 1980).

**TABLE 6-1.** The estimated mass of carbon (organic and inorganic) in various Earth's reservoirs and the transfer fluxes of carbons between the different reservoirs and their average  $\delta^{13}\text{C}$  compositions (from Anderson and Arthur, 1980).

| <b>RESERVOIRS</b>  | <b>MASS</b> ( $10^{15}$ gmC)          | <b><math>\delta^{13}\text{C}</math></b> (‰, PDB) |
|--|---------------------------------------|--|
| 1) Atmosphere (pre-1850 CO <sub>2</sub> )<br>(~ 290 ppm)         | 610                                   | -6.0 to -7.0                                     |
|  | range 560 – 692                       | —  |
| 2) Oceans -TDC   | 35,000                                | 0  |
| -DOC   | 1,000                                 | -20  |
| -POC   | 3                                     | -22  |
| 3) Land Biota (biomass)  | range 592 – 976                       | -25  |
|  | (~ 10% may be C4 plants ?)            | -12  |
| 4) Soil Humus  | range 1,050 – 3,000                   | -25  |
| 5) Sediments (Total)   | range 500,000 – 10,000,000            | —  |
| Inorganic carbon   | 423,670                               | +1   |
| Organic carbon   | 86,833                                | -23  |
| 6) Fossil Fuels  | > 5,000                               | -23  |
| <b>FLUXES</b> ( $10^{15}$ gC/yr)                                 | <b>RATES OF MASS TRANSFER</b>         | <b><math>\delta^{13}\text{C}</math></b> (‰, PDB) |
| 1) Atmosphere/Ocean CO <sub>2</sub> exchange                     | 100                                   | —  |
| 2) Atmosphere/land biota-photosynthesis<br>(Estuaries-marshes).. | range 53 – 78; average 63<br>(~ 1.4 ) | —  |
| 3) Ocean Photosynthesis  | range 15 – 126; average 45            | —  |
| 4) Land to Ocean   | range 0.38 – 0.44                     | —  |
| -TDC   | 0.4                                   | -6.0 to -9.0                                     |
| -DOC   | 0.1 ( 0.215) 2                        | -25  |
| -POC   | 0.06 ( 0.180) 2                       | -26  |
| 5) Ocean Deposition  | range 1 - 10                          | —  |
| Inorganic carbon   | range 0.5 – 5 ; probable 1-2          | +1.0   |
| Organic carbon   | 0.095 (probably too low)              | -20  |
| 6) Fossil Fuel Combustion  | 5 (can be presently higher)           | -23  |
| 7) Volcanic CO <sub>2</sub>                                      | 0.08 (mantle) 3                       | -7   |
| 8) Organic carbon leaving photic zone                            | 4.1 – 10.0                            | -20  |

are the reservoirs of organic carbon and the reservoirs of inorganic or carbonate carbon (Mackenzie and Pigott, 1981). The organic carbon reservoir consists of the second largest volume of carbon which has a highly negative  $\delta^{13}\text{C}$  value. This value results from a large fractionation of carbon isotopes during photosynthetic fixation of carbon by plants and organic matter which preferentially incorporate  $^{12}\text{C}$  from atmospheric  $\text{CO}_2$ . For the carbonate reservoirs, precipitation of inorganic carbon (largely from total dissolved carbon of  $\text{HCO}_3^-$  in the ocean) as carbonate minerals (i.e. high-Mg calcite, low-Mg calcite, aragonite, dolomite and others) either directly by organisms or from inorganic processes (e.g. cementation) usually contribute a much smaller isotope fractionation relative to the  $\delta^{13}\text{C}$  values of bicarbonate species in the seawater. Mackenzie and Pigott (1981) and later Veizer et al. (1999) have illustrated that the variation of carbon isotope compositions of carbonate minerals in either marine fossils or whole rock carbonates may be used to monitor the changes of the total dissolved carbon in seawater during the geologic past. The relationships among the major sedimentary or chemical carbon components and the ranges of  $\delta^{13}\text{C}$  values are illustrated in **Figure 6-2** and **Figure 6-3**.

### **6.3 CARBON ISOTOPES IN A SEQUENCE STRATIGRAPHIC FRAMEWORK**

#### **6.3.1 Positive $\delta^{13}\text{C}_{\text{carb}}$ excursion**

Two types of  $\delta^{13}\text{C}_{\text{carb}}$  excursions may be observed on the vertical carbon isotope trend in a stratigraphic framework, the positive and negative excursions. The positive  $\delta^{13}\text{C}_{\text{carb}}$  excursion which occurs on a global scale record is due to a worldwide increased organic carbon accumulation during oceanic anoxic conditions or an increased organic production indicating the Earth's carbon cycle shifting towards the organic carbon reservoir (i.e. Scholle et al., 1980; Follmi et al., 1994; Jenkyns et al., 1994; Weissert et al., 1998; Jarvis et al., 2001). Marine carbonates, and hence their carbon isotopic compositions, are basically controlled by seawater

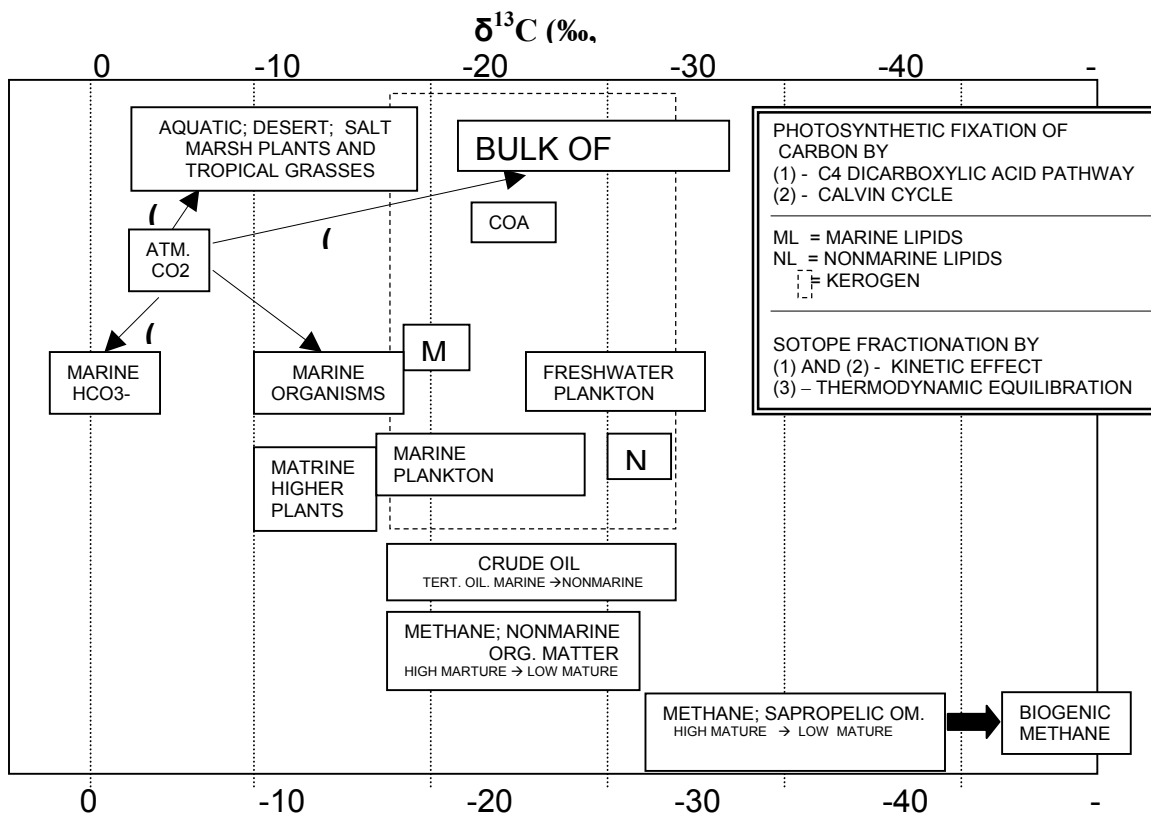


**Figure 6-2.** Schematic of major sedimentary and chemical carbon components and their average range of  $\delta^{13}\text{C}$  values (from Anderson and Arthur, 1980).

### THE NONMARINE CARBON CYCLE

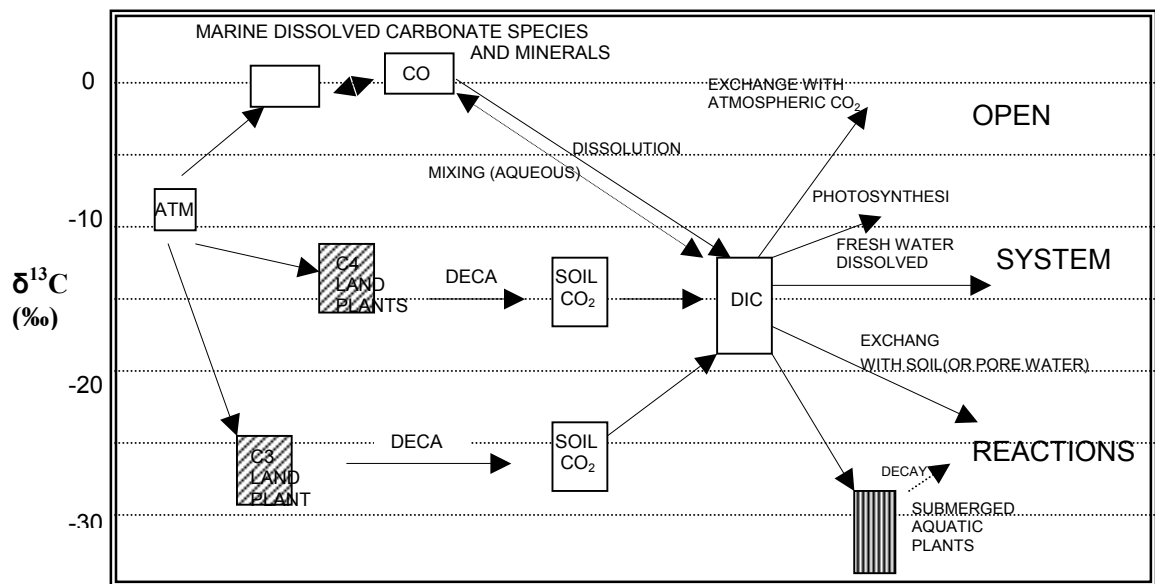


**Figure 6-3.** Components of nonmarine carbon cycle and their inter-relationships of the  $\delta^{13}\text{C}$  values (from Anderson and Arthur, 1980).

composition at the time sedimentation occurred (Veizer and Hoefs, 1976; Given and Lohmann, 1985; Popp et al., 1986; Lohmann, 1988). Studies have shown that the fluctuation of carbon isotope compositions of carbonates through geological time most likely resulted from variations in the carbon isotope composition of seawater (i.e. bicarbonates) due to the changes in carbon budget (e.g. Veizer and Hoefs, 1976; Scholle and Arthur, 1980; Poppe et al., 1986; Lohmann, 1988; Margaritz, 1989; Weissert and Lini, 1991; Lini et al., 1992; Kaufman et al., 1993; Follmi et al., 1994; Jenkyns., 1994). Thus, carbon isotope composition of carbonate sediments or organisms which consist of stabilized carbonate mineral may be observable and correlated in a time-stratigraphic framework. The studies which initially introduced these data as useful tracer for the fluctuation of carbon cycling through time were conducted on Cretaceous pelagic sequences (e.g. Scholle and Arthur, 1980; Renard, 1986; Jenkyns, 1988; Weissert, 1989). During the Cretaceous, it was believed that there were low-frequency ( $>10^5$  yrs) and high amplitude  $\delta^{13}\text{C}_{\text{carb}}$  fluctuations ( $>1.5\%$ ) which reflected mass being transferred between the global  $\text{C}_{\text{org}}$  and  $\text{C}_{\text{carb}}$  burial rates (Schidlowski, 1987). During the Cretaceous oceanic anoxic event (OAE), the widespread black-shale deposits, which increased the global sedimentary organic carbon accumulation rate, affected the global carbon cycle by transferring carbon to organic carbon reservoir. The large difference in carbon isotopic composition between these two carbon reservoirs thus affected the  $^{13}\text{C}/^{12}\text{C}$  ratio shift in the atmosphere  $\text{CO}_2$  and in the seawater  $\text{HCO}_3^-$  component. An increased  $^{13}\text{C}/^{12}\text{C}$  ratio in the  $\text{HCO}_3^-$  in the seawater and  $\text{CO}_2$  in the atmosphere as the  $^{12}\text{C}$  had been largely incorporated by an increase of global organic carbon accumulations. Carbonates precipitated from marine water at this specific period of time, therefore, reflect the  $^{12}\text{C}$  depleted (or  $^{13}\text{C}$  enriched) seawater and exhibit the positive  $\delta^{13}\text{C}_{\text{carb}}$  excursion. In  $\delta^{13}\text{C}_{\text{carb}}$  stratigraphy, the positive  $\delta^{13}\text{C}_{\text{carb}}$  excursion, if it occurred in parallel to  $\delta^{13}\text{C}_{\text{org}}$  variation, can be used to infer the time interval when the increased organic accumulation had occurred (Jenkyns, 1988 and 1995). In sequence stratigraphy, total organic carbon accumulation can be enhanced during the maximum flooding surface or a condensed section because of increasing productivity and/or anoxic conditions. Thus, the positive

$\delta^{13}\text{C}_{\text{carb}}$  excursion observed on the carbonate sequence is usually interpreted as the maximum flooding surface or a condensed section during period of increase  $^{13}\text{C}/^{12}\text{C}$  in the seawater. Shackleton and Pisias (1985) suggested that an increase in the  $^{13}\text{C}/^{12}\text{C}$  in the seawater occurred not only in the deep ocean basin but was also in the global surface seawater as well. In addition to pelagic carbonates, the  $\delta^{13}\text{C}_{\text{carb}}$  stratigraphy of carbonate sequences has been conducted successfully on shallow water carbonates or on a correlation between carbonate platform to basin (Vahrenkamp, 1996; Ferreri et al., 1997). However, the magnitude of positive  $\delta^{13}\text{C}_{\text{carb}}$  excursion at the maximum flooding surface on the shallow-water carbonate sediments may not always be distinctive due to a limited ocean water circulation where the structural enclosure may prevent full connection to the open marine system (Vahrenkamp, 1996).

### **6.3.2 Negative $\delta^{13}\text{C}_{\text{carb}}$ excursion**

In addition to positive excursions, negative excursions of  $\delta^{13}\text{C}_{\text{carb}}$  can be observed in the carbonate carbon isotope stratigraphy (e.g. Buggisch et al., 2003; Stephens and Sumner, 2003). Even though carbon isotope variation in carbonates may possibly be used to infer a large scale fluctuation of major carbon reservoirs, the variation of carbon isotope compositions of ancient carbonates also reflect their carbonate deposition and diagenetic environments which occurred during changes in relative sea level and water salinity (e.g. Margaritz and Stemmerik, 1989; Joachimski and Buggisch, 1993; Saltzman et al., 1995; Kaufman and Knoll, 1995; Saltzman et al., 1998). On a carbonate platform, it is not uncommon that its shallowing condition related to falling relative sea level fall or subaerial exposure can also be influenced by meteoric diagenetic alteration. On a local scale, carbonate diagenesis under meteoric water zone can affect  $\delta^{13}\text{C}_{\text{carb}}$  values by causing a negative  $\delta^{13}\text{C}_{\text{carb}}$  excursion which has also been suggested to be useful for local stratigraphic correlation (Allan and Matthews, 1982). Allan and Matthews (1977 and 1982) reported that during subaerial exposure meteoric diagenesis can have a significant role for

changing the  $\delta^{13}\text{C}$  values in ancient carbonates. They recognized that carbonates from immediately beneath a subaerial exposure surface generally consist of  $\delta^{13}\text{C}$  compositions that are more negative than values of sediments which are derived from greater depth below the exposure surface. These more negative and depth-dependent  $\delta^{13}\text{C}$  values are suggested to result from the incorporation of isotopically light carbon from soil gas carbon dioxide ( $\text{CO}_2$ ) into the carbonate lattice during recrystallization and cementation in the shallow meteoric vadose zone (**Figure 6-4**). The variations of carbon and also oxygen isotope compositions of carbonates produced during different diagenetic conditions and their distinct patterns, therefore, are useful for identifying the subaerial exposure horizons and zone of meteoric diagenesis within the ancient limestone sequences (**Figure 6-5**).

According to Allan and Matthews (1982), six potential isotope patterns could be used to view stable isotope data within a stratigraphic framework on a local and/or a regional scale, if worldwide falling relative sea level occurs. These patterns are: 1) the strongly  $^{12}\text{C}$ -enriched (or  $^{13}\text{C}$ -depleted) limestone at subaerial exposure surface and the heavier (more positive)  $\delta^{13}\text{C}$  compositions of the underlying carbonates; 2) the possibility of a slightly heavier  $\delta^{18}\text{O}$  value in carbonates at the subaerial exposure surface due to evaporation; 3) an abrupt shift in  $\delta^{18}\text{O}$  values from the deeper sediments to the shallow sediments at the exposure surface; 4) the positive covariance between the  $\delta^{13}\text{C}$  and the  $\delta^{18}\text{O}$  compositions of sediments which were altered in the marine-meteoric mixing zone; 5) the sharp increase of  $\delta^{13}\text{C}$  values at the boundary between the vadose to phreatic zones; and 6) a narrow variation of  $\delta^{18}\text{O}$  but a larger variation of  $\delta^{13}\text{C}$  values for a single contemporaneous meteoric diagenetic alteration occurring under a restricted environment.

Subsequently, Magaritz and Stemmerik (1989) reported the depleted  $\delta^{13}\text{C}$  values to be observed during the regressive phase or relative sea level lowstand. They suggested the more negative  $\delta^{13}\text{C}$  values in sediments were not always necessarily influenced only by the local  $^{12}\text{C}$ -enriched organic-derived  $\text{CO}_2$ , but might also be the reflection from a large scale variation in

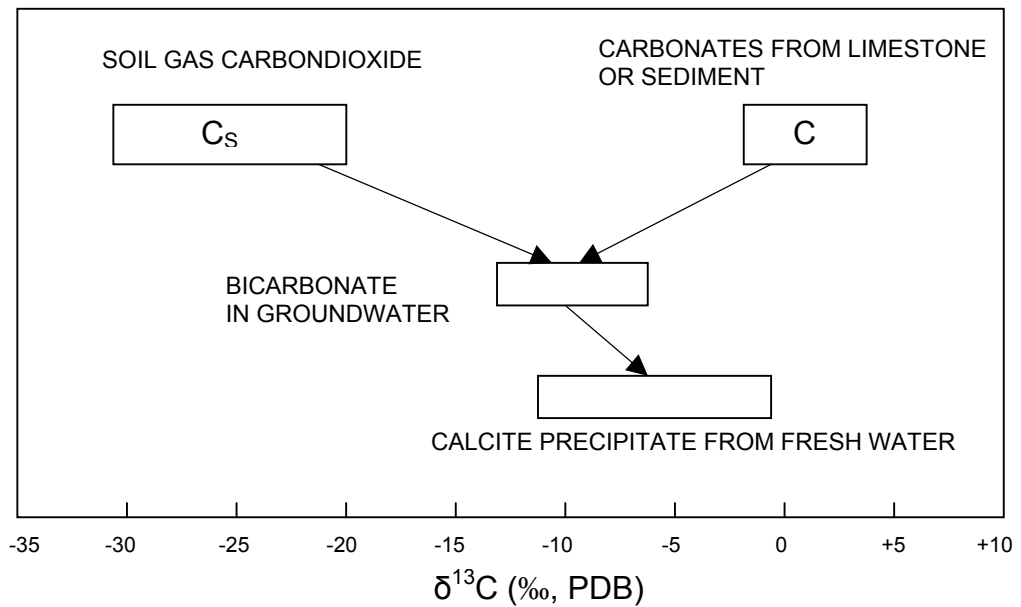


**Figure 6-4.** Diagram illustrating effect of meteoric water diagenesis on  $\delta^{13}C$  composition of limestone sediments that results from mixing of carbon from metastable marine sediments with carbon from soil-gas carbon dioxides ( $CO_2$ ). It is suggested that  $\delta^{13}C$  composition of carbonates depends on the molar ratio  $C_L/C_{SG}$  ( $C_L$ = No. of moles carbon derived from limestone sediment;  $C_{SG}$ =No. of moles carbon

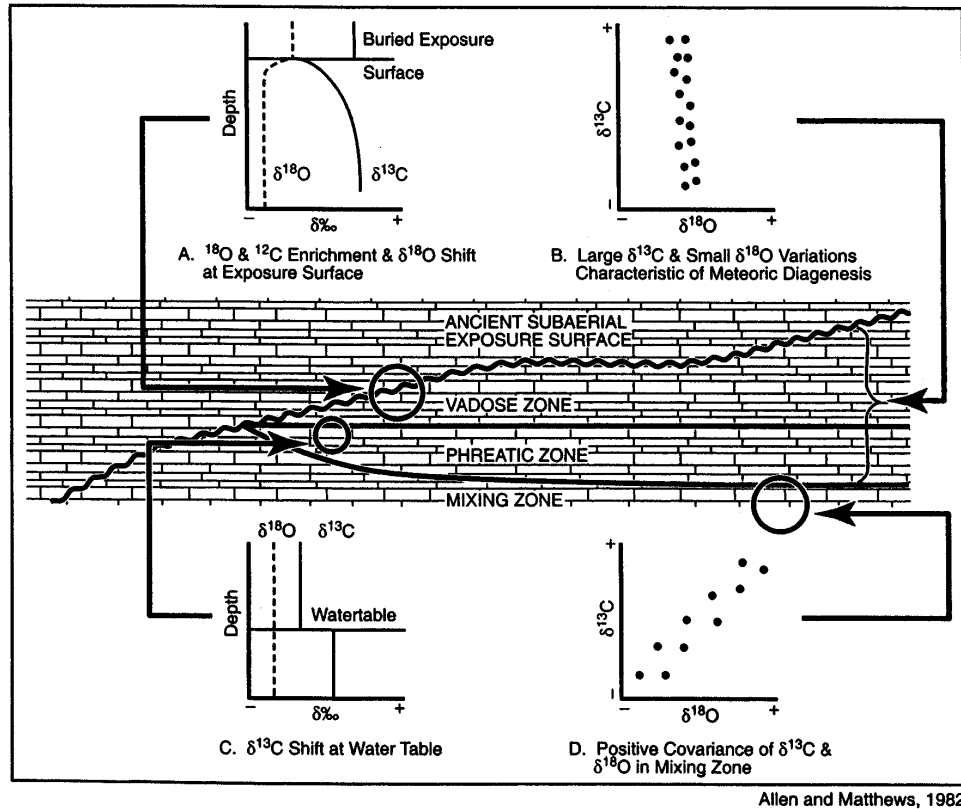


**Figure 6-5.** Figure illustrating potential patterns of  $\delta^{18}\text{O}$  and  $\delta^{13}\text{C}$  variations in the ancient carbonate rocks which can be useful for interpreting diagenetic depositional environments on the vertical trends in a time-stratigraphic framework that possibly are relative to changes of sea level (from Allan and Matthews, 1982).

carbon budget. During a regressive period, because of decreased organic productivity and/or increased rate of organic material oxidation ( $^{12}\text{C}$ -enriched) during the exposure of the platform, the dissolved inorganic carbon in the ocean would become depleted in  $^{13}\text{C}/^{12}\text{C}$  ratios which would result in lighter  $\delta^{13}\text{C}_{\text{carb}}$  values in carbonates. During the transgression, seawater  $\text{HCO}_3^-$  is more enriched in  $^{13}\text{C}$  so that carbonate precipitates consist of more positive  $\delta^{13}\text{C}_{\text{carb}}$  values. Because carbonate transgressive-regressive cycles usually correspond to the changes in sea level cycles, the more negative  $\delta^{13}\text{C}_{\text{carb}}$  values of the sediments can be used to infer the falling sea level cycle in addition to the heavier  $\delta^{13}\text{C}_{\text{carb}}$  values (Magaritz and Stemmerik, 1989). Vahrenkamp (1996) described a correlation of carbon isotope trends, sea level and sediment depositional system which can be applied to carbonate deposition: 1) the positive  $\delta^{13}\text{C}_{\text{carb}}$  trend characterizes the rising sea level during the transgressive system tract (showing backstepping sedimentation and a condensed section in the downdip area), 2) the constant  $\delta^{13}\text{C}_{\text{carb}}$  trend characterizes the stable or stillstand sea level during the highstand system tract (high carbonate production of aggradation and progradation) and 3) the negative  $\delta^{13}\text{C}_{\text{carb}}$  trend characterizes the falling relative sea level during forced regression or the lowstand system tract (this trend may not be present in the updip area due to exposure). Many sequence stratigraphy studies of carbonates from ramp platforms demonstrated that the  $\delta^{13}\text{C}_{\text{carb}}$  variation of the carbonate sediments could be correlated to the relative sea level changes of the third-order eustatic cycles (e.g. Valladares et al., 1996; Vahrenkamp, 1996; Buggisch et al., 2003).

### 6.3.3 SAMPLE ANALYSIS

The isotope composition values of material (both carbon and oxygen isotopes) in carbonate and organic components are denoted by a conventional notation  $\delta$  in a unit of part per thousand (‰). This notation represents the difference of an isotopic ratio (i.e.  $^{13}\text{C}/^{12}\text{C}$  or  $^{18}\text{O}/^{16}\text{O}$ ) in the sample compared to the ratio in the international standard which commonly is the Pee Dee

Belemnite (PDB) carbonates. Usually, even though the Standard Mean Oceanic Water (SMOW) is also used as a standard for oxygen isotope composition, the value relative to the SMOW generally is converted and reported to value relative to PDB standard. The equations for calculating the  $\delta^{13}\text{C}$  and  $\delta^{18}\text{O}$  (‰) relative to the standard in each sample have been illustrated in Chapter 3. For this study, both carbon and oxygen isotope values are reported relative to the PDB standard.

Carbonate samples that are used for investigating  $\delta^{13}\text{C}_{\text{carb}}$  stratigraphy can come from calcareous fossils such as foraminifera (Popp et al., 1986; Bill et al., 1995; Li et al., 2000) or a bulk rock carbonates (Scholle and Arthur, 1980; Weissert and Lini, 1991; Varenkamp, 1996). The advantages of using bulk samples are based upon the faster technique and homogeneity averaging the vital effect due to variable organisms and the diagenetic alterations (Scholle and Arthur, 1980). Even though original carbonate minerals (i.e. aragonite, high-Mg calcite, low-Mg calcite) can have different degrees of diagenetic alteration on their trace elements and isotopic compositions, in fact, the alteration of carbon isotope composition in the stable recrystallized (diagenetic) low-Mg calcite mineral is relatively minor because of much smaller volume of pore water compared to the bulk rock volume (Brand and Veizer, 1980 and 1981; Allan and Matthews, 1982). However, it is expected that if there was involved meteoric diagenesis effect, the  $^{12}\text{C}$  from a soil-dissolved  $\text{CO}_2$  would contribute to the more negative  $\delta^{13}\text{C}$  values (Brand and Veizer, 1981; Allan and Matthews, 1982).

Core observations and elemental analyses of the Smackover described in the previous chapters have indicated that there are vertical and lateral variations in sedimentary texture and diagenetic environment between the Smackover deposits in the Conecuh Embayment and in the Manila Embayment. Although the low-Mg calcite mudstone samples are the most preferred materials, as they represent the more stable, potentially less diagenetically altered materials, to characterize Smackover  $\delta^{13}\text{C}$  stratigraphy, wackestone, grainstone, packstone and dolomite, which likely included more heterogeneous compositions of carbonate minerals, are also presented

in order to obtain results for the complete Smackover sequence. Indeed, this sedimentary indiscrimination of using samples from different lithofacies and diagenetic alteration might be an effective approach to investigate the  $\delta^{13}\text{C}$  composition of carbonates from different depositional environment if there is any correlation which is independent to a local variation including diagenesis and burial. It has been suggested by Emrich et al. (1970) that temperature effect in the burial environment has small effect on  $\delta^{13}\text{C}$  alteration compared to the effect on the  $\delta^{18}\text{O}$  values. Holser (1997) has also reported that late diagenesis including dolomitization might also have minimal effect on the changes of  $\delta^{13}\text{C}$  values of the sediment samples.

## 6.4 RESULTS

### 6.4.1 Carbon Isotopic Composition of the Smackover carbonates

Carbon isotope values ( $\delta^{13}\text{C}_{\text{carb}}$ ) of the whole rock Smackover sediments from the T.R. MILLER MILLS 17-11, #1 of the Conecuh Embayment and from the #1 NEAL ET AL UNIT 30-1 of the Manila Embayment illustrate the variation ranging from 1‰ to 6‰ (PDB) (**Figure 6-6**). Exceptions occur in a few samples just above the reworked sandstone unit at the base of the Smackover in the #1 NEAL ET AL UNIT, 30-1 which consist of negative  $\delta^{13}\text{C}_{\text{carb}}$  values of -0.71‰ and -0.16‰. In the Conecuh Embayment, the sandstone samples of the Norphlet Formation underlying the Smackover carbonates were also analyzed but yielded too little carbonate carbon for  $\delta^{13}\text{C}_{\text{carb}}$  analysis. On the long vertical trend, both Smackover units illustrate some comparable short-term  $\delta^{13}\text{C}_{\text{carb}}$  variations regardless of the lithology, sediment thickness and diagenesis. In the T.R. MILLER MILLS 17-11, #1, three short-term negative and positive  $\delta^{13}\text{C}_{\text{carb}}$  fluctuation trends are clearly observable. The first short-term negative  $\delta^{13}\text{C}_{\text{carb}}$  trend (as the  $\delta^{13}\text{C}_{\text{carb}}$  become more negative values) in the T.R. MILLER MILLS 17-11, #1 core starts from the base of the Smackover from 13845 ft to approximate 13795 ft. The  $\delta^{13}\text{C}_{\text{carb}}$  values decrease from around 3.5‰ to about 2.3‰. The second trend is observed from 13737 ft to around 13680 ft and

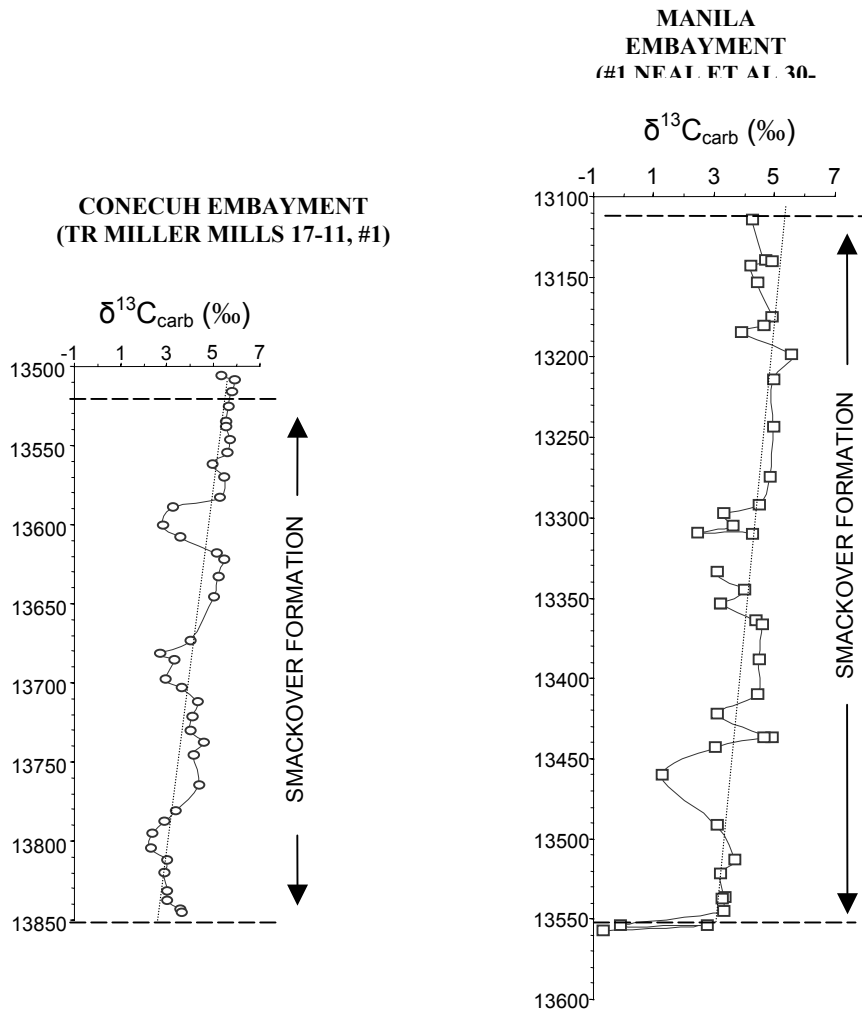


**Figure 6-6.** Carbon isotope variation ( $\delta^{13}C_{carb}$ ) from the whole rock samples of the Smackover Formation from the T.R. MILLER MILLS 17-11, #1 well of the Conecuh Embayment and from

the  $\delta^{13}\text{C}_{\text{carb}}$  vary from 4.5‰ to about 2.7‰. The third trend is from 13623 ft to around 13590 ft showing the  $\delta^{13}\text{C}_{\text{carb}}$  values vary from about 5.4‰ to less than 3‰. The carbonates above this part to the top of the Smackover Formation illustrate constant and heavy  $\delta^{13}\text{C}_{\text{carb}}$  compositions ranging from 4.9‰ to around 6‰. The mixed anhydrite-carbonate sample of the Buckner Anhydrite have  $\delta^{13}\text{C}_{\text{carb}}$  values of 5.88‰. In the #1 NEAL ET AL UNIT 30-1 core from the Manila Embayment, negative  $\delta^{13}\text{C}_{\text{carb}}$  excursions are also distinguished although showing some differences if compared to the Smackover in the Conecuh Embayment. In the #1 NEAL ET AL UNIT 30-1 core, the first negative  $\delta^{13}\text{C}_{\text{carb}}$  excursion to values of -0.71‰ and -0.16‰ is observed at the base of the Smackover. The negative  $\delta^{13}\text{C}_{\text{carb}}$  trend then presents showing values which decreases from 3.2‰ to less than 2‰ to about 3‰ at depths from 13460 ft to 13420 ft. Again, smaller-scale fluctuations are observed during this interval. The next  $\delta^{13}\text{C}_{\text{carb}}$  negative trend begins around 13367 ft and extends to around 13298 ft showing  $\delta^{13}\text{C}_{\text{carb}}$  values decreasing from above 4.5‰ to around 2.5‰ to 3.5‰. Above this interval the  $\delta^{13}\text{C}_{\text{carb}}$  compositions of the carbonate to the top of the Smackover Formation exhibit heavier values from 4.4‰ to almost 5.5‰, but with a small fluctuation to a lighter  $\delta^{13}\text{C}_{\text{carb}}$  value of 3.88‰. In this well, the  $\delta^{13}\text{C}_{\text{carb}}$  of carbonate from the Buckner Anhydrite is around 4.2‰.

#### 6.4.2 Oxygen isotopes

The oxygen isotope compositions ( $\delta^{18}\text{O}_{\text{carb}}$ , relative to PDB) of the Smackover carbonate samples from the T.R. MILLER MILLS 17-11, #1 and the #1 NEAL ET AL UNIT 30-1 cores in the Conecuh and the Manila Embayments illustrate different vertical fluctuations in the  $\delta^{18}\text{O}_{\text{carb}}$  values (**Figure 6-7**). In the Conecuh Embayment, the  $\delta^{18}\text{O}_{\text{carb}}$  values of the samples vary from -4‰ to 4‰ and show a relative narrow fluctuation in the middle part of the core compared to the carbonates from the Manila Embayment. Samples with heavier  $\delta^{18}\text{O}_{\text{carb}}$  values more than -1‰ mainly occur in the upper lower and the middle Smackover. The lighter  $\delta^{18}\text{O}_{\text{carb}}$  values less than

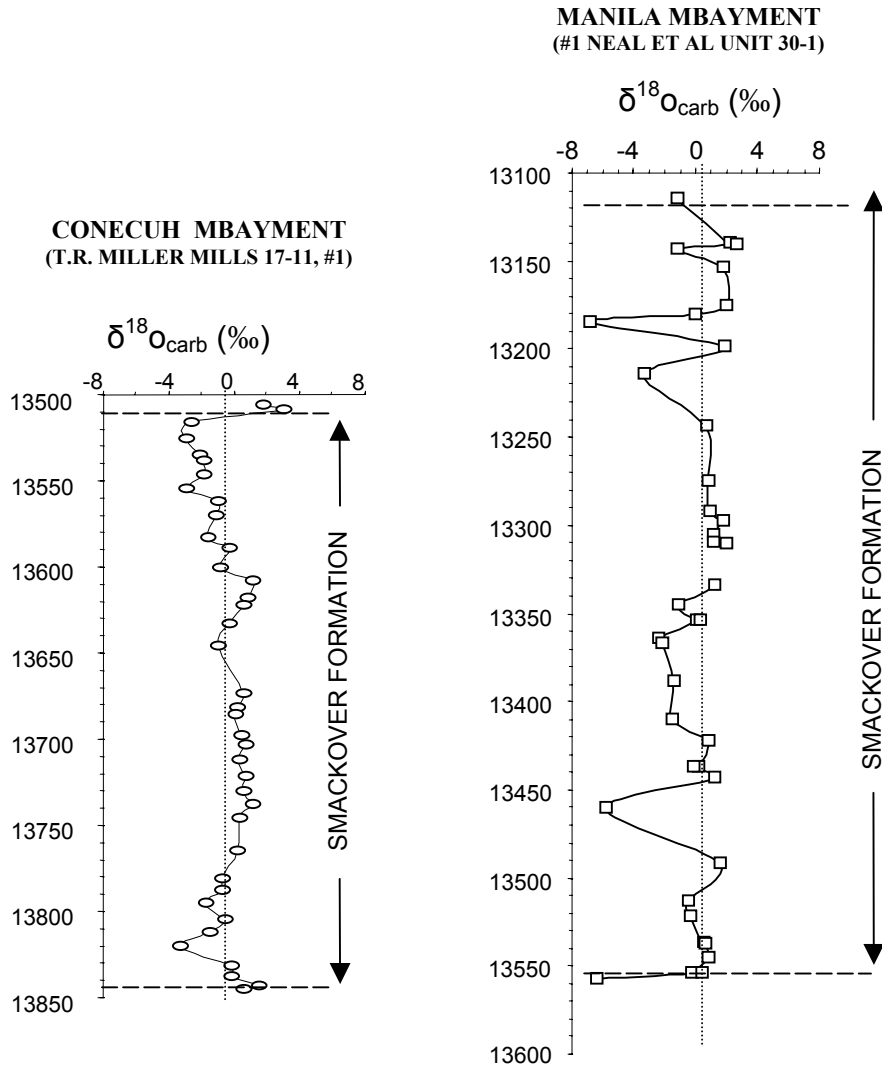


**Figure 6-7.** Oxygen isotope variation ( $\delta^{18}\text{O}_{\text{carb}}$ ) from the whole rock samples of the Smackover Formation from the T.R. MILLER MILLS 17-11, #1 well of the Conecuh Embayment and from

-1‰ occur near the base of the lower and in the upper Smackover sedimentations. The Buckner Anhydrite samples above the Smackover have  $\delta^{18}\text{O}_{\text{carb}}$  values ranging from 1‰ to 3‰. In the Manila Embayment, the  $\delta^{18}\text{O}_{\text{carb}}$  values vary from -7‰ to 4‰. A relative large negative  $\delta^{18}\text{O}_{\text{carb}}$  value, greater than 6‰, is observed in sample above the reworked Norphlet sandstone unit. Compared to samples from the Conecuh Embayment, the Smackover sequence of the Manila Embayment generally reflects a larger  $\delta^{18}\text{O}_{\text{carb}}$  fluctuation especially in the upper part of the core. A sample from carbonate mixed inside the Buckner anhydrite in the top part of the #1 NEAL ET AL UNIT 30-1 core consists of negative  $\delta^{18}\text{O}_{\text{carb}}$  value less of than -1‰.

## **6.5 DISCUSSION**

### **6.5.1 Diagenetic Effects**

The ranges of carbon isotope values from 1‰ to 6‰ (relative to PDB) observed in the Smackover samples from the Conecuh Embayment and the Manila Embayment of this study are comparable to the  $\delta^{13}\text{C}_{\text{carb}}$  values of the Smackover carbonates and dolomites from the Escambia County of Alabama (Vinet, 1984; Saller and Moore, 1986; Haywick et al., 2000). The oxygen isotope compositions of samples from the #1 NEAL ET AL UNIT 30-1 well exhibit some larger negative values (to -7‰), but samples from the T.R. MILLER MILLS 17-11, #1 well consist of the same  $\delta^{18}\text{O}_{\text{carb}}$  distribution between -4‰ to 4‰ as previously reported. Even though vertical variation of the  $\delta^{13}\text{C}_{\text{carb}}$  values of shallow carbonates, especially the recrystallized low-Mg calcite have been indicated to be useful for stratigraphic correlation (Allan and Matthews, 1977 and 1982; Given and Lohmann, 1985; Lohmann, 1988), the susceptibility of carbonates to diagenesis requires that the variation of  $\delta^{13}\text{C}_{\text{carb}}$ ,  $\delta^{18}\text{O}_{\text{carb}}$ , and some trace elements in these Smackover samples should be examined for the diagenetic influence on their isotope compositions.

For diagenetic stabilization of carbonate constituents, the processes are usually

accompanied by changes in sediment texture and chemical composition (Brand and Veizer, 1981). Strong alteration from diagenesis occurs in the meteoric diagenetic environment because of difference in the chemical compositions between the interstitial pore waters and the sediments. With the increase in the degree of post-depositional alteration, the textural maturity of sediments changes from original carbonate phases i.e. aragonite (A), high-Mg calcite (HMC), low-Mg calcite (LMC), into the stabilized carbonate phase of diagenetic low-Mg calcite (dLMC). Carbonate diagenesis can take place in different depositional environments i.e. fresh water, near-surface marine and deep burial environment. In general, there are six different processes that affect diagenesis and these are: dissolution, cementation, micritization, neomorphism, compaction and dolomitization (Tucker and Wright, 1990, Chapter 7). Although carbonate diagenesis varies due to the depositional environment, for a shallow-marine carbonate, early near-surface meteoric diagenesis is common due to the shallow paleowater depth condition. Several common reactions which occur in this meteoric diagenetic zone are dissolution, cementation and reprecipitation. Because of different chemical compositions of seawater in which the carbonate sediments were formed and in fresh water (as shown in Table 5-1), diagenetic reactions usually affect changes in chemical composition of the stabilized dLMC manifested by a decrease of  $\text{Sr}^{2+}$  and  $\text{Na}^{2+}$  and an increase in  $\text{Mn}^{2+}$  and  $\text{Fe}^{2+}$  concentrations. During these diagenetic, wet dissolution-reprecipitation steps (Bathurst, 1975), not only are the minor or trace elements in carbonates altered in order to reach equilibration with the meteoric water, but the isotopic composition of the oxygen and carbon in the minerals ( $^{18}\text{O}/^{16}\text{O}$  and  $^{13}\text{C}/^{12}\text{C}$  ratios) are also affected. In a shallow carbonate, if the stabilization processes occur in the phreatic and vadose freshwater zones, changes in the  $\delta^{13}\text{C}_{\text{carb}}$  and  $\delta^{18}\text{O}_{\text{carb}}$  compositions result from diagenetic exchanges between an original marine carbonate phase and dissolved  $\text{HCO}_3^-$  of the meteoric water ( i.e.  $^{13}\text{C}^{18}\text{O}_3^{2-} + \text{H}_2^{16}\text{O} + ^{12}\text{CO}_2 \leftrightarrow ^{12}\text{C}^{16}\text{O}_3^{2-} + \text{H}_2^{18}\text{O} + ^{13}\text{CO}_2$  ) (Land, 1970; Matthews, 1974; Allan and Matthews, 1977; Brand and Veizer, 1981). Depletions in  $\delta^{18}\text{O}_{\text{carb}}$  and  $\delta^{13}\text{C}_{\text{carb}}$  from diagenesis are affected by an enrichment of  $^{16}\text{O}$  and the  $^{12}\text{C}$  in dissolved  $\text{CO}_2$ , if soil-derived, in meteoric freshwater (Vogel, 1959; Allan and

Mathews, 1977 and 1982 ). In general, the degree of isotopic exchange depends on the proportions of the isotopes in the stabilized phase derived from the carbonate precursor and in the interstitial water. The greater the influence of the interstitial water the more open the sediments are to the diagenetic environment, the closer the isotopic equilibrium between the water and the precipitate dLMC. The influences of meteoric diagenesis on changes in the carbonate components are briefly described in **Figure 6-8**. The rate of changes in these chemical compositions are also dependent upon: 1) the stability of the original carbonate phases; 2) the water/rock ratio or the openness of the diagenetic system; 3) the difference in chemical composition of seawater and diagenetic meteoric water; and 4) the deviation of a particular partition coefficient (fractionation factor) (Brand and Veizer, 1981). Diagenetic effects on the Smackover samples therefore can play a partial role on the variations of sedimentary texture and chemical compositions. .

The variations of the  $\delta^{13}\text{C}_{\text{carb}}$  and  $\delta^{18}\text{O}_{\text{carb}}$  values with depth observed in the Smackover cores, shown in Figure 6-6 and Figure 6-7, suggest there were variable diagenetic environments during the Smackover depositional sequence. Similar fluctuations in the  $\delta^{13}\text{C}_{\text{carb}}$  values between more negative and positive values suggest a possible stratigraphic correlation which could occur on a local and/or global scale variations. In contrast, the difference between the  $\delta^{18}\text{O}_{\text{carb}}$  trends indicates the lateral variation which affected differences in isotope exchanges between the  $\delta^{18}\text{O}$  of the pore waters and carbonates. These observations support different sedimentary environments and facies in the core as described in the previous chapter. The Conecuh Embayment samples, the dominated mudstone and wackestone (from 13775 ft to 13650 ft) of low-Mg calcite minerals (micrite, pellet and peloid allochems) were probably not significantly affected by a large change in chemical composition because of their closer concentrations to the dLMC. The semi-enclosed structural setting of the embayment likely restricted open-marine circulation and thus might induce slight hypersalinity of the water which would enrich the water to a heavier  $\delta^{18}\text{O}_{\text{carb}}$  composition. Since the  $\delta^{18}\text{O}_{\text{carb}}$  exchanges from recrystallization would likely occur from the same single freshwater reservoir in the subsurface, the  $\delta^{18}\text{O}_{\text{carb}}$  values in most of this part of the

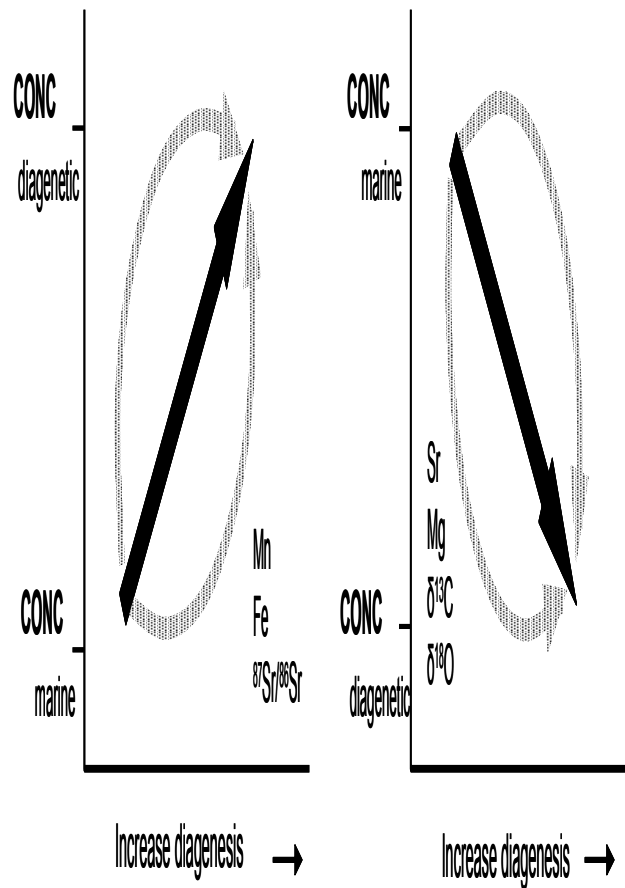


Figure 6-8. Diagrams illustrating diagenetic influence on multi-component in carbonate systems. According to Brand and Veizer (1980 and 1981), geochemical reactions affect the shifting of concentration of these components into equilibrium in diagenetic environment. It is noted that the schematic examples are given only the common diagenetic trends in decreasing or increasing concentrations during meteoric and burial environments. The actual geochemical changes in an individual carbonate or component are dependent upon the diagenetic history of the sediment and the availability of specific ions or isotopes (from Marshall, 1992).

Smackover core consisted of small variations but with a slightly heavier  $\delta^{18}\text{O}_{\text{carb}}$  values compared to other ancient carbonate isotope compositions (Brand and Veizer, 1981; Figure 2 and Figure 4). On the contrary, the packstone and grainstone which dominated in the upper part of this core basically might have consisted of aragonite and high-Mg calcite mineral phases. The dissolution and reprecipitation processes occurred as a result of the passage of the freshwater pore-fluids undersaturated with respect to these mineral phases where the isotopic exchanges between the interstitial water in the pores and rock minerals became very effective. By increasing pore water/rock ratio, the  $\delta^{18}\text{O}_{\text{carb}}$  of the recrystallized minerals become isotopically lighter due to the isotopically lighter meteoric water. In the present day, organic and inorganic carbonates in equilibrium with present-day seawater  $\delta^{18}\text{O}_{\text{carb}}$  are between +1‰ to -2‰ (Milliam, 1974) and between -2‰ to -30‰ with the freshwater  $\delta^{18}\text{O}_{\text{carb}}$  values. In the upper Smackover (from 13587 ft to the top of the Smackover) the lighter  $\delta^{18}\text{O}_{\text{carb}}$  values (less than -1‰) are interpreted to be influenced by the susceptibility of the original mineral phases and an increased pore fluid/rock ratio for the  $^{18}\text{O}$  and  $^{16}\text{O}$  isotopic exchange in the meteoric water zone. This effect however could be much smaller for the  $\delta^{13}\text{C}_{\text{carb}}$  values in these samples since there is much more bulk carbon in the carbonate rock relative to the pore fluids. Unless the  $\delta^{13}\text{C}_{\text{carb}}$  composition of the pore-fluids is altered during subaerial processes, compared to oxygen isotopes, carbon isotope composition of the carbonate rock could be a reliable signature for the carbon isotope composition of the possible precursor sediment (Land, 1986).

For the Manila Embayment, a large negative  $\delta^{18}\text{O}_{\text{carb}}$  fluctuation observed throughout the core is also interpreted to result from isotopic exchanges of meteoric water diagenesis associated with less stabilized original carbonate mineral phases (i.e. high-Mg calcite and aragonite). Burial diagenesis and elevated subsurface temperature might have affected on oxygen isotopes but they probably were not the major contribution to the different  $\delta^{18}\text{O}_{\text{carb}}$  values observed in these two Smackover sequences as both were derived from the same platform and comparable subsurface depth interval. Located on a paleostructural high (Wade et al., 1987), the Manila Embayment

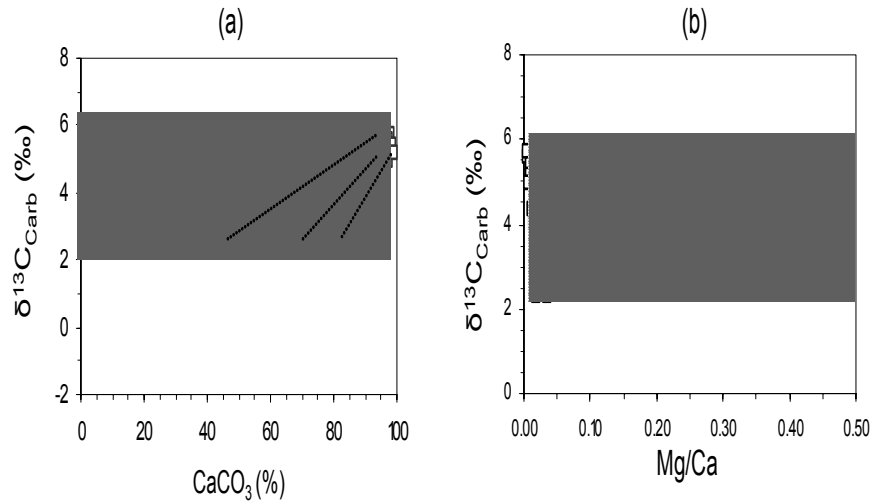
could have relative shallower paleowater-depth compared to paleoenvironment in the Conecuh Embayment. As described in Chapter 4, interpretation of the sedimentary facies suggested a tidal-flat depositional environment for the Manila Embayment and the restricted marine-lagoonal systems for the Conecuh Embayment. The shallower paleowater depth in the Manila Embayment probably increases susceptibility of meteoric diagenesis to carbonate sediment under the shallower vadose zone than the phreatic zone. Because freshwater is undersaturated with respect to carbonate sediment, dissolution can also take place illustrating an abundance of possible dissolved pores and vugs, especially in the #1 NEAL ET AL UNIT 30-1 core. As the water moved down through the vadose zone, its composition had become supersaturated with respect to carbonates and reprecipitations occur. From the phreatic zone, pore spaces were fluid-filled all the time. With increasing depth, the freshwater could move downwards to the more saline water at depths of several hundred meters or more where the mixing zone between phreatic meteoric water and the seawater occur and dolomites occurred. Dolomitization of carbonate sediments could have occurred under several conditions (i.e. evaporative-hypersaline, seepage- reflux, mixing zone, normal marine, and burial dolomitization) (Tucker and Wright, 1990, Chapter 8), but examination of the mechanism for dolomitization of the Smackover carbonate is beyond the scope of this study. From the literature, various models for dolomitization have been reported for Smackover deposition in the Escambia County of Alabama. For example, the evaporative-hypersaline and the seepage-reflux or evaporative drawdown models from Saller and Moore (1986); and the hypersaline, mixing zone and hydrothermal models from Haywick et al. (2000). The similar ranges of the  $\delta^{13}\text{C}_{\text{carb}}$  values observed in those above studies of dolomites (from 4.4‰ to 5.7‰ and 5.2‰ to 6.0‰ for  $\delta^{13}\text{C}_{\text{carb}}$  and from 1.4 to 4.5‰ and -1.8‰ to for  $\delta^{18}\text{O}_{\text{carb}}$  reported by Saller and Moore, 1986; from 2‰ to 6‰ for the  $\delta^{13}\text{C}_{\text{carb}}$  and -7‰ to 4‰ for the reported by Haywick et al., 2000) when compared to the  $\delta^{13}\text{C}_{\text{carb}}$  values from the Smackover of this study, suggest that carbon isotope compositions of dolomite were probably not altered significantly from the original carbonate phase. The XRD analysis of some Smackover samples from the T.R.

MILLER MILLS 17-11, #1 core (Table 6 listed in Appendix 5-1) support that dolomitization is minor for the samples from the Conecuh Embayment in the vicinity of this well.

Variations of  $\delta^{13}\text{C}_{\text{carb}}$  values with the carbonate and dolomite components are examined in cross-plots of carbonate mineral content (include dolomite, from HCl dissolution) and the Mg/Ca ratio (**Figure 6-9**). Mg/Ca value is used to indicate dolomitization based on the fact that dolomite consists of higher  $\text{Mg}^{2+}$  or  $\text{MgCO}_3$  (~50 mole%) than the common original carbonate minerals (i.e. LMC: less than 4 mol%; HMC: between 4-30 mol%) (Veizer, 1983). According to Land (1986), naturally occurring dolomite ( $\text{CaMg}(\text{CO}_3)_2$ ) can have variable compositions ranging from  $\text{Ca}_{1.16}\text{Mg}_{0.84}(\text{CO}_3)_2$  to  $\text{Ca}_{0.96}\text{Mg}_{1.04}(\text{CO}_3)_2$  resulting in Mg/Ca ratios varying from 0.72 to 1.083. With increasing dolomitization, the Mg/Ca ratio in carbonate rocks is expected to increase at least 0.72. Most samples from the Conecuh Embayment illustrate Mg/Ca ratios even smaller than 0.1 which suggests insignificant dolomitization has occurred. Except for a few samples, the high Mg/Ca ratios around 0.3 to 0.5 could represent dolomites that occurred near the base and the top of the Smackover in this area. In the Manila Embayment, samples from the #1 NEAL ET AL UNIT 30-1 have Mg/Ca ratios higher than 1.08 confirming dolomite observed in the core and thin sections.

For both cores, the  $\delta^{13}\text{C}_{\text{carb}}$  values range from 1‰ to 6‰ illustrate different distribution between the dominant carbonate sediment from the Conecuh Embayment and the dominant dolomite sediment from the Manila Embayment. However, with respect to the  $\delta^{13}\text{C}_{\text{carb}}$  values, a similar range of the  $\delta^{13}\text{C}_{\text{carb}}$  values between two cores indicate dolomite was not specifically responsible for changes in the  $\delta^{13}\text{C}_{\text{carb}}$  values, especially in the #1 NEAL ET AL UNIT 30-1 sample from the Manila Embayment. In contrast, for samples from the Conecuh Embayment, the distribution of data indicates positive correlation between carbonate contents and  $\delta^{13}\text{C}_{\text{carb}}$  values and illustrates more than one positive trends. The correlation between carbonate contents and  $\delta^{13}\text{C}_{\text{carb}}$  values is recognizable; the higher the carbonate content, the more positive the  $\delta^{13}\text{C}_{\text{carb}}$  values. These observations not only suggest that dolomitization did not have significant

CONECUH EMBAYMENT (T.R. MILLER MILLS 17-11, #1)



MANILA EMBAYMENT (#1 NEAL ET AL UNIT 30-1)

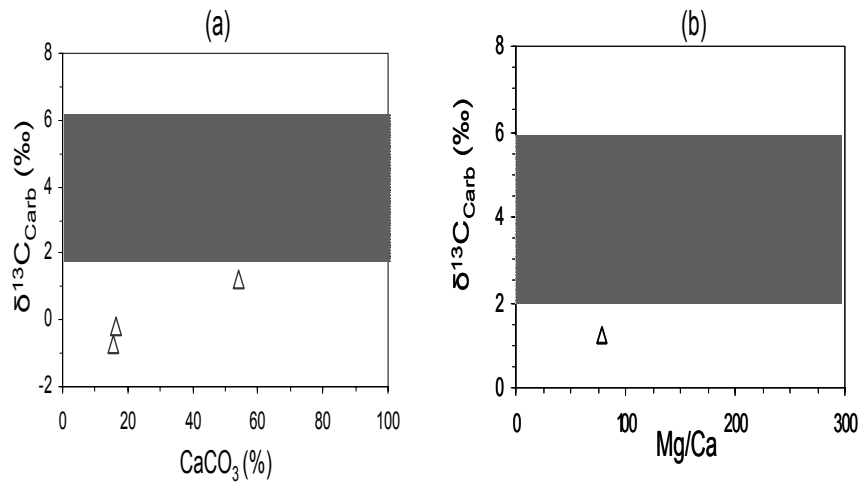
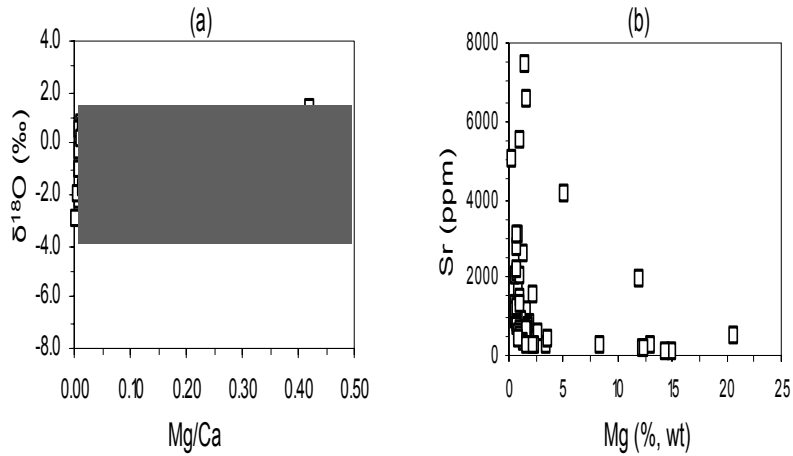


**Figure 6-9** Cross-plots illustrating the distribution between (a) the  $\delta^{13}C_{\text{carb}}$  values and the carbonate content (including dolomite) analyzed by acid dissolution (HCl) and (b) the  $\delta^{13}C_{\text{carb}}$  values and the Mg/Ca ratio for dolomite presented in these two cores.

alteration on the  $\delta^{13}\text{C}_{\text{carb}}$  values to these Smackover samples, but the more positive  $\delta^{13}\text{C}_{\text{carb}}$  values tend to exist in samples with the higher carbonate contents. Because the positive  $\delta^{13}\text{C}_{\text{carb}}$  values in the high carbonate content samples appear to form during the relatively high sea level, the observation from the T.R. MILLER MILLS 17-11, #1 samples suggests there was variation of sea level conditions which affected carbonate sedimentation. In the case of the #1 NEAL ET AL UNIT 30-1 samples, it is possible that dolomitization had obscured this correlation or it was because carbonate sediments were derived from the tidal environment, where the fluctuation was principally controlled by the local tide currents (not from open marine condition), this correlation was then not distinctive.

Again, the effects of dolomitization on these two Smackover set of samples are checked by the of  $\delta^{18}\text{O}_{\text{carb}}$  variation and by the variation of elements, Mg and Sr, which are sensitive to carbonate diagenesis (**Figure 6-10**). The plot with Mg/Ca (Figure 6-10a) shows that dolomitization did not have strong influence on the variation of the  $\delta^{18}\text{O}_{\text{carb}}$  values in these Smackover rocks. Diagenesis also has an effect on the changes of the Mg and Sr concentrations in carbonate or dolomitized rocks. In carbonate-dominated rocks, diagenetic alteration would present a positive correlation between Mg and Sr (Figure 6-8). However, with the dolomitization effect, while the Sr concentration decreases, Mg would increase. This relationship is clearly observable for samples from the #1 NEAL ET AL UNIT 30-1 core (Figure 6-10b). With respect to Sr concentration in carbonate rocks, Veizer (1983) reported that Sr concentrations in ancient dolomites usually should not exceed 600 ppm (from 20 to 600 ppm) unless dolomite precipitations occur from hypersaline solutions. In general, aragonite and high-Mg calcite minerals, which can dominate in shallow-water carbonates, can be enriched in Sr concentrations (compared to low-Mg calcite). Therefore, dolomites that evolve from an original aragonite phase may consist of high Sr concentration, but usually still less than 550 ppm. The ancient dolostones, if they were formed and affected by early diagenetic conditions, were reported to have Sr concentration ranging from 100-1000 ppm, and from 30-100 ppm if they were affected by late

CONECUH EMBAYMENT (T.R. MILLER MILLS 17-11, #1)



MANILA EMBAYMENT (#1 NEAL ET AL UNIT 30-1)

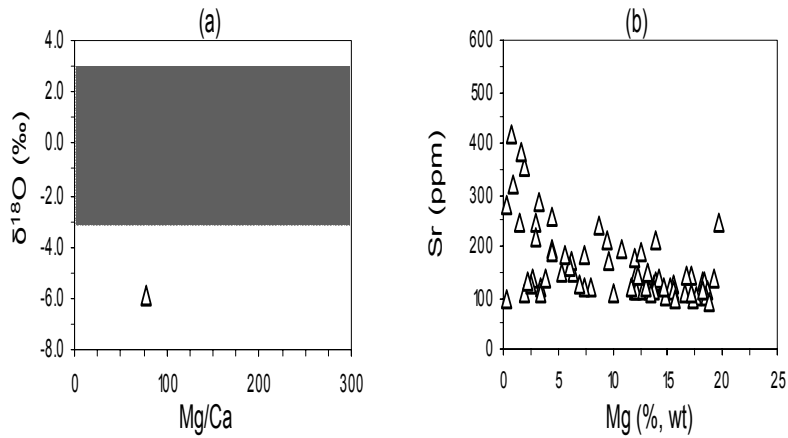


**Figure 6-10.** Cross-plots between (a) the  $\delta^{18}\text{O}_{\text{carb}}$  values of the Smackover samples and the Mg/Ca ratios illustrating different diagenetic environment on dolomitization between the two embayments and (b) the Sr and the Mg concentration for the effect from diagenesis where both elements would be reduced. The negative correlation between Sr and Mg suggests to variation of original calcite mineral in the sediment (high-mg vs low-Mg calcite), and the variation of dolomitization effect between the two depositional areas.

diagenetic condition (Veizer and Demovic, 1971; Veizer et al., 1974). In this study (Figure 6-10b), the Sr concentrations in dolomitized samples from the #1 NEAL ET AL UNIT 30-1 show a variation from less than 100 ppm to about 400 ppm. Based upon the information above, the Sr concentrations in the #1 NEAL ET AL UNIT 30-1 samples suggest that dolomite precipitation in the Manila Embayment probably occurred during early diagenesis environment and did not occur under hypersaline conditions. If this is true for the dolomitization environment, it also means the mixing zone between meteoric fresh water and seawater under its shallow carbonate setting could have strong effect for the changes of Sr in the Smackover sediment of the Manila Embayment.

While low Sr and Mg contents in samples from the Manila Embayment could be primarily affected by diagenesis and dolomitization, the relatively higher Sr contents in samples from the T.R. MILLER MILLS 17-11, #1 well in the Conecuh Embayment can not be explained in a similar way. As shown earlier in Figure 6-8, stabilization processes, the three different original carbonate phases (A, HMC and LMC) to diagenetic low-Mg calcite (dLMC), will also involve with the presence of the elemental concentration during diagenetic alterations (decreasing or increasing). As previously discussed in Chapter 5, samples with high Ca contents also have high Sr concentrations of more than 1500 ppm. The original aragonitic mineral phase (i.e. oolitic packstone and grainstone in the upper Smackover) appears to have unusually high Sr contents (> 5000 ppm). In these Smackover core samples, if Sr is primarily influenced by diagenetic alteration, the positive correlation with the Mg content and systematic decrease in concentration would be expected. The siliciclastic influence is excluded, since most samples with the significant Sr concentration occurred as carbonates (which means siliciclastic contamination would be minimal). Therefore, this leads to the possibility that the eustatic sea level variation could have influenced the cyclic variation on the Sr content but excluding the upper Smackover grainstones and packstones where original carbonate mineral was dominated by aragonite.

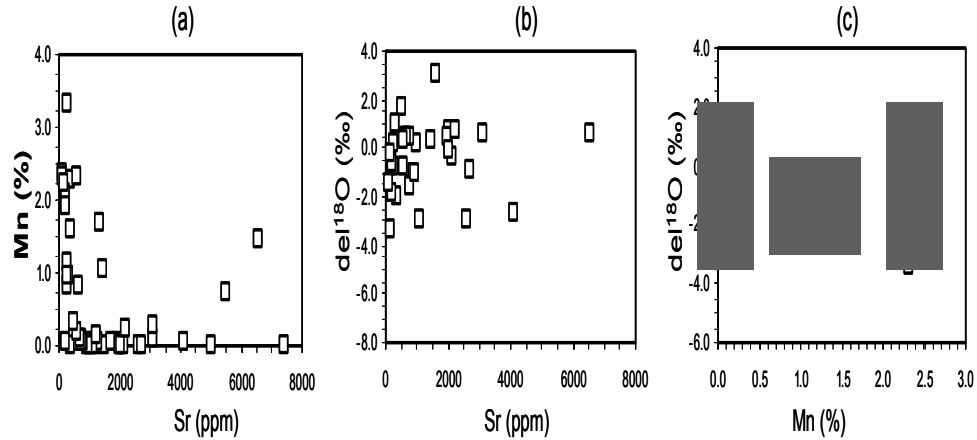
Variation of the Sr and Mn concentrations, especially for samples from the T.R. MILLER MILLS 17-11, #1 core, are examined along with the variation of the  $\delta^{18}\text{O}_{\text{carb}}$  values (**Figure 6-**

11). The different and unusual high Sr and Mn concentrations in the T.R. MILLER MILLS 17-11, #1 samples from the Conecuh Embayment are interpreted to be influenced by additional factors besides original carbonate minerals and diagenetic alterations and sedimentary facies (Figure 6-11a). The positive correlation between Sr and  $\delta^{18}\text{O}_{\text{carb}}$  from the diagenetic effect in samples from both of the study areas shows no clear correlation (Figure 6-11b). The correlation between Mn and  $\delta^{18}\text{O}_{\text{carb}}$  values, especially from samples in the T.R. MILLER MILLS 17-11, #1 core, (Figure 6-11c) suggests that Mn occurred in these Smackover samples by at least three separate environment depositional conditions during the long Smackover deposition.

### 6.5.2 $\delta^{13}\text{C}_{\text{carb}}$ and $\delta^{18}\text{O}_{\text{carb}}$ correlation

A correlation between the  $\delta^{13}\text{C}_{\text{carb}}$  and  $\delta^{18}\text{O}_{\text{carb}}$  values also helps to evaluate the effects from the original signals versus diagenetic overprinting. The cross-plots between the  $\delta^{13}\text{C}_{\text{carb}}$  and  $\delta^{18}\text{O}_{\text{carb}}$  from the two cores are illustrated in **Figure 6-12**. Except a few samples from the Manila Embayment, almost of the data from of the two cores are distributed in the same  $\delta^{13}\text{C}_{\text{carb}}$  and  $\delta^{18}\text{O}_{\text{carb}}$  ranges. The larger variation in the  $\delta^{18}\text{O}_{\text{carb}}$  values than in the  $\delta^{13}\text{C}_{\text{carb}}$  values is interpreted to result from different rates of oxygen isotope fractionation during diagenetic stabilization at early and probable at variable burial depths. The lateral and vertical variation of sedimentary depositional environment involves different stability of the major and minor original carbonate phases within different diagenetic environments during Smackover deposition. Due to the different structural setting and the distance from land, the openness of the diagenetic system (referred as the pore water/rock ratio) between the two embayments were probable different even though chemical compositions of seawater and diagenetic meteoric water would not be significantly different. In the Manila Embayment, the higher degree of diagenetic alterations in the sedimentary texture and trace elements (from major aragonite and high-Mg calcite to stabilized diagenetic low-Mg calcite and dolomite) apparently resulted in more altered and more

CONECUH EMBAYMENT (T.R. MILLER MILLS 17-11, #1)



MANILA EMBAYMENT (#1 NEAL ET AL UNIT 30-1)

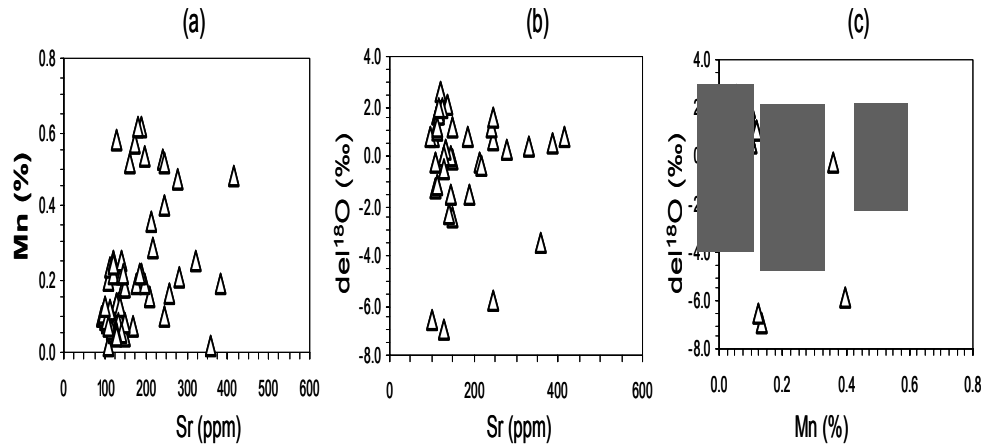


**Figure 6-11.** Cross-plots between (a) the Sr and Mn concentrations, (b) the Sr concentration and  $\delta^{18}\text{O}_{\text{carb}}$  values, and (c) the Mn concentration and  $\delta^{18}\text{O}_{\text{carb}}$  values illustrating diagenetic variation on chemical composition of the Smackover depositions in southwest Alabama. It is noted for the similar range of the  $\delta^{18}\text{O}_{\text{carb}}$  values for diagenetic alteration. The greater concentrations of the Sr and Mn in the T. R. MILLER MILLS 17-11, #1 well samples are interpreted as a possible influence from changes of seawater composition as the Conech Embayment was probably more connected to an open marine condition during relative sea level rise and a highstand. Mn and  $\delta^{18}\text{O}_{\text{carb}}$  correlation indicates separate trends of diagenetic effect on samples with different range of Mn concentrations.

**CONECUH EMBAYMENT**  
(T.R. MILLER MILLS 17-11, #1)

**MANILA EMBAYMENT**  
(#1 NEAL ET A UNIT 30-1)

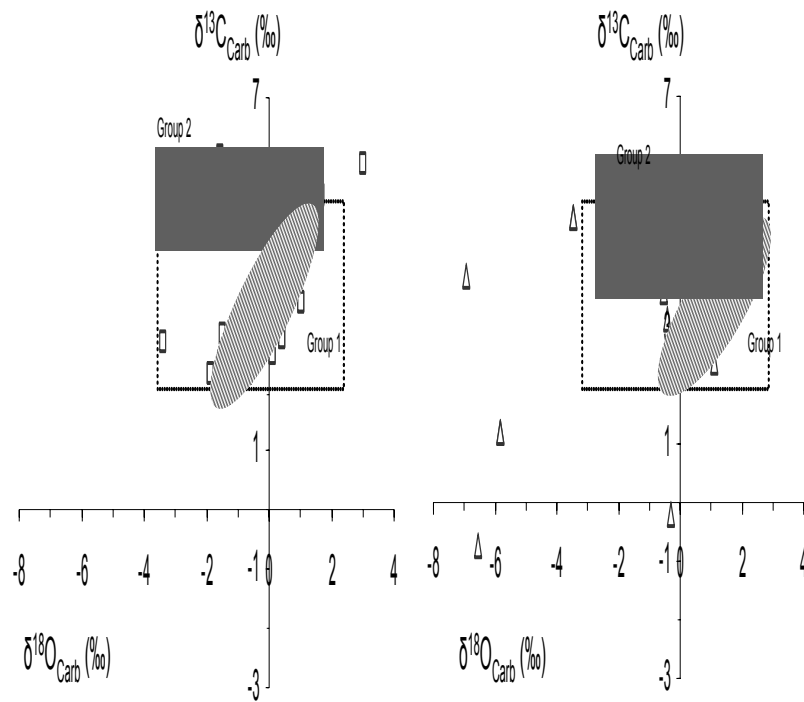


**Figure 6-12.** Cross-plots between the  $\delta^{13}\text{C}_{\text{carb}}$  and  $\delta^{18}\text{O}_{\text{carb}}$  values from whole rock samples of the Smackover Formation in the Conecuh Embayment and the Manila Embayment. Except in a few samples, the  $\delta^{13}\text{C}_{\text{carb}}$  and  $\delta^{18}\text{O}_{\text{carb}}$  values of samples fall in almost similar ranges. Two distinctive trends are recognized; the first trend illustrates diagenetic alteration on both  $\delta^{13}\text{C}_{\text{carb}}$  and  $\delta^{18}\text{O}_{\text{carb}}$  values and the second trend illustrates diagenetic effect mostly on the  $\delta^{18}\text{O}_{\text{carb}}$  values.

variable  $\delta^{18}\text{O}_{\text{carb}}$  values. The large differences in concentrations of the major and trace element in carbonates (i.e. Mg, Mn and Sr) which are usually good indicators for carbonate diagenesis can be influenced by different degrees of diagenetic alteration and additional controls on the Smackover deposition. Even though the  $^{18}\text{O}$  content of the ocean water has been reported to probably decrease with increasing geologic age and thus the  $\delta^{18}\text{O}_{\text{carb}}$  values of the carbonates (Brand and Veizer, 1980), it is not possible that this factor could be the cause for the  $\delta^{18}\text{O}_{\text{carb}}$  difference in these Smackover samples. Diagenetic effects on different carbonate mineral phases can be variable. For recent sediments, Brand and Veizer (1980) reported that the  $\delta^{18}\text{O}_{\text{carb}}$  depletion of about 2‰ occurred for the high-Mg calcite and aragonite and about 1‰ for the low-Mg calcite. It is possible that differences in the original carbonate phase of these sediments can have different effects on changes of the  $\delta^{18}\text{O}_{\text{carb}}$  values in addition to diagenetic environments.

Diagenetic effects on the  $\delta^{13}\text{C}_{\text{carb}}$  values show smaller variations. On the cross-plots between  $\delta^{13}\text{C}_{\text{carb}}$  and  $\delta^{18}\text{O}_{\text{carb}}$  values, two distinct trends based on the  $\delta^{13}\text{C}_{\text{carb}}$  values can be distinguished. The first trend was grouped by samples which illustrate the depletion in both  $\delta^{13}\text{C}_{\text{carb}}$  and the  $\delta^{18}\text{O}_{\text{carb}}$  values and are interpreted as the diagenetic equilibrium trend. The second trend was grouped by samples of variable  $\delta^{18}\text{O}_{\text{carb}}$  values but illustrate less change in the  $\delta^{13}\text{C}_{\text{carb}}$  values. From the Manila Embayment, Smackover sediments of this group are more or less stable in the  $\delta^{13}\text{C}_{\text{carb}}$  values but they consist slightly heavier  $\delta^{13}\text{C}_{\text{carb}}$  values in the Conecuh Embayment. In the study of Brand and Veizer (1980), the separation of the  $\delta^{13}\text{C}_{\text{carb}}$  values by about 1‰ apart into two distinct groups was also observed in the carbonate samples of their study. They pointed that this bimodal distribution was not likely affected by geological ages, original mineralogy or the degree of diagenetic alteration. Their speculation was that other factors, which related to environment of deposition and physiological conditions, could be important. The higher rate of carbonate precipitation could occur during the concentration of organisms which were directly related to the high relative sea level and thus affected the positive shift of the  $^{13}\text{C}/^{12}\text{C}$  ratio in the precipitated carbonates (a pers. comm with J. Turner (1980) by Brand and Veizer, 1980). Many

studies also reported the bimodal distribution on the cross-plot between  $\delta^{13}\text{C}_{\text{carb}}$  and the  $\delta^{18}\text{O}_{\text{carb}}$  values in recent and ancient carbonate sediments (e.g. Epstein and Lowenstam, 1953, Gross and Tracey, 1966; Ginsburg and Schroeder, 1973; Davies and Krouse, 1975). The explanation for the cause of this distribution was not clear until later when Allan and Matthews (1982) observed that the limestones which undergo mineralogical stabilization near the soil zone or under the influence of  $^{12}\text{C}$  enrichment of organic carbon can have  $\delta^{13}\text{C}_{\text{carb}}$  values depleted by 2 to 4‰. Magaritz and Stemmerik (1989) reported from their carbonate samples from the Paleozoic Permian sequence of East Greenland that the  $\delta^{13}\text{C}_{\text{carb}}$  values could be related to the changes of sea level and seawater salinity. During the variation of relative sea level, the carbon isotope in carbonates could be different by 2-4‰ under the rising and falling sea level periods. Magaritz and Stemmerik (1989) believed that the variation of the  $\delta^{13}\text{C}_{\text{carb}}$  values that occurred in carbonate samples was not primarily controlled by basinal conditions but rather by the changes of global carbon cycle. The enrichment of  $^{13}\text{C}$  in marine carbonates was suggested to increasing  $\text{CO}_2$  in the atmosphere and in the ocean water resulting from an increase in organic carbon storage either on land (in forests or soils) (Shackleton, 1977) or during marine flooding (Broecker and Takahashi, 1984). The relative fall in sea level which could cause the platform exposure increases the oxidation of organic matter on the platform and/or land (e.g coal beds) and increases the  $^{12}\text{C}$  in the seawater or depleted  $\delta^{13}\text{C}_{\text{carb}}$  values in carbonates. From Magaritz and Stemmerik 's report, the  $\delta^{13}\text{C}_{\text{carb}}$  values recorded in carbonate deposited during the transgression were from 4‰ to 6‰, and during the regression were from 0‰ to 2‰. Therefore, the separation of  $\delta^{13}\text{C}_{\text{carb}}$  data points on the plots in Figure 6-12 is interpreted to result from the changing in sea level cycles

### **6.5.3 $\delta^{13}\text{C}_{\text{carb}}$ trends of the Smackover in a stratigraphic framework**

The covariance of the  $\delta^{13}\text{C}_{\text{carb}}$  trends of the two Smackover depositions from the Conecuh Embayment and the Manila Embayment which appears to be independent of their different

sedimentary facies and diagenetic environments strongly suggests sequence stratigraphy of the Smackover Formation may be constrained by using a  $\delta^{13}\text{C}_{\text{carb}}$  chemostratigraphic approach.

The  $\delta^{13}\text{C}_{\text{carb}}$  and  $\delta^{18}\text{O}_{\text{carb}}$  variations on the depth scale of the two core samples are shown together and are correlated in a time-stratigraphic framework (**Figure 6-13**). The  $\delta^{18}\text{O}_{\text{carb}}$  variations during the Smackover depositions were affected by diagenesis and carbonate mineral differences so they are not considered as a time stratigraphic marker. Because of the depleted  $\delta^{13}\text{C}_{\text{carb}}$  samples represented carbonates formed during the lowstand sea level and/or associated with sequence boundary, the correlation of the  $\delta^{13}\text{C}_{\text{carb}}$  values between the two Smackover sequences complimented by their core observations indicate that the lowest sequence boundary occurred probably during Early Oxfordian is not coincident with the boundary between the Norphlet and the Smackover Formations. This observation has been pointed out by Wade and Moore (1993) from the Smackover deposition in the Manila Embayment as illustrated by #1 NEAL ET AL UNIT 30-1 core sequence. The boundary at the Norphlet-Smackover contact of the Smackover deposition was probably not equivalent in time when compared to the same boundary in the Conecuh Embayment area. On the T.R. MILLER MILLS 17-11, #1 core, the contact between the Norphlet-Smackover Formation (13845-13847 ft) might possibly be a sequence boundary where the rapid marine transgression (shown by positive  $\delta^{13}\text{C}_{\text{carb}}$  values between 2‰ to 3‰) overlying the siliciclastic eolian sandstone on the erosional surface. The missing sample at this contact, however, limits this interpretation. The same boundary, which is interpreted as possible sequence boundary and being equivalent to the boundary of the Norphlet-Smackover contact of the T.R. MILLER MILLS 17-11, #1 core, is interpreted to occur in the #1 NEAL ET AL UNIT 30-1 core at depth about 13587 ft (see core photographs in Appendix A and Appendix B). The difference in this boundary is interpreted to be due to the different depositional setting of the Manila Embayment which was located on a structural high (Wade et al., 1987). The first marine transgression into the Manila Embayment during the early Smackover time was probably not high nor stable enough for stable carbonate deposition to take place but only a thin carbonate interval

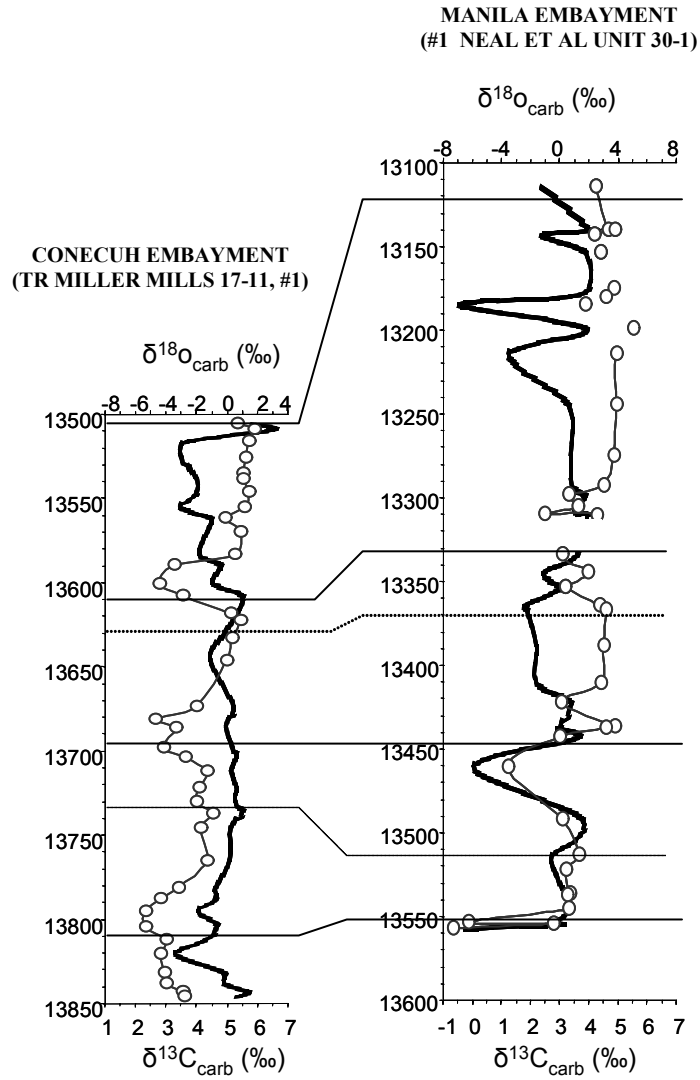


**Figure 6-13.** The correlation between the  $\delta^{13}\text{C}_{\text{carb}}$  and  $\delta^{18}\text{O}_{\text{carb}}$  values of the Smackover Formation from the Conecuh Embayment and the Manila Embayment. The different variation between dark

occurred at around 13568.5 ft. The regression of sea level, however, caused marine reworking on the early sandstone deposits of the Norphlet Formation and resulted in clean and massive sand unit underlying the major Smackover carbonates. The reworked sandstone interval next to the Smackover carbonate in the #1 NEAL ET AL UNIT 30-1 is thus interpreted to occur at the same time of the lower Smackover carbonate near its base in the T.R. MILLER MILLS 17-11, #1 core. However, because no carbon isotopic data was applied for this interpretation, the correlation in this lower part of the sequence which includes the upper Norphlet Formation can be only partially conducted from the  $\delta^{13}\text{C}_{\text{carb}}$  data which are available from the carbonate section.

The first  $\delta^{13}\text{C}_{\text{carb}}$  negative excursion observed in the T.R. MILLER MILLS 17-11, #1 core (13805ft to 13875 ft) is interpreted to correlate with the  $\delta^{13}\text{C}_{\text{carb}}$  negative excursion at the base of the Smackover in the #1 NEAL ET AL UNIT 30-1 core. Besides this first  $\delta^{13}\text{C}_{\text{carb}}$  excursion, there are two other intervals where the  $\delta^{13}\text{C}_{\text{carb}}$  compositions of the carbonates become  $^{13}\text{C}$ -depleted. These intervals are around 13710-13675 ft and 13610-13588 ft in the T.R. MILLER MILLS 17-11, #1 core and around 13460-3420 ft and 13365-13293 ft in the #1 NEAL ET AL UNIT 30-1 core. It is important to note the values of  $\delta^{13}\text{C}_{\text{carb}}$  in sediments during these time intervals are relatively lighter by about 1‰ to 3‰ than the  $\delta^{13}\text{C}_{\text{carb}}$  values in the carbonates beneath or above. This observation may be compared to the carbonate diagenesis pattern near the exposure surface presented by Allan and Matthew (1982) (Figure 6-5). The difference is that in the Conecuh Embayment, the exposure surface was not occurred where the deeper part of the basin is located which means basinal can be just restricted and non-sediment surface instead of exposure condition. Increasing siliciclastic influx (on core observation and elemental analysis) should not be uncommon during this period of time as river channels could prograde more seaward. However, the nearshore location affected high siliciclastic background in the carbonate sediment deposited in the Manila Embayment, cyclicity by siliciclastic input was therefore not so clear as it is shown in the Conecuh Embayment area. Nevertheless, the shallower conditions and stronger diagenetic freshwater effect affected dolomitization, evaporitic or/and anhydrite nodules

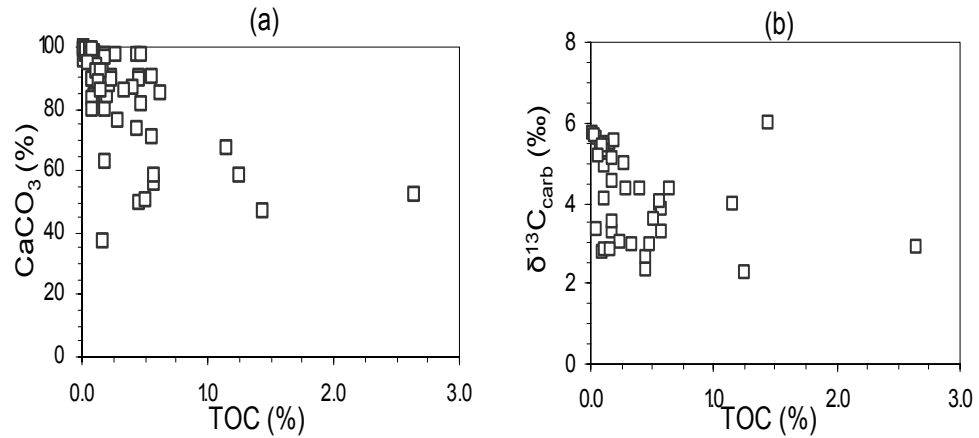
to be increased in the Manila Embayment area. The variation of  $\delta^{13}\text{C}_{\text{carb}}$  and  $\delta^{18}\text{O}_{\text{carb}}$  patterns in these two cores are interpreted, using the pattern from Figure 6-5, to result from different conditions related to meteoric diagenesis. In the Manila Embayment, shallower structural setting could promote meteoric diagenesis under the vadose freshwater zone where larger negative fluctuations of  $\delta^{18}\text{O}_{\text{carb}}$  values occurred. In the Conecuh embayment, subtidal conditions limited carbonate diagenesis in the phreatic zone because of smaller changes in pore fluid compositions relative to carbon isotope changes from the bulk sediment. The changes from low-Mg calcite minerals to diagenetic calcite in the T.R. MILLER MILLS 17-11, #1 sediments probable caused smaller changes of the  $\delta^{18}\text{O}_{\text{carb}}$  values in addition that the restricted condition during the falling relative sea level in the Conecuh Embayment would also caused  $\delta^{18}\text{O}_{\text{carb}}$  values to become heavier. The heavier  $\delta^{13}\text{C}_{\text{carb}}$  values with high carbonate concentration in samples above the three negative  $\delta^{13}\text{C}_{\text{carb}}$  intervals indicate an increase relative sea level after a regression. Different trends between the  $\delta^{18}\text{O}_{\text{carb}}$  values and covariant trends between the  $\delta^{13}\text{C}_{\text{carb}}$  values confirm the cause for the  $\delta^{13}\text{C}_{\text{carb}}$  compositions was independent from sedimentary facies and diagenetic environments. Between these two sequences, carbonate intervals with heavier  $\delta^{13}\text{C}_{\text{carb}}$  composition can be correlated and suggest that they likely formed during the similar relatively high sea level cycles. Using the  $\delta^{13}\text{C}_{\text{carb}}$  correlation, four or three and a half smaller sea level cycles changes (depending on the contact of the Norphlet-Smackover) are interpreted to occur during the long term Smackover deposition in the Conecuh Embayment and three smaller sea level cycles occurred in the Smackover deposition in the Manila Embayment.

In order to further investigate whether carbon isotope variations of the Smackover carbonates were the consequence of local effects and/or changes of the carbon isotopic composition of the global reservoir, the correlation between the  $\delta^{13}\text{C}_{\text{carb}}$  and  $\delta^{13}\text{C}_{\text{org}}$  values and the correlation between the  $\delta^{13}\text{C}_{\text{carb}}$  of the Smackover sequence and the other sediment sequences which are equivalent age to the Smackover (Oxfordian) also need to be discussed.

#### 6.5.4 TOC and the variations between the $\delta^{13}\text{C}_{\text{carb}}$ and $\delta^{13}\text{C}_{\text{org}}$ values

By comparing TOC with the variation of the  $\delta^{13}\text{C}_{\text{carb}}$  and the  $\delta^{13}\text{C}_{\text{org}}$ , the mixing between organic source inputs which could have affected the  $^{13}\text{C}/^{12}\text{C}$  of the seawater and carbonate and organic carbon of the Smackover sediments can be estimated. Total organic carbon (TOC) content in the whole rock samples from the two cores are correlated with their carbonate (including dolomite) concentrations ( $\text{CaCO}_3$ ) and the  $\delta^{13}\text{C}_{\text{carb}}$  values (**Figure 6-14**). Most of samples from both cores generally consist of TOC less than 1% and have negative correlation with the  $\text{CaCO}_3$  content. The correlation between TOC content and  $\delta^{13}\text{C}_{\text{carb}}$  values however was not clearly distinguished. On the TOC and  $\text{CaCO}_3$  correlation, the different slope between the two plots suggests the accumulation of the TOC in samples from the two cores were negatively affected differently by the variation of the carbonate precipitation which indicates to different organic facies. It is important to reiterate that on a global scale, an increase TOC accumulation rate would result a positive shift in both  $\delta^{13}\text{C}_{\text{org}}$  and  $\delta^{13}\text{C}_{\text{carb}}$  compositions. Therefore, a positive correlation between  $\delta^{13}\text{C}_{\text{org}}$  and  $\delta^{13}\text{C}_{\text{carb}}$  values can be expected. The cross-plots between TOC and  $\delta^{13}\text{C}_{\text{org}}$  and between the  $\delta^{13}\text{C}_{\text{carb}}$  and  $\delta^{13}\text{C}_{\text{org}}$  values are illustrated in **Figure 6-15**. Data from the TOC and the  $\delta^{13}\text{C}_{\text{org}}$  plots illustrate different correlations which suggest different organic accumulation during the Smackover depositions between the two areas. In the Conecuh Embayment, samples from the T.R. MILLER MILLS 17-11, #1 well consist of TOC relatively lower compared to samples from the #1 NEAL ET AL UNIT 30-1 well of the Manila Embayment. While a positive correlation is appeared for samples from the Manila Embayment, a negative correlation is observed between TOC and  $\delta^{13}\text{C}_{\text{org}}$  for the Conecuh Embayment. Although the positive correlation observed in the #1 NEAL ET AL UNIT 30-1 might seem to indicate the global variation between the TOC and the  $\delta^{13}\text{C}_{\text{org}}$  variation, the different organic source input could also have some effect on the  $\delta^{13}\text{C}_{\text{org}}$  variation between samples derived from these two areas. For the T.R. MILLER MILLS 17-11, #1 samples, the  $\delta^{13}\text{C}_{\text{org}}$  values vary from -27 ‰ to -21.5‰ and

**CONECUH EMBAYMENT (T.R. MILLER MILLS 17-11, #1)**



**MANILA EMBAYMENT (#1 NEAL ET AL UNIT 30-1)**

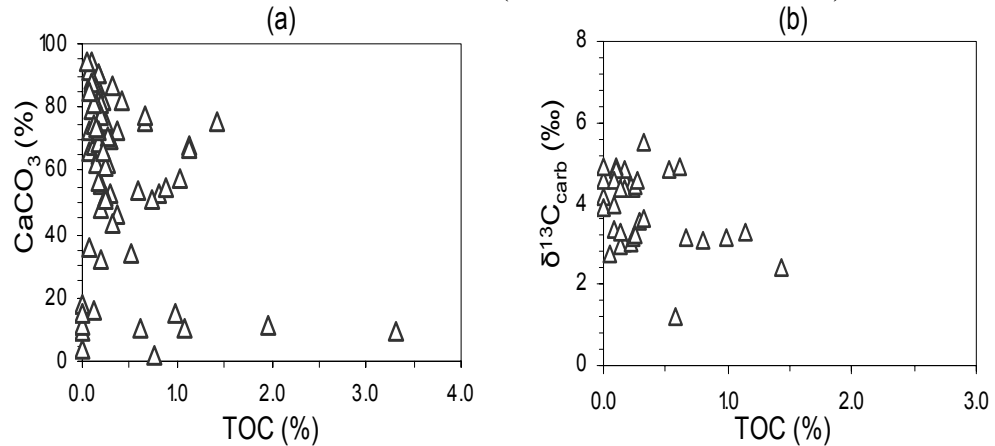
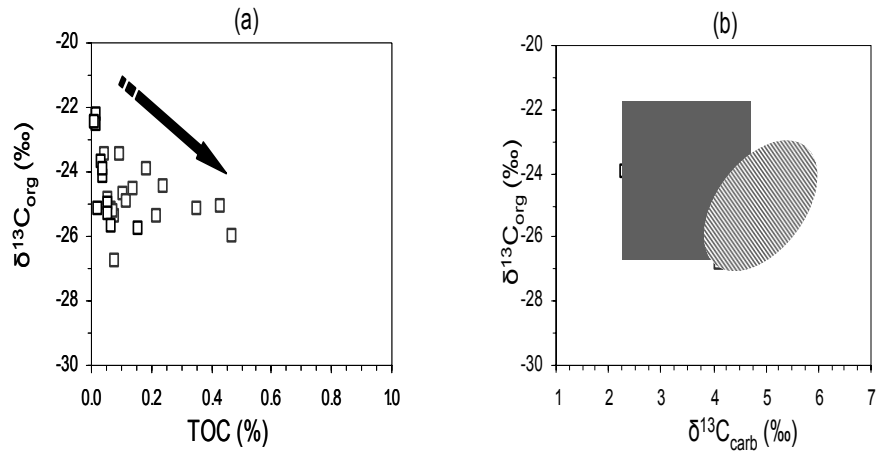


**Figure 6-14.** Cross-plots illustrating the correlations between (a) the TOC and the  $\text{CaCO}_3$  concentration and, (b) the TOC and the  $\delta^{13}\text{C}_{\text{carb}}$  values. Negative correlation between the TOC and the  $\text{CaCO}_3$  is observed in both cores but with a different relationship. The variation of the TOC content in the Smackover samples illustrates indistinct correlation with the  $\delta^{13}\text{C}_{\text{carb}}$  values.

CONECUH EMBAYMENT (T.R. MILLER MILLS 17-11, #1)



MANILA EMBAYMENT (#1 NEAL ET AL UNIT 30-1)

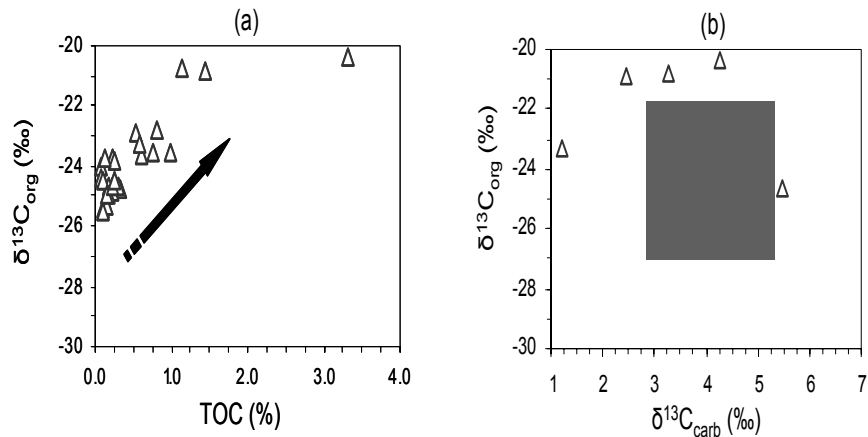


**Figure 6-15.** Cross-plots between (a) the TOC and the  $\delta^{13}\text{C}_{\text{org}}$  values and (b) the  $\delta^{13}\text{C}_{\text{carb}}$  and the  $\delta^{13}\text{C}_{\text{org}}$  values. Different correlations between the TOC and  $\delta^{13}\text{C}_{\text{org}}$  values suggest a possible variation in original organic carbon sources between the two Smackover depositional environments. In the Conecuh Embayment, data plotted between the  $\delta^{13}\text{C}_{\text{carb}}$  and the  $\delta^{13}\text{C}_{\text{org}}$  values are separated into two groups; the first group illustrating a positive correlation which is interpreted to be affected by increasing terrigenous organic source materials and the second group illustrating a negative correlation which possibly due to an increase in marine organic input.

samples are dominated by lighter or more negative  $\delta^{13}\text{C}_{\text{org}}$  compositions. For the #1 NEAL ET AL UNIT 30-1 samples, the  $\delta^{13}\text{C}_{\text{org}}$  values range from -26‰ to -20‰. The positive correlation between  $\delta^{13}\text{C}_{\text{org}}$  and the TOC content observed in the #1 NEAL ET AL UNIT 30-1 samples indicates that increasing TOC probably has effect for the  $\delta^{13}\text{C}_{\text{org}}$  values to become more positive. The different variation on the TOC and  $\delta^{13}\text{C}_{\text{org}}$  values occurred in samples from these two well areas is interpreted to affect by variable organic source materials that consist of different carbon isotope compositions. The explanation will be later discussed in the next paragraph. From the cross-plots between  $\delta^{13}\text{C}_{\text{carb}}$  and  $\delta^{13}\text{C}_{\text{org}}$  values, samples of the Manila Embayment illustrate no distinct correlation while samples of the Conecuh Embayment illustrate two separate correlations. The indistinctive correlation between the  $\delta^{13}\text{C}_{\text{carb}}$  and  $\delta^{13}\text{C}_{\text{org}}$  values in samples of the Manila Embayment cancel their TOC and the  $\delta^{13}\text{C}_{\text{org}}$  to be related to the global scale effect caused by shifting of the organic carbon reservoir. From the Conecuh Embayment, the  $\delta^{13}\text{C}_{\text{carb}}$  and  $\delta^{13}\text{C}_{\text{org}}$  positive correlation is observed in samples with  $\delta^{13}\text{C}_{\text{carb}}$  values higher than 4‰ whereas the negative correlation is observed in samples with  $\delta^{13}\text{C}_{\text{carb}}$  values less than 4‰. These different correlations therefore suggest the variation of organic source types could play a significant role for the  $\delta^{13}\text{C}_{\text{org}}$  variation in these samples. In addition, different correlations among the  $\text{CaCO}_3$ , TOC,  $\delta^{13}\text{C}_{\text{carb}}$  and  $\delta^{13}\text{C}_{\text{org}}$  support a speculation that the variation of the  $\delta^{13}\text{C}_{\text{org}}$  and the TOC occurred on a local organic facies control rather than the global control which affected the  $\delta^{13}\text{C}_{\text{carb}}$  of the carbonates. Maturation effect on the  $\delta^{13}\text{C}_{\text{org}}$  values is excluded since these two Smackover wells are similar in age and occurred on the same carbonate platform. Therefore it is possible to theorize that whereas relative sea level changes could be a major control for the  $\delta^{13}\text{C}_{\text{carb}}$  variation, the different depositional settings between Smackover depositions in the Conecuh and the Manila Embayments affect organic facies and variable organic source inputs and/or organic processes.

#### **6.5.5 $\delta^{13}\text{C}_{\text{org}}$ Variation and Organic Carbon Sources**

In order to confirm that the difference of the organic carbon sources can be a primary effect for the  $\delta^{13}\text{C}_{\text{org}}$  variation between samples from these two Smackover core areas, organic carbon compositions in the saturate carbon fraction of some samples from these two cores are examined. The vertical and lateral variations of the n-alkane distribution in samples of these two cores are illustrated in **Figure 6-16** and **Figure 6-17**.

According to Hayes (1993), carbon isotopic compositions of naturally synthesized organic compounds depend on four different factors during biosynthesis. These factors are the original carbon source; the isotope effect during carbon assimilation by organisms, the isotope effect during metabolism and biosynthesis, and carbon budget at each step of these processes. Different types and quantities of carbon sources can affect the  $\delta^{13}\text{C}$  values in sedimentary organic carbon. Many studies (i.e. Arthur et al., 1985; Dean et al., 1986; Popp et al., 1989; Kenig et al., 1994; Hofmann et al., 2000) have reported that carbon isotope compositions of marine and terrestrial organic carbon were different in the past relative to today. In the present day, the  $\delta^{13}\text{C}$  composition of marine organic matter is more positive than it was in ancient times. On average,  $\delta^{13}\text{C}$  values reported for contemporary marine organisms and terrestrial organic matters are between -20‰ to -23‰ and between -27‰ to -30‰, respectively (Galimov, 1975). In contrast, the  $\delta^{13}\text{C}$  values of organic matter in sedimentary rocks of the Late Albian (Early Cretaceous) from different sites of the North Atlantic Ocean, on average, were -29‰ for the marine derived liptinite and -23.3‰ for the terrigenous derived vitrinite and intertinite components (Hofmann et al., 2000). Algal material, which can also be a significant component for organic carbon in TOC has  $\delta^{13}\text{C}$  values around -18‰ (Hollerbach et al., 1977). From a study of the Oxford Clay sediments (Middle Callovian to Lower Oxfordian) of central and southern England (Kenig et al., 1994),  $\delta^{13}\text{C}$  value of terrestrial materials are estimated to be around -23.5‰ while the  $\delta^{13}\text{C}$  value estimated for the marine primary input material was -28.2‰. In the study of Kenig et al. (1994), due to the dominant marine organic input and the limited contribution from the terrestrial organic matter observed in the samples, the variation of the  $\delta^{13}\text{C}$  values from -23.1‰ to -27.7‰ was

**CONECH EMBAYMENT**  
(T.R.MILLER MILLS 17-11, #1)

**MANILA EMBAYMENT**  
(#1 NEAL ET AL UNIT 30-1)

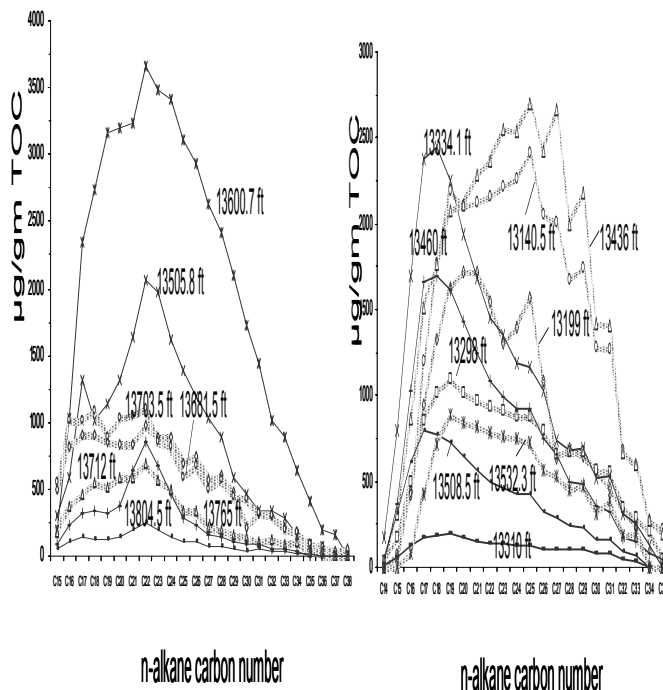


**Figure 6-16.** Gas chromatograms of the saturate fraction from the extracted organic matter of the Smackover samples from the two depositional areas. The T.R.MILLER MILLS 17-11, #1 samples from the Conecuh Embayment characterize major marine organic matter ( $n-C_{22}$ ) with mixed algal ( $n-C_{17}$ ) and terrigenous ( $n-C_{26-30}$ ) materials. The #1 NEAL ET AL UNIT 30-1 samples from the Manila Embayment illustrated the dominant algal source ( $n-C_{17}$ ) and the terrigenous organic material ( $n-C_{26-30}$ ).

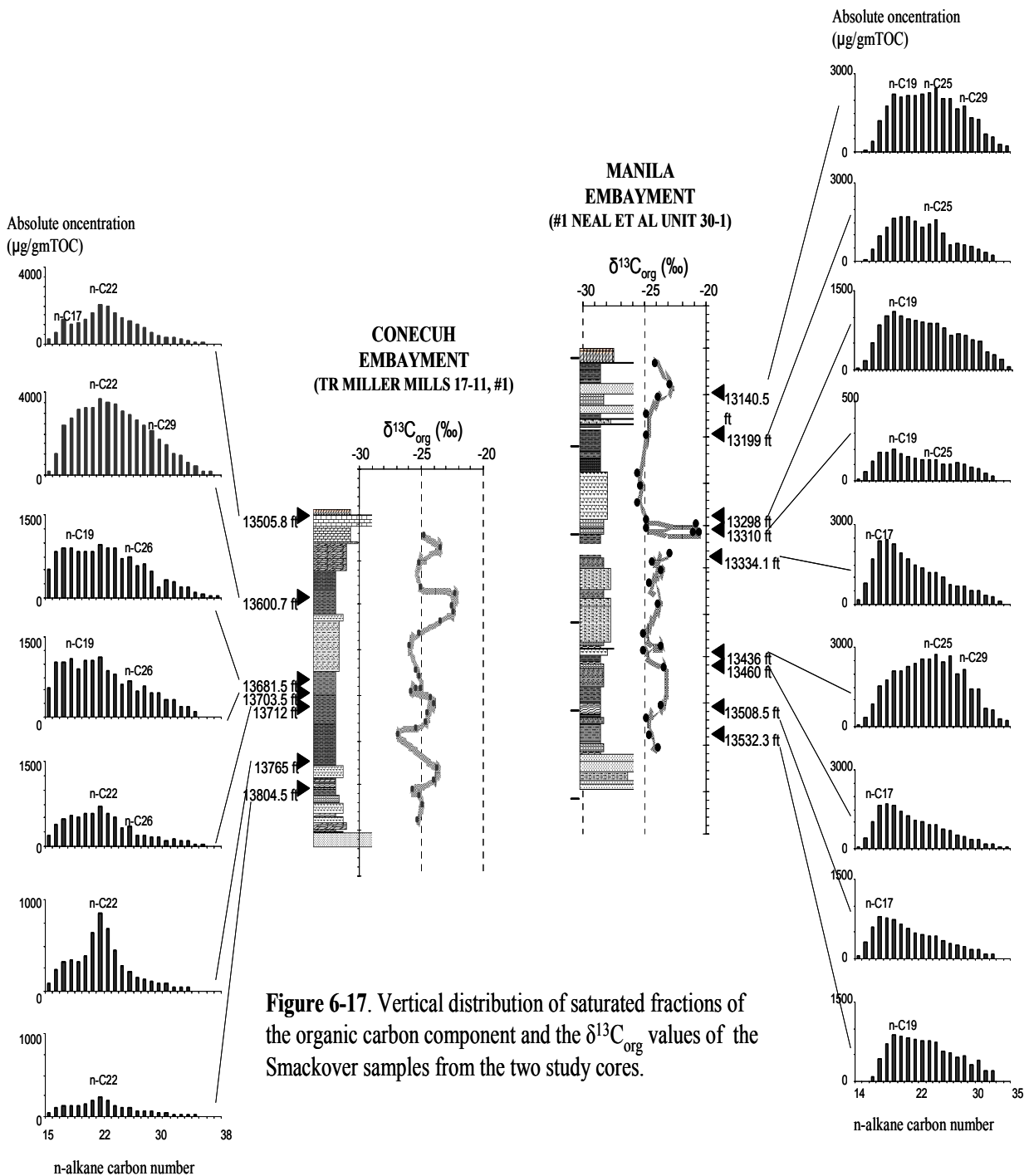


**Figure 6-17.** Vertical distribution of saturated fractions of the organic carbon component and the  $\delta^{13}\text{C}_{\text{org}}$  values of the Smackover samples from the two study cores.

was interpreted as being affected from the heterotrophic reworking processes causing an oxidative remineralization of organic carbons. For the Gulf of Mexico area, the  $\delta^{13}\text{C}$  values of land-derived organic matters in surface sediment from the Gulf of Mexico have been reported by Goni et al. (1998) were between -19.7‰ to 21.7‰. In this study, the Smackover samples from the two cores consist of variable  $\delta^{13}\text{C}_{\text{org}}$  values range between -27‰ to -20‰ which are interpreted to be affected by mixing organic carbon sources. According to Hayes (1993), biological reworking of organic carbon could affect the enrichment of the  $^{13}\text{C}$  in organic carbons due to the loss of lighter of the  $^{12}\text{C}$  carbons. Although the effect from organic reworking processes can not be excluded for the Smackover  $\delta^{13}\text{C}_{\text{org}}$  values, it is reasonable to believe that local primary organic source variation could have a significant effect on these  $\delta^{13}\text{C}_{\text{org}}$  values.

Gas chromatograms of the saturate fraction from the extracted fraction at different depths indicate that both lateral and vertical differences for the major organic inputs occurred between these two Smackover cores (Figure 6-16). In the Conecuh Embayment, one major organic input was derived from marine organisms which are dominated by the n-C<sub>22</sub> alkane. However, marine algae and the terrestrial material are also present at different depths and characterized by a predominance of n-C<sub>17</sub> and n-C<sub>26</sub> to n-C<sub>30</sub>. In the Manila Embayment, saturate distributions illustrate that the influence of marine organic input characterized by n-C<sub>22</sub> is limited when compared to the n-C<sub>22</sub> concentrations observed in the Conecuh Embayment. The dominant n-alkane components occur around n-C<sub>17</sub> and around n-C<sub>25</sub> to n-C<sub>30</sub> which suggests that major organic inputs for the TOC accumulation of this area were mainly marine algae and terrestrial organic material. The vertical distributions of n-alkane organic components shown in Figure 6-17 indicate the  $\delta^{13}\text{C}$  values of the TOC can possibly be related to the ratio of different primary inputs which varied spatially at the same times. However, the  $\delta^{13}\text{C}$  values are measured from the TOC which consists of different volume fractions of all organic compounds, i.e. aromatic, asphaltene, reworked organic materials and others with more complex structures, which could have different  $\delta^{13}\text{C}$  values. Unless, the  $\delta^{13}\text{C}$  values and the fractions of the organic carbon components are

known, all effects, from variable ratios of primary organic inputs, environment conditions during and after organic burial including reworking processes, are still possible. In order to conclude which major control(s) that vertically and laterally affected  $\delta^{13}\text{C}_{\text{org}}$  variations on the Smackover Formation from the Conecuh Embayment and the Manila Embayment, more details from the isotope and geochemical investigations are needed. However, those data are beyond the purpose of this study for characterizing the Smackover stratigraphic framework at this time. The essential point in illustrating the correlation between the TOC and the  $\delta^{13}\text{C}$  values and the distribution of organic components (saturate fraction) from the TOC is to support the speculation that the  $\delta^{13}\text{C}_{\text{org}}$  values of the Smackover principally resulted from local variation rather than the global control.

The variation between the TOC,  $\delta^{13}\text{C}_{\text{org}}$  and  $\delta^{13}\text{C}_{\text{carb}}$  values in the two Smackover cores are plotted on the vertical scale and correlated based upon the  $\delta^{13}\text{C}_{\text{carb}}$  stratigraphy (**Figure 6-18**). The  $\delta^{13}\text{C}_{\text{org}}$  of the Smackover illustrates shorter trends where  $\delta^{13}\text{C}_{\text{org}}$  values become heavier during the depleted  $\delta^{13}\text{C}_{\text{carb}}$  values of the carbonates. The heavier  $\delta^{13}\text{C}_{\text{org}}$  values are interpreted to result from increased terrestrial organic material associated with higher siliciclastic input during relative sea level lowstand periods rather than the increasing in  $^{12}\text{C}$ -enriched TOC which could cause  $^{13}\text{C}$ -enriched in the sea water and positive  $\delta^{13}\text{C}_{\text{carb}}$  excursion. Unless organic carbon has been shown to be derived from a single organic source, the variation of the  $\delta^{13}\text{C}_{\text{org}}$  values in the TOC might not truly reflect the global variation. It was not only an increased TOC ( $^{12}\text{C}$ -enriched) which could cause positive excursion in the  $\delta^{13}\text{C}_{\text{org}}$  but also by an increased terrigenous organic input during relative low sea level. For the Smackover deposition in southwest Alabama basins, while the  $\delta^{13}\text{C}_{\text{org}}$  variation can not be used to represent the global variation due to local variation of the organic facies, the  $\delta^{13}\text{C}_{\text{carb}}$  variation and the correlation between the two study areas suggest that the regional or a combination of both regional and local effects did not obliterate its potential for using in a time-stratigraphic framework on a local and probably also on a global scale.

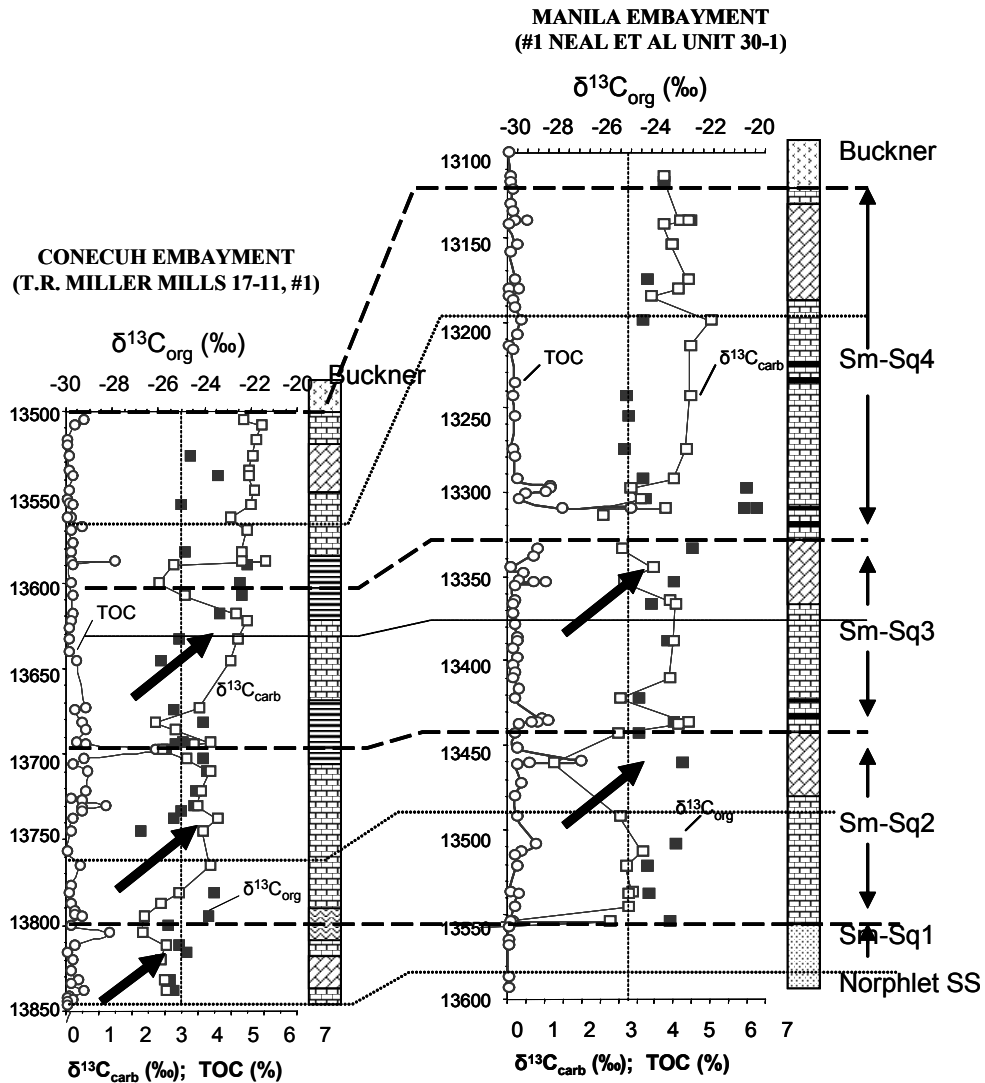


**Figure 6-18.** The vertical variations of the TOC,  $\delta^{13}\text{C}_{\text{org}}$  and  $\delta^{13}\text{C}_{\text{carb}}$  values of the Smackover carbonate depositions in the Conech Embayment and in the Manila Embayment. The variations of the  $\delta^{13}\text{C}_{\text{org}}$  in the Smackover sedimentary organic matter in these Smackover samples illustrate the mixing in the primary organic input and probably reworking processes during organic matter burial rather than changes by global increased of TOC accumulation. The  $\delta^{13}\text{C}_{\text{org}}$  shifts to heavier values are caused by increasing algal and terrigenous material during shallower paleowater-depth and relative low sea level where the  $\delta^{13}\text{C}_{\text{carb}}$  values become depleted due to diagenetic alteration.

### 6.5.6 The $\delta^{13}\text{C}_{\text{carb}}$ stratigraphy of the global Oxfordian sequences

To identify the possibility of global variation on the  $\delta^{13}\text{C}_{\text{carb}}$  signals recorded in the Smackover sequence, the  $\delta^{13}\text{C}_{\text{carb}}$  trend of the Smackover should be compared to the  $\delta^{13}\text{C}_{\text{carb}}$  variations of the other Upper Jurassic Oxfordian sequences. In Jenkyns (1996),  $\delta^{13}\text{C}_{\text{carb}}$  stratigraphy of different sediment sequences aged from Upper Callovian to Upper Oxfordian from southern France and north Italy were reported (**Figure 6-19**). Although Jenkyns (1996) only emphasized the positive  $\delta^{13}\text{C}_{\text{carb}}$  excursion in the Lower-Middle Oxfordian which he suggested as an evidence of the synchronized global bathymetric deepening, several short-term negative-positive  $\delta^{13}\text{C}_{\text{carb}}$  trends can be recognized in these sequences. The values of the  $\delta^{13}\text{C}_{\text{carb}}$  and the  $\delta^{18}\text{O}_{\text{carb}}$  illustrated in the cross-plots vary from 1‰ to 4‰ and from -2.5‰ to 0.5‰, respectively (in Figure 6, Jenkyns, 1996). Carbon isotopes from several fossil groups using echinoids and crinoids from four different sections of the Liesberg Beds (Lower Oxfordian to Middle Oxfordian) were reported by Bill et al. (1995). In the study of Bill et al. (1995), a negative  $\delta^{13}\text{C}_{\text{carb}}$  shift of 1‰ to 1.5‰ was observed near the base of the Liesberg Beds before increasing toward the middle and the upper part of section. These  $\delta^{13}\text{C}_{\text{carb}}$  negative shifts were interpreted as an original signal resulting from variation of isotopic compositions of dissolved  $\text{HCO}_3^-$  in the seawater. They proposed that the negative shift to the lowest  $\delta^{13}\text{C}_{\text{carb}}$  values correspond to a large input of dissolved nutrients to the platform under oxidizing conditions. An ensuing positive  $\delta^{13}\text{C}_{\text{carb}}$  shift to about 2-2.3‰ in the middle and upper part of the Liesberg Beds was interpreted as a general trend for the opening up of the platform and a connection to open marine water. In Bartolini et al. (1996 and 1999), details of the Callovian-Oxfordian sequence, which is part of the continuous carbon isotope stratigraphy of the Middle-Upper Jurassic pelagic carbonate rocks from central Italy, also illustrated the short negative-positive  $\delta^{13}\text{C}_{\text{carb}}$  trends. It is noted that in these reports mainly positive  $\delta^{13}\text{C}_{\text{carb}}$  shifts would be emphasized as a global variation due to an increased organic carbon extraction from the ocean reservoir. It was not until Padden et al. (2001)

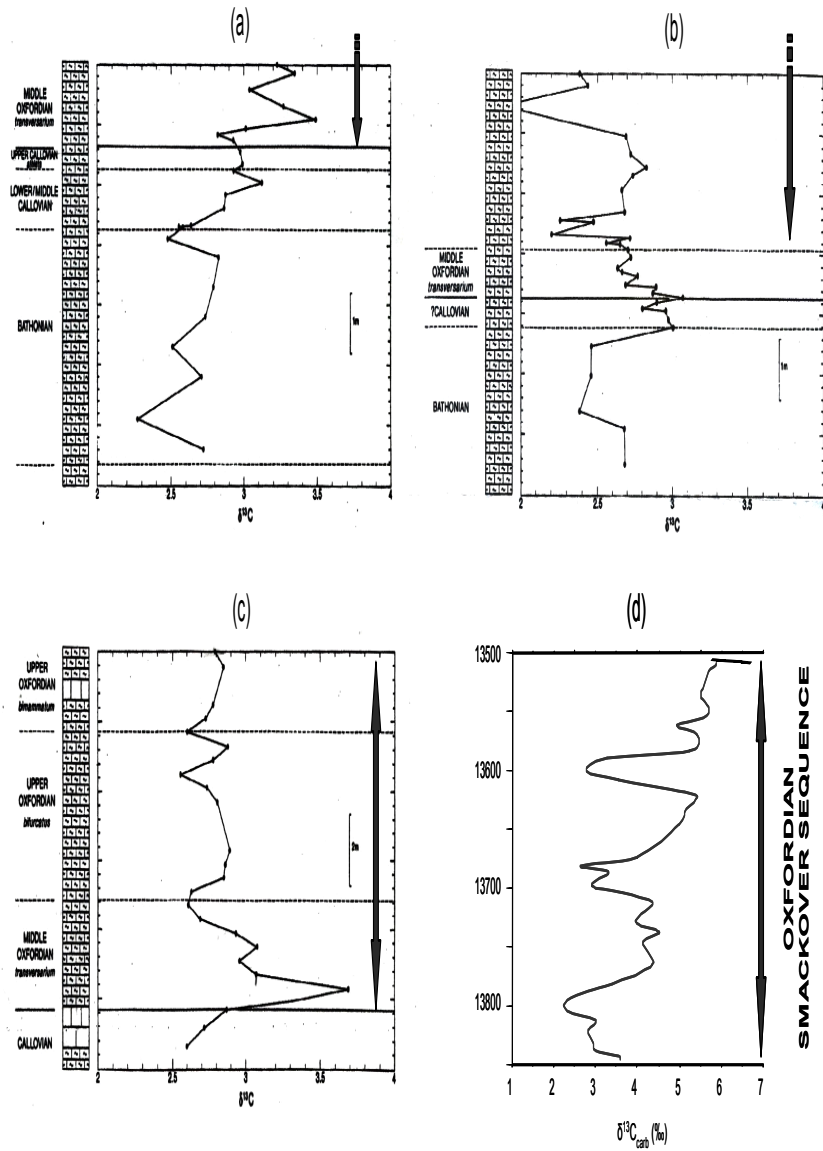


Figure 6-19. Carbon isotope stratigraphy of the Callovian to the Oxfordian sequences from (a) the Rovere Veronese, north Italy, (b) the Camposilvano, north Italy, (c) the Chabrieres, southern France (from Jenkyns, 1996) and, (d) the Smackover Sequence (the Conecuh Embayment, southwest Alabama, USA; this study).

proposed from the  $\delta^{13}\text{C}_{\text{carb}}$  stratigraphic records from the northern continental margin of the ancient Tethys Sea, that the negative  $\delta^{13}\text{C}_{\text{carb}}$  excursion in the middle Oxfordian (defined as the *transversarium zone*) was affected by the release of the frozen methane hydrate along the continental margin. For supporting their theory from the US Gulf Coast area, the negative carbon isotope excursion observed in the Upper Smackover from Louisiana reported by Humphrey et al (1986) was suggested as a possible result from a releasing of these methane gas hydrates. However, according Humphrey et al (1986) these depleted  $^{13}\text{C}$  values (by 1.5‰) which occurred in the porous Upper Smackover suggested to result from an isotopically depleted soil gases from the meteoric water vadose zone. For the Smackover sequence of southwest Alabama in this study, the results from core observation, elemental and isotopic analysis suggest the variation of the  $\delta^{13}\text{C}_{\text{carb}}$  values of the Smackover sequence were probably affected from local and larger scale variations which could have been related to relative sea level changes. These variations were meteoric diagenetic alteration, changes in seawater composition due to widespread organic oxidation during period of exposed platform and changes of siliciclastic weathering rate on the continent.

## 6.6 CONCLUSIONS

The preceding observations suggest a degree of interdependence between sea level change, sedimentary facies, and diagenesis. The observed vertical variations of the  $\delta^{18}\text{O}_{\text{carb}}$  values and cross-plot correlations with  $\delta^{13}\text{C}_{\text{carb}}$  values and elements with variable diagenetic susceptibilities suggest different diagenetic environments which in turn are related to sedimentary facies variations between the two embayments. Under the long-term trends interpreted as a regressive sequence, the  $\delta^{13}\text{C}_{\text{carb}}$  stratigraphy of the Smackover sequence in southwest Alabama illustrates four shorter negative-positive cycles which do not chronologically coincide with the formation boundary observed in one of the two Smackover cores. Core observations and  $\delta^{13}\text{C}_{\text{carb}}$

values suggest that the lowest Smackover sequence boundary, possibly a type 2 boundary, might occur at the base of the Smackover in the Conecuh Embayment, but possibly occurs during the siliciclastic Norphlet deposition in the Manila Embayment. The lower Smackover in the T.R. MILLER MILLS 17-11, #1 core of Conecuh Embayment was interpreted to be time-equivalent to the reworked marine sandstone at the top of the Norphlet Formation in the #1 NEAL ET AL UNIT 30-1 core of the Manila Embayment. During the early Oxfordian, the first rapid marine transgression established a carbonate environment in the Conecuh Embayment, but it was probably of insufficient amplitude and stability for carbonate precipitation to occur in the area of the Manila Embayment. The base of the Smackover from the #1 NEAL ET AL UNIT 30-1 characterized predominant marine reworked sands of the earlier siliciclastic sediments of the Norphlet Formation which resulted in the white, massive marine sandstone unit underlying the Smackover carbonates. Cross-plots of  $\delta^{13}\text{C}_{\text{carb}}$ ,  $\delta^{18}\text{O}_{\text{carb}}$  values and carbonate related elements (i.e. Sr, Mn, Mg) suggest different diagenetic environments between the two Smackover depositional areas. The relation between the  $\delta^{18}\text{O}_{\text{carb}}$  values and Mn illustrated the separation which could be related to third-order sea level cycles. An unusually high Mn concentration in samples from the Conecuh Embayment suggests a possibility of a direct increase in Mn content in the seawater where carbonate precipitation occurred. The cross-plot between  $\delta^{13}\text{C}_{\text{carb}}$  and  $\delta^{18}\text{O}_{\text{carb}}$  values suggest two different groups of Smackover samples. The first group consists of samples affected by diagenetic alteration showing decreasing both  $\delta^{13}\text{C}_{\text{carb}}$  and  $\delta^{18}\text{O}_{\text{carb}}$  values. The second group illustrates high carbonate samples of more positive and stable  $\delta^{13}\text{C}_{\text{carb}}$  values with variable  $\delta^{18}\text{O}_{\text{carb}}$  values from diagenesis.

A correlation between the  $\delta^{13}\text{C}_{\text{carb}}$  vertical trends of the two Smackover cores suggests  $\delta^{13}\text{C}_{\text{carb}}$  values can be used as time stratigraphic constraints. During a long term Smackover sequence, four (or possibly three and a half) and three short-term negative-positive  $\delta^{13}\text{C}_{\text{carb}}$  cycles are observed in the T.R. MILLER MILLS 17-11, #1 and #1 NEAL ET AL UNIT 30-1 cores, respectively, and suggest possible combined effects on global and local- scale variations. On a

global scale, a positive  $\delta^{13}\text{C}_{\text{carb}}$  excursion which represents a stratigraphic interval where there is an increased burial rate of organic carbon is not distinguishable in these two Smackover core sequences which could be due to shallow marine conditions. On the contrary, depleted  $\delta^{13}\text{C}_{\text{carb}}$  values are more evident under these cores. In the Conecuh Embayment, three negative  $\delta^{13}\text{C}_{\text{carb}}$  intervals occurred and are associated with carbonate sediments which received higher siliciclastic materials. In the Manila Embayment, the first negative  $\delta^{13}\text{C}_{\text{carb}}$  interval occurred at the base of the Smackover and the other two intervals were observed in sediment of increasing dolomitization and evaporitic anhydrites. The depleted  $\delta^{13}\text{C}_{\text{carb}}$  values suggest diagenetic alteration might be associated from mixing organic rich ( $^{12}\text{C}$ -enriched) water from the near surface or from the increasing of riverine influx to the ocean during relative sea level lowstand. The regional and global variation would occur due to changes of seawater composition and become enriched in  $^{12}\text{C}$  by organic oxidation during increasing weathering of the exposed platform. The ensuing shift to positive  $\delta^{13}\text{C}_{\text{carb}}$  values above these depleted  $\delta^{13}\text{C}_{\text{carb}}$  intervals is interpreted to be an open to more open marine environment during the transgressive and highstand sea level.

The variation of  $\delta^{13}\text{C}_{\text{org}}$  values in the sedimentary organic matter of the Smackover samples suggest variable ratios in the marine/terrestrial organic input during changes of depositional environment and probably distant from the land. The different carbon isotopic composition of the marine (-27‰) and terrigenous (-23‰) materials reported in the Oxfordian sediments (Kenig et al., 1994) and the  $\delta^{13}\text{C}_{\text{org}}$  values derived from terrigenous source (-20‰) of the Gulf Coast region area support the possibility of mixed organic sources and recycled organic material during burial processes. Increasing positive value of the  $\delta^{13}\text{C}_{\text{org}}$  values is interpreted to be influenced by an increasing input of terrigenous organic material associated with an enhanced siliciclastic influx during relative sea level lowstand period. The differences in the cross-plots between  $\delta^{13}\text{C}_{\text{org}}$  values and TOC content of the two areas suggest different major organic inputs. In the Manila Embayment, with increasing sedimentary organic carbon, TOC, the  $\delta^{13}\text{C}_{\text{org}}$  values become more positive (-23‰ to -20‰) suggesting a possibility of an increased of terrigenous and

algal organic materials under the tidal flat environment. In the Conecuh Embayment, affected by a more distal paleoenvironment setting and deeper lagoonal-marine system, marine organic material was more abundant when relative sea level was highstand and a times of high carbonate precipitation. The organic carbon derived from marine organic source is reflected in the  $\delta^{13}\text{C}_{\text{org}}$  values of the TOC showing more negative carbon isotope values (less than -25‰). The organic carbon analysis from saturate fraction of the extracted organic component from the two Smackover core samples supports the variation of the major organic carbon source during Smackover deposition. It is therefore concluded that while the  $\delta^{13}\text{C}_{\text{org}}$  variation characterizes the mixed isotope signals derived from variable organic source ratios (i.e marine vs. terrigenous vs. algal) including a possible reworking of organic material in the sedimentary environments, only the  $\delta^{13}\text{C}_{\text{carb}}$  variation of the Smackover sequence can be used to constrain both the local and global effects on a time-stratigraphic framework.

## 6.7 FURTHER SUGGESTED STUDIES

The correlation between the  $\delta^{13}\text{C}_{\text{carb}}$  trends in the T. R. MILLER MILLS 17-11, #1 and the #1 NEAL ET AL UNIT 30-1 cores from the Conecuh Embayment and the Manila Embayment suggests that sequence stratigraphic framework of the Smackover deposition on the U.S. Gulf Coast can possibly be constrained using the  $\delta^{13}\text{C}_{\text{carb}}$  isotope stratigraphic concept. Variation of the  $\delta^{13}\text{C}_{\text{org}}$  values, which show no parallel variations with the  $\delta^{13}\text{C}_{\text{carb}}$  trend and vary with changes of organic composition, however, suggest a possible local effect resulting from mixed original organic carbon sources (marine vs. terrestrial vs. algae). Padden (2001) declared that the negative  $\delta^{13}\text{C}_{\text{org}}$  excursion during the Oxfordian period resulted from the release of methane gas hydrates due to global climate changes. To improve the detail of this Smackover stratigraphic study, the following studies are suggested: 1) sample at shorter intervals in order to increase stratigraphic resolution which would also to increase number of samples of both

carbonate and organic carbon isotope for higher resolution; 2) clarify the local and regional/global variation on the  $\delta^{13}\text{C}_{\text{carb}}$  of these Smackover samples by conducting the  $\delta^{13}\text{C}_{\text{carb}}$  stratigraphic correlation of many Smackover wells from platform to basin; 3) compare the  $\delta^{13}\text{C}_{\text{carb}}$  values analyzed from variable fossils (different original calcite mineral) and compared to the whole rock for vital effect; 4) clarify the theory that the decreased  $\delta^{13}\text{C}_{\text{carb}}$  during the Oxfordian was a global effect caused by the released methane gas hydrates by isotope analysis (hydrogen and carbon) of both carbonate and organic carbons; 5) identify the local mixing in organic sources in more detail by the organic (biomarkers) and isotope geochemical analysis, 6) incorporate other time-stratigraphic parameters (i.e. biostratigraphy on nannofossils,  $^{87}\text{Sr}/^{86}\text{Sr}$  ratios) for global correlation and absolute time precision.

## CHAPTER 7

### 7.1 SYNTHESIS: THE SMACKOVER DEPOSITIONAL MODEL

This study has presented chemostratigraphic and lithostratigraphic evidence that carbonate platform sedimentation is dynamic owing to a variety of different variables that occurred in the depositional system. The vertical accumulation of platform sediment is usually governed by the interplay between carbonate growth, rate of sea level change and platform morphology (Jones and Desrochers, 1992). The rate of sea level change is important because different rates of flooding will provide different responses from the carbonate factory on the platform. For southwest Alabama, sedimentary facies and chemostratigraphy from the Smackover Formation in the Conecuh Embayment and the Manila Embayment suggest although the structural setting and platform morphology had significant effect on carbonate depositional and diagenetic environments, eustatic sea level change was likely the primary control. Therefore, both in order to synthesize the preceding analysis and interpretations and to provide a test for future studies of the Jurassic, it is appropriate that a model be constructed for the Jurassic Smackover ramp. The models are proposed based upon parameters interpreted on a depositional setting of a carbonate ramp platform for Smackover deposition. Chemostratigraphic correlations used to constrain the proposed Smackover depositional models which were time-equivalent between the two study areas are summarized in **Figure 7-1** to **7-3**.

The proposed depositional model and changes of the Smackover sequence that occurred in the Conecuh Embayment and which combine the major observations made from the core lithofacies, elemental composition and carbon isotope variations are illustrated in **Figure 7-4**. In the Conecuh Embayment, the lowest boundary of the first sequence (Sm-S1) may or may not be coincident with the boundary between the Smackover and the Norphlet Formations. This is dependent upon the nature of missing core (~2 ft) at the contact. However, in the underlying

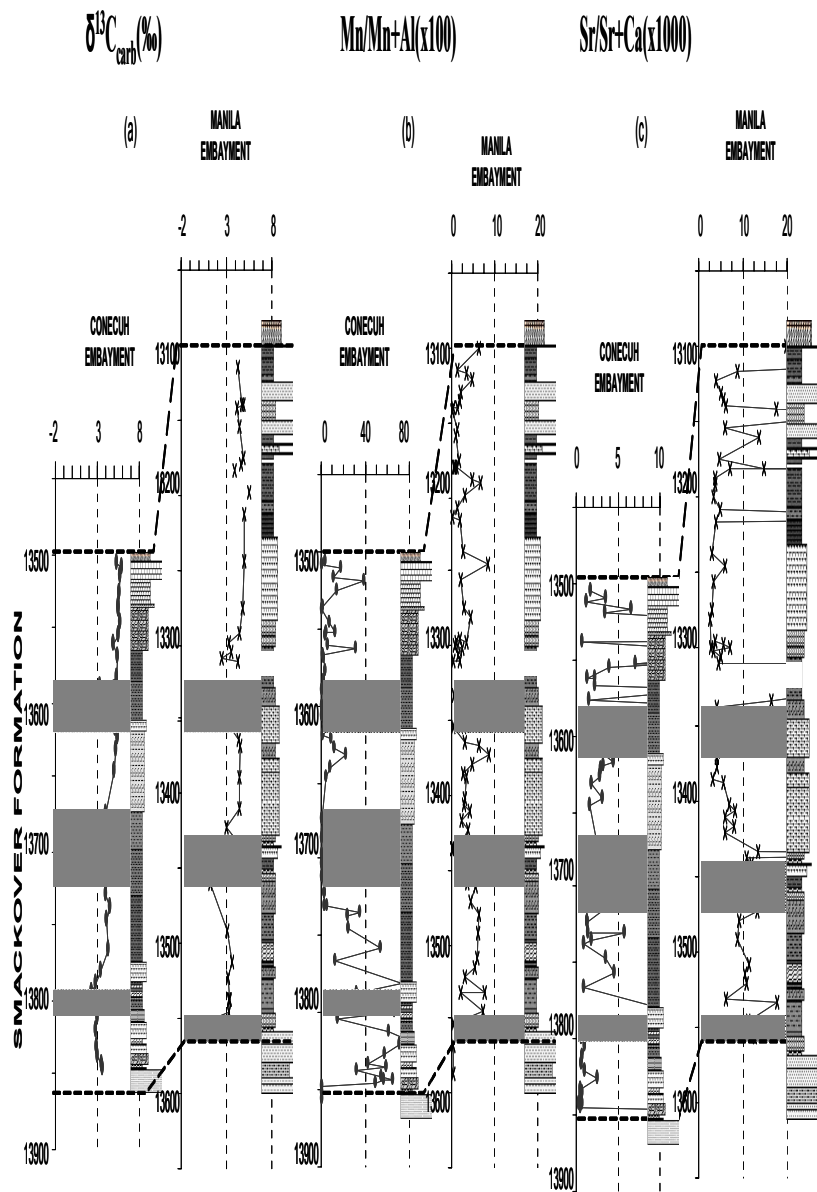


Figure 7-1. Carbon isotope and elemental stratigraphic correlations used for synthesizing the Smackover depositional models corresponded to relative sea level changes. (a)  $\delta^{13}C_{carb}$  for local and global variation of relative sea level rise and fall (transgressive-regressive cycle) due to changes of carbon budgets, (b) Mn for a possible global hydrothermal activities and (c) Sr for local and global variation of Sr in the seawater.

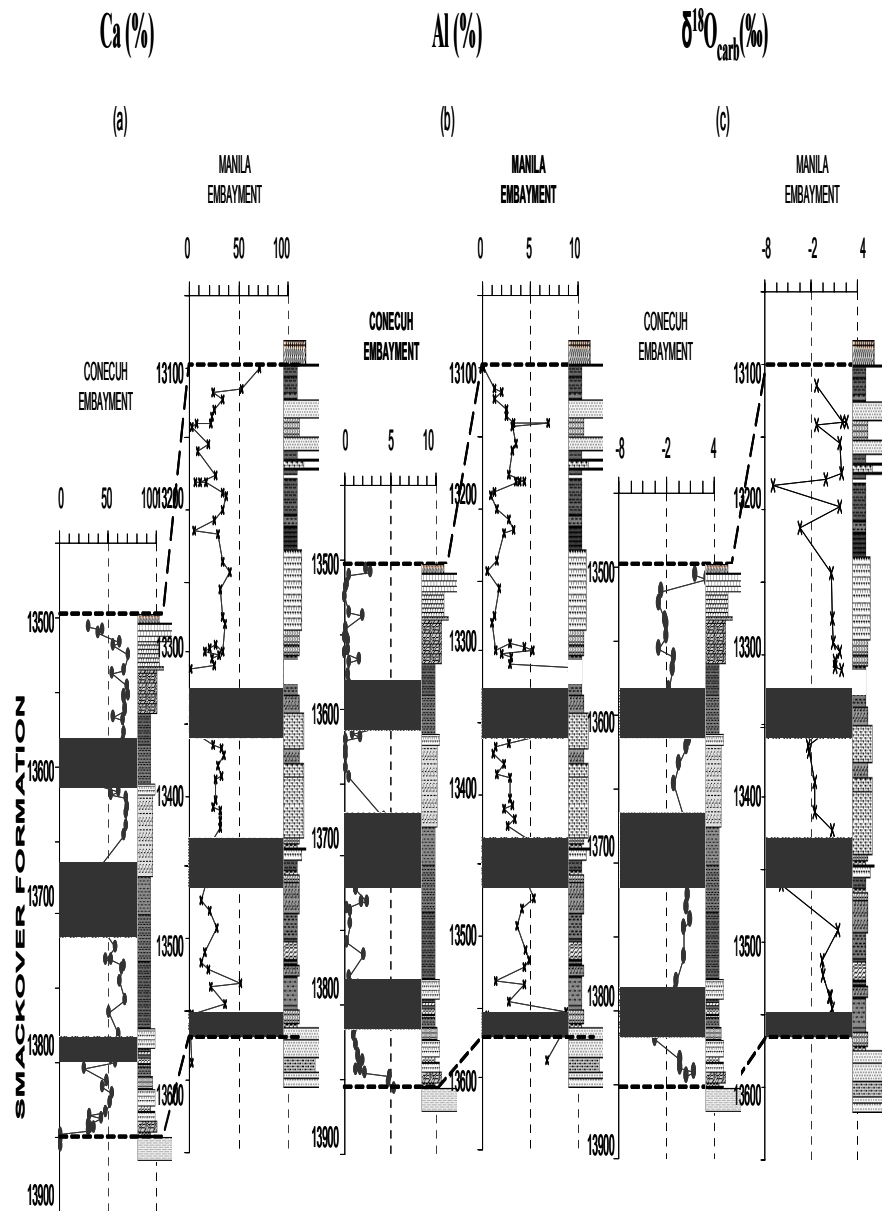


Figure 7-2. Elemental and oxygen isotope correlations between the Smackover sequences during local variations used for synthesizing depositional model for the Conecuh and the Manila Embayments, (a) and (b) carbonate and siliciclastic component (Ca and Al) for depositional environments, (c)  $\delta^{18}\text{O}_{\text{carb}}$  for diagenetic environment.

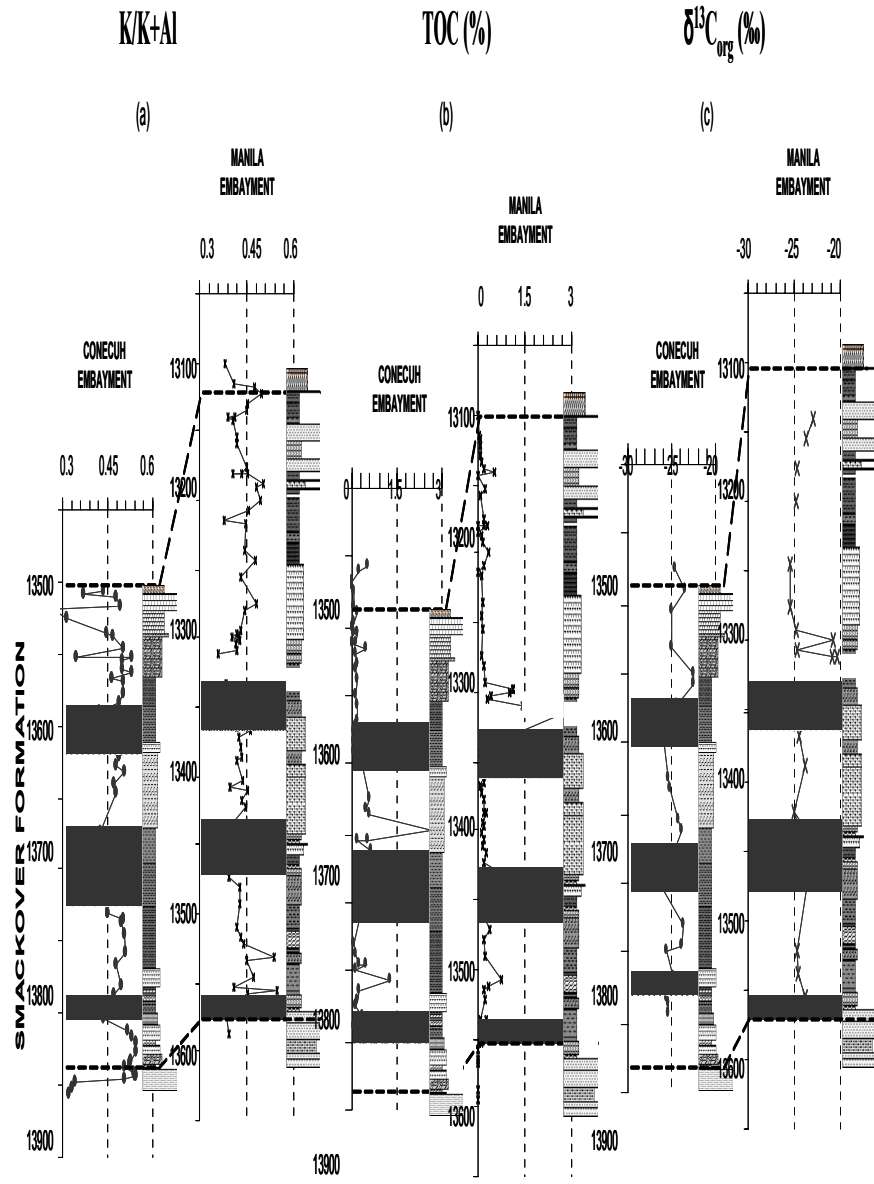
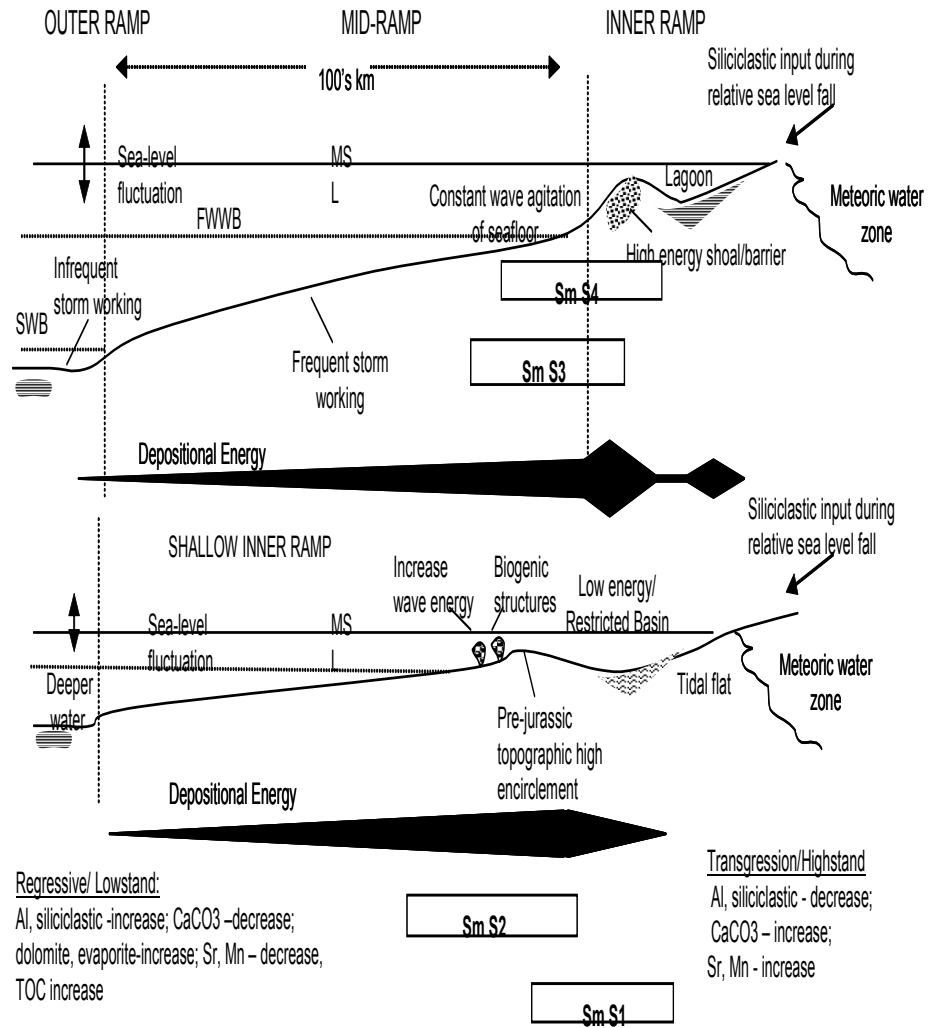


Figure 7-3. Elemental, organic carbon content and  $\delta^{13}C_{org}$  correlations between Smackover sequences from the Conecuh and the Manila Embayments (a) K/K+Al ratios for siliclastic variation of different related minerals because of local (and global?) chemical weathering cycle, (b) TOC for organic carbon accumulation associated with source input and/or depositional condition, (c)  $\delta^{13}C_{org}$  for local effect caused from mixed organic source input during relative sea level variation.

## DEPOSITIONAL MODEL - CONECUH EMBAYMENT (T.R. MILLER MILLS 17-11, #1)



**Figure 7-4.** Schematic depositional model related to relative sea level changes proposed for the Smackover deposition in the Conech Embayment. The lowest sequence, the Sm-S, formed during the major flooding for Smackover carbonates may include the upper siliclastic Norphlet as the lowstand deposit. The Sm-S2 sequence earlier occurred in a partially restricted condition but became more normal marine during the later stage of high sea level. The Sm-S2 and the Sm-S3 sequence were interrupted by falling sea level period showing increasing siliclastic influx. The Sm-S4 deposited on top of the next lowstand cycle occurred during long-term Smackover progradation where depositional energy became high. At the top of the Smackover Formation of the Sm-S4 sequence, relative sea level fell illustrated by an erosional surface and increased dolomite and evaporite. Different parameters can be used to recognize the variation of sea level and sediment deposition of different system tracts.

Norphlet sediment interval (~13 ft), that absence of a distinct discontinuity surface might suggest a sequence boundary similar to that appearing in the #1 NEAL ET AL UNIT 30-1 in the Manila Embayment. The major Oxfordian marine flooding which established the carbonate Smackover could have occurred on top of the erosional surface in the Conecuh Embayment. From this contact, a sufficient accommodation space allowed subtidal carbonate sedimentation. According to Jones and Desrochers (1992), shallow carbonate depositional cycles on the platform, especially on ramps, could occur as the repetitive meter-scale subtidal cycles without either an erosional break or subaerial exposure. Shorter Smackover cycles (meter scale) are typified by an upward increase in grain size, bed thickness and high energy sedimentary structure. These types of shallowing upward cycles have been recorded in many carbonate sedimentary sequences (i.e. Lohmann, 1976; Aigner, 1985; Calvet and Tucker, 1988; Osleger, 1991). During the Sm-S1 sequence, the abundance of carbonate mud and scarcity of normal marine fossils indicate that the Smackover deposition in the Conecuh Embayment area at this period of time was still under low energy and partially restricted conditions likely caused from the nearby paleostructural highs. During the transgressive sea level to highstand, where terrigenous input was minimal, some organic algal biohermal build-ups could have formed and continued into the late highstand phase. It is not uncommon for the late highstand organic build-ups to reflect the higher frequency sea level fluctuations and later to be partially drowned by the following sea level transgressive event. These build-up structures may only exhibit shallowing, but not necessarily exposure (Burchette and Wright, 1992). In the lower Smackover, a brief falling or decreased rate of eustatic sea level rising probably occurred but was insufficient to expose the highstand deposit of the Sm-S1 sequence. However a fluctuation of higher-frequency sea level cycles appeared to superimpose a stacking of several small cycles (centimeters scale) (13787 ft to 13805 ft). These small upward-shoaling cycles consist of algal laminated mudstone and the algal organic reef structures associated with evaporite nodules and some terrestrial materials.

As the eustatic sea level resumed rising again, interpreted as the Sm-S2 sequence, the subtidal carbonate deposit continued without distinct transitional sedimentation. Carbonate precipitation became productive under open marine waters, as evidenced by the presence of normal marine fossils. The condensed section is interpreted from the core (13755 ft to 13761 ft) as the carbonate mudstone intercalated with dark very thin layers that are probably the marine organic black shale. In the late highstand and the next lowstand periods where the rate of eustatic sea level changes started to fall, although the mean sea level was probably still above the fair-weather wave base, river channels that transported siliciclastic sediments (aluminosilicate, Al) to the ocean (from the ancestral Mississippi river or small rivers to the northeast), could prograde seaward along the platform. The fine grain siliciclastic sediments were transported by wave and ocean currents from the channel mouth in the Mississippi area to be deposited farther away. Increased siliciclastic sediment influx has been shown to be associated with period of relative sea level fall for many carbonate ramp stratigraphic sequences (i.e. Choi and Simo, 1998; Pittet et al., 2000; Spalletti et al., 2000). Burchette and Wright (1992) pointed out that because of the low slope angle of the platform, change in the character of the ramp sediment between highstand and lowstand system tracts might be minimal and hardly distinguishable if the relative sea level fall is small. The type 2 sequence boundary which was formed on the low gradient platform might show no greater contrast in the nature of the facies above and below the boundary (Tucker et al., 1993). The sabkha, lacustrine, fluvial and other supratidal/non-marine environments which commonly develop during the lowstand sea level occurred predominantly under the type 1 sequence (with sea level falling below the shelf break).

In the next sea level cycle, interpreted as Sm-S3, depositional energy increased as it prograded landward toward the carbonate shoal/barrier. Some higher energy grains i.e. oncoids, packstones and wackestones under an open marine environment developed. Under these conditions where depositional energy was high with very low to no siliciclastic contamination, carbonate deposition was dominant but without a condensed interval or distinguishable maximum

flooding surface. Toward the falling period of the next sea level, small evaporite replacement became noticeable in the highstand carbonate deposit. The increasing of siliciclastic sediment and evaporite nodules in the carbonate deposit at this time was interpreted as the lowstand deposit in which more siliciclastic sediment was brought into the platform.

Under the next sea level cycle, the upper Smackover deposition was formed and is interpreted as the Sm-S4. In this sequence, depositional energy in the environment became high as sedimentation approached a shoaling environment. Although siliciclastic sediment was still low, siliciclastic elements interpreted as being associated with high energy conditions (Ti/Ti+Al) increased. The Sr content became unusually high owing to the precipitation and deposition of aragonitic carbonate minerals of the carbonate grains. At the end of the upper Smackover, a large eustatic sea level fall occurred and caused some exposure in the grainstone highstand sediment before deposition of the Buckner Anhydrite formation. The effect of eustatic sea level changes on the T.R. MILLER MILLS 17-11, #1 Smackover core is interpreted based upon the variation of the  $\delta^{13}\text{C}_{\text{carb}}$  variation which can be globally correlated with the other rock sequences of equivalent Oxfordian age. On a local scale, during the lowstand when the ramp was more attached to the land, meteoric input with high  $^{12}\text{C}$  from organic material from the surface soils might affect decreasing of the  $\delta^{13}\text{C}_{\text{carb}}$  values in addition to their original isotopic signal. At the same time, the regional scale (and global) falling eustatic sea level increased sediment erosion and organic matter oxidation from land into the ocean and caused the bicarbonate ions to become enriched in  $^{12}\text{C}$  which would lower the  $^{13}\text{C}/^{12}\text{C}$  or the  $\delta^{13}\text{C}_{\text{carb}}$  values of the carbonate and thus negative  $\delta^{13}\text{C}_{\text{carb}}$  values. The  $\delta^{13}\text{C}_{\text{carb}}$  depleted values for shallow platform carbonate sedimentation during the falling relative sea level are believed to be a distinctive stratigraphic marker which can cut across the variation of sedimentary facies and diagenetic environment in the Conecuh Embayment and the Manila Embayment areas where the Smackover deposition occurred.

Analogously, the proposed depositional model for explaining the changes of the Smackover sequences of the Manila Embayment is illustrated in **Figure 7-5**. For the Manila

## DEPOSITIONAL MODEL - MANILA EMBAYMENT (#1 NEAL ET AL UNIT 30-1)

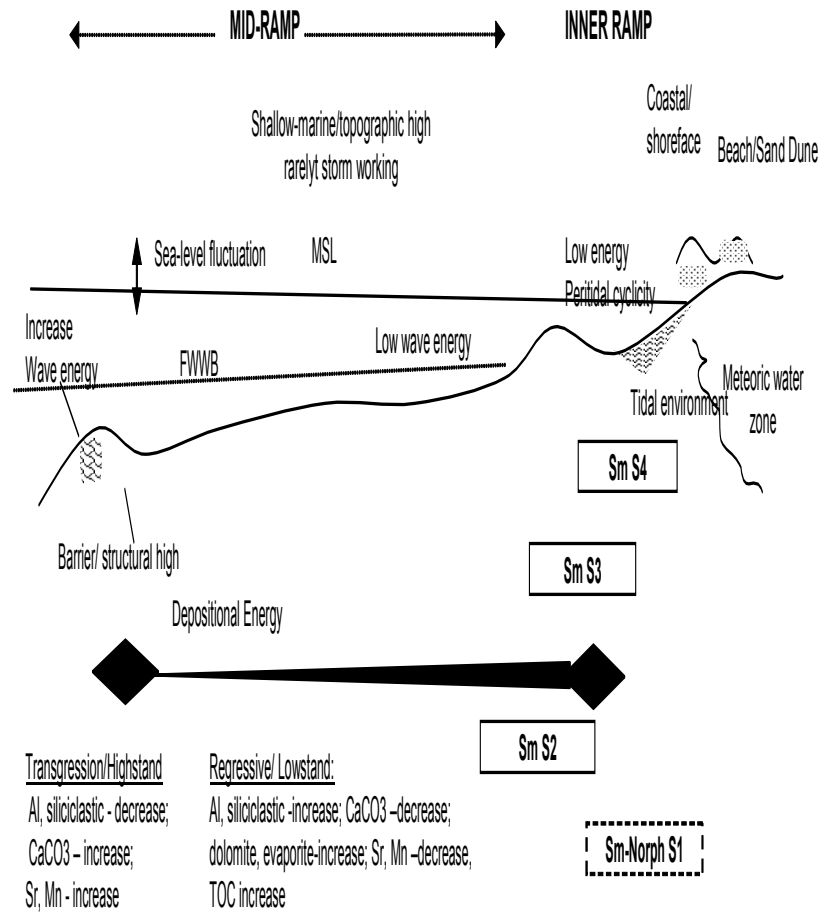


**Figure 7-5.** Schematic depositional model related to relative sea level changes proposed for the Smackover deposition in the Manila Embayment. The lowest sequence, the Sm-S1, formed during the major flooding for Smackover carbonates but consists mostly the massive, marine reworked siliciclastic sandstone in the uppermost Norphlet Formation. The next two sequences, the Sm-S2 and the Sm-S3, illustrate shallowing-upward cycles in a peritidal environment where the sediments in the uppermost intervals were affected from meteoric diagenesis and subaerial exposure. The Sm-S4 sequence formed during the high energy sea level condition of the long term progradational Smackover sequence. Coastal/shoreface mixed siliciclastic-carbonate intercalation occurred near the shoreline. Because of the high structural setting condition, Smackover depositional sequences experienced strong diagenetic alteration and dolomitization. Similar parameters can be recognized during the variation of sea level and sediment deposition of different system tracts.

Embayment location, the data suggest a depositional model where the Smackover was deposited on a tidal flat environment which was attached to the coastal and shoreline environment. During the early and late Smackover periods, although the Smackover developed in different environments, the depositional energy was still low as it was in the Conecuh Embayment. A high-energy environment occurred later in the upper Smackover deposition under higher-energy shoreface/beach conditions. Sedimentary facies and elemental compositions differ in characteristics of the shorter Smackover sequences in the Manila Embayment and occur as peritidal cyclicity, especially in the lower and middle Smackover. Upward shoaling successions on meters scale from subtidal to supratidal are observable but for the majority of the sediment there are repeated facies representing intertidal conditions (“ribbon rocks”). Due to the characteristic of the cycle which was capped by subaerial diagenesis during the supratidal, these shorter depositional sequences (of long meters scale) for the Smackover of the Manila Embayment might be characterized as diagenetic cycles (Jones and Desrochers (1992).

The relationship between sea level fluctuation and the stacking characteristic of the peritidal shallowing-upward succession is illustrated in **Figure 7-6** and **Figure 7-7**. During the Smackover long-term sequence, there were several shallowing-upward cycles that probably were controlled by the higher frequency sea level cycles occurred as sea level fluctuated up and down and thus back and forth across the platform. During the relative sea level falls, the highstand sediments became strongly overprinted by diagenetic alteration including dolomitization due possible subaerial exposure. A sequence boundary can be observed but instead of exhibiting a single surface, it instead presents as a zone where the sediment deposition illustrates higher sea level fluctuation and early meteoric diagenetic effects. The  $\delta^{13}\text{C}_{\text{carb}}$  values become depleted and can be correlated with the  $\delta^{13}\text{C}_{\text{carb}}$  values of the lowstand deposit intervals in the Conecuh Embayment. The variation of the elemental composition on the siliciclastic sediment is less obvious as higher siliciclastic sediment background which has already mixed with the carbonate sedimentation in this area. The relatively higher siliciclastic sediments in the carbonate

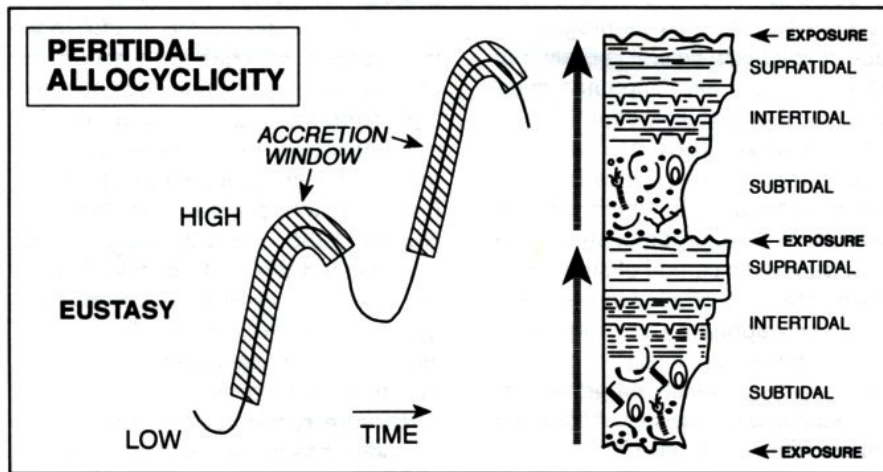


**Figure 7-6.** A diagram illustrating the possible relationship between the fluctuation of sea level and the short-term peritidal cycles observed during the long-term Smackover sequence in the #1 NEAL ET AL UNIT 30-1 well of the Manila Embayment. In the NEAL ET AL. 30-1 core sequence, the stacking of these cycles formed during the higher order eustatic sea level cycles can be observed but it is interpreted that only during the major fall in relative sea level (third order) which interrupted the continuous carbonate production and resulted in subaerial exposure and diagenesis (from Pratt et al., 1992).

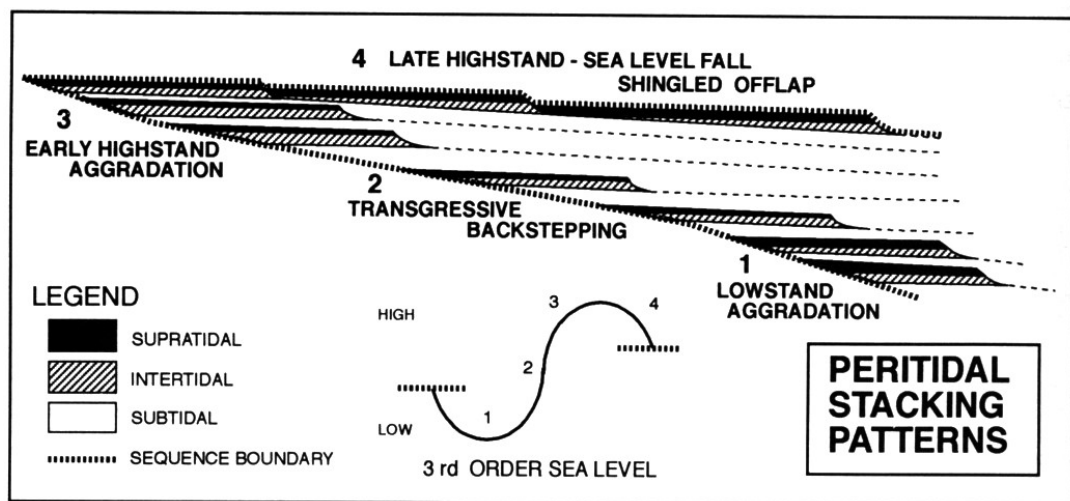


**Figure 7-7.** A diagram illustrating the hypothetical stratigraphy of meter-scale, peritidal, successions which could possibly occur between the two sequence boundaries in the #1 NEAL ET AL UNIT 30-1 core of the Manila Embayment. Each succession formed by sediment progradation, which was most likely associated with the higher frequency sea level fluctuation. The balance between sea level changes, sedimentation and subsidence rate affected the stacking pattern of the tidal flat sediment succession (from Pratt et al., 1992).

environment of the Manila Embayment might have been transported from the Mississippi Interior Salt Basin as Shew (1991) had earlier reported the influx of several large siliciclastic sandstones which interrupted Smackover carbonate deposition (**Figure 7-8**). From core observations and  $\delta^{13}\text{C}_{\text{carb}}$  correlations, the lowest short-term Smackover sequence in the Manila Embayment (Sm-S1) is interpreted as the upper sandstone deposits of the Norphlet Formation. In the Manila Embayment, three short sequences are interpreted as being controlled by the relative sea level changes and can be correlated with the Smackover sequences in the Conecuh Embayment. These short sequences are interpreted as being affected by third-order eustatic sea level fluctuation controlling carbonate diagenetic cycles in this embayment. The upper boundaries of the cycles, affected by eustatic sea level falls, are manifested as sediment deposition which associated with subaerial exposure and diagenesis. In the #1 NEAL ET AL UNIT 30-1 core sequence, the variation between carbonate and siliciclastic influx as shorter Smackover cyclicality was not as clearly distinguished as in the T.R. MILLER MILLS 17-11, #1 of the Conecuh Embayment. However, the diagenetic alteration during the allocyclic peritidal cycles (affected by relative sea level change) is distinctive and does illustrate the stratigraphy which can be correlated between the Smackover depositional sequence in these two southwest Alabama basins. During the fluctuation of relative sea level, the organic carbon content and its carbon isotope composition were locally affected by the depositional environment, structural setting of the embayment and distance from the land. Because of the different carbon isotope compositions between algae, marine organisms and terrigenous higher plants, the mixing ratio between these original organic carbon sources for the Smackover TOC appeared to have dominated influence on the  $\delta^{13}\text{C}_{\text{org}}$  values rather than the  $^{13}\text{C}/^{12}\text{C}$  variation in the ocean. The regional stratigraphy and depositional model of the Smackover in southwest Alabama interpreted by using the  $\delta^{13}\text{C}_{\text{carb}}$  values in this study can be correlated to the Smackover stratigraphy interpreted from south Arkansas and north Louisiana. Troell and Robinson (1987) detected four progradational carbonate sequences of the Smackover which occurred parallel to the ancestral Gulf shoreline. Each progradation consisted

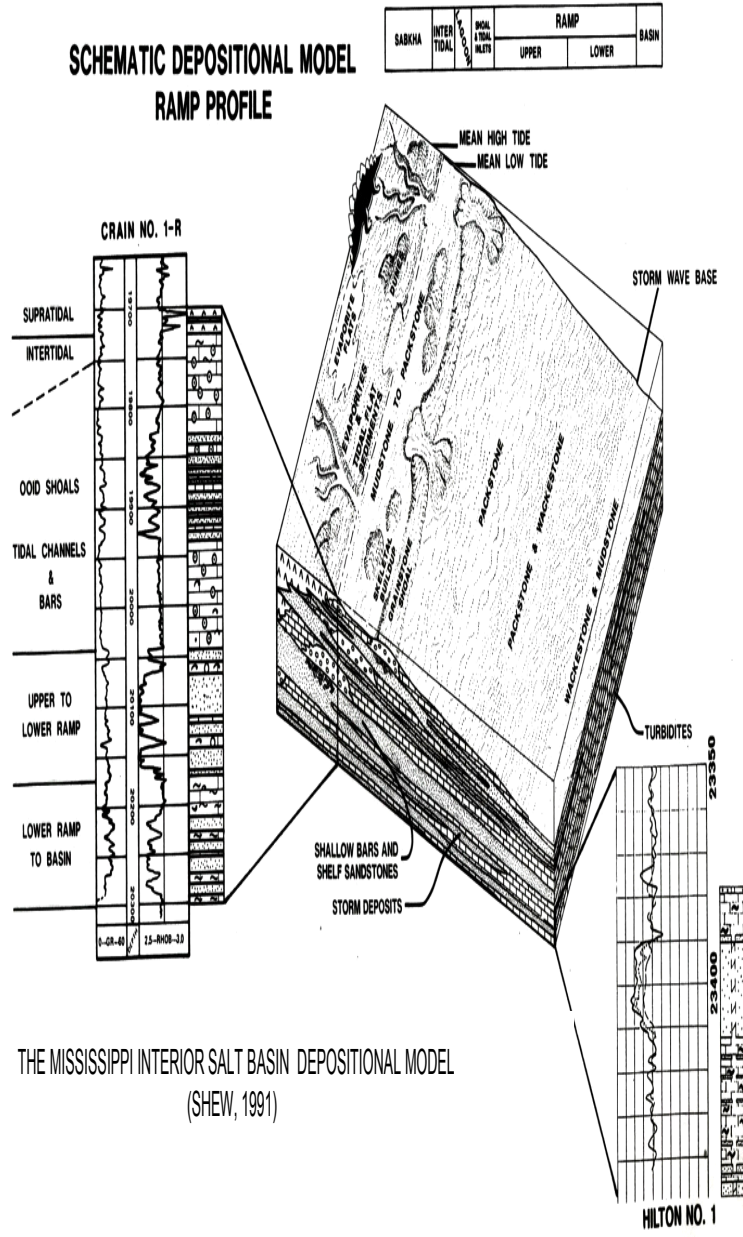


Figure 7-8. Depositional model proposed for the Smackover upward-shoaling sequence in the Mississippi Interior Salt Basin, central Mississippi and described as the lower, middle and upper Smackover by Shew (1991). It is noted that the Smackover carbonates were interrupted by several episodes of siliciclastic sediment influx which probably contributed to siliciclastic observed in the Smackover deposition of the Manila Embayment (from Shew, 1991).

of calcarenite rock bodies or banks which prograded basinward on top of the previous cycles. For southwest Alabama area, the higher structural setting which was less open to normal marine high energy environment lead to a weakening of the marine wave energy during the three lower Smackover sequences required for high energy grainstone formation. Not until the last Smackover cycle (Sm-Sq4), where the long term Smackover sea level was high and marine wave energy was increased close to the shoal area or the shoreface did the high-energy Smackover sediment became recognizable in the southwest Alabama area.

## **7.2 OXFORDIAN SEA LEVEL VARIATION AND TECTONIC ACTIVITY**

In general, the two possible causes of global sea-level change are the melting and the freezing of the polar icecaps (glacioeustasy) and the changing volume of oceanic basin bound up with the creation and destruction of the oceanic ridges (tectonoeustasy) (Hallam, 1992). Hallam (2001) reported that the change associated with the change of the oceanic volume due to the oceanic ridge activities are usually three times lower than glacioeustatic changes. According to Frakes et al., 1992; Hallam, 1993), during the Jurassic period the influence from the changing of the polar ice volume affecting eustatic sea level changes had no evidence compared to the significant ice volume on this present day. Wignall (1991) earlier suggested from the upper Jurassic, Kimmeridgian of England and northern France, that the synchronous development of unconformities in several basin margins especially in northwest Europe could have been affected from sea level falling or widespread tectonic movements which were unrelated to the local intrabasinal tectonic activities. The opening of the Atlantic Ocean in its central sector between the North America and north-western Africa was speculated to be possibly associated with the rise in the late Callovian to the Early Oxfordian (Hallam, 2001). However, the pulses of the subsequent rising in the Late Oxfordian and Kimmeridgian were not believed by Hallam (2001) to be caused by activities from the central Atlantic Ocean through its opening owing to a more or less uniform

rate of the sea floor spreading (Kiltgord and Schouten, 1986). Halam (2001) instead hypothesized that the effect might come from the initial breakup of the eastern Gondwanaland which led to an opening and creating the new sea floor of the Indian Ocean.

The effects of the tectonoeustasy on the Oxfordian eustatic sea level variation have also been reported. Allenbach (2002) suggested from sedimentary facies and structure observation of the Oxfordian sediment sequence occurred from the Swiss Jura Mountain in northern Switzerland that the active local and regional tectonisms could have play the role in addition to eustasy and sedimentation rate on the developments of the Oxfordian epicontinental basins as well as on the shallow-water deposition. Allenbach (2002) also suggested that eustatic sea level fluctuations might have an important role on the development of shallow-water facies patterns, but subordinately on a role for the creation of accommodation space in the basin. He proposed that tectonic activities could possibly still be active and affect differential basin subsidence. This synsedimentary tectonic movement could lead to a diachronous boundary between the two shallow basins. In the Gulf of Mexico region, Llinás (2002) interpreted from a seismic data derived from the eastern margin of the Manila basin and embayment and suggested that the tectonic subsidence associated with faulted basement blocks could contribute and thus affected the Smackover deposition in the southwest Alabama area. He reported that a differential subsidence resulting from salt movement accompanying the tectonic movements could have a strong role for rapid and significant marine inundation for the Smackover deposition instead of eustatic sea level changes. However, from this study, the shorter depositional cycles are observed in a long-term Smackover sequence from the deeper part of the Manila Basin in the #1 NEAL ET AL UNIT 30-1. The stratigraphic evidences illustrated by a  $\delta^{13}\text{C}_{\text{carb}}$  correlation with the Smackover sequence in the Conecuh Embayment and the subaerial exposure intervals observed in the #1 NEAL ET AL UNIT 30-1 core tend to support that sea level fluctuation was still likely the primary control for Smackover depositions in these southwest Alabama basins.

### 7.3 LATE JURASSIC PALEOCLIMATES

Climate conditions can be important and affect the magnitude on carbonate productivity in shallow carbonate environments because of changing carbonate favorable factors (e.g. Lees, 1975; Isern et al., 1996; Riding 1996; Homewood, 1996). Under the climate major control, an increased siliciclastic influx which is usually associated with falling sea level may not necessarily be directly controlled by the falling of the sea level but instead become accelerated by an increased intensity of weathering processes on the continent (Weissert and Mohr, 1996). During humid and wet periods, weathering processes can affect the water, nutrient and organic carbon recycling from land to the ocean (Cecil, 1990; Weissert, 1990). According to Hallam (1984), Late Jurassic climate was exceptionally warm and humid compared to the earlier Mesozoic climates. The intense humidity corresponded to an elevated energy level of the biosphere and the distribution of an increased rainfall was controlled by the seasonal (monsoonal) climate which was progressively replaced by a more zonal climate by the beginning of the Cretaceous (Weissert and Mohr, 1996). The widespread carbonate sedimentation which peaked during the Late Oxfordian and Early Kimmeridgian still suggests a global high sea level. Weissert and Mohr (1996) believed that an increased organic carbon accumulation in the ocean and high siliciclastic influx during the Late Jurassic was influenced by the specific conditions of increased weathering, erosion and water run-off from land. In contrast, increasing siliciclastic and fine grain suspension as well as nutrient loads in the coastal waters would interrupt the carbonate factory in the shallow water environment. A high global sea level and more open paleoceanographic conditions become favorable for both carbonate platform growth and increases organic carbon burial rate. Because of the fluctuating carbonate and organic carbon burial rate during the Late Jurassic, Weissert and Mohr (1996) suggested the positive  $\delta^{13}\text{C}_{\text{carb}}$  variation during the Upper Jurassic time might not be an accurate proxy from an increased global organic carbon accumulation rate which affected the change on the  $^{13}\text{C}$  and  $^{12}\text{C}$  of global reservoirs. Weissert and Mohr (1996) proposed the global

paleoclimate change model in which an elevated atmospheric CO<sub>2</sub> was the cause for change of the global climates related to water cycling, rainfall and the seasonality. An increase in chemical weathering during the warm and humid climate owing to the elevated CO<sub>2</sub> level in the atmosphere caused weathering and thus increased siliclastic influx and nutrients transferred into the oceans. An increase of organic carbon production rate in the ocean thus affected the  $\delta^{13}\text{C}$  composition in the carbonate to fluctuate showing trends which were controlled by changes in paleoclimate and paleoceanic conditions. The relation of various components related to driving mechanism for the cycles of the Weissert and Mohr (1996) model is illustrated in **Figure 7-9**.

#### 7.4 CONCLUSIONS

On a gently sloping carbonate ramp, small vertical changes in sea level could lead to large lateral changes in marine transgressions and regressions. Distinguishing the effects of global causes and local causes for the major and minor elemental compositions, organic carbon content, and stable isotopic ratios of carbon and oxygen can be complicated by a variety of factors, especially diagenesis and climatic effects. However, a few clear signals from this study of Smackover carbonate sedimentation of southwest Alabama as analyzed from two wells of the Manila Embayment and the Conecuh Embayments can be defined. In general,  $\delta^{13}\text{C}_{\text{carb}}$  corresponds to vertical global changes in sea level whereas  $\delta^{13}\text{C}_{\text{org}}$  corresponds to local horizontal changes in transgressions and regressions, while  $\delta^{18}\text{O}$  mostly provide a tell-tale signal of diagenetic alteration. Certain minor elemental associations clearly indicate the proximity of clastic influx and help track transgressions and regressions. The sedimentation was primarily controlled by relative sea level cycles and modified by the paleotopography associated with basin configuration and depositional environments related to paleowater-depths. The variation of the sedimentary facies and diagenetic environments of the Smackover depositions could be the reason the carbonate depositional sequence, relative to changes of sea level and/or climates in this

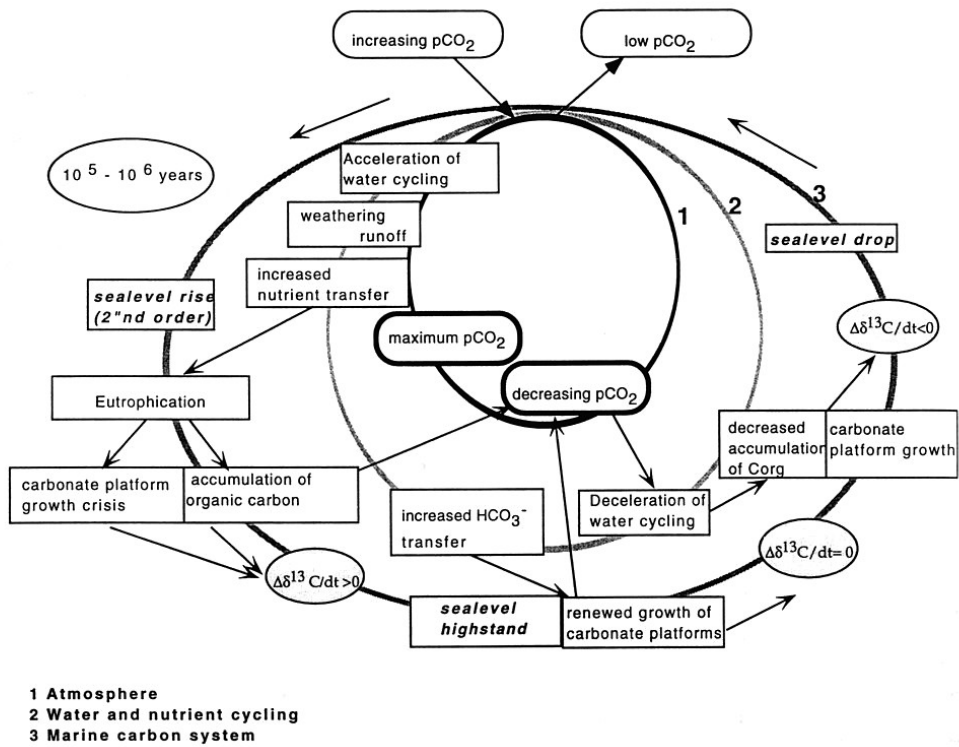


**Figure 7-9.** The global paleoclimate model proposed by Weissert and Mohr (1996) and illustrated the link between different components during the Late Jurassic global water and carbon recyclings due an increased atmospheric CO<sub>2</sub>.

particular area, not being clearly distinguishable and the inability to be correlated to the Smackover sequence stratigraphy proposed from a nearby basin (i.e. the Mississippi Interior Salt Basin) and to the sea level model which has been applied to other sedimentary basins of the Gulf of Mexico.

In particular, the conclusions that can be drawn from this depositional sequence study of the Smackover Formation in the two southwest Alabama basins are:

- 1) Although sea level was a primary control for sedimentary cycles, the paleotopography and depositional setting affected sedimentation and subsidence rates and modified the basic components (the system tract) of the depositional sequence.
- 2) The low slope gradient on the platform and the variation in the structural setting in the two embayments caused the changes between system tracts to become less distinctive. The bounding surface does not show an abrupt facies change or a discontinuity surface but instead a change due to depositional energy and type of carbonate sedimentation. The sequence boundary is not always a subaerial exposure but is disconformable or shows a subaqueous omission or the superimposition of the higher frequency sedimentary cycles which could be related to climate effects.
- 3) On the shallow platform carbonate, because the markers or keys for a stratigraphic boundary (i.e. first transgressive surface, maximum flooding surface, sequence boundary) were not always distinguishable, the correlation based upon these component might not be explicit.
- 4) Diagenetic effects of carbonates on a shallow platform can be variable. The extensive alterations can obliterate early sedimentary characteristics (texture, fabric and structure) which are important for lateral stratigraphic observation.
- 5) Sequence interpretation from sedimentary facies and elemental analysis can be variable if sedimentary facies and elemental variation affected by local modification under different conditions.

6) Sequence boundaries which are not coincident with the formation boundary could make correlation problematic.

7) For ramp sequence stratigraphy with a disconformable transition, during an early transgressive system tract, increasing accommodation space with carbonates trying to catch-up with sea level and increased siliciclastic by a landward sea transgression could possibly end up with mixed carbonate-siliciclastic sediment depositing on top of the lowstand siliciclastic sediment. However, because of no distinguishable surface, the condensed intervals resulting from low sedimentation rates and mixing of sediments may be hardly separated from the lowstand sediment from the previous sea cycle unless they are marked by dark organic rich marine sediment deposit.

8) The superimposition of the high frequency sea level cycle effects which is not necessary expressed in every core sequence, especially sedimentation that occurred some distant from the land, reduce the effectiveness of the higher frequency sea level cycle correlation.

9) On a shallow carbonate platform, the effects from mixing primary organic carbon sources (marine vs. terrestrial vs. algae) and organic oxidation or reworking process can affect the organic total organic accumulation rate and the carbon isotope values.

10) While sedimentary facies, depositional environment and diagenesis might be problematic for the correlation due to several related effects, the carbon isotope stratigraphy can be used for the stratigraphic correlation. By combining the different results (core characterization, element compositions, oxygen and carbon isotopes), the effects of these variations during the sedimentary cycles related to relative sea level changes are recognizable.

11) Carbon isotope stratigraphy of the Smackover depositional sequence was recorded on the carbonate carbon isotope composition controlled by the effects of regional/global scale sea level variation (or climate?) and/or local diagenesis during falling relative sea level period. The organic carbon isotope varied along the long-term Smackover trend and was controlled by different ratios of mixed marine and terrigenous organic materials which contained variable

carbon isotope compositions. The correlation between carbonate and organic carbon isotope would illustrate positive covariation to changes of global carbon reservoirs if the organic carbon content was derived primarily from a single organic source (i.e. marine or terrestrial) which has to be clarified.

12) Global climate conditions could be an important factor for the variation of carbonate deposition and the  $\delta^{13}\text{C}_{\text{carb}}$  variation in addition to sea level changes. To verify this conclusion, the correlation between carbonate and organic carbon isotopes on a stratigraphic framework related to chemical weathering cycles during the Smackover sequence need to be further studied.

13) The  $\delta^{13}\text{C}_{\text{carb}}$  stratigraphy of the Smackover carbonate in southwest Alabama indicates four short-term sequences which were probably controlled by third-order eustatic sea level cycles during the long-term Smackover regressive sequence (second order?). The sequence boundaries, especially of the lowest sequence, were not coincident with the formation boundary between the Norphlet and the Smackover Formations.

14) Regional sequence stratigraphic correlation of the Smackover deposition on the northern Gulf of Mexico basins using the major and minor elemental analyses as well as the  $\delta^{13}\text{C}_{\text{carb}}$  stratigraphy should be expanded in order to study the effects of both local and global controls

## REFERENCES

- Aceredo A. C. (1998) Geometry and facies dynamics of Middle Jurassic carbonate ramp sand bodies, west-central Portugal. In *Carbonate Ramp* (Edited by V.P. Wright and T.P. Burchette), Geological Society, London, Special Publication, 149, 281-314.
- Ahr W. M. (1973) The carbonate ramp: an alternative to the shelf model. *Gulf Coast Assoc. Trans.* 23, 221-225.
- Ahr W. M. and Palko G. J. (1981) Depositional and diagenetic cycles in Smackover limestone-sandstone sequences, Lincoln Parish, Louisiana. *Gulf Coast Assoc. Trans.* 31, 7-17.
- Aigner T. (1984) Dynamic stratigraphy of epicontinental carbonates, Upper Muschelkalk (M. Triassic), South-German Basin. *Neues Jahrb. Geol. Paläontol.* 169, 127-159.
- Allan J. R. and Matthews R. K. (1982) Isotope signatures associated with early meteoric diagenesis. *Sedimentology* 29, 797-817.
- Allan J. R. and Matthews R. K. (1977) Carbon and oxygen isotopes as diagenetic and stratigraphic tools: surface and subsurface data, Barbados, West Indies, *Geology* 5, 16-20.
- Allenbach R. P. (2002) The ups and downs of Tectonic Quiescence – recognizing differential subsidence in the epicontinental sea of the Oxfordian in the Swiss Jura Mountains. *Sedimentary Geology* 150, 323-342.
- Amy J. P., Schmitz D. W. and Baria L. R. (1995) Distribution of illite and mixed-layered illite in the Smackover Formation of the Manila Embayment of southwest Alabama (Wilcox, Clarke and Monroe Counties). *Gulf Coast Assoc. Tran.* 45, 13-20.
- Anderson, T. F. and Arthur, M. A. (1983) Stable isotopes of oxygen and carbon and their application to sedimentologic and paleoenvironmental problems. In *Stable Isotopes in Sedimentary Geology* (Edited by Arthur M.A.), SEPM Short Course 10, Chapter 1, 1-151.
- Arthur M. A., Dean W. E. and Schlanger S. O. (1985) Variations in the global carbon cycle during the Cretaceous related to climate, volcanism, and changes of atmospheric CO<sub>2</sub>. In *The carbon cycle and Atmospheric CO<sub>2</sub>: Natural Variations Archean to Present* (Edited by E.T.S. Sundquist and W.S. Broecker), Geophys. Monogr. 32, 504-529.
- Arthur M. A. and Dean W. E. (1991) A holistic geochemical approach to cyclomania: examples from Cretaceous pelagic limestone sequences. In *Cycles and Events in stratigraphy* (Edited by G. Einsele, A. Seilacher and W. Ricken), Springer, Berlin, 126-166.
- Bachmann M. and Kuss J. (1998) The Middle Cretaceous carbonate ramp of the northern Sinai: sequence stratigraphy and facies distribution. In *Carbonate Ramp* (Edited by V.P. Wright and T.P. Burchette), Geological Society, London, Special Publication, 149, 253-280.

- Badon C. W. (1973) Petrology and combine reservoir potential of the Smackover Formation, Clark County, Mississippi. *Gulf Coast Assoc.Trans.* 24, 163-174.
- Barrett D. (1998) Upper Smackover depositional model, Kildare Field, Cass County, Texas. *Gulf Coast Assoc.Trans.* 48, 1-8.
- Barrett M. L. (1987) The dolomitization and digenesis of the Jurassic Smackover Formation, southwest Alabama. *Ph.D. diss.*, Johns Hopkins University, 361p
- Baria L., Stoudt D. L., Harris P. M. and Crevallo P. D. (1982) Upper Jurassic reef of the Smackover Formation, Clark County, Mississippi. *AAPG Bull.* 66, 10, 1449-1482.
- Bathurst R. G. C. (1975) *Carbonate Sediments and Their Diagenesis*. Elsevier Sci. Publ.Com, Amsterdam, Netherlands.
- Benson D. J. (1985) Diagenetic controls on reservoir development and quality, Smackover Formation of southwest Alabama. *Gulf Coast Assoc Trans.* 25, 317-326.
- Benson D. J. (1988) Depositional history of the Smackover Formation in southwest Alabama. *Gulf Coast Assoc.Trans.* 38, 197-205.
- Benson D. J. and Mancini E. A. (1984) Porosity development and reservoir characteristics of the Smackover Formation in southwest Alabama. In *The Jurassic of the Gulf Rim* (Edited by W.P.S. Ventress, D.G. Bebout, B.F. Perkins, and C.H. Moore), Gulf Coast Section, SEPM Foundation Third Annual Research Conference Proceeding, 1-18.
- Benson D. J., Pultz L. M. and Bruner D. D. (1996) Paleotopographic vs. eustatic controls on deposition of the Smackover Formation, Appleton Field, Escambia County, Alabama. Abstract with Programs, *AAPG Bull.* 80, 1495.
- Bill M., Baumgartner P. O., Hunziker J. C. and Sharp Z. D. (1995) Carbon isotope stratigraphy of the Liesberg Beds Member (Oxfordian, Swiss Jura). *Eclogae Geologicae Helveticae* 88, 135-155.
- Bingham C. L. (1937) Developments in Arkansas-Louisiana-Texas area, 1936-1937. *AAPG Bull.* 21, 1066-1073.
- Bishop W. F. (1973) Late Jurassic contemporaneous faults in north Louisiana and south Arkansas. *AAPG Bull.* 57, 858-877.
- Bradford C. A. (1984) Transgressive-regressive carbonate facies of the Smackover Formation, Escambia County, Alabama. In *The Jurassic of the Gulf Rim* (Edited by W.P.S. Ventress, D.G. Bebout, B.F. Perkins, and C.H. Moore), Gulf Coast Section, SEPM Foundation Third Annual Research Conference Proceeding, 27-39.
- Brand U. and Veizer J. (1980) Chemical diagenesis of a multicomponent carbonate system-1: trace elements. *Jour. Sed. Petrology* 50, 1219-1236.
- Brand U. and Veizer J. (1981) Chemical diagenesis of a multicomponent carbonate system-2: stable isotopes. *Jour. Sed. Petrology* 51, 987-997.

- Broecker W. S. and Takahashi T. (1984) Is there a tie between atmospheric CO<sub>2</sub> content and the ocean circulation? *Am. Geophys. Union Geophys. Monogr.* 28, 314-326.
- Budd D. A. and Loucks R. G. (1981) Smackover and Lower Buckner Formations, south Texas: depositional systems on a Jurassic carbonate ramp. *Bureau of Economic Geology, report of investigation No. 112*, 38p.
- Buggisch W., Keller M. and Lehnert O. (2003) Carbon isotope record of Late Cambrian to early Ordovician carbonates of the Argentine Precordillera. *Palaeogeogr. Palaeoclimatol. Palaeoecol.* 195, 357-373.
- Burchette T. P. and Wright V. P. (1992) Carbonate ramp depositional systems. *Sedimentary Geology* 79, 3-57.
- Calvet F. and Tucker M. E. (1988) Outer ramp carbonate cycles in the Upper Muschelkalk, Catalan Basin, N.E. Spain. *Sed. Geol.* 57, 185-159.
- Calvert S. E. (1976) The mineralogy and geochemistry of near-shore sediments. In *Chemical Oceanography* (Edited by J.P. Riley and R. Chester), Chapter 33, 187-280
- Calvert S. E. and Pedersen T. F. (1993) Geochemistry of recent oxic and anoxic marine sediments: implications for geological record. *Mar. Geol.* 113, 67-88.
- Calvert S. E. and Pederson T. F. (1996) Sedimentary Geochemistry of Manganese: Implications for the Environment of Formation of Manganiferous Black Shales. *Economic Geology* 91, 1996.
- Cecil C. B. (1990) Pleoclimate control on stratigraphic repetition of chemical and siliciclastic rocks. *Geology* 18, 533-536.
- Chester R. (1990) *Marine Geochemistry*. Unwin Hyman, London.
- Chimene C. A (1976) Upper Jurassic reservoir, Walker Creek Field area, Lafayette and Columbia counties, Arkansas. In *North American Oil and Gas Fields*. AAPG Memoir 24, 117-204.
- Choi Y. S. and Simo J. A. (1998) Ramp facies and sequence stratigraphic models in an epeiric sea: the Upper Ordovician mixed carbonate-siliciclastic Glenwood and Platteville Formations, Wisconsin, USA. In *Carbonate Ramp* (Edited by V.P. Wright and T.P. Burchette), Geological Society, London, Special Publication, 149, 437-456
- Church K. D. and Coe A. L. (2003) Processes controlling relative sea-level change and sediment supply. In *The Sedimentary Record of Sea-Level Changes* (Edited by A.L. Coe), Chapter 5, 99-117, Cambridge University Press. London.
- Claypool G. E. and Mancini A. E. (1989) Geochemical relationship of petroleum in Mesozoic reservoirs to carbonate rocks of Jurassic Smackover Formation, southwest Alabama. *AAPG Bull.* 73, 7, 904-924.
- Corbin J. C., Person A., Iatzioura A., Ferre B. and Renard M. (2000) Manganese in pelagic carbonates: indication of major tectonic events during the geodynamic evolution of a

passive continental margin (the Jurassic European margin of the Tethys-Ligurian Sea). *Palaeogeogr.Palaeoclimatol. Palaeoecol.* 156, 123-138.

- Craig H. (1957) Isotope standards for carbon and oxygen fractionation factors for mass spectrometric analysis of carbon dioxide. *Geochim.Cosmochim.Acta* 12, 133-149.
- Cunningham A. E. (1984) Lithofacies, depositional environment, and diagenesis alteration of the Smackover Formation in the Manila Embayment of southwest Alabama. *Master's thesis*, University of Alabama, 198p.
- Davies G. R. and Krouse H. R. (1975) Carbon and oxygen isotopic composition of late Palaeozoic calcite cements, Canadian Archilelago-preliminary results and interpretation. *Geol. Surv. Can. Paper* 15, 215-220.
- De Rafelis M., Emmanuel L., Renard M., Atrops F. and Jan Du Chene R. (2001) Geochemical characterization (MnO content) of third order eustatic sequences in the upper Jurassic pelagic carbonates of the Vocontian Trough (SE France). *Eclogae Geologicae Helveticae* 94, 145-152.
- Dickinson K. A. (1968) Upper Jurassic stratigraphy of some adjacent parts of Texas, Louisiana and Arkansas, *USGS Professional Paper*, 594E, 25P.
- Dinkins T. H., Oxley M. L., Minihan E. and Ridgeway J. M. (1968) Jurassic stratigraphy of the Mississippi. *Mississippi Geology, Economic and Topographical Survey Bull.* No.109, 77p.
- Dolenec T., Lojen S. and Ramovs A. (2001) The Permian-Triassic boundary in Western Slovenia (Idrijca Valley section): Magnetostratigraphy, stable isotopes, and elemental variations. *Chemical Geology* 175, 175-190.
- Duval B., Cramez C. and Vail P. R. (1992) Types and hierarchy of stratigraphic cycles. Abstract from Sequence Stratigraphic of European Basins Conference, CNRS-IFP, Dijon, France 44-45.
- Edmond J. M., Campbell A. C., Palmer M. R. and German C. R. (1990) Geochemistry of hydrothermal fluids from the Mid-Atlantic Ridge: TAG and MARK 1990. *Eos* 71, 1650-1651.
- Emrich K., Ehhalt D. H. and Vogel J. C. (1970) Carbon isotope fractionation during the precipitation of calcium carbonate. *Earth and Planetary Science Letters* 8, 363-369.
- Epstein S. and Lowenstam H. A. (1953) Temperature-shell-growth relations of recent and interglacial Pleistocene shoal-water biota from Bermuda. *Jour. Geology* 61, 424-438.
- Esposito Jr. A. R. (1987) Stratigraphic analysis and depositional environments of the Smackover Formation in the Conecuh basin, Escambia County, southeastern Alabama. *Master's thesis*, Auburn University, Alabama, 125p.
- Esposito Jr. A. R. and King Jr. D. T. (1987) Facies analysis, sea level history, and platform evolution of the Jurassic Smackover Formation, Conecuh Basin, Escambia, County, Alabama. *Gulf Coast Assoc Trans.* 37, 335-344.

- Ferreri V., Weissert H., Argenio B. D. and Buonocunto F. P. (1997) Carbon isotope stratigraphy: a tool for basin to carbonate platform correlation. *Terra Nova* 9, 57-61.
- Folk R. L. and Land L. S. (1975) Mg/Ca ratio and salinity: two controls over crystallization of dolomite. *AAPG Bull.* 59, 60-68.
- Follmi K. B., Weissert H., Bisping M. and Funk H. P. (1994) Phosphogenesis, carbon isotope stratigraphy, and carbonate platform evolution along the Lower Cretaceous northern Tethyan margin. *Geol. Soc. Am. Bull.* 106, 729-746.
- Frakes L. F., Francis J. E. and Syktus J. I. (1992) *Climate modes of the Phanerozoic*. Cambridge Univ. Press. Cambridge.
- Galimov E. M. and Shirinsky V. G. (1975) Ordered distributions of carbon isotopes in compounds and components of the lipid fraction in organisms. *Geochem. Int.* 12, 157-180.
- Ginsburg R. N. and Schroeder J. H. (1973) Growth and submarine fossilization of algal cup reefs, Bermuda. *Sedimentology* 20, 575-614.
- Given R. K. and Lohmann K. C. (1985) Petrographic and isotopic examination of reef dolomite in the Permian Reef complex, West Texas and New Mexico. *Abstracts with Programs, Geol. Soc. Am.* 17, 593.
- Goni M. A., Ruttenberg K. C. and Eglinton T. I. (1998) A reassessment of the sources and importance of land-derived organic matter in surface sediments from the Gulf of Mexico. *Geochim. Cosmochim. Acta* 62, 3055-3075.
- Gordeev V. V. and Demina L. L. (1979) Direct observation of hydrotherms at the Pacific bottom (Galapagos active zone, Hess depression). *Geokhimija* 6, 902-917.
- Gross M. G. and Tracey J. I. Jr. (1966) Oxygen and carbon isotopic composition of limestones and dolomites, Bikini and Eniwetok atolls. *Science* 151, 1082-1084.
- Hallam A. (1992) *Phanerozoic Sea-Level Changes*. Columbia Univ. Press, New York. 266p.
- Hallam A. (1993) Jurassic climates as inferred from sedimentary and fossil record. *Philos. Trans. R. Soc. London* B341, 287-296.
- Hallam A. (2001) A review of a broad pattern of Jurassic sea-level changes and their possible cause in the light of current knowledge. *Palaeogeogr. Palaeoclimatol. Palaeoecol.* 167, 23-37.
- Haq B. U., Hardenbole J. and Vail P. R. (1988) Mesozoic and Cenozoic chronostratigraphy and cycles of sea level change. In *Sea-level changes - An integrated approach* (Edited by C.K. Wilgus, C.A. Ross, and J.C. Van Wagoner), SEPM Special Publication 42, 71-108.
- Hayes J. M. (1993) Factors controlling  $^{13}\text{C}$  of sedimentary organic compounds: Principles and evidence. *Marine Geology* 113, 111-125.

- Haywick D., Hall-Brown M. B. and Pfeiffer L. (2000) Smackover reservoir diagenesis in the Appleton Field, Escambia County, Alabama. *Gulf Coast Assoc. Trans.* 50, 43-53.
- Heydari E. (2002) Sequence Stratigraphy of the Smackover Formation, northcentral U.S. Gulf Coast. *Abstracts with Programs, Geol. Soc. Am.* 34. 336.
- Heydari E. and Moore C. H. (1994) Paleogeographic and paleoclimate controls on ooid mineralogy of the Smackover Formation, Mississippi Salt Basin: Implications for Late Jurassic sea water composition. *Jour. Sed. Research* A64, 101-114
- Heydari E., Wade W. J. and Anderson L. C. (1995) Depositional environments and accumulation of organic matter in the Smackover Formation in the north-central Gulf of Mexico. *Gulf Coast Assoc. Trans.* 45, 251-258.
- Heydari E., Wade W. J. and Anderson L. C. (1997) Depositional environments, organic carbon accumulation, and solar-forcing cyclicity in Smackover Formation lime-mudstones, Northern Gulf Coast. *AAPG Bull.* 81, 760-774.
- Heydari E. and Wade W. J. (2002) Massive recrystallization of low-Mg calcite at high temperature in hydrocarbon source rocks: Implications for organic acids as factors in diagenesis. *AAPG Bull.* 86, 1285-1303.
- Hillgartner H. (1998) Discontinuity surfaces on a shallow-marine carbonate platform (Berrisian, Valanginian, French and Switzerland). *Jour. Sed. Research* 68, 1098-1108.
- Hirst D. M. (1962a) The geochemistry of modern sediments from the Gulf of Paria; [Part] 1, The location and distribution of trace elements. *Geochim. Cosmochim. Acta* 26, 309-334.
- Hirst D. M. (1962b) The geochemistry of modern sediments from the Gulf of Paria; [Part] 2, The location and distribution of trace elements. *Geochim. Cosmochim. Acta* 26, 1147-1187.
- Hofmann P., Ricken W., Schwark L. and Leythaeuser, D. (2000) Carbon-sulfur-iron relationship and  $\delta^{13}\text{C}$  of organic matter for late Albian sedimentary rocks from the North Atlantic Ocean: paleoceanographic implications. *Palaeogeogr. Palaeoclimatol. Palaeoecol.* 163, 97-113
- Hollerbach A. and Hagemann H. W. (1977) Alteration of non-aromatic hydrocarbons during maturation. *Abstracts with Program, International Congress on Organic Geochemistry* 8, 49.
- Holser T. W. (1997) Geochemical events documented in inorganic carbon isotopes. *Palaeogeogr. Palaeoclimatol. Palaeoecol.* 132, 173-182.
- Homewood P. W. (1996) The carbonate feedback system: interaction between stratigraphic accommodation, ecological succession and the carbonate factory. *Bull. Soc. Geol. France* 167, 701-715
- Humphrey J. D., Ransom K. L. and Matthews R. K. (1986) Early meteoric diagenetic control of Upper Smackover production, Oaks Field, Louisiana. *AAPG Bull.* 70, 70-85.

- Imlay R. W. (1943) Jurassic formations of the Gulf region. *AAPG Bull.* 27, 1407-1533.
- Imlay R. W. and Herman G. (1984) Upper Jurassic ammonites from the subsurface of Texas, Louisiana and Mississippi. In *The Jurassic of the Gulf Rim* (Edited by W.P.S. Ventress, D.G. Bebout, B.F. Perkins, and C.H. Moore), Gulf Coast Section, SEPM Foundation Third Annual Research Conference Proceeding, 149-170.
- Isern A. R., McKenzie J. A. and Feary D. A. (1996) The role of sea-surface temperature as a control on a carbonate platform develop in the Western Coral Sea. *Palaeogeogr. Palaeoclimatol. Palaeoecol.* 124, 247-272.
- Jarvis I., Murphey A. M. and Gale A. S. (2001) Geochemistry of pelagic and hemipelagic carbonates: criteria for identifying systems tracts and sea level change. *Jour. Geol. Soc. London* 158, 685-696.
- Jenkyns H. C. (1988) The early Toarcian (Jurassic) anoxic events: stratigraphic sedimentary, and geochemical evidences. *Am. Jour. Sci.* 228, 101-151.
- Jenkyns H. C. (1996) Relative sea-level change and carbon isotopes: data from the upper Jurassic (Oxfordian) of central and southern Europe. *Terra Nova* 8, 75-85.
- Jenkyns H. C., Gale A. S. and Corfield R. M. (1994) Carbon- and oxygen isotope stratigraphy of the English chalk and Italian Scaglia and its paleoclimatic significance. *Geol. Mag.* 131, 1-34.
- Jenkyns H. C. and Strasser A. (1995) Lower Cretaceous oolites from the Mid-Pacific Mountains (Resolution Guyot, Site 866). Scientific Results, *Proceedings of the Ocean Drilling Program* 143, 111-118.
- Joachimski M. M. and Buggisch W. (1993) Anoxic event in the late Frasnian: causes of Frasnian-Famennian faunal crisis? *Geology* 21, 675-678.
- Jones B. and Desrochers A. (1992) Shallow platform carbonate. In *Facies Models: Response to Sea Level change* (Edited by R.G. Walker and N.P. James), Geol. Soc. Canada, Chapter15, 277-301.
- Jones C. E., Jenkyns H. C., Coe A. L. and Hesselbo S. P. (1994) Sr-isotope variations in Jurassic and Cretaceous seawater. *Geochim. Cosmochim. Acta* 58, 3061-3074.
- Judice P. C. and Mazzullo S. J. (1982) The gray sandstones (Jurassic) in Terryville Field, Louisiana; basinal depositional and exploration model. *Gulf Coast Assoc. Trans.* 32, 23-43.
- Kastner M. (1999) Oceanic minerals; their origin, nature of their environment, and significance. *National Academy of Sciences USA Proceedings* 96, No. 7, 3380-3387.
- Kaufman A. J., Jacobson S. B. and Knoll A. H. (1993) The Vendian record of Sr and C isotopic variations in sea water: implications for tectonic and plaeoclimate. *Earth and Planet Science Letters* 120, 409-430.

- Kaufman A. J. and Knoll A. H. (1995) Neoproterozoic variations in the C-isotopic composition of sea water: stratigraphic and biogeochemical implications. *Precambrian Research* 73, 27-49.
- Kenig F., Hayes J. M., Popp B. N. and Summons R. E. (1994) Isotopic biogeochemistry of the Oxford Clay Formation (Jurassic), UK. *Jour. Geol. Soc. London* 151, 149-173.
- Kiltgord K. D. and Schouten H. (1986) Plate kinematics of the central Atlantic. In *The western North Atlantic Ocean Region. The Geology of North America* (Edited by P.R. Vogt and B.E. Tucholke), 19-55.
- King Jr. D. T. and Hargrove E. G. (1991) Sequence stratigraphy of the Smackover Formation in the northern half of the Manila Embayment, Alabama. *Gulf Coast Assoc. Trans.* 41, 359-363.
- King Jr. D. T. and Moore D. K. (1992) Jurassic Smackover sequence stratigraphy, southern Manila Embayment, Alabama. *Gulf Coast Assoc. Trans.* 42, 503-510.
- Klinkhammer G. P., Elderfield H., Greaves M., Rona P. and Nelson T. (1986) Manganese geochemistry near high temperature events in Mid-Atlantic Ridge rift valley. *Earth Planet Science Letters* 80, 230-240.
- Koepnick R. B., Denison R. E. Burke W. H., Hetherington E. A. and Dahl D. A. (1990) Construction of the Triassic and Jurassic portion of the Phanerozoic curve of sea water  $^{87}\text{Sr}/^{86}\text{Sr}$ . *Chemical Geology* 80, 327-349.
- Kopaska-Merkel D. C. (1994) Oncoids to reefs: rolling stones come to rest in the Smackover Formation. *Gulf Coast Assoc. Trans.* 44, 347-353.
- Kopaska-Merkel D. C. and Mann S. D. (1992) Regional variation in microscopic and megascopic reservoir heterogeneity in the Smackover formation, southwest Alabama. *Gulf Coast Assoc. Trans.* 42, 189-212.
- Krishnaswami S. (1976) Authigenic transition elements in pelagic clays. *Geochim. Cosmochim Acta* 40, 425-434.
- Kump L. R. and Arthur M. A. (1999) Interpreting carbon-isotope excursions: carbonates and organic matter. *Chemical Geology* 161, 181-198.
- Land L. S. (1970) Late Pleistocene diagenesis and dolomitization, northern Jamaica. *Sedimentology* 14, 187-200.
- Land L. S. (1986) Environments of limestone and dolomite diagenesis: some geochemical considerations. In *Studies in Diagenesis* (Edited by Bodine M.W. Jr.), USGS Bulletin, Report 1578, 129-137.
- Lees A. (1975) Possible influences of salinity and temperature on modern shelf carbonate sedimentation. *Marine Geology* 13, 1767-1773.
- Li L., Keller. G., Adatte T. and Stinnesbeck W. (2000) Late Cretaceous sea-level changes in Tunisia: a multi-disciplinary approach. *Jour. Sed. Soc. London* 157, 447-458.

- Lini, A. Weissert, H. and Erba, E. (1992) The Valanginian carbon isotope event: a first episode of greenhouse climate condition during the cretaceous. *Terra Nova* 4, 374-384.
- Llinás J. C. (2002) Carbonate sequence stratigraphy: Influence of paleotopography, eustasy, and tectonic subsidence: Upper Jurassic Smackover Formation, Vocation Field, Manila subbasin (eastern coastal plain), USA. Abstracts with Programs, Geol. Soc. Am. Annual Meeting 2002.
- Lloyd J. M., Ragland P. C., Pagland J. M. and Parker W. C. (1986) Diagenesis of the Jurassic Smackover Formation, Jay Field, Florida. *Gulf Coast Assoc. Trans.* 36, 201-211.
- Lohmann K. C. (1976) Lower Dresbachian (Upper Cambrian) platform-to-basin transition in eastern Nevada and western Utah: *Brigham Young University Geology Studies*, No. 23, 111-122.
- Lohmann K. C. (1988) Geochemical patterns of meteoric diagenetic systems and their application to studies of paleokarst. In *Paleokarst* (Edited by N.P. James and P.W. Choquette), Springer-Verlag, New York, 58-80.
- Loutit T. S., Hardenbol J., Vail P. R. and Baum G. R. (1988) Condensed sections: the key to age dating and correlation of continental margin sequences. In *Sea-level changes - An integrated approach* (Edited by C.K. Wilgus, B.S. Hasting, C.G.St.C. Kendall, H.W. Posamentier, A. Ross and J.C. Van Wagoner), Soc. Econ. Paleontol. Mineral. Spec. Publ. 42, 183-213
- Lyle M., Owen R. M. and Leinen M. (1986) History of hydrothermal sedimentation at the East Pacific Rise, 19°S. *Init. Rep. DSDP* 92, 585-596.
- Mackenzie F. T. and Pigott J. D. (1981) Tectonic controls of Phanerozoic sedimentary rock cycling. *Jour. Geol. Soc.* 138, 183-196.
- Mann M. C. and Thomas W. A. (1968) The ancient Mississippi River. *Gulf Coast Assoc. Trans.* 18, 187-197.
- Mann S. D. and Kopaska-Merkel D. C. (1992) Depositional history of the Smackover-Buckner transition, eastern Mississippi Interior Salt Basin. *Gulf Coast Assoc. Trans.* 42, 245-265.
- Mancini E. A. and Benson D. J. (1980) Regional stratigraphy of Upper Smackover carbonates of southwest Alabama. *Gulf Coast Assoc. Trans.* 30, 151-165.
- Mancini E. A., Tew B. H. and Mink R. M. (1990) Jurassic sequence stratigraphy in the Mississippi Interior Salt Basin of Alabama. *Gulf Coast Assoc. Trans.* 40, 521-529.
- Mancini E. A. and Tew B. H. (1991) Relationships of Paleogene stage and planktonic foraminifera zone boundaries to lithostratigraphic and allostratigraphic contacts in the eastern Gulf Coastal Plain. *Journal of Foraminiferal Research* 21, 48-66.
- Mancini E. A., Tew B. H. and Mink R. M. (1993) Petroleum source rock potential of Mesozoic condensed section deposits of southwest Alabama. In *Source rock in a Sequence*

*Stratigraphic Framework* (Edited by K.B. J. Katz and L.M. Pratt), AAPG Studies in Geology 37, 147-162.

- Markello J. R. and Read J. F. (1981) Carbonate ramp-to-deeper shale shelf transitions of an Upper Cambrian intrashelf basin, Nolichucky Formation, southwest Virginia Appalachians. *Sedimentology* 28, 573-597.
- Margaritz M. and Stemmerik L. (1989) Oscillation of carbon and oxygen isotope compositions of carbonate rocks between evaporative and open marine environments, Upper Permian of East Greenland. *Earth and Planetary Science Letters* 93, 233-240.
- Markland L. A. (1992) Depositional history of the Smackover Formation, Appleton Field, Escambia County, Alabama. *Master's thesis*, University of Alabama, 145p.
- Marshall J. D. (1992) Climatic and oceanographic isotopic signals from the carbonate rock record and their preservation. *Geol. Mag.* 129, 143-160.
- Martin R. G. (1978) Northern and eastern Gulf of Mexico continental margin: stratigraphic and structural framework, In *Framework, facies, and oil-trapping characteristics of the upper continental margin* (Edited by A.H. Bouma, G.T. Moore and J.M. Coleman), AAPG Studies in Geology 7, 21-42.
- Matthews R. K. (1974) A process approach to diagenesis reefs and reefs associated limestones. *Soc. Econ. Paleontologists Mineralogists Spec. Pub.* 18, 234-256.
- McDonald T. J. and Kennicutt M. C. (1992) Fractionation of crude oils by HPLC and quantitative determination of aliphatic and aromatic biological markers by GC-MS with selected ion monitoring. *LC-GC* 10, 935-938
- Meendsen F. C., Moore C. H., Heydari E. and Sassen R. (1987) Jurassic depositional systems and hydrocarbon potential of southeast Mississippi. *Gulf Coast Assoc. Trans.* 37, 161-174.
- Milliam J. D. (1974) *Marine carbonates*. Springer-Verlag, Berlin, 375p
- Moore C. H. (1984) The Upper Jurassic of the Gulf rim: depositional systems, diagenesis, porosity evolution and hydrocarbon production. In *The Jurassic of the Gulf Rim* (Edited by W.P.S. Ventress, D.G. Bebout, B.F. Perkins, and C.H. Moore), Gulf Coast Section, SEPM Foundation Third Annual Research Conference Proceeding, 283-307.
- Moore D. K. (1991) Carbonate depositional environments and facies stratigraphy of the Jurassic Smackover Formation, southwestern portion of the Manila Embayment, southwest Alabama. *Master's thesis*, Auburn University, Alabama, 150p.
- Morse J. W. and Mackenzie F. T. (1990) *Geochemistry of sedimentary carbonates*. Development in sedimentology No. 48, Elsevier, Amsterdam, 707p.
- Murray R. W. and Leinen M. (1996) Scavenged excess aluminum and its relationship to bulk titanium in biogenic sediment from the central Equatorial Pacific Ocean. *Geochim. Cosmochim. Acta* 60, 3869-3878.

- Oglesby T. W. (1976) A model for the distribution of manganese, iron, and magnesium in authigenic calcite and dolomite cements in the upper Smackover in eastern Mississippi. *Master's thesis*, The University of Missouri, Columbia, Missouri, 122p
- Osleger D. (1991) Subtidal carbonate cycles: implications for allocyclic vs. autocyclic controls. *Geology (Boulder)* 19, 917-920.
- Ottman R. D., Keyes P. L. and Ziegler (1973) Jay Field- A Jurassic stratigraphy trap. *Gulf Coast Assoc. Trans.* 23, 146-157.
- Padden M., Weissert H., and De Rafelis M. (2001) Evidence for Late Jurassic methane hydrate release: opening of the Pangean gateway. *Geology* 29, 223-226.
- Pittet B., Strasser A. and Dupraz C. (1995) Plaeoecology, paleoclimatology and cyclostratigraphy of shallow-water carbonate-siliciclastic transitions in the Oxfordian of the Swiss Jura. *IAS-16<sup>th</sup> Regional Meeting of Sedimentology*, Publication ASF, Paris, 23, 225-254.
- Pittet B. and Gorin G. (2000) Distribution of sedimentary organic matter in a mixed carbonate-siliciclastic platform environment: Oxfordian of the Swiss Jura Mountains. *Sedimentology* 44, 915-937.
- Popp B. N., Anderson T. F. and Sandberg P. A. (1986) Brachiopods as indicators of original isotopic compositions of some Paleozoic limestone. *Geol. Soc. Am. Bull.* 97, 1262-1296.
- Popp B. N., Takigiku R., Hayes J. M., Lauda J. W. and Baker E. W. (1989) The post-Paleozoic chronology and mechanism of <sup>13</sup>C depletion in primary organic matter. *Am. Jour. Sci.* 289, 436-454.
- Prather B. E. (1992) Evolution of a Late Jurassic carbonate/evaporite platform, Conecuh embayment, northeastern Gulf Coast, U.S.A. *AAPG Bull.* 71, 164-190.
- Pratt B. R., James N. P. and Cowan C. A. (1992) Peritidal carbonates. In *Facies Models: Response to Sea Level change* (Edited by R.G. Walker and N.P. James), Geol. Soc. Canada, Chapter 16, 303-321.
- Price N. B. and Wright P. L. (1971) The geology of the east Atlantic continental margin; 2, Europe. Report - Natural Environment Research Council, Institute of Geological Sciences 70, 17-31.
- Rachold V. and Brumsack H. (2001) Inorganic geochemistry of Albian sediments from the Lower Saxony Basin NW Germany: paleoenvironmental constraints and orbital cycles. *Palaeogeogr. Palaeoclimatol. Palaeoecol.* 174, 121-143.
- Read J. F. (1980) Carbonate Ramp-to-basin transitions and Foreland basin Evolution, Middle Ordovician, Virginia Appalachians. *AAPG Bull.* 64, 10, 1575-1612
- Read J. F. (1982) Carbonate platforms of passive (extensional) continental margins - types, characteristics and evolution. *Tectonophysics* 81, 195-212
- Read J. F. (1985) Carbonate platform models. *AAPG Bull.* 69, 1-21.

- Reinhardt L. and Ricken W. (2000) The stratigraphic and geochemical record of playa cycles: monitoring a Pangean monsoon-like system (Triassic, Middle Keuper, S. Germany). *Palaeogeogr. Palaeoclimatol. Palaeoecol.* 161, 205-227.
- Renard M. (1986) Pelagic carbonate chemostratigraphy (Sr, Mg,  $^{18}\text{O}$ ,  $^{13}\text{C}$ ). *Marine Micropaleontology* 10, 117-164
- Rhode J. A. and Maxwell G. B. (1993) Jurassic Stratigraphy of the Wiggins Arch, Mississippi. *Gulf Coast Assoc. Trans.* 43, 333-344.
- Riding R. (1983) Cyanoliths (cyanoids): oncoids formed by calcified cyanophytes. In *Coated Grains* (Edited by T.M. Peryt), Springer-Verlag, Berlin., 277-283.
- Riding R. (1996) Long-term changes in marine  $\text{CaCO}_3$  precipitation. *Memoir. Soc. Geol. France* 169, 157-166.
- Saller A. H. and Moore B. R. (1986) Dolomitization in the Smackover Formation, Escambia County, Alabama. *Gulf Coast Assoc. Trans.* 36, 275-282.
- Saltzman M. R., Davidson J.P., Holden P., Runnigar B. and Lohmann K. C. (1995) Sea level changes in ocean chemistry at an Upper Cambrian extinction horizontal. *Geology* 23, 893-896.
- Saltzman M. R., Runnigar B. and Lohmann K. C. (1998) Carbon isotope stratigraphy of sequences Upper Cambrian (Steptoean Stage) of the eastern Great Basin: Record on a global oceanic event. *Geol. Soc. Am. Bull.* 110, 285-297.
- Salvador A. (1987) Late Triassic-Jurassic paleogeography and origin of Gulf of Mexico basin: *AAPG Bull.* 71, 419-451.
- Sarg J. F. (1982) Off-reef Salina deposition (Silurian), southern Michigan Basin: implication of reef genesis. In *Depositional and diagenetic spectra of Evaporites* (Edited by C.R. Handford), Society of Economic Paleontologists Mineralogists Core Workshop, no.3, 354-384.
- Sarg J. F. (1983) Eustatic control of cyclic carbonate-evaporite deposition (Silurian), southern Michigan Basin. *Programs with Abstracts, Geol. Soc. Am. National Meeting*, Indianapolis, 678p.
- Sassen R. and Moore C. H. (1988) Framework of hydrocarbon Generation and destruction in Eastern Smackover Trend. *AAPG Bull.* 72, 6, 648-663.
- Shackleton N. J. (1977) Carbon-13 in *Uvigerina*: tropical rainforest history and the equatorial Pacific carbonate dissolution cycles. In *The Fate of Fossil Fuel  $\text{CO}_2$  in the Oceans* (Edited by N.R. Anderson and A. Malahoff), Plenum Press, New York, 401-427.
- Shackleton N. J. and Pisias N. G. (1985) Atmospheric carbon dioxide, orbital forcing and climate. *Am. Geophys. Union Geophys. Monogr.* 32, 303.

- Scholle P. A. (1977) Diagenesis of Upper Cretaceous Chalks from England, Northern Ireland, and the North Sea . In *Pelagic Sediments: on Land and under the Sea* (Edited by K.J. Hsu and H.C. Jenkyns), Spec. Publ. Inter. Asso. Sedimentologist 1, 177-210.
- Scholle P. A. and Arthur M. A. (1980) Carbon isotope fluctuations in Cretaceous pelagic limestones: potential stratigraphic and petroleum exploration tool. *AAPG Bull.* 64, 67-87.
- Shew R. D. (1991) Upward-shoaling sequence of mixed siliciclastics and carbonates from the Jurassic Smackover Formation from the Jurassic Smackover Formation of central Mississippi. In *Mixed carbonate-siliciclastic sequences* (Edited by A.J. Lomando and P.M. Harris), SEPM Core Workshop No.15, 135-167.
- Sigsby J. R. (1976) Paleoenvironmental analysis of the Big Escambia Creek-Jay-Blackjack Creek field area.. *Gulf Coast Assoc. Trans.* 26, 258-278.
- Spalletti L. A., Franzese J. R., Matheos S. D. and Schwarz E. (2000) Sequence stratigraphy of a tidally dominated carbonate-siliciclastic ramp; the Tithonian-Early Berriasian of the southern Neuquen Basin, Argentina. *Jour. Geol. Soc., London* 157, 433-446.
- Spencer D. W., Degens E. T. and Kulbicki G. (1968) Factors affecting element distributions in sediment. In *Origin and Distribution of the Elements* (Edited by L.H. Ahrens), Int. Ser.Mon. Earth Sci. 30, 981-998.
- Stephens N. P. and Sumner D. Y. (2003) Late Devonian carbon isotope stratigraphy and sea level fluctuations, Canning Basin, Western Australia. *Palaeogeogr. Palaeoclimatol. Palaeoecol.* 191, 203-219.
- Sun S. Q. (1989) A new interpretation of the Corallian (Upper Jurassic) cycles of the Dorset Coast, southern England. *Geological Journal* 24, 139-158.
- Swain F. M. (1949) Upper Jurassic of northeastern Texas. *AAPG Bull.* 33, 1206-1250.
- Swart P. K., Burm S. J. and Leder J. J. (1991) Fractionation of the stable isotopes of oxygen and carbon in carbon dioxide during the reaction of calcite with phosphoric acid as a function of temperature and technique. *Chemical Geology* 86, 89-96.
- Tew B. H., Mink R. M., Mancini E. A., Mann S. D. and Kopaska-Merkel D.C. (1993) Geological framework of the upper Jurassic (Oxfordian) Smackover formation, Alabama and Panhandle Florida coastal water area and adjacent Federal waters area. *Geological Survey of Alabama Bull.* 154, 60p.
- Todd R. G., and Mitchum R. M. Jr., (1977) Seismic stratigraphy and global changes of sea level, part 8: Identification of the upper Triassic, Jurassic and Lower Cretaceous seismic sequence in Gulf of Mexico and offshore west Africa. In *Seismic stratigraphy- Application to hydrocarbon exploration* (Edited by C.E. Playton), AAPG Memoir 26, 145-163.
- Tolson J. S., Copeland C. W. and Bearden B. L. (1983) Stratigraphic profiles of Jurassic strata in the western part of the Alabama Coastal Plain. *Alabama Geological Survey Bull.* 122, 145 p.

- Troell A. R. and Robinson J. D. (1987) Regional stratigraphy of the Smackover Limestone (Jurassic) in south Arkansas and north Louisiana, and the geology of the Chalybeat Springfield oil field. *Gulf Coast Assoc. Trans.* 37, 255-262.
- Tucker M. E. (2001) *Sedimentary Petrology: An introduction to the origin of sedimentary rocks*. Blackwell Scientific Publications, 262p
- Tucker M. E. and Wright V. P. (1990) *Carbonate Sedimentology*. Blackwell Scientific Publications, 482p.
- Tucker M. E., Calvert F. and Hunt D. (1993) Sequence stratigraphy of carbonate ramps: system tracts, models and application to the Muschelkalk carbonate platforms of eastern Spain. In *Sequence stratigraphy and facies association* (Edited by H.W. Posamentier, C.P. Summerhayes, B.U. Haq and G.P. Allen), Assoc. Sedimentol. Spec. Publ. 18, 394-415.
- Turner J. V. (1982) Kinetic fractionation of carbon-13 during calcium carbonate precipitation. *Geochim. Cosmochim. Acta* 46, 1183-1191.
- Urey H. C. Lowenstam H. A., Epstein S. and Mckinney C. R. (1951) Measurement of paleotemperatures and temperatures of the Upper Cretaceous of England, Denmark, and the southeastern of United States. *Bull. Geol. Soc. America* 62, 399-416.
- Vail P. R., Hardenbol J. and Todd R. G. (1984) Jurassic unconformities, chronostratigraphy and sea-level changes from seismic stratigraphy and biostratigraphy. In *The Jurassic of the Gulf Rim* (Edited by W.P.S. Ventress, D.G. Bebout, B.F. Perkins, and C.H. Moore), Gulf Coast Section, SEPM Foundation Third Annual Research Conference Proceeding, 347-364.
- Valladares I., Recio C. and Lendinez A. (1996) Sequence stratigraphy and stable isotopes ( $\delta^{13}\text{C}$ ,  $\delta^{18}\text{O}$ ) of the Late Cretaceous carbonate ramp of the western margin of the Iberian Chain (Soria, Spain). *Sedimentary Geology* 105, 11-28.
- van Wagoner J. C., Posamentier H. W., Mitchum R. M., Vail P. R., Sarg J. F., Loutit T. S. and Hardenbol J. (1988) An overview of the fundamentals of sequence stratigraphy and key definitions. In *Sea-level change: An integrated approach* (Edited by C.K. Wilgus, B.S. Hasting, C.G.St.C. Kendall, H.W. Posamentier, A. Ross and J.C. Van Wagoner), Soc. Econ. Paleontol. Mineral. Spec. Publ. 42, 39-45.
- van Wagoner J. C., Mitchum R. M. Jr., Campion K. M. and Rahmanian V. D. (1990) Siliciclastic Sequence Stratigraphy in well logs, Cores and Outcrop: Concepts for high resolution correlation of time and facies. *AAPG Methods in Exploration series* 7, 55p
- Varenkamp V. C. (1996) Carbon isotope stratigraphy of the upper Kharai and Shuaiba Formations: Implication for the early Cretaceous Evolution of the Arabian Gulf Region. *AAPG Bull.* 80, 5, 647-662.
- Veizer J. and Demovic R. (1974) Strontium as a tool in facies analysis. *Jour. Sed. Petrology* 44, 93-115.
- Veizer J. and Hoefs J. (1976) The nature of  $^{18}\text{O}/^{16}\text{O}$  and  $^{13}\text{C}/^{12}\text{C}$  secular trends in sedimentary carbonate rocks. *Geochim. Cosmochim. Acta* 40, 1387-1395.

- Veizer J., Demovic, R. and Turan, J. (1971) Possible use of strontium in sedimentary carbonate rocks as a paleoenvironmental indicator. *Sed. Geology* 5, 5-22.
- Veizer J. (1983) Chemical diagenesis of carbonates: theory and application of trace element technique. In *Stable Isotopes in Sedimentary Geology* (Edited by M.A. Arthur), SEPM Short Course 10, Chapter 3, 1-100.
- Veizer J., Ada D., Azmy K. and 12 others (1999)  $^{87}\text{Sr}/^{86}\text{Sr}$ ,  $\delta^{13}\text{C}$  and  $\delta^{18}\text{O}$  evolution of the Phanerozoic seawater. *Chemical Geology* 161, 59-88.
- Vinet M. J. (1984) Geochemistry and origin of Smackover and Buckner dolomites ( Upper Jurassic) Jay Field area, Alabama-Florida. In *The Jurassic of the Gulf Rim* (Edited by W.P.S. Ventress, D.G. Bebout, B.F. Perkins, and C.H. Moore), Gulf Coast Section, SEPM Foundation Third Annual Research Conference Proceeding, 365-374.
- Vogel J. C. (1959) Über den isotonen Gehalt des Kohlenstoffs in Süßwasser Kalkablagerungen. *Geochim. Cosmochim. Acta* 16, 236-245
- Von Damm K. L. (1995) Temporal and compositional diversity in seafloor hydrothermal fluids. *Reviews of Geophysics*, 33, II, 1297-1305.
- Wade J. W., Sassen R. and Chinn E. W. (1987) Stratigraphy and source potential of the Smackover Formation in the northern Manila Embayment, southwest Alabama. *Gulf Coast Assoc. Trans.* 37, 277-285.
- Wade W. J. and Moore C. H. (1993) Jurassic sequence stratigraphy of southwest Alabama. *Gulf Coast Assoc. Trans.* 43, 431-443.
- Weissert H. (1989) Carbon isotope stratigraphy, a monitor of paleoenvironmental change: a case study from the Early Cretaceous. *Surveys in Geophysics* 10, 1-61.
- Weissert H. (1990) Siliciclastic in the Early Cretaceous Tethys and Atlantic oceans: Documents of periodic greenhouse climate conditions. *Mem. Soc. Geol. Ital.* 44, 59-69.
- Weissert H. and Lini A. (1991) Ice age interludes during the time of cretaceous greenhouse climate. In *Controversies in modern Geology* (Edited by D.W. Muller, J.A. Mckenzie and H. Weissert), London, Academic press, 173-191.
- Weissert H. and Mohr H. (1996) Late Jurassic climate and its impact on carbon cycling. *Palaeogeogr. Palaeoclimatol. Palaeoecol.* 122, 27-43.
- Weissert H., Lini A., Follmi K. B. and Kuhn O. (1998) Correlation of Early Cretaceous isotope stratigraphy and platform drowning events: a possible link? *Palaeogeogr. Palaeoclimatol. Palaeoecol.* 137, 189-203.
- Weissert H., Mckenzie J. A. and Channell J. E. T. (1985) Natural variations in the carbon cycle during the Early Cretaceous. In *The carbon cycle and Atmospheric CO<sub>2</sub>: Natural Variations Archean to Present* (Edited by E.T.S. Sundquist and W.S. Broecker), Geophys. Monogr. 32, 531-545.

- Wignall P. B. (1991) Model for transgressive black shale? *Geology* 19, 167-170.
- Wilkerson R. P. (1981) Environments of deposition of the Norphlet Formation (Jurassic ) in south Alabama. *Master's thesis*, University of Alabama, 141p.
- Wilson J. L (1975) *Carbonate facies in geologic history*. New York, Springer-Verlag, 471p.
- Wood M. L. and Walper J. L. (1974) The evolution of the interior Mesozoic basin and the Gulf of Mexico. *Gulf Coast Assoc. Trans.* 24, 31-41.

# **APPENDIX A**



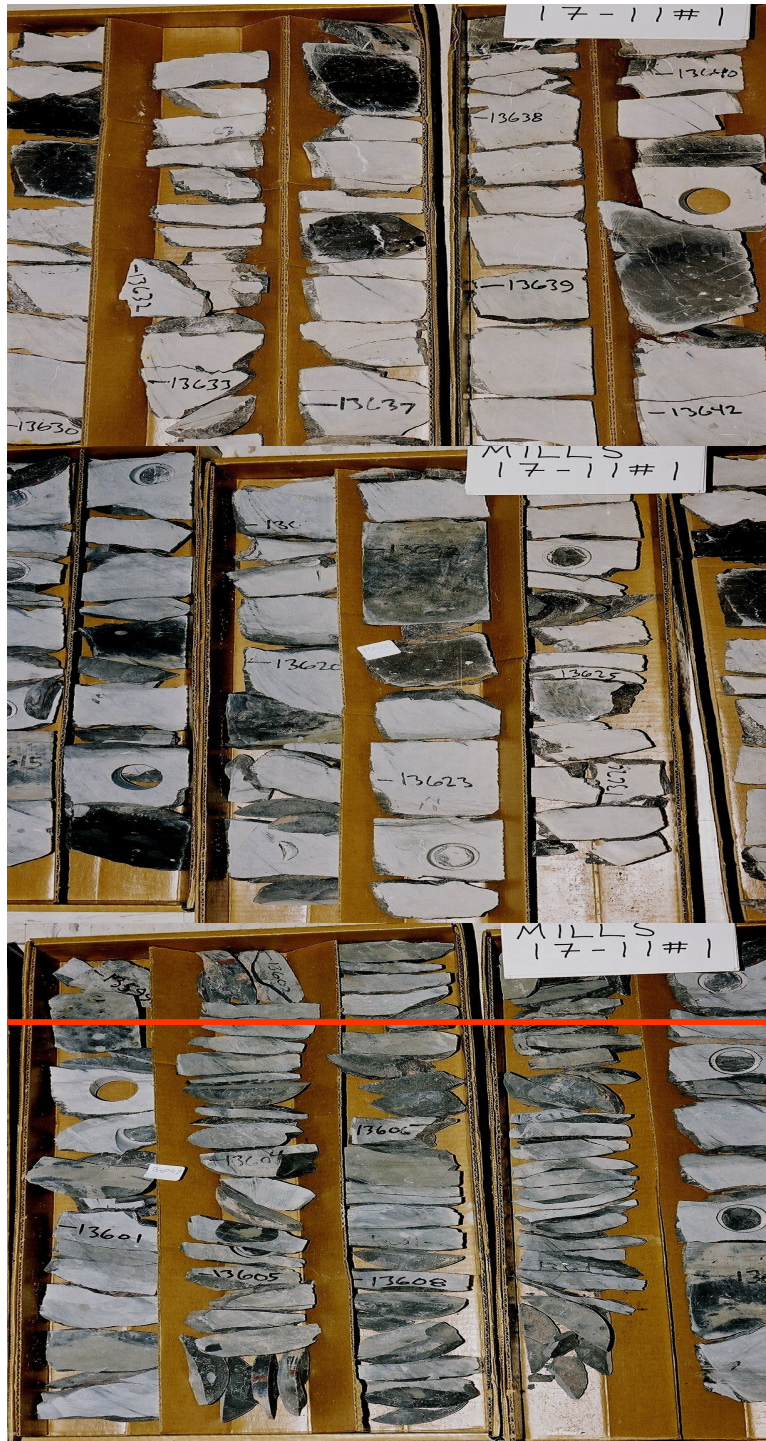
Photographs of core from the T.R. MILLER MILLS 17-11, #1 well of the Conecuh Embayment of depth between **13504-13528 ft** illustrating the Buckner Anhydrite overlying on top of the Smackover Formation at 13510.2 ft .



Photographs of core from the T.R. MILLER MILLS 17-11, #1 well of the Conecuh Embayment of depth between **13528-13560 ft** dominated by oolitic packstones and grainstones facies.



Photographs of core from the T.R. MILLER MILLS 17-11, #1 well of the Conecuh Embayment of depth between **13560-13591 ft** illustrating an upward decreasing of siliciclastic materials. The Smackover sediments changed from mixed mudstone-siliciclastic into more carbonate dominated wacke/packstones and grainstone facies.



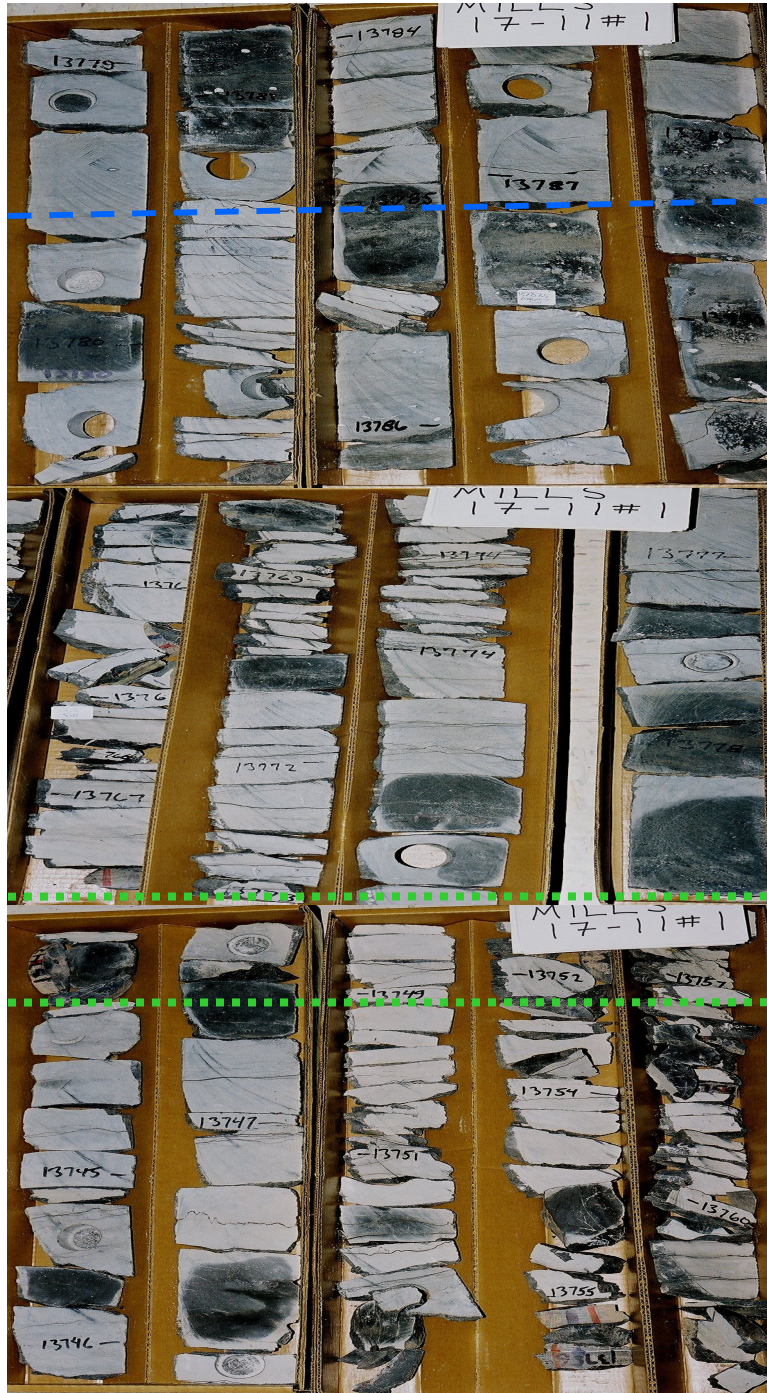
Photographs of core from the T.R. MILLER MILLS 17-11, #1 well of the Conecuh Embayment of depth between 13599- 13642 ft. The upper depth shows interval where Smackover carbonate (mudstone) was mixed with high siliciclastic incoming, the middle shows a transition from the dominated wacke/packestone facies in the lower depth. It is noted that the evaporite/anhydrite nodules were presented before carbonate became mixing with siliciclastic materials which interpreted as a transition from a late highstand deposit into lowstand deposit during falling sea level. The exposure was not occurred, either because the rate of sea level fall was small or the embayment was still deep, or a comonation of both (one photograph of core was missing from 13599 ft to 13591 ft in previous page).



Photographs of core from the T.R. MILLER MILLS 17-11, #1 well of the Conech Embayment of depth between **13646-13685 ft** illustrating an upward decreasing of siliclastic materials. Smackover deposit became dominant of carbonate ranging from mudstone, wackestone to packstone facies.



Photographs of core from the T.R. MILLER MILLS 17-11, #1 well of the Conecuh Embayment of depth between **13685-13740 ft** illustrating an upward increasing of siliciclastic materials.



Photographs of core from the T.R. MILLER MILLS 17-11, #1 well of the Concuah Embayment of depth between **13744-13791 ft** illustrating a shallow marine subtidal carbonate sedimentation dominated by mudstone. It is noted that a condensed interval is observable shown by intercalation of the carbonate mudstone with the dark organic-riched layers (from 13756 -13761 ft). The bottom part illustrated a transition from the organic reef boundstone of the an algal bioherm into normal mudstone which is interpreted as an ensuing of high sea level.



Photographs of core from the T.R. MILLER MILLS 17-11, #1 well of the Conecuh Embayment of depth between 13791- 13825 ft illustrating an upward slight increasing of siliclastic materials and changing from massive carbonate or less dominated cyclic deposit into carbonate of higher sedimentary cycles. The sediments illustrate shallowing upward cycles where the algal boundstones (microreefs) presented in a shallower section (white box) and associated with evaporite/anhydrite nodules. Carbonate sediment from 13805 ft to about 13787 ft (previous) is interpreted to deposit during falling sea level period without subaerial exposure in the Smackover deposition in the Conecuh Embayment or where which this well located. During relative low sea level, higher frequency sea level cycles (fourth- and fifth-cycles) became prominent and superimposed on the third-order sea level cycles.



Photographs of core from the T.R. MILLER MILLS 17-11, #1 well of the Conecuh Embayment of depth between **13824-13862 ft** illustrating the transition from the siliciclastic eolian sandstone of the Norphlet Formation into the carbonate sediments of the Smackover Formation. The presence of small cyclicity, an abundance of algal lamination associated with bioturbation structure and siliciclastic intraclasts suggested a high energy oxic water of the intertidal-subtidal condition instead of a deep anoxic open marine condition. It is noted that core sample was missing at the contact between the Smackover and the Norphlet Formation (13845 ft) which could possibly suggest a sequence boundary if it is assuming due to erosional process during subaerial exposure.

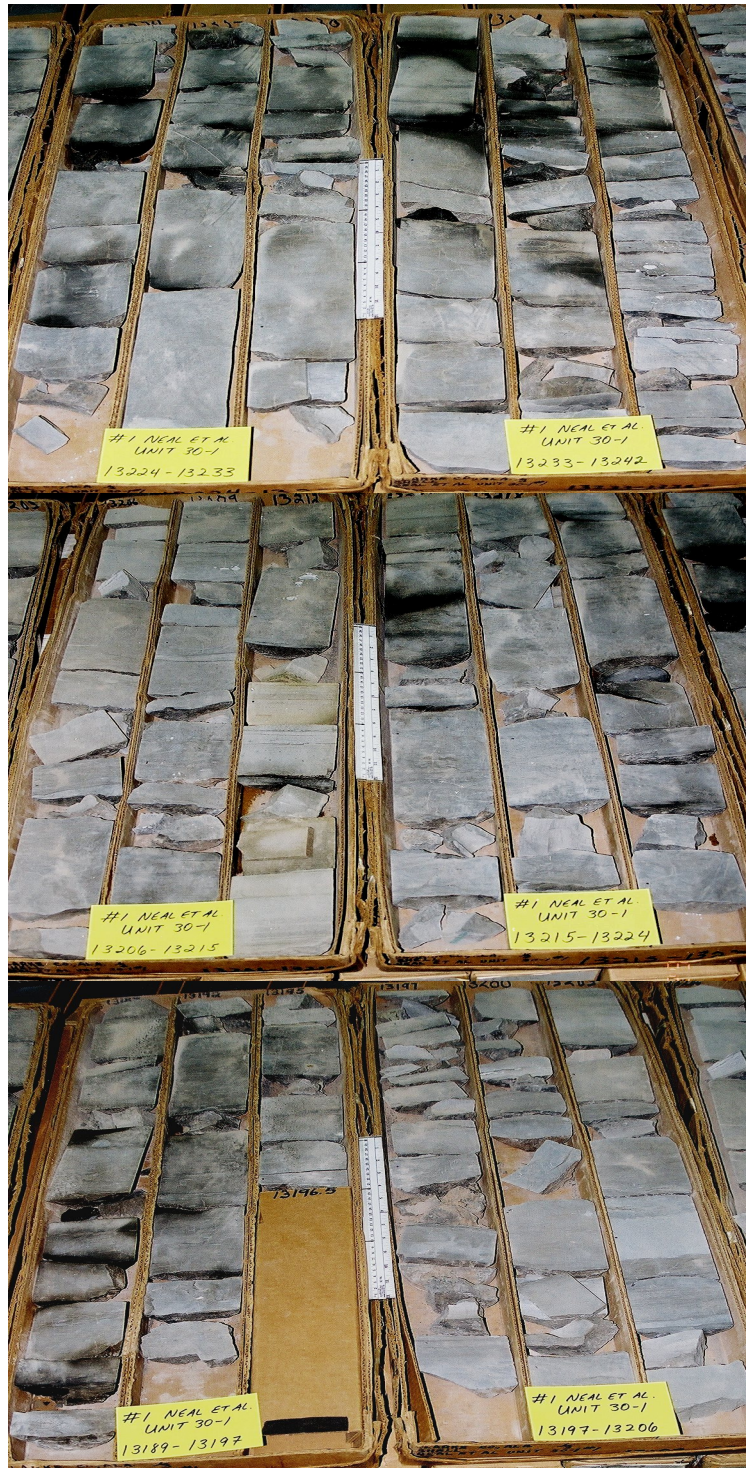
## **APPENDIX B**



Photographs of core from the #1 NEAL ET AL UNIT 30-1 well of the Manila Embayment of depth from **13093 to 13135 ft** illustrating an abrupt transition from the Buckner Member of the Haynesville Formation from mixed carbonate-anhydrite to an underlying dolostone of the Smackover Formation. Note at this boundary contact (13510.2 ft) marked by thin flaser structures associated with carbonate mudstone and dark organic materials.



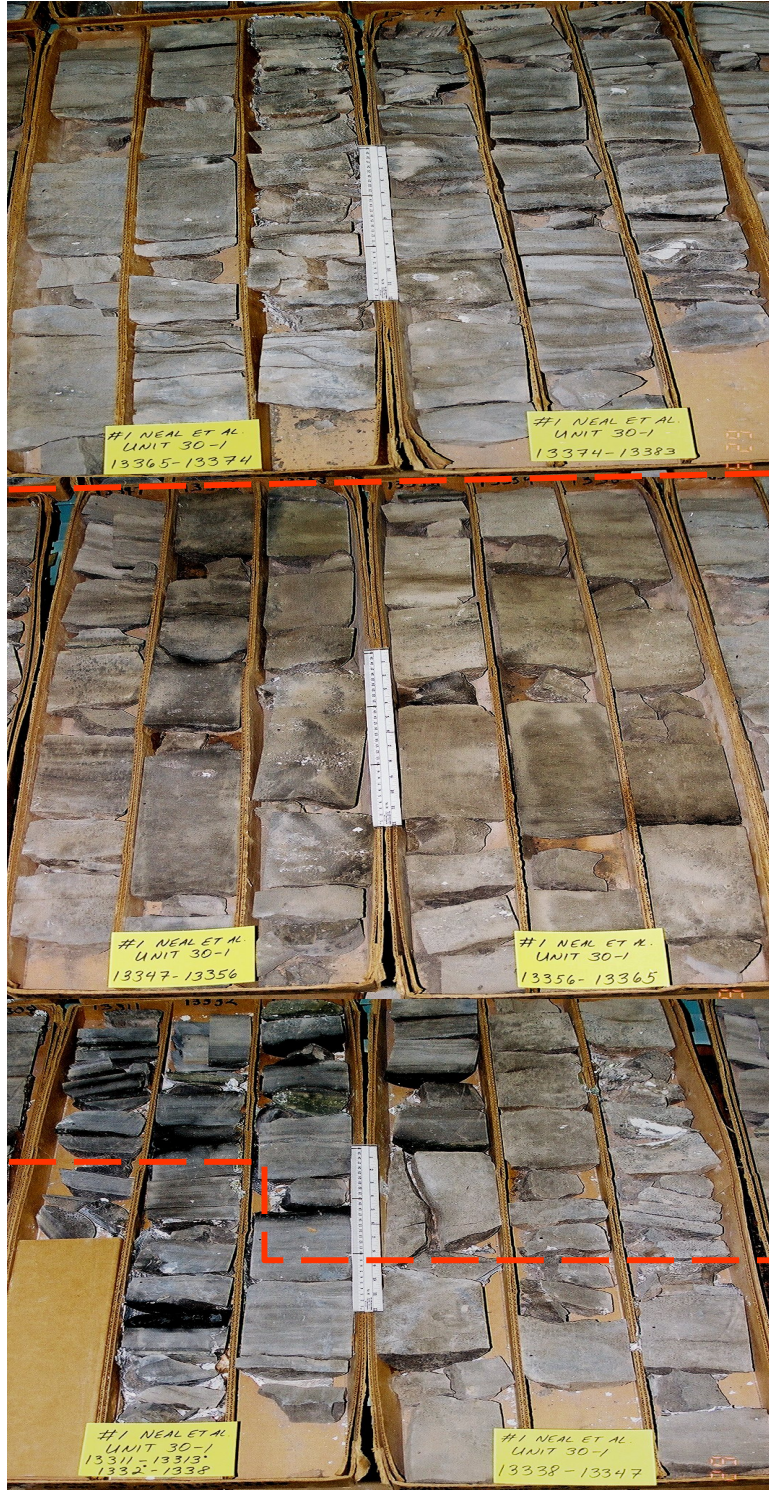
Photographs of core from the #1 NEAL ET AL UNIT 30-1 well of the Manila Embayment of depth from **13135 to 13189 ft** illustrating a mixing of dolomitic carbonate to dolostone with high siliciclastic input and associated with dark organic beds of coal materials. Sedimentary structures are vague and vary from massive to highly bioturbated.



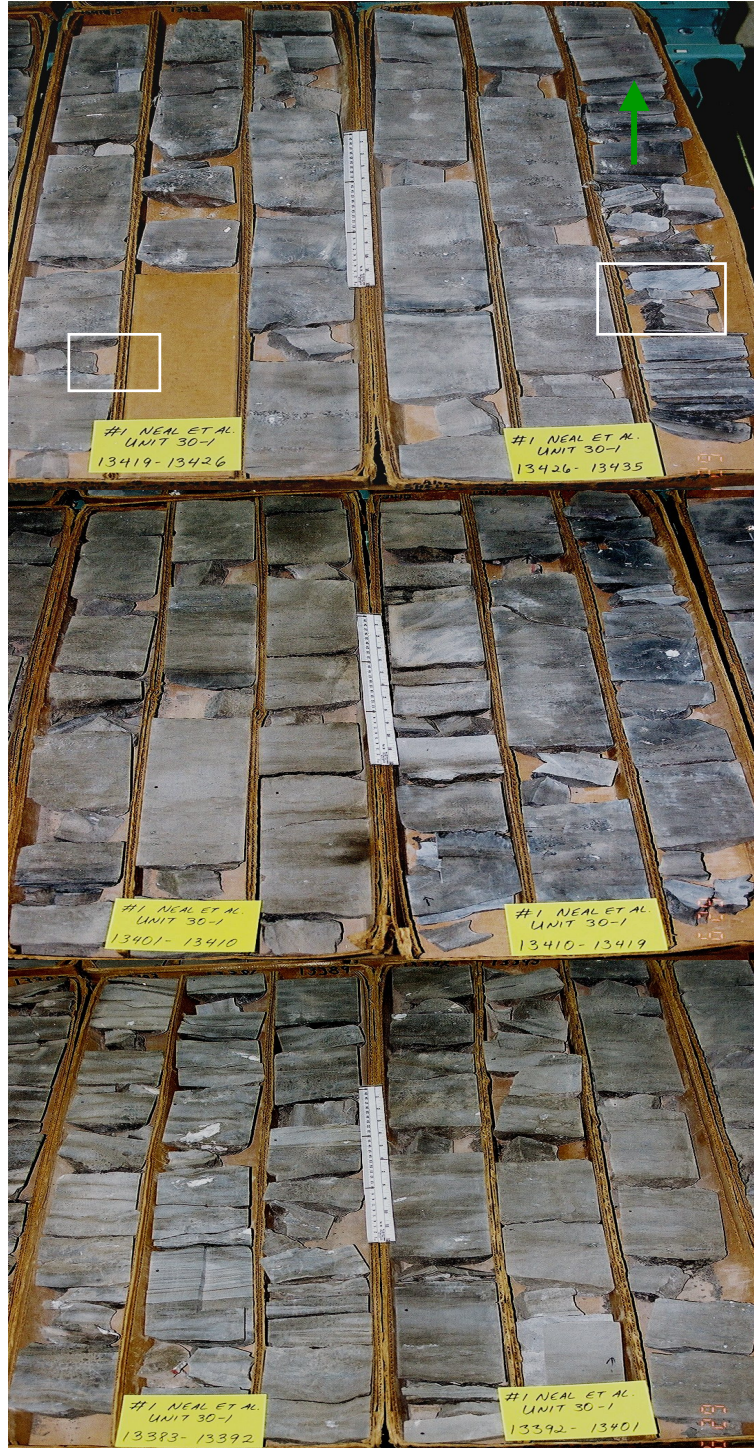
Photographs of core from the #1 NEAL ET AL UNIT 30-1 well of the Manila Embayment of depth from **13189 to 13242 ft** illustrating dolomitized Smackover carbonates becoming interbedded with multiple sandstone beds, which are interpreted as shoreface sand deposits. Sedimentary structures vary from highly dolomitized and bioturbated in carbonates to laminated in the sandstones and abundance of dark and thin organic layers of coal materials with scattered evaporite/anhydrite nodules.



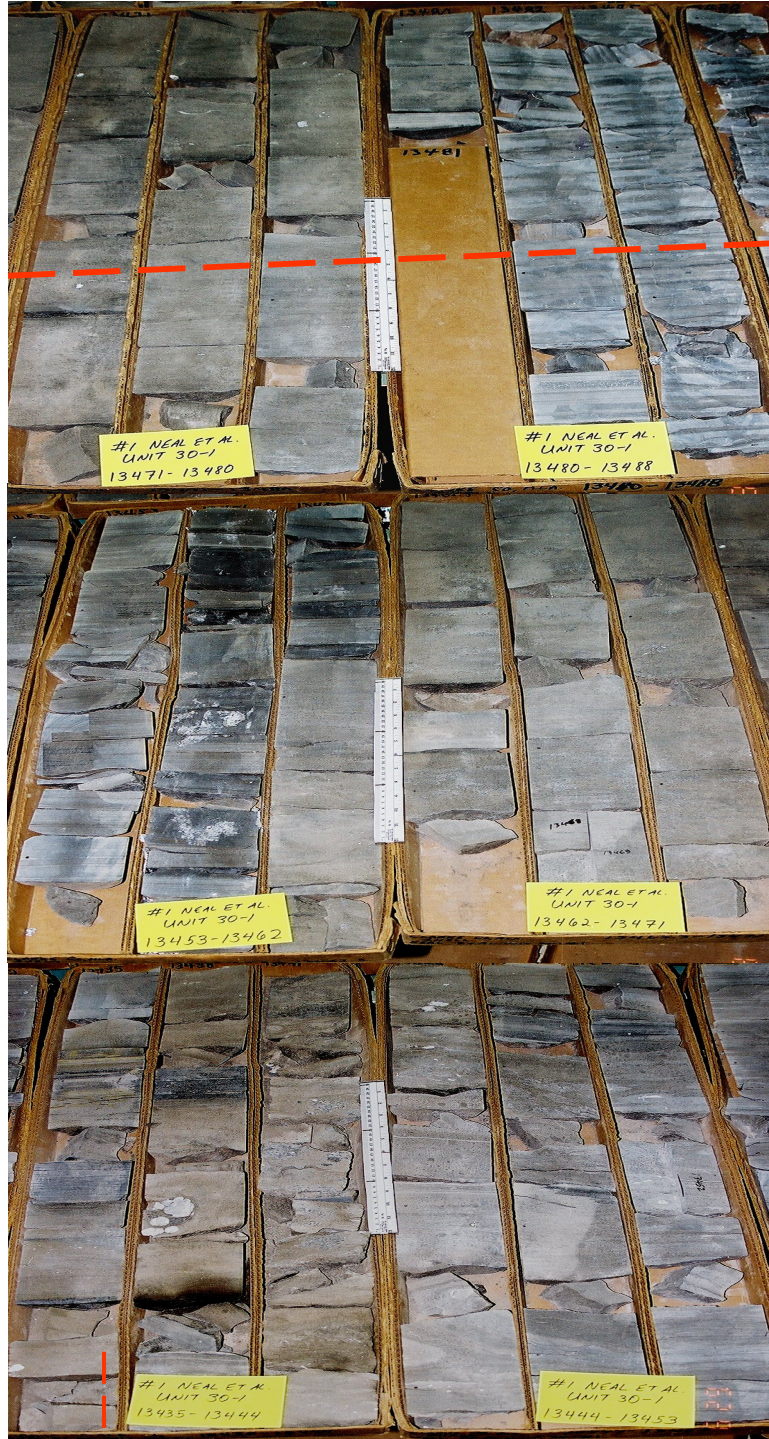
Photographs of core from the #1 NEAL ET AL UNIT 30-1 well of the Manila Embayment of depth from 13242 to 13311 ft illustrating shallowing upward successions from shallow subtidal or lower intertidal to upper intertidal. Sediments are dominated by interbedded mudstone/wackestone to dominated dolomitic bioturbated wackestone facies. Dark organic-rich layers of coals materials are abundant but associated mainly with the wackestone/mudstone facies. Sedimentary structures show abundant evaporite/anhydrite nodules and biogenic structures from organisms showing borings and small burrows filled with evaporites.



Photographs of core from the #1 NEAL ET AL UNIT 30-1 well of the Manila Embayment of depth from 13311 to 13383 ft illustrating a shallowing upward succession dolostones where the shallow sediment on the top of cycle experiencing strong diagenetic alterations of dolomitization and significant evaporite precipitation, interpreted as a subaerial exposure interval occurred during falling sea level.



Photographs of core from the #1 NEAL ET AL UNIT 30-1 well of the Manila Embayment of depth from 13383 to 13435 ft illustrating a peritidal sedimentation interpreted as lower intertidal to upper intertidal carbonates (probably original wackestones) with dolomitized diagenetic alteration. Sedimentary structures of “ribbon rock” became vague and highly alternated but associated with evaporite/anhydrite nodules.



Photographs of core from the #1 NEAL ET AL UNIT 30-1 well of the Manila Embayment of depth from **13435 to 13488 ft** illustrating multi cycles of high frequency shallowing upward succession which are interpreted to express a subarrial exposure during the third-order falling relative sea leve. Dark organic-riched mudstone on a smaller scale variation suggested to a subtidal deposit formed during high frequency sea level cycles which was superimposed by a larger sea level falling cycle.



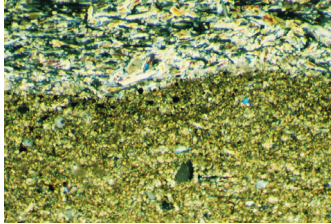
Photographs of core from the #1 NEAL ET AL UNIT 30-1 well of the Manila Embayment of depth from **13488 to 13544 ft** illustrating a carbonate sedimentation predominated by carbonates algal mudstone and wackestone facies. Stable sedimentary structures of “ribbon rock” suggest stable marine water energy subtidal to intertidal with occasionally increased probable by wave current or surging storms.



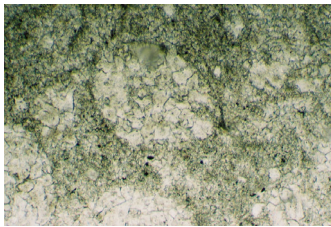
Photographs of core from the #1 NEAL ET AL UNIT 30-1 well of the Manila Embayment of depth from **13144 to 13594 ft** which is the end of the core. Abrupt transition from the reworked marine sandstone of the Norphlet Formation to the Smackover carbonate is occurred at approximate 13557.5 ft (1), and interpreted as a flooding surface on top of the regressive Norphlet sandstone. Rising sea level at the base of the Smackover is showed by dark organic mudstone deposit at about 13554 ft(2). A contact which observed at 13587.5 ft (3) is interpreted as sequence boundary, and time-equivalent to the boundary between the Smackover and Norphlet Formation in the Conecuh Embayment core. Thin carbonate bed of flasers structure (4) is interpreted as the maximum transgression of the Smackover first sea level cycle in the Manila Embayment.

## **APPENDIX C**

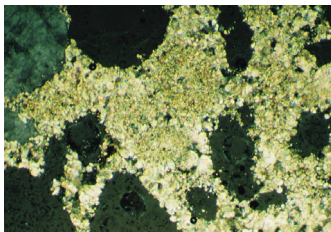
Photomicrographs of thin sections from the T. R. MILLER MILLS17-1, #1 core of the Conecuh Embayment (1)



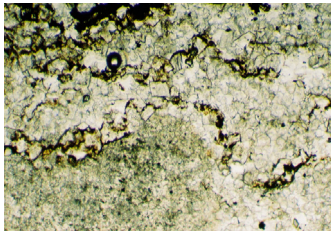
**13505.8 ft** : Interbedded anhydrite and mudstone. *Upper*: fibrous anhydrite, *Lower*: coarse to fine calcilutite, coarse to fine silty quartz dolomicrosparite (10x10; cross nicol)



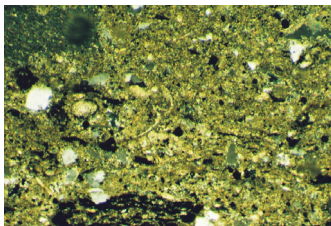
**13516.7 ft** : Dolomitized ooid grains with no porosity. Medium calcarenite: sparse silty quartz, oodolo microsparite (ooid grainstone)(10x10; plane light).



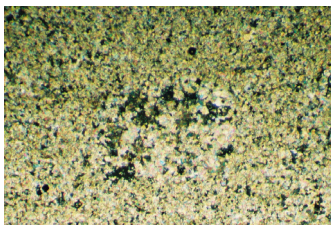
**13526 ft** : Ooid packstone showing pore vugs from dissolution. Medium to fine calcarenite: finely to very finely crystalline, sparse fine sand quartz, peldoloosparite. Most ooid grains are now vugs, but peloids are still Preserved (10x10; cross nicol)



**13555 ft** : Algal lamination showing schizohaline condition during dolomitization. Sparse silty quartz, peloidal (ooid?), blue-green algal, limpid dolomitic Pelbiolithite (10x10; plane light)



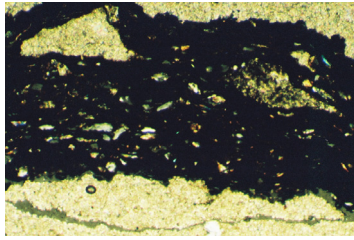
**13600.7 ft** : Mixed siltstone/wackestone showing coarse to fine silty quartz grains, micaceous phyllarenite, pyrite replacement in the *Favreina* pellet, peloid, ostracods and shell fragments (10x10; cross nicol)



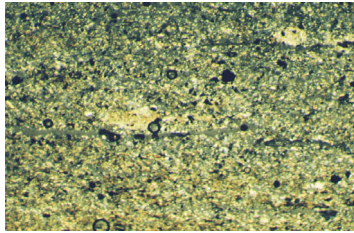
**13622.5 ft** : Wackestone showing sparse peloid that was recrystallized. Micrite shows very finely crystals. Fine to very fine silty quartz are also abundant (10x10; cross

0.5

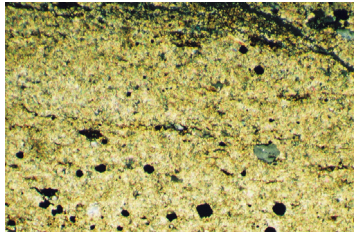
Photomicrographs of thin sections from the T. R. MILLER MILLS 17-11, #1 core of the Conecuh Embayment (2)



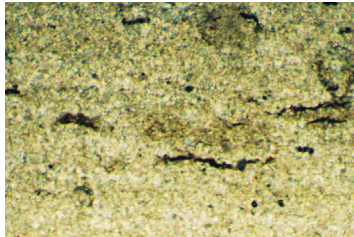
**13646 ft :** Algal laminae in the sparse algal mudstone. Brachiopod shells and abundant medium to fine silty quartz grains, very fine spicules in the algal layers (10x10; cross nicol).



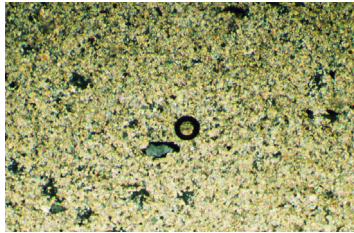
**13703.5 ft :** Mixed claystone/mudstone showing clay partings and pellets (10x10; cross nicol).



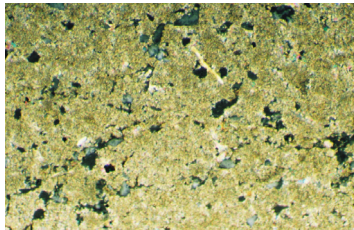
**13712 ft :** Algal boundstone/mudstone with pellets, sparse coarse to fine silty quartz and pyrite (10x10; cross nicol).



**13737 ft :** Mudstone showing intraclast of algal fragments (10x10; cross nicol)



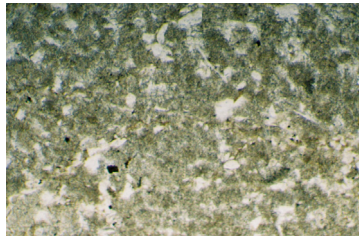
**13765 ft :** Mudstone (finely crystalline) with very sparse medium to fine silty quartz (10x10; cross nicol).



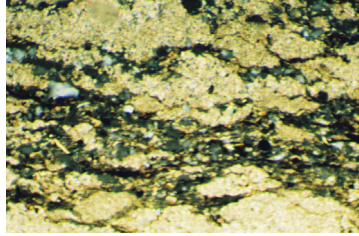
**13787.5 ft :** Pelletoid mudstone with scattered medium to fine silty quartz. Fenestral pores and broken spicules abundant (10x10; cross nicol)

0.5

Photomicrographs of thin sections fromf the T. R. MILLER MILLS 17-11, #1 core of the Conecuh Embayment (3)



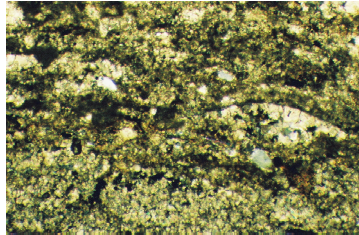
**13787.5 ft** : Pelletoid mudstone showed under plane light (10x10, plane light).



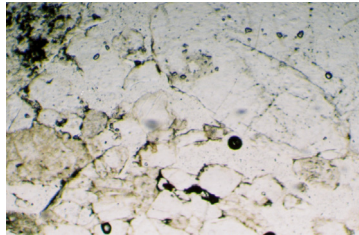
**13804.9 ft** : Algal boundstone/mudstone with abundant medium to fine silty quartz along the layers (10x10; cross nicol).



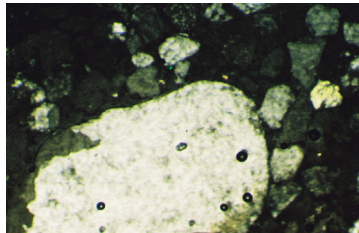
**13843 ft** : Algal layers in the agal laminated mudstone. Abundant and scattered fine silty quartz in the mud which was partially dolomitized under schizohaline (brackish) condition (10x10; cross nicol).



**13845.5 ft** : Algal boundstone showing growth layers. Abundant fossils are dolomitized. Ostracods is Sparsely present as well as scattered fine silty (10x10; cross nicol).



**13847.2 ft** : Sandstone showing submature metamorphic litharenite and small organic materials (10x10) plane light).

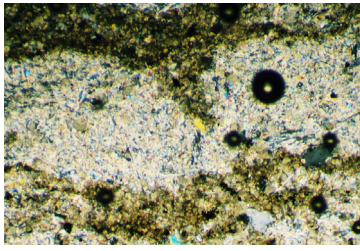


**13856.5 ft** : Sandstone showing well sorted, very fine grains, with submature coarse sand size metamorphic rock fragment and micaceous bearing (10x10; cross nicol)

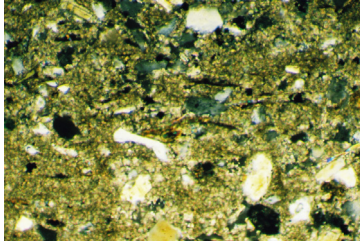
0.5

## **APPENDIX D**

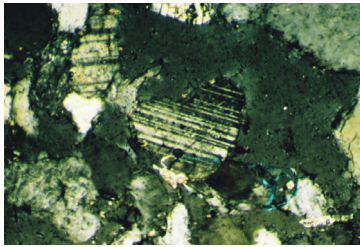
Photomicrographs of thin sections from the #1 NEAL ET AL UNIT 30-1 of the Manila Embayment (1)



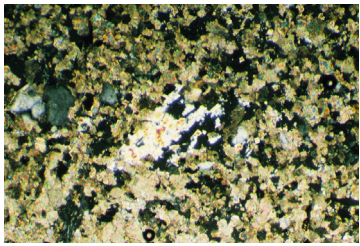
**13114.5 ft** : Nodular anhydrite with intermixed mudstone. Sparse very fine sand size quartz and organic materials are within the micrite (*10x10; cross nicol*).



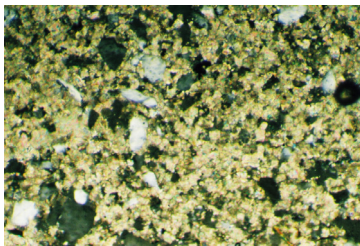
**13130 ft** : Fossiliferous/spiculiferous wackestone with sparse organic materials and abundant coarse to fine silty quartz (*10x10; cross nicol*).



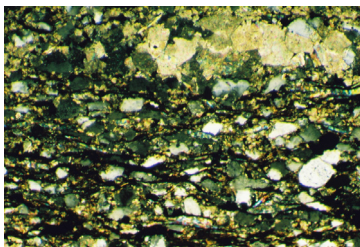
**13143 ft** : Medium sandstone with silica cement and sparse chert metamorphic rock fragments subarkose. Grain contact suggests strong compaction (*10x10; cross nicol*).



**13230 ft** : Dolomitic mudstone with evaporitic ghost Dolospar and coarse to fine silty quartz (*10x10; cross nicol*).



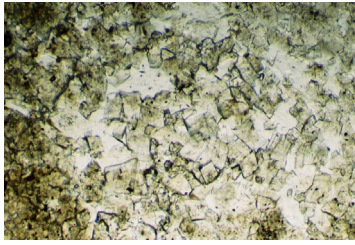
**13275 ft** : Finely crystalline dolosparite (probable originally wackestone) with abundant coarse to fine silty quartz (*10x10; cross nicol*).



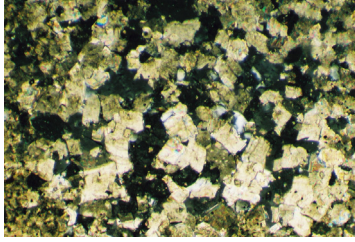
**13302 ft** : Silty dolomitic algal boundstone with mica Flakes and slight mud (*10x10; cross nicol*)

0.5

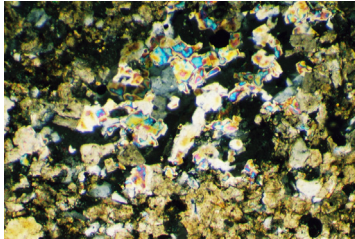
Photomicrographs of thin sections from the #1 NEAL ET AL UNIT 30-1 of the Manila Embayment (2)



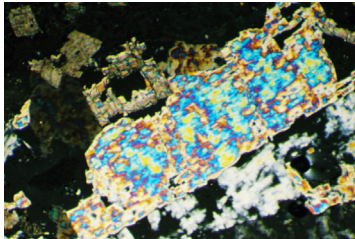
**13345 ft :** Medium crystalline dolosparite (probaple originally wackestone to packstone). Dolomite crystal is called limpid dolomite suggesting schizohaline or



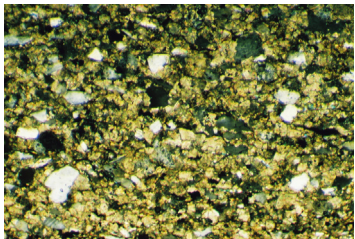
**13345 ft :** Medium crystalline dolosparite similar to above, but under cross nicol (*10x10*).



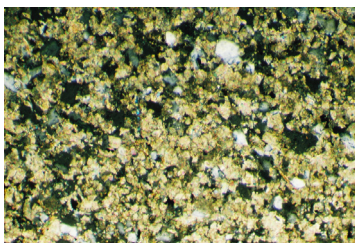
**13354.5 ft :** Medium to fine crystalline anhydritic dolosparite (probaple originally wackestone) with.



**13372.5 ft :** Evaporitic ghost dolospar crystal in a dolosparite (probaple originally wackestone/mudstone)



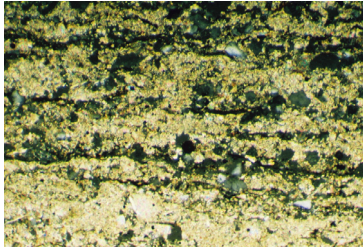
**13388.5 ft :** Dolomitic wackestone with abundant medium to fine silty quartz and small algal fragments



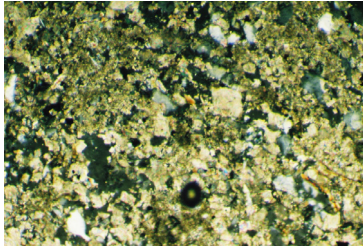
**13407 ft :** Dolomitic wackestone with abundant fine silty quartz and small algal fragments

0.5

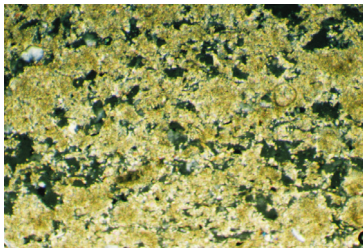
Photomicrographs of thin sections from the #1 NEAL ET AL UNIT 30-1 of the Manila Embayment (3)



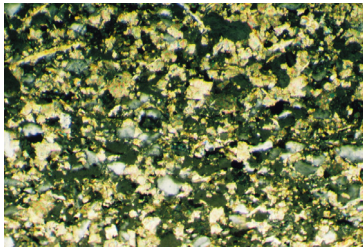
**13434 ft** : Algal boundstone/mudstone with abundant medium to fine silty quartz and some pellet and spicules (*10x10; cross nicol*).



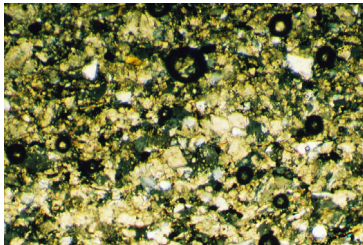
**13443 ft** : Spiculiferous/fossiliferous dolomitic wackestone with abundant medium to fine silty quartz, pellets and organic materials (*10x10; cross nicol*).



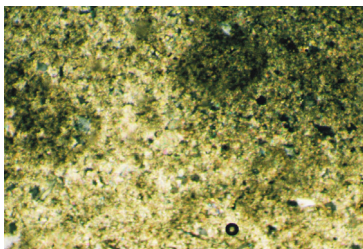
**13460 ft** : Pelloidal mudstone with scattered fine silty quartz and significant fenestral pores (*10x10; cross nicol*).



**13461 ft** : Spiculiferous dolomitic mudstone with high abundant medium to fine silty quartz, spicules and organic materials (*10x10; cross nicol*).



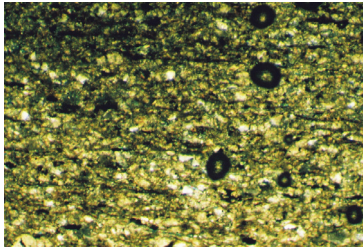
**13472.5 ft** : Spiculiferous dolomitic mudstone with abundant medium to fine silty quartz, spicules and organic materials (*10x10; cross nicol*).



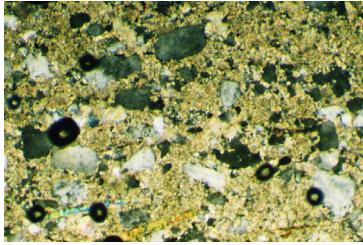
**13492 ft** : Dolomitic peloidal mudstone part in the alternated algal mudstone (ribbon rock), also showing sparse fine to very fine silty quartz and pellets (*10x10; cross nicol*).

0.5

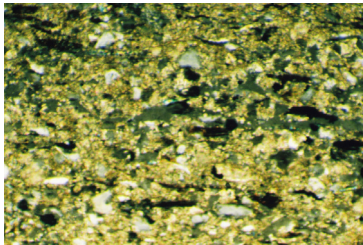
Photomicrographs of thin sections from the #1 NEAL ET AL UNIT 30-1 of the Manila Embayment (4)



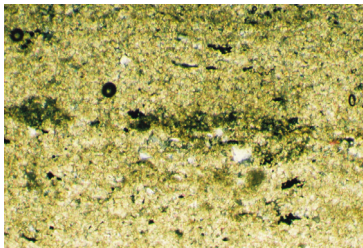
**13515 ft** : Mudstone with abundant spicules, small laminated algal organic materials (*10x10; cross*)



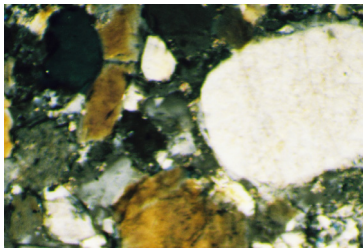
**13516 ft** : Mudstone with abundant fine to very fine sandy and silty quartz and some spicules (*10x10; cross nicol*).



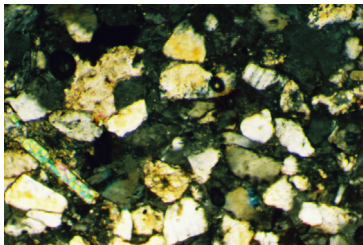
**13532.2 ft** : Spiculiferous mudstone with high abundant medium to fine silty quartz, spicules and organic materials (algal fragments) (*10x10; cross nicol*).



**13554 ft** : Peloidal algal mudstone with sparse fine to very fine silty quartz (*10x10; cross nicol*).



**13558 ft** : Sandstone showing bimodal grain sizes (of coarse sand and fine to very fine sand) with small mica and chert bearing (*10x10; cross nicol*).



**13594 ft** : Sandstone showing submature, moderated sorted grains with mica bearing (*10x10; cross nicol*).

0.5

# **APPENDIX E**

**Table 1.** Measured concentrations of major, minor and trace elements of the Smackover samples from the T.R. MILLER MILLS 17-11, #1 well of the Conecuh Embayment by XRF analysis.

| Depth (ft) | Ca (%) | Al (%) | Ti (%) | Si (%) | Fetotal (%) | K (%) | Mg (%) | Mn (%) | Sr (ppm) | Na (%) | P (%) |
|------------|--------|--------|--------|--------|-------------|-------|--------|--------|----------|--------|-------|
| 13505.8    | 30.384 | 2.356  | 0.117  | 13.442 | 1.306       | 1.811 | 11.862 | 0.082  | 537      | 0.198  | 0.023 |
| 13508.8    | 44.788 | 2.809  | 0.106  | 12.861 | 0.821       | 1.648 | 0.446  | 0.019  | 1589     | 0.285  | 0.029 |
| 13511.5    | 39.895 | 0.440  | 0.016  | 3.495  | 0.430       | 0.404 | 20.676 | 0.098  | 477      | 0.240  | 0.011 |
| 13516.4    | 62.026 | 0.287  | 0.006  | 1.672  | 0.071       | 0.278 | 5.113  | 0.036  | 4092     | 0.076  | 0.014 |
| 13520      | 56.013 | 0.076  | 0.006  | 0.381  | 0.426       | 0.027 | 11.927 | 0.048  | 1934     | 0.138  | 0.008 |
| 13526      | 70.796 | 0.054  | 0.006  | 0.140  | 0.007       | 0.024 | 0.269  | 0.009  | 17778    | 0.098  | 0.011 |
| 13535      | 66.888 | 0.504  | 0.007  | 1.720  | 0.117       | 0.409 | 0.562  | 0.009  | 59524    | 0.105  | 0.017 |
| 13538.5    | 54.346 | 2.016  | 0.072  | 6.803  | 0.452       | 1.770 | 1.491  | 0.015  | 385      | 0.124  | 0.025 |
| 13546.5    | 70.047 | 0.101  | 0.006  | 0.448  | 0.007       | 0.102 | 0.336  | 0.008  | 15734    | 0.094  | 0.011 |
| 13551.8    | 70.902 | 0.052  | 0.006  | 0.117  | 0.007       | 0.027 | 0.227  | 0.008  | 5032     | 0.088  | 0.007 |
| 13553.5    | 66.177 | 0.307  | 0.006  | 1.766  | 0.059       | 0.347 | 1.450  | 0.013  | 7437     | 0.078  | 0.008 |
| 13555      | 66.472 | 0.355  | 0.008  | 1.327  | 0.469       | 0.353 | 1.337  | 0.014  | 2620     | 0.102  | 0.011 |
| 13561.9    | 67.398 | 0.320  | 0.006  | 1.677  | 0.031       | 0.317 | 0.548  | 0.019  | 896      | 0.083  | 0.014 |
| 13562.3    | 67.997 | 0.048  | 0.006  | 0.279  | 0.112       | 0.055 | 2.293  | 0.023  | 1506     | 0.069  | 0.010 |
| 13568      | 55.142 | 1.630  | 0.048  | 7.307  | 0.385       | 1.410 | 0.927  | 0.020  | 1230     | 0.146  | 0.027 |
| 13570      | 66.052 | 0.448  | 0.016  | 1.837  | 0.159       | 0.451 | 1.119  | 0.011  | 10775    | 0.086  | 0.011 |
| 13576.9    | 67.013 | 0.384  | 0.014  | 1.833  | 0.019       | 0.390 | 0.545  | 0.016  | 1003     | 0.089  | 0.012 |
| 13583      | 65.425 | 0.508  | 0.014  | 2.213  | 0.242       | 0.484 | 0.987  | 0.012  | 19979    | 0.099  | 0.016 |
| 13589.5    | 27.755 | 4.749  | 0.199  | 19.748 | 1.576       | 3.464 | 1.663  | 0.035  | 1108     | 0.239  | 0.059 |
| 13600.7    | 23.768 | 5.161  | 0.235  | 21.039 | 2.351       | 3.850 | 1.935  | 0.041  | 781      | 0.226  | 0.060 |
| 13608      | 9.667  | 7.598  | 0.389  | 26.007 | 2.909       | 4.526 | 3.390  | 0.054  | 212      | 0.378  | 0.068 |
| 13618      | 61.234 | 0.856  | 0.020  | 4.395  | 0.595       | 0.858 | 0.710  | 0.022  | 2719     | 0.107  | 0.026 |
| 13620.2    | 53.496 | 1.769  | 0.048  | 7.994  | 0.676       | 1.654 | 0.857  | 0.026  | 1723     | 0.123  | 0.033 |
| 13622.5    | 68.902 | 0.182  | 0.006  | 0.795  | 0.159       | 0.173 | 0.572  | 0.019  | 2001     | 0.090  | 0.011 |
| 13627      | 69.806 | 0.074  | 0.006  | 0.427  | 0.007       | 0.068 | 0.626  | 0.010  | 2000     | 0.089  | 0.008 |
| 13632.9    | 69.366 | 0.101  | 0.006  | 0.687  | 0.007       | 0.104 | 0.597  | 0.029  | 1255     | 0.083  | 0.008 |
| 13640.5    | 68.584 | 0.137  | 0.006  | 0.976  | 0.072       | 0.121 | 0.766  | 0.012  | 2127     | 0.104  | 0.008 |
| 13646      | 67.117 | 0.448  | 0.020  | 1.628  | 0.106       | 0.411 | 0.531  | 0.020  | 1108     | 0.105  | 0.017 |
| 13673.9    | 34.297 | 4.284  | 0.151  | 16.550 | 1.340       | 3.168 | 1.230  | 0.037  | 914      | 0.290  | 0.048 |
| 13681.5    | 19.000 | 6.359  | 0.277  | 22.676 | 2.795       | 3.916 | 1.756  | 0.081  | 755      | 0.504  | 0.065 |
| 13686      | 22.542 | 6.000  | 0.238  | 21.054 | 2.515       | 3.784 | 1.728  | 0.058  | 626      | 0.433  | 0.055 |
| 13698      | 19.922 | 6.322  | 0.261  | 22.218 | 2.755       | 3.814 | 1.751  | 0.062  | 739      | 0.511  | 0.060 |
| 13703.5    | 19.792 | 6.534  | 0.267  | 21.998 | 2.813       | 4.022 | 1.692  | 0.054  | 660      | 0.527  | 0.060 |
| 13706.1    | 59.063 | 1.114  | 0.022  | 5.526  | 0.374       | 0.977 | 0.839  | 0.022  | 965      | 0.165  | 0.027 |
| 13712      | 47.210 | 2.600  | 0.071  | 10.993 | 0.695       | 1.888 | 1.007  | 0.021  | 2026     | 0.295  | 0.029 |
| 13721.9    | 57.635 | 1.251  | 0.051  | 6.286  | 0.424       | 1.000 | 0.788  | 0.038  | 774      | 0.192  | 0.024 |
| 13726.5    | 57.542 | 1.245  | 0.052  | 6.336  | 0.425       | 1.005 | 0.809  | 0.039  | 767      | 0.186  | 0.024 |
| 13730.2    | 47.808 | 2.519  | 0.076  | 10.573 | 0.708       | 2.071 | 0.983  | 0.076  | 685      | 0.234  | 0.036 |
| 13731      | 53.546 | 1.832  | 0.046  | 8.004  | 0.509       | 1.503 | 0.872  | 0.098  | 3097     | 0.198  | 0.027 |
| 13734      | 67.066 | 0.266  | 0.006  | 1.789  | 0.021       | 0.268 | 0.674  | 0.145  | 1230     | 0.097  | 0.019 |
| 13737.5    | 64.318 | 0.637  | 0.007  | 2.709  | 0.157       | 0.629 | 0.923  | 0.203  | 580      | 0.133  | 0.021 |
| 13745.8    | 61.997 | 0.637  | 0.021  | 4.399  | 0.110       | 0.653 | 0.701  | 0.208  | 2208     | 0.152  | 0.013 |
| 13756.8    | 67.869 | 0.221  | 0.006  | 1.241  | 0.007       | 0.231 | 0.711  | 0.261  | 3110     | 0.090  | 0.021 |

| Depth (ft) | Ca (%) | Al (%) | Ti (%) | Si (%) | Fetotal (%) | K (%) | Mg (%) | Mn (%) | Sr (ppm) | Na (%) | P (%) |
|------------|--------|--------|--------|--------|-------------|-------|--------|--------|----------|--------|-------|
| 13765      | 51.169 | 2.065  | 0.056  | 8.861  | 0.517       | 1.899 | 1.026  | 0.298  | 474      | 0.207  | 0.037 |
| 13781.2    | 61.310 | 0.540  | 0.013  | 3.508  | 0.227       | 0.529 | 1.573  | 1.463  | 6566     | 0.135  | 0.016 |
| 13787.5    | 52.873 | 1.499  | 0.063  | 8.342  | 0.461       | 1.341 | 1.039  | 0.706  | 5499     | 0.216  | 0.025 |
| 13793.5    | 25.552 | 4.665  | 0.232  | 20.361 | 1.860       | 3.621 | 1.645  | 0.817  | 638      | 0.493  | 0.046 |
| 13795.5    | 36.550 | 3.575  | 0.123  | 15.272 | 1.267       | 2.885 | 1.302  | 0.965  | 302      | 0.369  | 0.042 |
| 13797.4    | 53.081 | 1.218  | 0.049  | 8.295  | 0.566       | 1.201 | 0.998  | 1.051  | 1434     | 0.215  | 0.031 |
| 13800.5    | 57.903 | 0.789  | 0.022  | 5.680  | 0.470       | 0.801 | 0.842  | 1.587  | 370      | 0.151  | 0.017 |
| 13804.5    | 25.552 | 4.665  | 0.232  | 20.361 | 1.860       | 3.621 | 1.645  | 0.817  | 263      | 0.493  | 0.046 |
| 13811.9    | 48.685 | 1.434  | 0.062  | 7.976  | 0.677       | 1.537 | 3.562  | 2.291  | 366      | 0.210  | 0.030 |
| 13816.2    | 44.478 | 1.114  | 0.056  | 6.552  | 1.131       | 1.254 | 8.339  | 3.336  | 257      | 0.211  | 0.025 |
| 13820.5    | 54.378 | 0.930  | 0.035  | 5.798  | 0.387       | 1.110 | 2.754  | 2.316  | 562      | 0.158  | 0.022 |
| 13826.5    | 52.710 | 1.230  | 0.055  | 8.175  | 0.236       | 1.472 | 1.059  | 1.673  | 1326     | 0.198  | 0.026 |
| 13832      | 48.306 | 1.515  | 0.066  | 9.708  | 0.651       | 1.695 | 2.365  | 1.126  | 251      | 0.216  | 0.024 |
| 13834.5    | 31.295 | 1.452  | 0.086  | 11.953 | 0.682       | 1.596 | 13.085 | 2.098  | 208      | 0.305  | 0.029 |
| 13838      | 43.647 | 2.020  | 0.095  | 12.045 | 0.865       | 2.060 | 2.314  | 0.965  | 242      | 0.264  | 0.029 |
| 13841.5    | 29.972 | 1.576  | 0.097  | 13.243 | 0.835       | 1.841 | 12.267 | 1.901  | 202      | 0.268  | 0.026 |
| 13843      | 35.664 | 1.248  | 0.054  | 7.684  | 0.862       | 1.492 | 14.984 | 2.355  | 120      | 0.205  | 0.025 |
| 13843.5    | 31.676 | 1.733  | 0.101  | 9.856  | 1.091       | 2.036 | 14.369 | 2.297  | 117      | 0.241  | 0.031 |
| 13845.5    | 29.536 | 2.263  | 0.133  | 11.973 | 1.357       | 2.303 | 12.416 | 2.207  | 141      | 0.293  | 0.033 |
| 13847.2    | 0.758  | 4.960  | 0.368  | 37.486 | 0.836       | 2.587 | 1.076  | 0.021  | 165      | 1.926  | 0.033 |
| 13851.5    | 0.715  | 4.765  | 0.291  | 37.555 | 0.937       | 2.375 | 1.614  | 0.024  | 166      | 1.665  | 0.027 |
| 13856.5    | 1.025  | 5.376  | 0.440  | 34.886 | 1.981       | 2.561 | 2.574  | 0.041  | 204      | 2.081  | 0.040 |

**Table 2.** Trace element concentrations of Smackover samples from the #1 T.R. MILLER MILLS 17-11 of the Conecuh Embayment analyzed by XRF.

| Depth (ft) | Ca (%) | Pb (ppm) | Ba (ppm) | Zn (ppm) | Cu (ppm) | Ni (ppm) | Cr (ppm) | V (ppm) | Nb (ppm) | Rb (ppm) | Th (ppm) |
|------------|--------|----------|----------|----------|----------|----------|----------|---------|----------|----------|----------|
| 13505.8    | 30.384 | 5.880    | 50.042   | 10.793   | 98.053   | 15.138   | 13.468   | 19.450  | 2.768    | 25.985   | 0.500    |
| 13508.8    | 44.788 | 6.727    | 35.324   | 6.422    | 49.283   | 15.963   | 13.823   | 16.885  | 1.607    | 23.184   | 0.500    |
| 13511.5    | 39.895 | 2.971    | 27.010   | 2.130    | 6.764    | <2       | 4.164    | 3.197   | 0.821    | 10.043   | 0.500    |
| 13516.4    | 62.026 | 1.630    | 30.419   | <2       | 8.462    | 3.854    | 6.688    | 2.558   | <1       | 4.400    | 0.500    |
| 13520      | 56.013 | 2.530    | 24.583   | 25.432   | 10.506   | <2       | 4.334    | <2      | <1       | 3.907    | 0.500    |
| 13526      | 70.796 | 2.648    | 58.047   | <2       | 7.949    | 10.527   | 6.518    | <2      | <1       | <1       | 0.500    |
| 13535      | 66.888 | 9.198    | 171.816  | 3.691    | <2       | 28.539   | 19.609   | 12.411  | <1       | <1       | 0.500    |
| 13538.5    | 54.346 | 7.320    | 34.601   | 6.671    | 17.378   | 9.913    | 12.637   | 15.482  | 2.002    | 20.359   | 2.165    |
| 13546.5    | 70.047 | 2.870    | 47.822   | <2       | 10.042   | 11.399   | 6.662    | <2      | <1       | 0.919    | 0.500    |
| 13551.8    | 70.902 | <2       | 31.658   | <2       | 10.098   | 3.807    | 3.269    | <2      | <1       | 2.606    | 0.500    |
| 13553.5    | 66.177 | 3.077    | 33.259   | <2       | 9.825    | 8.502    | 3.257    | 1.910   | <1       | 2.054    | 0.500    |
| 13555      | 66.472 | 2.654    | 23.240   | <2       | 12.684   | 8.445    | 5.468    | 3.707   | <1       | 6.602    | 0.500    |
| 13561.9    | 67.398 | <2       | 38.320   | <2       | 11.880   | 6.146    | 2.697    | <2      | <1       | 5.361    | 0.500    |
| 13562.3    | 67.997 | <2       | 20.142   | <2       | 10.982   | <2       | <2       | 2.812   | 0.529    | 2.799    | 0.500    |
| 13568      | 55.142 | 2.754    | 35.583   | 2.004    | 17.339   | 10.892   | 9.950    | 15.800  | 1.569    | 15.920   | 1.868    |
| 13570      | 66.052 | 3.369    | 63.004   | 2.565    | 11.364   | 10.738   | 9.990    | 6.956   | <1       | 2.990    | 0.500    |
| 13576.9    | 67.013 | <2       | 34.240   | <2       | 13.930   | 7.582    | 5.012    | 2.256   | <1       | 5.883    | 0.500    |
| 13583      | 65.425 | 3.576    | 81.131   | 3.066    | 11.853   | 15.277   | 12.434   | 5.039   | <1       | 2.661    | 0.500    |
| 13589.5    | 27.755 | 6.318    | 105.351  | 18.382   | 23.061   | 21.123   | 32.887   | 49.209  | 6.500    | 59.421   | 2.000    |
| 13600.7    | 23.768 | 9.942    | 110.567  | 24.279   | 32.472   | 28.594   | 36.007   | 55.309  | 7.011    | 72.275   | 1.899    |
| 13608      | 9.667  | 3.893    | 218.812  | 36.540   | 38.406   | 33.776   | 57.609   | 102.203 | 11.634   | 114.406  | 9.463    |
| 13618      | 61.234 | 1.894    | 33.362   | 2.523    | 14.155   | 7.926    | 8.447    | 2.286   | 0.937    | 10.868   | 0.500    |
| 13620.2    | 53.496 | 1.973    | 37.390   | 4.333    | 15.274   | 8.400    | 9.591    | 17.156  | 1.689    | 20.506   | 0.500    |
| 13622.5    | 68.902 | <2       | 25.358   | <2       | 12.488   | 5.287    | 4.619    | <2      | <1       | 4.025    | 0.500    |
| 13627      | 69.806 | <2       | 13.738   | <2       | 10.546   | 3.664    | 4.123    | <2      | <1       | 2.709    | 0.500    |
| 13632.9    | 69.366 | <2       | 12.912   | <2       | 9.573    | 5.341    | 3.339    | <2      | <1       | 2.989    | 0.500    |
| 13640.5    | 68.584 | <2       | 18.748   | <2       | 12.477   | 6.645    | 3.666    | 3.684   | <1       | 3.470    | 0.500    |
| 13646      | 67.117 | 2.099    | 13.480   | 6.685    | 13.490   | 8.430    | 5.366    | <2      | 0.858    | 6.497    | 0.500    |
| 13673.9    | 34.297 | 5.185    | 87.689   | 14.565   | 25.085   | 23.947   | 27.612   | 38.815  | 4.967    | 52.242   | 3.427    |
| 13681.5    | 19.000 | 9.062    | 155.858  | 33.851   | 37.599   | 33.562   | 46.996   | 75.131  | 8.753    | 84.445   | 5.101    |
| 13686      | 22.542 | 6.635    | 119.760  | 28.106   | 33.509   | 36.253   | 41.731   | 64.128  | 7.138    | 74.935   | 5.342    |
| 13698      | 19.922 | 6.480    | 144.083  | 25.755   | 34.280   | 33.020   | 46.230   | 78.549  | 7.915    | 82.247   | 4.278    |
| 13703.5    | 19.792 | 7.961    | 134.426  | 31.392   | 36.817   | 34.536   | 49.231   | 74.970  | 7.919    | 85.759   | 5.629    |
| 13706.1    | 59.063 | 2.128    | 30.109   | 2.026    | 13.254   | 8.311    | 6.338    | 9.543   | 1.301    | 13.541   | 0.500    |
| 13712      | 47.210 | 3.257    | 56.911   | 17.315   | 18.880   | 16.477   | 15.399   | 29.123  | 0.829    | 22.981   | 3.709    |
| 13721.9    | 57.635 | 3.177    | 33.259   | 2.941    | 16.310   | 12.143   | 9.842    | 14.225  | 1.317    | 12.709   | 0.500    |
| 13726.5    | 57.542 | 1.923    | 34.963   | 4.174    | 16.035   | 13.919   | 11.337   | 16.831  | 1.606    | 13.399   | 1.569    |
| 13730.2    | 47.808 | 4.133    | 46.995   | 10.881   | 18.314   | 19.048   | 16.060   | 24.771  | 3.075    | 26.784   | 1.991    |
| 13731      | 53.546 | 3.248    | 78.807   | 7.306    | 16.813   | 15.409   | 12.307   | 19.772  | 0.780    | 17.446   | 1.635    |
| 13734      | 67.066 | <2       | 42.967   | <2       | 11.889   | 5.403    | 5.333    | 3.086   | <1       | 3.611    | 0.500    |
| 13737.5    | 64.318 | <2       | 21.433   | 2.536    | 13.435   | 6.339    | 6.302    | 5.507   | 1.067    | 8.329    | 0.500    |
| 13745.8    | 61.997 | <2       | 34.601   | <2       | 11.761   | 8.369    | 6.358    | <2      | <1       | 7.400    | 0.500    |
| 13756.8    | 67.869 | 1.724    | 57.995   | <2       | 10.338   | 6.376    | 4.537    | 3.812   | <1       | 4.641    | 0.500    |

| Depth<br>(ft) | Ca<br>(%) | Pb<br>(ppm) | Ba<br>(ppm) | Zn<br>(ppm) | Cu<br>(ppm) | Ni<br>(ppm) | Cr<br>(ppm) | V<br>(ppm) | Nb<br>(ppm) | Rb<br>(ppm) | Th<br>(ppm) |
|---------------|-----------|-------------|-------------|-------------|-------------|-------------|-------------|------------|-------------|-------------|-------------|
| 13765         | 51.169    | 2.602       | 36.151      | 7.150       | 16.586      | 15.316      | 11.120      | 18.389     | 2.292       | 22.433      | 2.434       |
| 13781.2       | 61.310    | 2.831       | 459.269     | <2          | 10.290      | 15.325      | 7.996       | 12.820     | <1          | 5.522       | 0.500       |
| 13787.5       | 52.873    | 4.703       | 198.102     | 5.171       | 14.350      | 35.137      | 11.950      | 12.515     | <1          | 10.349      | 0.500       |
| 13793.5       | 25.552    | 5.474       | 72.403      | 8.084       | 18.096      | 23.219      | 15.133      | 35.735     | 2.656       | 17.590      | 2.865       |
| 13795.5       | 36.550    | 16.557      | 74.004      | 13.257      | 25.875      | 27.970      | 22.138      | 73.288     | 3.782       | 42.226      | 3.390       |
| 13797.4       | 53.081    | 6.526       | 83.765      | 2.321       | 14.502      | 24.197      | 10.873      | 10.177     | 0.576       | 13.938      | 0.500       |
| 13800.5       | 57.903    | 6.703       | 27.475      | <2          | 14.840      | 13.305      | 5.499       | 12.652     | 1.492       | 9.513       | 0.500       |
| 13804.5       | 25.552    | 30.728      | 130.553     | 22.396      | 35.973      | 45.933      | 41.016      | 143.582    | 7.576       | 60.483      | 2.256       |
| 13811.9       | 48.685    | 13.397      | 43.484      | 8.216       | 15.053      | 24.517      | 12.078      | 31.894     | 2.792       | 16.608      | 0.500       |
| 13816.2       | 44.478    | 12.802      | 43.897      | 36.243      | 12.065      | 26.577      | 11.685      | 17.536     | 2.317       | 14.238      | 0.500       |
| 13820.5       | 54.378    | 4.749       | 49.629      | <2          | 13.168      | 14.155      | 9.856       | 11.702     | 1.589       | 11.663      | 0.500       |
| 13826.5       | 52.710    | 2.780       | 136.853     | 117.276     | 12.901      | 12.475      | 12.078      | 15.989     | 2.489       | 14.960      | 0.500       |
| 13832         | 48.306    | 21.125      | 45.343      | 3.969       | 15.066      | 15.425      | 9.682       | 25.083     | 2.131       | 20.242      | 2.866       |
| 13834.5       | 31.295    | 4.574       | 53.606      | 4.771       | 8.421       | 9.665       | 10.135      | 10.936     | 2.295       | 21.141      | 0.500       |
| 13838         | 43.647    | 22.030      | 58.357      | 6.811       | 18.334      | 24.353      | 13.861      | 41.361     | 3.576       | 25.943      | 0.500       |
| 13841.5       | 29.972    | 15.757      | 60.319      | 5.704       | 15.108      | 20.729      | 12.730      | 17.114     | 3.053       | 25.262      | 1.662       |
| 13843         | 35.664    | 11.654      | 38.733      | 3.017       | 38.044      | 12.056      | 9.334       | 11.338     | 2.655       | 16.572      | 0.500       |
| 13843.5       | 31.676    | 17.842      | 68.169      | 8.834       | 32.334      | 16.840      | 13.874      | 16.901     | 3.529       | 25.992      | 0.500       |
| 13845.5       | 29.536    | 24.142      | 88.258      | 8.016       | 35.201      | 24.716      | 17.531      | 25.271     | 3.906       | 27.488      | 2.877       |
| 13847.2       | 0.758     | 3.271       | 320.242     | 10.572      | 9.265       | 7.143       | 34.334      | 60.271     | 10.389      | 58.956      | 5.423       |
| 13851.5       | 0.715     | 3.949       | 302.734     | 10.170      | 7.539       | 7.942       | 22.383      | 46.674     | 8.544       | 59.427      | 3.137       |
| 13856.5       | 1.025     | 4.905       | 304.232     | 16.614      | 8.904       | 12.679      | 37.016      | 78.536     | 9.132       | 59.942      | 4.911       |

**Table 3.** Major, minor and trace elements of the Smackover from T.R. MILLER MILLS 17-11, #1 of the Conecuh Embayment normalized with respect to Al.

| Depth (ft) | Ca/Ca+Al | Ti/Ti+Al | Si/Si+Al | Fe/Fe+Al | K/K+Al | Na/Na+Al | P/P+Al | Sr/Sr+Al | Mn/Mn+Al (x100) | Mn/Mn+Ca (x1000) | Mg/Ca |
|------------|----------|----------|----------|----------|--------|----------|--------|----------|-----------------|------------------|-------|
| 13505.8    | 0.928    | 0.047    | 0.851    | 0.357    | 0.435  | 0.078    | 0.010  | 3.356    | 3.370           | 2.697            | 0.390 |
| 13508.8    | 0.941    | 0.036    | 0.821    | 0.226    | 0.370  | 0.092    | 0.010  | 3.809    | 0.656           | 0.414            | 0.010 |
| 13511.5    | 0.989    | 0.034    | 0.888    | 0.494    | 0.479  | 0.353    | 0.024  | 1.440    | 18.281          | 2.459            | 0.518 |
| 13516.4    | 0.995    | 0.021    | 0.854    | 0.198    | 0.492  | 0.208    | 0.046  | 1.287    | 11.039          | 0.574            | 0.082 |
| 13520      | 0.999    | 0.071    | 0.834    | 0.848    | 0.264  | 0.644    | 0.091  | 1.076    | 38.526          | 0.851            | 0.213 |
| 13526      | 0.999    | 0.102    | 0.722    | 0.120    | 0.312  | 0.646    | 0.165  | 1.054    | 14.381          | 0.127            | 0.004 |
| 13535      | 0.993    | 0.013    | 0.773    | 0.189    | 0.448  | 0.173    | 0.032  | 1.504    | 1.809           | 0.139            | 0.008 |
| 13538.5    | 0.964    | 0.035    | 0.771    | 0.183    | 0.467  | 0.058    | 0.012  | 3.016    | 0.738           | 0.276            | 0.027 |
| 13546.5    | 0.999    | 0.056    | 0.816    | 0.067    | 0.504  | 0.482    | 0.100  | 1.101    | 7.228           | 0.112            | 0.005 |
| 13551.8    | 0.999    | 0.102    | 0.694    | 0.120    | 0.346  | 0.630    | 0.115  | 1.052    | 12.765          | 0.107            | 0.003 |
| 13553.5    | 0.995    | 0.018    | 0.852    | 0.161    | 0.530  | 0.203    | 0.026  | 1.307    | 4.144           | 0.201            | 0.022 |
| 13555      | 0.995    | 0.021    | 0.789    | 0.569    | 0.498  | 0.223    | 0.029  | 1.355    | 3.725           | 0.207            | 0.020 |
| 13561.9    | 0.995    | 0.017    | 0.840    | 0.089    | 0.498  | 0.206    | 0.043  | 1.320    | 5.699           | 0.287            | 0.008 |
| 13562.3    | 0.999    | 0.108    | 0.852    | 0.699    | 0.532  | 0.588    | 0.173  | 1.048    | 31.711          | 0.331            | 0.034 |
| 13568      | 0.971    | 0.029    | 0.818    | 0.191    | 0.464  | 0.082    | 0.016  | 2.630    | 1.237           | 0.370            | 0.017 |
| 13570      | 0.993    | 0.034    | 0.804    | 0.262    | 0.502  | 0.161    | 0.024  | 1.448    | 2.474           | 0.172            | 0.017 |
| 13576.9    | 0.994    | 0.034    | 0.827    | 0.047    | 0.504  | 0.187    | 0.031  | 1.384    | 4.010           | 0.239            | 0.008 |
| 13583      | 0.992    | 0.026    | 0.813    | 0.322    | 0.488  | 0.163    | 0.030  | 1.508    | 2.391           | 0.190            | 0.015 |
| 13589.5    | 0.854    | 0.040    | 0.806    | 0.249    | 0.422  | 0.048    | 0.012  | 5.749    | 0.741           | 1.276            | 0.060 |
| 13600.7    | 0.822    | 0.043    | 0.803    | 0.313    | 0.427  | 0.042    | 0.011  | 6.161    | 0.788           | 1.723            | 0.081 |
| 13608      | 0.560    | 0.049    | 0.774    | 0.277    | 0.373  | 0.047    | 0.009  | 8.598    | 0.711           | 5.596            | 0.351 |
| 13618      | 0.986    | 0.023    | 0.837    | 0.410    | 0.500  | 0.111    | 0.030  | 1.856    | 2.558           | 0.367            | 0.012 |
| 13620.2    | 0.968    | 0.026    | 0.819    | 0.276    | 0.483  | 0.065    | 0.019  | 2.769    | 1.433           | 0.480            | 0.016 |
| 13622.5    | 0.997    | 0.031    | 0.814    | 0.466    | 0.487  | 0.330    | 0.055  | 1.182    | 9.274           | 0.270            | 0.008 |
| 13627      | 0.999    | 0.072    | 0.852    | 0.086    | 0.479  | 0.547    | 0.100  | 1.074    | 11.938          | 0.144            | 0.009 |
| 13632.9    | 0.999    | 0.054    | 0.872    | 0.065    | 0.507  | 0.451    | 0.071  | 1.101    | 22.228          | 0.416            | 0.009 |
| 13640.5    | 0.998    | 0.040    | 0.877    | 0.347    | 0.469  | 0.432    | 0.058  | 1.137    | 7.994           | 0.173            | 0.011 |
| 13646      | 0.993    | 0.042    | 0.784    | 0.191    | 0.479  | 0.189    | 0.038  | 1.448    | 4.295           | 0.299            | 0.008 |
| 13673.9    | 0.889    | 0.034    | 0.794    | 0.238    | 0.425  | 0.063    | 0.011  | 5.284    | 0.865           | 1.088            | 0.036 |
| 13681.5    | 0.749    | 0.042    | 0.781    | 0.305    | 0.381  | 0.073    | 0.010  | 7.359    | 1.252           | 4.225            | 0.092 |
| 13686      | 0.790    | 0.038    | 0.778    | 0.295    | 0.387  | 0.067    | 0.009  | 7.000    | 0.951           | 2.549            | 0.077 |
| 13698      | 0.759    | 0.040    | 0.778    | 0.304    | 0.376  | 0.075    | 0.009  | 7.322    | 0.977           | 3.120            | 0.088 |
| 13703.5    | 0.752    | 0.039    | 0.771    | 0.301    | 0.381  | 0.075    | 0.009  | 7.534    | 0.815           | 2.704            | 0.085 |
| 13706.1    | 0.981    | 0.020    | 0.832    | 0.251    | 0.467  | 0.129    | 0.023  | 2.114    | 1.896           | 0.364            | 0.014 |
| 13712      | 0.948    | 0.026    | 0.809    | 0.211    | 0.421  | 0.102    | 0.011  | 3.600    | 0.786           | 0.436            | 0.021 |
| 13721.9    | 0.979    | 0.039    | 0.834    | 0.253    | 0.444  | 0.133    | 0.019  | 2.251    | 2.944           | 0.658            | 0.014 |
| 13726.5    | 0.979    | 0.040    | 0.836    | 0.255    | 0.447  | 0.130    | 0.019  | 2.245    | 3.002           | 0.669            | 0.014 |
| 13730.2    | 0.950    | 0.029    | 0.808    | 0.219    | 0.451  | 0.085    | 0.014  | 3.519    | 2.932           | 1.589            | 0.021 |
| 13731      | 0.967    | 0.024    | 0.814    | 0.217    | 0.451  | 0.098    | 0.014  | 2.832    | 5.075           | 1.826            | 0.016 |
| 13734      | 0.996    | 0.021    | 0.871    | 0.075    | 0.502  | 0.268    | 0.067  | 1.266    | 35.230          | 2.152            | 0.010 |
| 13737.5    | 0.990    | 0.011    | 0.810    | 0.198    | 0.497  | 0.173    | 0.032  | 1.637    | 24.175          | 3.147            | 0.014 |
| 13745.8    | 0.990    | 0.031    | 0.873    | 0.147    | 0.506  | 0.193    | 0.020  | 1.637    | 24.573          | 3.337            | 0.011 |
| 13756.8    | 0.997    | 0.025    | 0.849    | 0.030    | 0.511  | 0.290    | 0.086  | 1.221    | 54.179          | 3.838            | 0.010 |
| 13765      | 0.961    | 0.026    | 0.811    | 0.200    | 0.479  | 0.091    | 0.018  | 3.065    | 12.616          | 5.792            | 0.020 |

| Depth<br>(ft) | Ca/Ca+Al | Ti/Ti+Al | Si/Si+Al | Fe/Fe+Al | K/K+Al | Na/Na+Al | P/P+Al | Sr/Sr+Al | Mn/Mn+Al<br>(x100) | Mn/Mn+Ca<br>(x1000) | Mg/Ca |
|---------------|----------|----------|----------|----------|--------|----------|--------|----------|--------------------|---------------------|-------|
| 13781.2       | 0.991    | 0.023    | 0.867    | 0.295    | 0.495  | 0.200    | 0.028  | 1.540    | 73.038             | 23.312              | 0.026 |
| 13787.5       | 0.972    | 0.040    | 0.848    | 0.235    | 0.472  | 0.126    | 0.016  | 2.499    | 32.019             | 13.179              | 0.020 |
| 13793.5       | 0.846    | 0.047    | 0.814    | 0.285    | 0.437  | 0.096    | 0.010  | 5.665    | 14.910             | 30.997              | 0.064 |
| 13795.5       | 0.911    | 0.033    | 0.810    | 0.262    | 0.447  | 0.094    | 0.012  | 4.575    | 21.252             | 25.720              | 0.036 |
| 13797.4       | 0.978    | 0.039    | 0.872    | 0.317    | 0.497  | 0.150    | 0.024  | 2.218    | 46.318             | 19.408              | 0.019 |
| 13800.5       | 0.987    | 0.028    | 0.878    | 0.373    | 0.504  | 0.161    | 0.021  | 1.789    | 66.791             | 26.676              | 0.015 |
| 13804.5       | 0.846    | 0.047    | 0.814    | 0.285    | 0.437  | 0.096    | 0.010  | 5.665    | 14.910             | 30.997              | 0.064 |
| 13811.9       | 0.971    | 0.041    | 0.848    | 0.321    | 0.517  | 0.128    | 0.021  | 2.434    | 61.506             | 44.943              | 0.073 |
| 13816.2       | 0.976    | 0.048    | 0.855    | 0.504    | 0.530  | 0.159    | 0.022  | 2.114    | 74.974             | 69.773              | 0.187 |
| 13820.5       | 0.983    | 0.036    | 0.862    | 0.294    | 0.544  | 0.145    | 0.023  | 1.930    | 71.346             | 40.856              | 0.051 |
| 13826.5       | 0.977    | 0.043    | 0.869    | 0.161    | 0.545  | 0.138    | 0.021  | 2.230    | 57.621             | 30.758              | 0.020 |
| 13832         | 0.970    | 0.042    | 0.865    | 0.300    | 0.528  | 0.125    | 0.016  | 2.515    | 42.641             | 22.786              | 0.049 |
| 13834.5       | 0.956    | 0.056    | 0.892    | 0.320    | 0.524  | 0.173    | 0.020  | 2.452    | 59.101             | 62.836              | 0.418 |
| 13838         | 0.956    | 0.045    | 0.856    | 0.300    | 0.505  | 0.116    | 0.014  | 3.020    | 32.334             | 21.637              | 0.053 |
| 13841.5       | 0.950    | 0.058    | 0.894    | 0.346    | 0.539  | 0.145    | 0.016  | 2.576    | 54.667             | 59.632              | 0.409 |
| 13843         | 0.966    | 0.042    | 0.860    | 0.409    | 0.545  | 0.141    | 0.020  | 2.248    | 65.369             | 61.942              | 0.420 |
| 13843.5       | 0.948    | 0.055    | 0.850    | 0.386    | 0.540  | 0.122    | 0.017  | 2.733    | 57.001             | 67.611              | 0.454 |
| 13845.5       | 0.929    | 0.055    | 0.841    | 0.375    | 0.504  | 0.114    | 0.014  | 3.263    | 49.373             | 69.524              | 0.420 |
| 13847.2       | 0.133    | 0.069    | 0.883    | 0.144    | 0.343  | 0.280    | 0.007  | 5.960    | 0.430              | 27.485              | 1.419 |
| 13851.5       | 0.130    | 0.058    | 0.887    | 0.164    | 0.333  | 0.259    | 0.006  | 5.765    | 0.500              | 32.411              | 2.257 |
| 13856.5       | 0.160    | 0.076    | 0.866    | 0.269    | 0.323  | 0.279    | 0.007  | 6.376    | 0.757              | 38.499              | 2.512 |

**Table 4.** Ca and trace element ratio normalized with respect to Al of the Smackover from the T.R. MILLER MILLS 17-11, #1 of the Conecuh Embayment.

| Depth<br>(ft) | Ca<br>(%) | Pb/Pb+Al<br>(x1000) | Ba/Ba+Al<br>(x1000) | Zn/Zn+Al<br>(x1000) | Cu/Cu+Al<br>(x1000) | Ni/Ni+Al<br>(x1000) | Cr/Cr+Al<br>(x1000) | V/V+Al<br>(x1000) | V/Cr   |
|---------------|-----------|---------------------|---------------------|---------------------|---------------------|---------------------|---------------------|-------------------|--------|
| 13505.8       | 30.384    | 0.250               | 2.120               | 0.458               | 4.145               | 0.642               | 0.571               | 0.825             | 0.692  |
| 13508.8       | 44.788    | 0.239               | 1.256               | 0.229               | 1.751               | 0.568               | 0.492               | 0.601             | 0.819  |
| 13511.5       | 39.895    | 0.675               | 6.106               | 0.484               | 1.536               | 0.114*              | 0.946               | 0.727             | 1.303  |
| 13516.4       | 62.026    | 0.568               | 10.490              | 0.174*              | 2.940               | 1.341               | 2.325               | 0.891             | 2.615  |
| 13520         | 56.013    | 3.313               | 31.295              | 32.341              | 13.619              | 0.657*              | 5.663               | 0.657*            | 4.334  |
| 13526         | 70.796    | 4.907               | 97.558              | 0.930*              | 14.588              | 19.229              | 11.993              | 0.930*            | 6.518  |
| 13535         | 66.888    | 1.821               | 32.954              | 0.731               | 0.099*              | 5.628               | 3.874               | 2.456             | 1.580  |
| 13538.5       | 54.346    | 0.363               | 1.713               | 0.331               | 0.861               | 0.491               | 0.626               | 0.767             | 0.816  |
| 13546.5       | 70.047    | 2.843               | 45.353              | 0.496*              | 9.878               | 11.198              | 6.575               | 0.496*            | 6.662  |
| 13551.8       | 70.902    | 0.966*              | 57.715              | 0.966*              | 19.163              | 7.311               | 6.285               | 0.966*            | 3.269  |
| 13553.5       | 66.177    | 1.000               | 10.701              | 0.163*              | 3.185               | 2.757               | 1.058               | 0.621             | 1.706  |
| 13555         | 66.472    | 0.746               | 6.499               | 0.141*              | 3.557               | 2.371               | 1.537               | 1.042             | 1.475  |
| 13561.9       | 67.398    | 0.156*              | 11.840              | 0.156*              | 3.701               | 1.918               | 0.843               | 0.156*            | 2.697  |
| 13562.3       | 67.997    | 1.030*              | 39.880              | 1.030*              | 22.145              | 1.030               | 1.030*              | 5.765             | 0.356  |
| 13568         | 55.142    | 0.169               | 2.179               | 0.123               | 1.063               | 0.668               | 0.610               | 0.969             | 0.630  |
| 13570         | 66.052    | 0.751               | 13.858              | 0.572               | 2.528               | 2.389               | 2.223               | 1.549             | 1.436  |
| 13576.9       | 67.013    | 0.130*              | 8.839               | 0.130*              | 3.615               | 1.971               | 1.304               | 0.587             | 2.222  |
| 13583         | 65.425    | 0.703               | 15.709              | 0.603               | 2.326               | 2.996               | 2.440               | 0.990             | 2.468  |
| 13589.5       | 27.755    | 0.133               | 2.214               | 0.387               | 0.485               | 0.445               | 0.692               | 1.035             | 0.668  |
| 13600.7       | 23.768    | 0.193               | 2.138               | 0.470               | 0.629               | 0.554               | 0.697               | 1.070             | 0.651  |
| 13608         | 9.667     | 0.051               | 2.872               | 0.481               | 0.505               | 0.444               | 0.758               | 1.343             | 0.564  |
| 13618         | 61.234    | 0.221               | 3.880               | 0.295               | 1.650               | 0.925               | 0.985               | 0.267             | 3.695  |
| 13620.2       | 53.496    | 0.112               | 2.109               | 0.245               | 0.863               | 0.475               | 0.542               | 0.969             | 0.559  |
| 13622.5       | 68.902    | 0.274*              | 13.726              | 0.274*              | 6.807               | 2.893               | 2.529               | 0.274*            | 4.619  |
| 13627         | 69.806    | 0.675*              | 18.233              | 0.675*              | 14.056              | 4.929               | 5.543               | 0.675*            | 4.123  |
| 13632.9       | 69.366    | 0.495*              | 12.630              | 0.495               | 9.395               | 5.264               | 3.297               | 0.495*            | 3.339  |
| 13640.5       | 68.584    | 0.366*              | 13.539              | 0.366*              | 9.052               | 4.841               | 2.676               | 2.690             | 0.995  |
| 13646         | 67.117    | 0.469               | 3.001               | 1.491               | 3.003               | 1.879               | 1.197               | 0.112*            | 5.366  |
| 13673.9       | 34.297    | 0.121               | 2.043               | 0.340               | 0.585               | 0.559               | 0.644               | 0.905             | 0.711  |
| 13681.5       | 19.000    | 0.142               | 2.445               | 0.532               | 0.591               | 0.528               | 0.739               | 1.180             | 0.626  |
| 13686         | 22.542    | 0.111               | 1.992               | 0.468               | 0.558               | 0.604               | 0.695               | 1.068             | 0.651  |
| 13698         | 19.922    | 0.102               | 2.274               | 0.407               | 0.542               | 0.522               | 0.731               | 1.241             | 0.589  |
| 13703.5       | 19.792    | 0.122               | 2.053               | 0.480               | 0.563               | 0.528               | 0.753               | 1.146             | 0.657  |
| 13706.1       | 59.063    | 0.191               | 2.695               | 0.182               | 1.188               | 0.745               | 0.569               | 0.856             | 0.664  |
| 13712         | 47.210    | 0.125               | 2.184               | 0.666               | 0.726               | 0.633               | 0.592               | 1.119             | 0.529  |
| 13721.9       | 57.635    | 0.254               | 2.652               | 0.235               | 1.303               | 0.970               | 0.786               | 1.136             | 0.692  |
| 13726.5       | 57.542    | 0.154               | 2.799               | 0.335               | 1.286               | 1.116               | 0.909               | 1.350             | 0.674  |
| 13730.2       | 47.808    | 0.164               | 1.862               | 0.432               | 0.726               | 0.755               | 0.637               | 0.982             | 0.648  |
| 13731         | 53.546    | 0.177               | 4.283               | 0.399               | 0.917               | 0.840               | 0.671               | 1.078             | 0.622  |
| 13734         | 67.066    | 0.188*              | 15.902              | 0.188*              | 4.451               | 2.028               | 2.002               | 1.159             | 1.728  |
| 13737.5       | 64.318    | 0.079*              | 3.354               | 0.398               | 2.105               | 0.994               | 0.989               | 0.864             | 1.144  |
| 13745.8       | 61.997    | 0.078*              | 5.402               | 0.078*              | 1.842               | 1.312               | 0.997               | 0.078*            | 12.716 |
| 13756.8       | 67.869    | 0.779               | 25.555              | 0.226*              | 4.653               | 2.875               | 2.047               | 1.721             | 1.190  |

| Depth<br>(ft) | Ca<br>(%) | Pb/Pb+Al<br>(x1000) | Ba/Ba+Al<br>(x1000) | Zn/Zn+Al<br>(x1000) | Cu/Cu+Al<br>(x1000) | Ni/Ni+Al<br>(x1000) | Cr/Cr+Al<br>(x1000) | V/V+Al<br>(x1000) | V/Cr  |
|---------------|-----------|---------------------|---------------------|---------------------|---------------------|---------------------|---------------------|-------------------|-------|
| 13765         | 51.169    | 0.126               | 1.748               | 0.346               | 0.803               | 0.741               | 0.538               | 0.890             | 0.605 |
| 13781.2       | 61.310    | 0.524               | 78.354              | 0.093*              | 1.901               | 2.829               | 1.478               | 2.368             | 0.624 |
| 13787.5       | 52.873    | 0.314               | 13.041              | 0.345               | 0.956               | 2.338               | 0.796               | 0.834             | 0.955 |
| 13793.5       | 25.552    | 0.117               | 1.550               | 0.173               | 0.388               | 0.498               | 0.324               | 0.766             | 0.423 |
| 13795.5       | 36.550    | 0.463               | 2.066               | 0.371               | 0.723               | 0.782               | 0.619               | 2.046             | 0.302 |
| 13797.4       | 53.081    | 0.536               | 6.832               | 0.191               | 1.190               | 1.983               | 0.892               | 0.835             | 1.068 |
| 13800.5       | 57.903    | 0.849               | 3.470               | 0.063*              | 1.877               | 1.683               | 0.697               | 1.601             | 0.435 |
| 13804.5       | 25.552    | 0.658               | 2.791               | 0.480               | 0.771               | 0.984               | 0.879               | 3.069             | 0.286 |
| 13811.9       | 48.685    | 0.933               | 3.024               | 0.573               | 1.049               | 1.707               | 0.842               | 2.219             | 0.379 |
| 13816.2       | 44.478    | 1.148               | 3.926               | 3.244               | 1.082               | 2.381               | 1.048               | 1.572             | 0.666 |
| 13820.5       | 54.378    | 0.510               | 5.307               | 0.054*              | 1.413               | 1.519               | 1.058               | 1.256             | 0.842 |
| 13826.5       | 52.710    | 0.226               | 11.002              | 9.443               | 1.048               | 1.013               | 0.981               | 1.298             | 0.755 |
| 13832         | 48.306    | 1.392               | 2.984               | 0.262               | 0.993               | 1.017               | 0.639               | 1.653             | 0.386 |
| 13834.5       | 31.295    | 0.315               | 3.678               | 0.328               | 0.580               | 0.665               | 0.697               | 0.753             | 0.927 |
| 13838         | 43.647    | 1.089               | 2.881               | 0.337               | 0.907               | 1.204               | 0.686               | 2.043             | 0.335 |
| 13841.5       | 29.972    | 0.999               | 3.812               | 0.362               | 0.958               | 1.313               | 0.807               | 1.085             | 0.744 |
| 13843         | 35.664    | 0.933               | 3.095               | 0.242               | 3.040               | 0.965               | 0.748               | 0.908             | 0.823 |
| 13843.5       | 31.676    | 1.029               | 3.919               | 0.510               | 1.863               | 0.971               | 0.800               | 0.974             | 0.821 |
| 13845.5       | 29.536    | 1.066               | 3.885               | 0.354               | 1.553               | 1.091               | 0.774               | 1.115             | 0.694 |
| 13847.2       | 0.758     | 0.066               | 6.415               | 0.213               | 0.187               | 0.144               | 0.692               | 1.214             | 0.570 |
| 13851.5       | 0.715     | 0.083               | 6.314               | 0.213               | 0.158               | 0.167               | 0.470               | 0.979             | 0.480 |
| 13856.5       | 1.025     | 0.091               | 5.627               | 0.309               | 0.166               | 0.236               | 0.688               | 1.459             | 0.471 |

**Note:** \* Samples that contain trace elements less than 2ppm and were given the 0.5 ppm concentration for the calculation purposes

**Table 5.** Carbonate, non-carbonate (residue) components, TOC and isotopic compositions of the Smackover samples from the T.R. MILLER MILLS 17-11, #1 of the Conecuh Embayment.

| Depth (ft) | CaCO <sub>3</sub> <sup>1</sup> (%) | nonCaCO <sub>3</sub> (%) | TOC <sup>2</sup> (%) | TOC* <sup>3</sup> (%) | δ <sup>13</sup> C <sub>carb</sub> (‰) | δ <sup>18</sup> O <sub>carb</sub> (‰) | δ <sup>13</sup> C <sub>org</sub> (‰) |
|------------|------------------------------------|--------------------------|----------------------|-----------------------|---------------------------------------|---------------------------------------|--------------------------------------|
| 13505.8    | 59.18                              | 40.82                    | 0.50                 | 1.23                  | 5.32                                  | 1.67                                  | n.a.                                 |
| 13508.8    | 2.66                               | 97.34                    | 0.21                 | 0.22                  | 5.88                                  | 3.02                                  | n.a.                                 |
| 13511.5    | n.a.                               | n.a.                     | n.a.                 | n.a.                  | n.a.                                  | n.a.                                  | n.a.                                 |
| 13516.4    | 95.61                              | 4.39                     | 0.02                 | 0.44                  | 5.71                                  | -2.67                                 | n.a.                                 |
| 13520      | 99.00                              | 1.00                     | 0.02                 | 1.75                  | n.a.                                  | n.a.                                  | n.a.                                 |
| 13526      | 97.69                              | 2.31                     | 0.04                 | 1.91                  | 5.6                                   | -2.92                                 | -24.69                               |
| 13535      | 89.75                              | 10.25                    | 0.08                 | 0.79                  | 5.5                                   | -2.21                                 | n.a.                                 |
| 13538.5    | 90.26                              | 9.75                     | 0.17                 | 1.71                  | 5.51                                  | -1.94                                 | -23.48                               |
| 13546.5    | 97.78                              | 2.22                     | 0.04                 | 1.65                  | 5.68                                  | -1.98                                 | n.a.                                 |
| 13551.8    | 99.82                              | 0.18                     | 0.01                 | 7.59                  | n.a.                                  | n.a.                                  | n.a.                                 |
| 13553.5    | 96.64                              | 3.36                     | 0.08                 | 2.47                  | n.a.                                  | n.a.                                  | n.a.                                 |
| 13555      | 97.59                              | 2.41                     | 0.19                 | 7.78                  | 5.54                                  | -3.02                                 | -25.07                               |
| 13561.9    | 97.53                              | 2.47                     | 0.12                 | 4.78                  | 4.94                                  | -1.02                                 | n.a.                                 |
| 13562.3    | 99.20                              | 0.80                     | 0.01                 | 1.85                  | n.a.                                  | n.a.                                  | n.a.                                 |
| 13568      | 90.33                              | 9.67                     | 0.45                 | 4.68                  | n.a.                                  | n.a.                                  | n.a.                                 |
| 13570      | 96.56                              | 3.44                     | 0.10                 | 3.04                  | 5.44                                  | -1.19                                 | n.a.                                 |
| 13576.9    | 97.19                              | 2.81                     | 0.18                 | 6.50                  | n.a.                                  | n.a.                                  | n.a.                                 |
| 13583      | 94.97                              | 5.03                     | 0.11                 | 2.25                  | 5.26                                  | -1.73                                 | -24.95                               |
| 13589.5    | 63.16                              | 36.84                    | 0.18                 | 0.49                  | 3.25                                  | -0.38                                 | -22.55                               |
| 13600.7    | 84.10                              | 15.90                    | 0.09                 | 0.60                  | 2.77                                  | -0.85                                 | -22.55                               |
| 13608      | 37.59                              | 62.41                    | 0.18                 | 0.28                  | 3.53                                  | 1.04                                  | -22.43                               |
| 13618      | 79.93                              | 20.07                    | 0.18                 | 0.91                  | 5.09                                  | 0.79                                  | -23.44                               |
| 13620.2    | n.a.                               |                          | n.a.                 | n.a.                  | n.a.                                  | n.a.                                  | n.a.                                 |
| 13622.5    | 98.65                              | 1.35                     | 0.10                 | 7.42                  | 5.42                                  | 0.52                                  | n.a.                                 |
| 13627      | 99.49                              | 0.51                     | 0.03                 | 6.74                  | n.a.                                  | n.a.                                  | n.a.                                 |
| 13632.9    | 98.98                              | 1.02                     | 0.07                 | 6.83                  | 5.17                                  | -0.37                                 | -25.15                               |
| 13640.5    | 98.23                              | 1.77                     | 0.08                 | 4.68                  | n.a.                                  | n.a.                                  | n.a.                                 |
| 13646      | 97.13                              | 2.87                     | 0.27                 | 9.47                  | 4.96                                  | -1.06                                 | -25.97                               |
| 13673.9    | 70.90                              | 29.10                    | 0.56                 | 1.92                  | 4                                     | 0.48                                  | -25.36                               |
| 13681.5    | 49.12                              | 50.88                    | 0.46                 | 0.90                  | 2.64                                  | 0.13                                  | -24.12                               |
| 13686      | 56.10                              | 43.90                    | 0.58                 | 1.32                  | 3.29                                  | -0.06                                 | n.a.                                 |
| 13698      | 51.83                              | 48.17                    | 2.64                 | 5.49                  | 2.9                                   | 0.42                                  | -25.75                               |
| 13703.5    | 50.66                              | 49.34                    | 0.51                 | 1.04                  | 3.6                                   | 0.63                                  | -24.16                               |
| 13706.1    | 93.36                              | 6.64                     | 0.16                 | 2.48                  | n.a.                                  | n.a.                                  | n.a.                                 |
| 13712      | 85.10                              | 14.90                    | 0.64                 | 4.27                  | 4.32                                  | 0.26                                  | -23.94                               |
| 13721.9    | 90.55                              | 9.45                     | 0.55                 | 5.86                  | 4.06                                  | 0.66                                  | -24.46                               |
| 13726.5    | n.a.                               | n.a.                     | n.a.                 | n.a.                  | n.a.                                  | n.a.                                  | n.a.                                 |
| 13730.2    | 67.00                              | 33.00                    | 1.15                 | 3.48                  | 3.96                                  | 0.56                                  | -24.55                               |
| 13731      | 89.33                              | 10.67                    | 0.46                 | 4.31                  | n.a.                                  | n.a.                                  | n.a.                                 |
| 13734      | 97.25                              | 2.75                     | 0.47                 | 17.13                 | n.a.                                  | n.a.                                  | -25.1                                |
| 13737.5    | 96.18                              | 3.82                     | 0.18                 | 4.81                  | 4.53                                  | 1                                     | n.a.                                 |
| 13745.8    | 93.91                              | 6.09                     | 0.11                 | 1.86                  | 4.12                                  | 0.28                                  | -26.79                               |

| Depth<br>(ft) | CaCO <sub>3</sub> <sup>1</sup><br>(%) | nonCaCO <sub>3</sub><br>(%) | TOC <sup>2</sup><br>(%) | TOC* <sup>3</sup><br>(%) | δ <sup>13</sup> C <sub>carb</sub><br>(‰) | δ <sup>18</sup> O <sub>carb</sub><br>(‰) | δ <sup>13</sup> C <sub>org</sub><br>(‰) |
|---------------|---------------------------------------|-----------------------------|-------------------------|--------------------------|--|--|---|
| 13756.8       | 98.42                                 | 1.58                        | n.a.                    | n.a.                     | n.a.                                     | n.a.                                     | n.a.                                    |
| 13765         | 86.67                                 | 13.33                       | 0.40                    | 2.99                     | 4.34                                     | 0.17                                     | n.a.                                    |
| 13781.2       | 95.01                                 | 4.99                        | 0.05                    | 0.93                     | 3.37                                     | -0.73                                    | -23.66                                  |
| 13787.5       | 91.66                                 | 8.34                        | 0.11                    | 1.38                     | 2.82                                     | -0.82                                    | n.a.                                    |
| 13793.5       | 87.97                                 | 12.03                       | 0.22                    | 1.80                     | n.a.                                     | n.a.                                     | n.a.                                    |
| 13795.5       | 73.88                                 | 26.12                       | 0.44                    | 1.69                     | 2.32                                     | -1.85                                    | -23.92                                  |
| 13797.4       | n.a.                                  | n.a.                        | n.a.                    | n.a.                     | n.a.                                     | n.a.                                     | -25.67                                  |
| 13800.5       | 91.82                                 | 8.18                        | 0.12                    | 1.48                     | n.a.                                     | n.a.                                     | n.a.                                    |
| 13804.5       | 58.30                                 | 41.70                       | 1.26                    | 3.02                     | 2.29                                     | -0.63                                    | n.a.                                    |
| 13811.9       | 89.30                                 | 10.70                       | 0.25                    | 2.29                     | 3  | -1.5                                     | -25.17                                  |
| 13816.2       | 89.98                                 | 10.02                       | n.a.                    | n.a.                     | n.a.                                     | n.a.                                     | -24.84                                  |
| 13820.5       | 92.31                                 | 7.69                        | 0.15                    | 1.99                     | 2.82                                     | -3.39                                    | n.a.                                    |
| 13826.5       | 88.76                                 | 11.24                       | 0.13                    | 1.17                     | n.a.                                     | n.a.                                     | n.a.                                    |
| 13832         | 85.62                                 | 14.38                       | 0.34                    | 2.38                     | 2.94                                     | -0.25                                    | -25.54                                  |
| 13834.5       | 82.88                                 | 17.12                       | 0.09                    | 0.51                     | n.a.                                     | n.a.                                     | n.a.                                    |
| 13838         | 81.03                                 | 18.97                       | 0.47                    | 2.50                     | 2.99                                     | -0.27                                    | -25.36                                  |
| 13841.5       | 80.02                                 | 19.98                       | 0.08                    | 0.39                     | n.a.                                     | n.a.                                     | n.a.                                    |
| 13843         | 89.47                                 | 10.53                       | n.a.                    | n.a.                     | 3.51                                     | 1.4                                      | -25.43                                  |
| 13843.5       | 85.65                                 | 14.35                       | 0.16                    | 1.09                     | n.a.                                     | n.a.                                     | n.a.                                    |
| 13845.5       | 82.23                                 | 17.77                       | n.a.                    | n.a.                     | 3.57                                     | 0.58                                     | n.a.                                    |
| 13847.2       | 5.43                                  | 94.57                       | n.a.                    | n.a.                     | n.a.                                     | n.a.                                     | n.a.                                    |
| 13851.5       | 5.31                                  | 94.69                       | 0.09                    | 0.10                     | n.a.                                     | n.a.                                     | n.a.                                    |
| 13856.5       | 8.95                                  | 91.05                       | n.a.                    | n.a.                     | n.a.                                     | n.a.                                     | n.a.                                    |

**Note:** CaCO<sub>3</sub><sup>1</sup> an average value from two analysis by HCl digestion of the whole rock samples.  
TOC<sup>2</sup> an average content of TOC in the whole rock from two analysis by TOC analyzer.  
TOC<sup>3</sup> a calculated TOC content in the non-carbonate (residue) fraction.

**Table 6.** Relative distribution of minerals presented in the core samples analyzed by XRD from the T.R. MILLER MLLS 17-11, #1 well of the Conecuh Embayment.

| Depth (ft) | Anhydrite | Calcite | Dolomite | Quartz | Quartz | Pyrite | $\delta^{13}\text{C}_{\text{carb}}$ (‰) | $\delta^{18}\text{O}_{\text{carb}}$ (‰) |
|------------|-----------|---------|----------|--------|--------|--------|---|---|
| 13505.8    | 550.1     | 0       | 938.2    | 207.3  | 49.7   |        | 5.32                                    | 1.67                                    |
| 13508.8    | 1685.7    | 0       | 81.7     | 88.6   | 20.3   |        | 5.88                                    | 3.02                                    |
| 13516.4    | 137.9     | 793.3   | 263.4    | 28.1   |        |        | 5.71                                    | -2.67                                   |
| 13526      |           | 1208.6  |          |        |        |        | 5.6                                     | -2.92                                   |
| 13535      |           | 942.9   |          |        |        |        | 5.5                                     | -2.21                                   |
| 13538.5    |           | 984.2   | 60.5     | 42.2   |        |        | 5.51                                    | -1.94                                   |
| 13555      |           | 1334    | 75.3     |        |        |        | 5.54                                    | -3.02                                   |
| 13583      |           | 1065.8  | 31.6     | 28.3   |        |        | 5.26                                    | -1.73                                   |
| 13600.7    |           | 511.9   | 17       | 285    | 43.1   | 36.4   | 2.77                                    | -0.85                                   |
| 13622.5    |           | 1082.9  |          |        |        |        | 5.42                                    | -0.52                                   |
| 13646      |           | 1307.7  |          |        |        |        | 4.96                                    | -1.06                                   |
| 13681.5    |           | 976.8   |          |        |        |        | 2.64                                    | 0.13                                    |
| 13703.5    |           | 609.5   |          | 249.2  | 80.6   | 35     | 3.6                                     | 0.63                                    |
| 13710      |           | 664.4   |          | 198.5  | 76.7   | 26.3   | 4.32                                    | 0.26                                    |
| 13737.5    |           | 997.3   |          | 68.2   |        |        | 4.53                                    | 1.00                                    |
| 13765      |           | 1087.9  |          | 63.7   |        |        | 4.34                                    | 0.17                                    |
| 13787.5    |           | 690.7   | 194.7    | 88.1   | 17.7   |        | 2.82                                    | -0.82                                   |
| 13804.9    |           | 757.5   |          | 331.1  | 53.8   |        | 2.29                                    | -0.63                                   |
| 13820.5    |           | 874.2   | 136.3    | 83.8   |        |        | 2.82                                    | -3.39                                   |
| 13843      |           | 116.5   | 1246     | 106.4  | 29.9   | 21.2   | 3.51                                    | 1.40                                    |
| 13845      |           | 46.1    | 757.6    | 173.9  | 42.4   | 23.6   | 3.64                                    | 0.57                                    |
| 13847.2    |           | 44.8    | 33.1     | 2317.2 | 444.5  |        | too small                               |   |
| 13856.5    |           | 34.4    | 52       | 1859.2 | 465.5  |        | too small                               |   |

## **APPENDIX F**

**Table 1.** Measured concentrations of major, minor and trace elements of the Smackover samples from the #1 NEAL ET AL UNIT 30-1 well of the Manila Embayment by XRF analysis.

| Depth (ft) | Ca (%) | Al (%) | Ti (%) | Si (%) | Fe <sub>total</sub> (%) | K (%) | Mg (%) | Mn (%) | Sr (ppm) | Na (%) | P (%) |
|------------|--------|--------|--------|--------|-------------------------|-------|--------|--------|----------|--------|-------|
| 13100      | 70.847 | 0.101  | 0.011  | 0.259  | 0.014                   | 0.062 | 0.115  | 0.015  | 1436     | 0.149  | 0.018 |
| 13114.5    | 52.519 | 1.284  | 0.052  | 7.883  | 0.400                   | 0.890 | 2.996  | 0.035  | 1332     | 0.324  | 0.028 |
| 13117.1    | 23.717 | 2.012  | 0.106  | 16.440 | 1.109                   | 1.830 | 13.836 | 0.148  | 210      | 0.529  | 0.033 |
| 13122      | 33.384 | 1.244  | 0.072  | 7.935  | 1.144                   | 1.232 | 18.139 | 0.132  | 134      | 0.346  | 0.026 |
| 13130      | 24.885 | 2.521  | 0.171  | 14.887 | 1.529                   | 2.078 | 13.769 | 0.115  | 126      | 0.452  | 0.033 |
| 13135      | 23.432 | 2.546  | 0.162  | 15.679 | 1.564                   | 2.091 | 13.877 | 0.106  | 130      | 0.505  | 0.034 |
| 13140      | 22.117 | 3.279  | 0.217  | 15.255 | 1.965                   | 2.303 | 14.222 | 0.086  | 136      | 0.436  | 0.038 |
| 13140.5    | 6.770  | 6.925  | 0.517  | 24.089 | 3.722                   | 4.413 | 8.033  | 0.052  | 121      | 0.801  | 0.051 |
| 13143      | 2.464  | 3.125  | 0.090  | 38.610 | 0.245                   | 2.125 | 1.983  | 0.018  | 108      | 1.216  | 0.021 |
| 13154      | 18.884 | 3.512  | 0.240  | 16.918 | 2.503                   | 2.530 | 13.794 | 0.096  | 114      | 0.554  | 0.041 |
| 13159      | 8.608  | 3.147  | 0.164  | 29.718 | 1.309                   | 2.257 | 7.363  | 0.057  | 119      | 0.941  | 0.033 |
| 13175      | 26.036 | 2.717  | 0.179  | 12.535 | 1.513                   | 2.226 | 15.535 | 0.097  | 124      | 0.431  | 0.034 |
| 13180.2    | 11.379 | 4.420  | 0.255  | 24.050 | 1.762                   | 3.374 | 9.670  | 0.067  | 169      | 0.834  | 0.044 |
| 13180.5    | 6.156  | 3.562  | 0.130  | 32.609 | 0.754                   | 2.445 | 5.386  | 0.042  | 149      | 1.201  | 0.037 |
| 13181      | 16.434 | 3.918  | 0.295  | 19.336 | 2.138                   | 3.248 | 11.971 | 0.090  | 117      | 0.604  | 0.041 |
| 13187.5    | 34.123 | 1.289  | 0.073  | 7.262  | 1.054                   | 1.303 | 18.387 | 0.135  | 129      | 0.306  | 0.025 |
| 13191.5    | 36.878 | 0.829  | 0.045  | 5.668  | 0.846                   | 0.767 | 19.253 | 0.127  | 137      | 0.299  | 0.018 |
| 13199      | 34.177 | 1.519  | 0.067  | 6.864  | 0.829                   | 1.477 | 18.674 | 0.098  | 115      | 0.320  | 0.026 |
| 13208      | 25.279 | 2.758  | 0.180  | 13.161 | 1.573                   | 2.310 | 15.176 | 0.079  | 123      | 0.493  | 0.031 |
| 13214      | 4.843  | 3.210  | 0.115  | 36.799 | 0.681                   | 1.950 | 1.970  | 0.017  | 357      | 1.187  | 0.027 |
| 13216.3    | 28.719 | 2.246  | 0.116  | 11.733 | 1.224                   | 1.803 | 15.513 | 0.092  | 114      | 0.376  | 0.027 |
| 13236.4    | 33.995 | 1.529  | 0.086  | 7.942  | 0.750                   | 1.219 | 17.650 | 0.086  | 102      | 0.351  | 0.022 |
| 13244.2    | 40.748 | 0.487  | 0.014  | 3.693  | 0.415                   | 0.447 | 19.639 | 0.099  | 247      | 0.220  | 0.015 |
| 13256      | 31.697 | 1.796  | 0.102  | 9.937  | 0.797                   | 1.356 | 16.525 | 0.080  | 107      | 0.393  | 0.023 |
| 13275      | 34.325 | 1.276  | 0.061  | 7.368  | 0.714                   | 1.183 | 18.540 | 0.081  | 106      | 0.289  | 0.019 |
| 13280.2    | 36.703 | 0.998  | 0.046  | 5.451  | 1.705                   | 0.800 | 18.767 | 0.095  | 93       | 0.294  | 0.025 |
| 13298.2    | 33.714 | 1.323  | 0.066  | 8.790  | 0.548                   | 0.972 | 17.381 | 0.099  | 97       | 0.353  | 0.024 |
| 13295.2    | 26.445 | 2.868  | 0.148  | 12.896 | 1.249                   | 2.183 | 14.804 | 0.109  | 101      | 0.449  | 0.039 |
| 13297      | 20.439 | 4.419  | 0.221  | 16.393 | 2.028                   | 3.177 | 12.100 | 0.097  | 116      | 0.505  | 0.049 |
| 13300      | 15.575 | 5.243  | 0.297  | 19.803 | 2.541                   | 3.555 | 10.032 | 0.089  | 111      | 0.580  | 0.049 |
| 13302      | 29.809 | 2.028  | 0.114  | 11.337 | 1.004                   | 1.519 | 15.707 | 0.110  | 98       | 0.402  | 0.028 |
| 13305      | 22.885 | 2.958  | 0.178  | 16.784 | 1.161                   | 2.103 | 12.730 | 0.096  | 114      | 0.547  | 0.033 |
| 13310      | 25.233 | 2.936  | 0.155  | 14.485 | 1.624                   | 2.123 | 13.358 | 0.115  | 114      | 0.512  | 0.046 |
| 13310.5    | 1.412  | 9.080  | 0.560  | 28.299 | 4.636                   | 5.072 | 3.367  | 0.065  | 118      | 0.796  | 0.058 |
| 13334.1    | 8.927  | 6.991  | 0.408  | 24.176 | 3.531                   | 4.388 | 6.354  | 0.084  | 149      | 0.705  | 0.059 |
| 13339      | 26.359 | 2.692  | 0.152  | 14.290 | 1.309                   | 1.852 | 13.397 | 0.197  | 107      | 0.464  | 0.030 |
| 13345      | 37.022 | 0.850  | 0.040  | 6.593  | 0.572                   | 0.616 | 18.171 | 0.232  | 111      | 0.304  | 0.018 |
| 13348.2    | 24.343 | 3.200  | 0.156  | 15.119 | 1.316                   | 2.393 | 12.994 | 0.246  | 122      | 0.466  | 0.039 |
| 13353      | 21.906 | 3.907  | 0.193  | 16.736 | 1.672                   | 2.659 | 11.658 | 0.215  | 122      | 0.455  | 0.044 |
| 13353.6    | 27.661 | 2.745  | 0.134  | 14.207 | 1.376                   | 2.007 | 12.195 | 0.174  | 146      | 0.458  | 0.047 |
| 13354      | 2.861  | 8.793  | 0.534  | 27.433 | 4.366                   | 4.991 | 3.872  | 0.078  | 135      | 0.804  | 0.064 |
| 13364.5    | 24.432 | 2.797  | 0.158  | 15.643 | 1.041                   | 2.014 | 13.237 | 0.180  | 150      | 0.504  | 0.030 |

| Depth<br>(ft) | Ca<br>(%) | Al<br>(%) | Ti<br>(%) | Si<br>(%) | Fe <sub>total</sub><br>(%) | K<br>(%) | Mg<br>(%) | Mn<br>(%) | Sr<br>(ppm) | Na<br>(%) | P<br>(%) |
|---------------|-----------|-----------|-----------|-----------|----------------------------|----------|-----------|-----------|-------------|-----------|----------|
| 13367         | 32.523    | 1.434     | 0.072     | 9.309     | 0.610                      | 1.230    | 17.222    | 0.210     | 141         | 0.400     | 0.023    |
| 13372.5       | 34.627    | 1.182     | 0.049     | 8.903     | 0.497                      | 0.878    | 16.654    | 0.248     | 140         | 0.341     | 0.020    |
| 13378.5       | 29.146    | 2.222     | 0.103     | 12.357    | 0.765                      | 1.684    | 14.716    | 0.236     | 121         | 0.406     | 0.031    |
| 13386.2       | 32.816    | 1.521     | 0.082     | 9.179     | 0.586                      | 1.169    | 17.208    | 0.085     | 106         | 0.380     | 0.024    |
| 13388.5       | 26.093    | 2.934     | 0.167     | 14.980    | 1.164                      | 2.116    | 12.303    | 0.212     | 145         | 0.520     | 0.037    |
| 13402.5       | 25.978    | 2.851     | 0.137     | 15.509    | 0.990                      | 2.211    | 11.966    | 0.187     | 179         | 0.475     | 0.043    |
| 13407         | 23.852    | 3.072     | 0.174     | 17.550    | 1.142                      | 2.015    | 10.837    | 0.184     | 196         | 0.517     | 0.032    |
| 13410.5       | 31.189    | 2.289     | 0.093     | 12.453    | 0.859                      | 1.895    | 12.566    | 0.216     | 188         | 0.422     | 0.036    |
| 13417         | 31.606    | 3.387     | 0.186     | 16.761    | 1.237                      | 2.616    | 4.498     | 0.159     | 257         | 0.439     | 0.040    |
| 13422.5       | 30.984    | 2.677     | 0.153     | 15.813    | 1.292                      | 2.158    | 7.328     | 0.218     | 185         | 0.451     | 0.033    |
| 13434         | 20.722    | 5.366     | 0.273     | 21.611    | 2.291                      | 3.619    | 3.314     | 0.208     | 283         | 0.568     | 0.052    |
| 13436         | 0.920     | 9.463     | 0.578     | 28.131    | 5.203                      | 5.548    | 2.700     | 0.049     | 140         | 0.841     | 0.059    |
| 13436.3       | 1.044     | 8.693     | 0.536     | 28.942    | 5.402                      | 5.272    | 2.525     | 0.058     | 128         | 0.810     | 0.058    |
| 13436.6       | 2.121     | 7.791     | 0.512     | 30.676    | 3.718                      | 4.806    | 2.167     | 0.041     | 130         | 0.810     | 0.071    |
| 13437.5       | 19.265    | 3.831     | 0.230     | 19.836    | 1.858                      | 2.888    | 9.399     | 0.360     | 213         | 0.581     | 0.045    |
| 13443         | 19.749    | 3.638     | 0.226     | 20.615    | 1.364                      | 2.476    | 8.793     | 0.525     | 240         | 0.585     | 0.042    |
| 13452         | 24.644    | 3.792     | 0.230     | 20.324    | 1.614                      | 2.853    | 4.395     | 0.537     | 196         | 0.554     | 0.042    |
| 13460         | 21.504    | 5.042     | 0.255     | 22.697    | 2.051                      | 3.812    | 1.517     | 0.397     | 245         | 0.599     | 0.061    |
| 13461.5       | 16.438    | 4.607     | 0.273     | 22.895    | 2.169                      | 3.168    | 6.283     | 0.573     | 174         | 0.580     | 0.046    |
| 13472.5       | 11.956    | 5.434     | 0.333     | 24.855    | 2.420                      | 3.522    | 6.060     | 0.515     | 161         | 0.640     | 0.047    |
| 13480         | 20.756    | 4.138     | 0.246     | 22.368    | 1.480                      | 3.098    | 4.474     | 0.611     | 191         | 0.587     | 0.043    |
| 13492         | 27.742    | 3.608     | 0.206     | 19.857    | 1.369                      | 2.712    | 2.975     | 0.514     | 247         | 0.512     | 0.041    |
| 13508.5       | 15.771    | 4.495     | 0.275     | 23.216    | 3.109                      | 3.219    | 5.647     | 0.609     | 181         | 0.652     | 0.048    |
| 13516         | 12.020    | 4.819     | 0.282     | 24.868    | 2.051                      | 3.657    | 6.916     | 0.577     | 128         | 0.623     | 0.047    |
| 13522         | 19.816    | 4.363     | 0.255     | 23.774    | 1.841                      | 3.446    | 2.911     | 0.284     | 218         | 0.556     | 0.045    |
| 13537         | 52.157    | 1.360     | 0.061     | 9.144     | 0.503                      | 1.586    | 0.910     | 0.247     | 322         | 0.217     | 0.027    |
| 13537.5       | 21.186    | 4.317     | 0.256     | 24.026    | 1.629                      | 3.545    | 1.639     | 0.188     | 385         | 0.577     | 0.048    |
| 13545.5       | 36.521    | 2.799     | 0.151     | 17.193    | 0.795                      | 2.488    | 0.754     | 0.478     | 415         | 0.391     | 0.038    |
| 13554         | 1.973     | 8.726     | 0.537     | 27.866    | 4.372                      | 6.055    | 3.415     | 0.070     | 108         | 0.720     | 0.079    |
| 13554.5       | 63.780    | 0.509     | 0.015     | 3.336     | 0.325                      | 0.618    | 0.367     | 0.472     | 278         | 0.134     | 0.019    |
| 13557.5       | 7.672     | 3.153     | 0.104     | 36.296    | 0.304                      | 2.613    | 0.356     | 0.125     | 99          | 0.816     | 0.028    |
| 13568.5       | 0.959     | 8.325     | 0.548     | 29.351    | 3.418                      | 5.099    | 4.156     | 0.054     | 110         | 0.918     | 0.069    |
| 13586.5       | 1.872     | 6.807     | 0.354     | 30.257    | 4.473                      | 4.398    | 2.676     | 0.048     | 190         | 2.303     | 0.049    |

**Table 2.** Trace element concentrations of Smackover samples from the #1 NEAL ET AL UNIT 30-1 of the Manila Embayment analyzed by XRF.

| Depth<br>(ft) | Ca<br>(%) | Pb<br>(ppm) | Ba<br>(ppm) | Zn<br>(ppm) | Cu<br>(ppm) | Ni<br>(ppm) | Cr<br>(ppm) | V<br>(ppm) | Nb<br>(ppm) | Rb<br>(ppm) | Th<br>(ppm) |
|---------------|-----------|-------------|-------------|-------------|-------------|-------------|-------------|------------|-------------|-------------|-------------|
| 13100         | 70.847    | <2          | 13.790      | <2          | 13.530      | 5.475       | 4.566       | 4.817      | 0.818       | 2.171       | 2.356       |
| 13114.5       | 52.519    | 3.850       | 45.601      | 3.548       | 12.470      | 9.272       | 9.308       | 9.217      | 1.200       | 12.357      | <2          |
| 13117.1       | 23.717    | 6.048       | 88.671      | 8.490       | 8.386       | 4.502       | 9.180       | 16.148     | 3.005       | 26.089      | <2          |
| 13122         | 33.384    | 5.333       | 44.620      | 8.945       | 8.561       | 2.530       | 7.668       | 10.790     | 2.348       | 15.829      | <2          |
| 13130         | 24.885    | 9.321       | 100.084     | 11.940      | 10.937      | 7.748       | 13.998      | 23.918     | 3.613       | 30.767      | 1.503       |
| 13135         | 23.432    | 8.852       | 109.948     | 10.299      | 9.510       | 9.490       | 15.926      | 24.002     | 4.048       | 33.212      | <2          |
| 13140         | 22.117    | 9.460       | 120.896     | 16.258      | 11.278      | 11.729      | 19.946      | 33.471     | 4.899       | 40.274      | 2.204       |
| 13140.5       | 6.770     | 25.049      | 312.805     | 45.205      | 21.987      | 36.668      | 57.033      | 103.137    | 13.277      | 102.219     | 8.167       |
| 13143         | 2.464     | 4.654       | 298.705     | 3.240       | 2.980       | <2          | 9.020       | 12.448     | 3.473       | 45.360      | <2          |
| 13154         | 18.884    | 12.475      | 152.347     | 16.925      | 13.244      | 15.787      | 23.342      | 42.270     | 5.943       | 48.892      | 2.807       |
| 13159         | 8.608     | 10.772      | 214.577     | 10.684      | 9.562       | 7.348       | 18.942      | 22.926     | 5.778       | 46.910      | <2          |
| 13175         | 26.036    | 9.248       | 109.483     | 13.144      | 11.113      | 9.295       | 15.970      | 29.183     | 4.558       | 36.000      | <2          |
| 13180.2       | 11.379    | 10.965      | 221.239     | 19.114      | 13.310      | 10.664      | 23.811      | 45.826     | 6.910       | 60.979      | 3.647       |
| 13180.5       | 6.156     | 8.201       | 235.854     | 5.264       | 5.551       | 3.686       | 12.305      | 19.852     | 4.237       | 47.810      | <2          |
| 13181         | 16.434    | 15.585      | 168.666     | 24.449      | 14.296      | 15.724      | 25.759      | 43.297     | 6.380       | 57.934      | 2.596       |
| 13187.5       | 34.123    | 5.588       | 62.075      | 5.019       | 7.369       | 1.663       | 5.784       | 14.899     | 1.698       | 17.267      | <2          |
| 13191.5       | 36.878    | 5.019       | 36.099      | <2          | 7.068       | 3.318       | 4.596       | 6.184      | 2.290       | 11.163      | <2          |
| 13199         | 34.177    | 6.928       | 50.611      | 11.301      | 8.701       | 3.601       | 7.309       | 11.386     | 1.704       | 19.683      | <2          |
| 13208         | 25.279    | 13.193      | 116.610     | 15.377      | 11.651      | 12.344      | 17.248      | 29.882     | 3.962       | 37.611      | <2          |
| 13214         | 4.843     | 10.866      | 223.614     | 6.219       | 5.064       | <2          | 10.213      | 16.651     | 3.933       | 44.944      | <2          |
| 13216.3       | 28.719    | 6.608       | 69.253      | 9.401       | 8.566       | 8.493       | 10.006      | 17.426     | 3.496       | 25.992      | <2          |
| 13236.4       | 33.995    | 5.577       | 63.934      | 14.455      | 7.034       | 2.774       | 8.125       | 14.044     | 2.657       | 17.577      | <2          |
| 13244.2       | 40.748    | <2          | 29.437      | 3.577       | 6.951       | <2          | 2.394       | 3.772      | 0.642       | 6.776       | <2          |
| 13256         | 31.697    | 6.407       | 61.869      | 5.720       | 9.050       | 3.116       | 7.472       | 14.259     | 2.857       | 19.551      | <2          |
| 13275         | 34.325    | 5.000       | 53.503      | 4.373       | 6.154       | 3.137       | 5.695       | 12.858     | 2.092       | 16.003      | <2          |
| 13280.2       | 36.703    | 5.921       | 75.089      | 3.017       | 7.113       | 4.645       | 7.489       | 11.194     | 2.016       | 12.778      | <2          |
| 13298.2       | 33.714    | 4.541       | 60.681      | 4.537       | 5.807       | 4.303       | 8.813       | 7.033      | 1.882       | 14.210      | <2          |
| 13295.2       | 26.445    | 7.861       | 85.211      | 10.133      | 12.641      | 14.272      | 13.929      | 28.743     | 3.474       | 34.921      | 2.679       |
| 13297         | 20.439    | 10.006      | 145.633     | 22.340      | 19.148      | 16.936      | 25.221      | 45.712     | 6.281       | 61.237      | 3.514       |
| 13300         | 15.575    | 8.458       | 176.980     | 30.266      | 24.099      | 24.965      | 33.987      | 61.700     | 8.254       | 77.386      | 5.796       |
| 13302         | 29.809    | 2.989       | 94.610      | 6.306       | 10.241      | 7.807       | 9.488       | 20.587     | 3.203       | 22.699      | <2          |
| 13305         | 22.885    | 4.994       | 106.229     | 12.116      | 9.316       | 9.196       | 16.350      | 23.473     | 4.190       | 34.859      | 3.421       |
| 13310         | 25.233    | 4.542       | 113.304     | 10.575      | 12.342      | 10.352      | 14.348      | 33.120     | 3.944       | 32.970      | 2.341       |
| 13310.5       | 1.412     | 19.143      | 366.982     | 65.552      | 47.422      | 48.864      | 74.828      | 156.179    | 13.879      | 150.021     | 15.554      |
| 13334.1       | 8.927     | 12.839      | 245.254     | 46.607      | 38.695      | 36.199      | 52.989      | 110.404    | 11.229      | 116.915     | 11.494      |
| 13339         | 26.359    | 3.319       | 94.300      | 8.098       | 9.845       | 7.426       | 13.873      | 21.985     | 3.778       | 29.874      | <2          |
| 13345         | 37.022    | 2.084       | 39.508      | 1.550       | 7.433       | <2          | 4.101       | 9.803      | 0.632       | 10.098      | <2          |
| 13348.2       | 24.343    | 3.953       | 99.361      | 11.301      | 10.869      | 12.084      | 16.845      | 31.727     | 4.706       | 37.055      | 2.351       |
| 13353         | 21.906    | 5.351       | 115.628     | 15.389      | 13.235      | 13.805      | 21.142      | 36.122     | 4.722       | 43.951      | 3.625       |
| 13353.6       | 27.661    | 3.533       | 93.009      | 11.040      | 10.747      | 11.586      | 13.257      | 26.480     | 3.800       | 28.457      | <2          |
| 13354         | 2.861     | 18.233      | 341.107     | 64.509      | 48.331      | 53.436      | 74.723      | 144.784    | 13.728      | 148.842     | 15.435      |

| Depth<br>(ft) | Ca<br>(%) | Pb<br>(ppm) | Ba<br>(ppm) | Zn<br>(ppm) | Cu<br>(ppm) | Ni<br>(ppm) | Cr<br>(ppm) | V<br>(ppm) | Nb<br>(ppm) | Rb<br>(ppm) | Th<br>(ppm) |
|---------------|-----------|-------------|-------------|-------------|-------------|-------------|-------------|------------|-------------|-------------|-------------|
| 13364.5       | 24.432    | 3.711       | 85.263      | 11.446      | 8.428       | 6.006       | 14.493      | 19.990     | 3.719       | 32.445      | 3.312       |
| 13367         | 32.523    | 2.998       | 57.376      | 3.098       | 7.045       | 3.754       | 7.480       | 10.522     | 2.273       | 17.532      | <2          |
| 13372.5       | 34.627    | 2.259       | 43.691      | 2.476       | 7.061       | 5.578       | 5.393       | 6.699      | 1.087       | 13.518      | <2          |
| 13378.5       | 29.146    | 4.027       | 72.765      | 4.911       | 8.997       | 6.621       | 10.210      | 17.808     | 3.147       | 22.435      | 1.783       |
| 13386.2       | 32.816    | 5.484       | 54.948      | 4.679       | 8.542       | 2.825       | 7.321       | 9.635      | 2.542       | 16.679      | 1.849       |
| 13388.5       | 26.093    | 5.423       | 104.473     | 10.747      | 12.238      | 13.489      | 15.381      | 29.677     | 4.161       | 33.261      | 5.904       |
| 13402.5       | 25.978    | 4.633       | 85.056      | 9.200       | 11.323      | 10.329      | 15.382      | 20.766     | 3.909       | 34.141      | 2.637       |
| 13407         | 23.852    | 4.600       | 107.675     | 9.700       | 9.896       | 12.916      | 17.814      | 27.073     | 5.366       | 33.462      | 3.339       |
| 13410.5       | 31.189    | 2.426       | 58.460      | 6.241       | 10.073      | 8.648       | 9.838       | 22.668     | 2.680       | 26.215      | 2.013       |
| 13417         | 31.606    | 5.636       | 102.717     | 15.619      | 16.476      | 17.726      | 20.611      | 31.618     | 4.629       | 41.458      | <2          |
| 13422.5       | 30.984    | 5.775       | 79.169      | 12.471      | 13.238      | 13.617      | 16.474      | 23.150     | 3.984       | 32.098      | 2.010       |
| 13434         | 20.722    | 13.254      | 177.083     | 25.389      | 31.168      | 35.603      | 40.501      | 82.431     | 7.697       | 70.898      | 6.064       |
| 13436         | 0.920     | 23.099      | 400.809     | 75.581      | 54.855      | 53.729      | 100.881     | 196.014    | 16.378      | 187.926     | 17.425      |
| 13436.3       | 1.044     | 17.988      | 375.503     | 68.172      | 58.165      | 53.549      | 85.649      | 161.805    | 13.940      | 153.380     | 13.866      |
| 13436.6       | 2.121     | 16.206      | 305.833     | 41.259      | 32.072      | 39.806      | 56.879      | 98.189     | 13.096      | 109.646     | 13.523      |
| 13437.5       | 19.265    | 8.477       | 131.793     | 19.096      | 14.739      | 14.194      | 25.026      | 43.945     | 7.041       | 48.703      | 5.093       |
| 13443         | 19.749    | 6.077       | 139.642     | 13.838      | 8.891       | 12.701      | 19.717      | 32.817     | 5.706       | 42.459      | 3.100       |
| 13452         | 24.644    | 7.399       | 122.497     | 17.662      | 16.013      | 23.354      | 25.523      | 42.622     | 5.994       | 45.930      | 3.337       |
| 13460         | 21.504    | 11.557      | 158.853     | 24.924      | 29.670      | 32.281      | 36.348      | 72.660     | 6.853       | 59.889      | 5.898       |
| 13461.5       | 16.438    | 6.955       | 160.093     | 19.575      | 15.658      | 17.948      | 28.900      | 47.949     | 6.830       | 50.968      | 7.240       |
| 13472.5       | 11.956    | 8.690       | 202.492     | 38.920      | 19.142      | 26.095      | 38.911      | 63.615     | 9.159       | 66.462      | 5.808       |
| 13480         | 20.756    | 9.385       | 141.346     | 19.764      | 19.090      | 25.605      | 30.211      | 44.803     | 7.409       | 52.931      | 6.360       |
| 13492         | 27.742    | 7.281       | 129.468     | 17.414      | 17.254      | 23.621      | 27.054      | 43.970     | 4.986       | 42.487      | 3.891       |
| 13508.5       | 15.771    | 16.046      | 225.216     | 23.877      | 28.788      | 32.595      | 32.021      | 65.910     | 7.991       | 57.185      | 7.511       |
| 13516         | 12.020    | 7.575       | 186.225     | 25.859      | 11.457      | 14.962      | 34.047      | 46.378     | 8.105       | 69.476      | 4.475       |
| 13522         | 19.816    | 9.636       | 150.229     | 21.513      | 18.141      | 20.508      | 32.590      | 50.511     | 7.731       | 58.383      | 6.372       |
| 13537         | 52.157    | 4.719       | 65.173      | 5.308       | 12.353      | 9.452       | 11.776      | 14.816     | 2.498       | 16.928      | <2          |
| 13537.5       | 21.186    | 11.618      | 191.233     | 20.351      | 17.136      | 17.063      | 30.051      | 48.409     | 7.342       | 53.946      | 6.283       |
| 13545.5       | 36.521    | 12.014      | 118.158     | 28.530      | 15.817      | 18.156      | 23.377      | 19.222     | 4.800       | 33.114      | 2.527       |
| 13554         | 1.973     | 14.057      | 352.572     | 77.003      | 192.897     | 61.964      | 89.648      | 190.782    | 14.707      | 193.119     | 13.784      |
| 13554.5       | 63.780    | 7.543       | 21.949      | <2          | 21.952      | 7.365       | 4.352       | 7.269      | 1.104       | 7.724       | <2          |
| 13557.5       | 7.672     | 7.564       | 198.773     | 6.111       | 26.826      | 4.012       | 10.203      | 21.145     | 3.998       | 48.371      | 1.509       |
| 13568.5       | 0.959     | 10.368      | 365.071     | 44.376      | 557.445     | 58.369      | 82.359      | 132.321    | 12.298      | 109.493     | 11.367      |
| 13586.5       | 1.872     | 13.484      | 315.388     | 35.943      | 10.417      | 36.790      | 56.492      | 108.744    | 9.258       | 104.425     | 9.071       |

**Table 3.** Major, minor and trace elements of the Smackover from #1 NEAL ET.UNIT 30-1well of the Manila Embayment normalized with respect to Al.

| Depth<br>(ft) | Ca/Ca+Al | Ti/Ti+Al | Si/Si+Al | Fe/Fe+Al | K/K+Al | Na/Na+Al | P/P+Al | Sr/Sr+Al | Mn/Mn+Al<br>(x100) | Mn/Mn+Ca<br>(x1000) | Mg/Ca |
|---------------|----------|----------|----------|----------|--------|----------|--------|----------|--------------------|---------------------|-------|
| 13100         | 0.999    | 0.102    | 0.720    | 0.120    | 0.382  | 0.597    | 0.148  | 0.934    | 12.765             | 0.208               | 0.002 |
| 13114.5       | 0.976    | 0.039    | 0.860    | 0.237    | 0.409  | 0.201    | 0.021  | 0.509    | 2.619              | 0.657               | 0.057 |
| 13117.1       | 0.922    | 0.050    | 0.891    | 0.355    | 0.476  | 0.208    | 0.016  | 0.094    | 6.866              | 6.216               | 0.583 |
| 13122         | 0.964    | 0.055    | 0.864    | 0.479    | 0.498  | 0.218    | 0.020  | 0.097    | 9.613              | 3.946               | 0.543 |
| 13130         | 0.908    | 0.063    | 0.855    | 0.378    | 0.452  | 0.152    | 0.013  | 0.047    | 4.347              | 4.583               | 0.553 |
| 13135         | 0.902    | 0.060    | 0.860    | 0.381    | 0.451  | 0.165    | 0.013  | 0.049    | 4.009              | 4.517               | 0.592 |
| 13140         | 0.871    | 0.062    | 0.823    | 0.375    | 0.413  | 0.117    | 0.011  | 0.040    | 2.570              | 3.894               | 0.643 |
| 13140.5       | 0.494    | 0.069    | 0.777    | 0.350    | 0.389  | 0.104    | 0.007  | 0.017    | 0.739              | 7.553               | 1.187 |
| 13143         | 0.441    | 0.028    | 0.925    | 0.073    | 0.405  | 0.280    | 0.007  | 0.033    | 0.559              | 7.076               | 0.805 |
| 13154         | 0.843    | 0.064    | 0.828    | 0.416    | 0.419  | 0.136    | 0.012  | 0.031    | 2.655              | 5.046               | 0.730 |
| 13159         | 0.732    | 0.050    | 0.904    | 0.294    | 0.418  | 0.230    | 0.010  | 0.036    | 1.787              | 6.610               | 0.855 |
| 13175         | 0.906    | 0.062    | 0.822    | 0.358    | 0.450  | 0.137    | 0.012  | 0.044    | 3.462              | 3.728               | 0.597 |
| 13180.2       | 0.720    | 0.055    | 0.845    | 0.285    | 0.433  | 0.159    | 0.010  | 0.037    | 1.504              | 5.897               | 0.850 |
| 13180.5       | 0.634    | 0.035    | 0.902    | 0.175    | 0.407  | 0.252    | 0.010  | 0.040    | 1.175              | 6.833               | 0.875 |
| 13181         | 0.808    | 0.070    | 0.832    | 0.353    | 0.453  | 0.134    | 0.010  | 0.029    | 2.247              | 5.451               | 0.728 |
| 13187.5       | 0.964    | 0.053    | 0.849    | 0.450    | 0.503  | 0.192    | 0.019  | 0.091    | 9.498              | 3.948               | 0.539 |
| 13191.5       | 0.978    | 0.052    | 0.872    | 0.505    | 0.481  | 0.265    | 0.022  | 0.142    | 13.276             | 3.429               | 0.522 |
| 13199         | 0.957    | 0.042    | 0.819    | 0.353    | 0.493  | 0.174    | 0.017  | 0.071    | 6.069              | 2.864               | 0.546 |
| 13208         | 0.902    | 0.061    | 0.827    | 0.363    | 0.456  | 0.152    | 0.011  | 0.043    | 2.768              | 3.096               | 0.600 |
| 13214         | 0.601    | 0.035    | 0.920    | 0.175    | 0.378  | 0.270    | 0.008  | 0.100    | 0.531              | 3.523               | 0.407 |
| 13216.3       | 0.927    | 0.049    | 0.839    | 0.353    | 0.445  | 0.143    | 0.012  | 0.048    | 3.941              | 3.197               | 0.540 |
| 13236.4       | 0.957    | 0.053    | 0.839    | 0.329    | 0.444  | 0.187    | 0.014  | 0.062    | 5.306              | 2.515               | 0.519 |
| 13244.2       | 0.988    | 0.028    | 0.883    | 0.460    | 0.478  | 0.311    | 0.029  | 0.336    | 16.932             | 2.432               | 0.482 |
| 13256         | 0.946    | 0.054    | 0.847    | 0.307    | 0.430  | 0.179    | 0.013  | 0.056    | 4.278              | 2.526               | 0.521 |
| 13275         | 0.964    | 0.046    | 0.852    | 0.359    | 0.481  | 0.185    | 0.015  | 0.076    | 5.935              | 2.341               | 0.540 |
| 13280.2       | 0.974    | 0.044    | 0.845    | 0.631    | 0.445  | 0.228    | 0.024  | 0.085    | 8.715              | 2.589               | 0.511 |
| 13298.2       | 0.962    | 0.048    | 0.869    | 0.293    | 0.423  | 0.211    | 0.018  | 0.068    | 6.974              | 2.933               | 0.516 |
| 13295.2       | 0.902    | 0.049    | 0.818    | 0.303    | 0.432  | 0.135    | 0.013  | 0.034    | 3.671              | 4.116               | 0.560 |
| 13297         | 0.822    | 0.048    | 0.788    | 0.315    | 0.418  | 0.103    | 0.011  | 0.026    | 2.148              | 4.724               | 0.592 |
| 13300         | 0.748    | 0.054    | 0.791    | 0.326    | 0.404  | 0.100    | 0.009  | 0.021    | 1.660              | 5.650               | 0.644 |
| 13302         | 0.936    | 0.053    | 0.848    | 0.331    | 0.428  | 0.165    | 0.014  | 0.046    | 5.143              | 3.675               | 0.527 |
| 13305         | 0.886    | 0.057    | 0.850    | 0.282    | 0.416  | 0.156    | 0.011  | 0.037    | 3.141              | 4.174               | 0.556 |
| 13310         | 0.896    | 0.050    | 0.831    | 0.356    | 0.420  | 0.149    | 0.015  | 0.038    | 3.784              | 4.556               | 0.529 |
| 13310.5       | 0.135    | 0.058    | 0.757    | 0.338    | 0.358  | 0.081    | 0.006  | 0.013    | 0.708              | 43.828              | 2.385 |
| 13334.1       | 0.561    | 0.055    | 0.776    | 0.336    | 0.386  | 0.092    | 0.008  | 0.021    | 1.181              | 9.276               | 0.712 |
| 13339         | 0.907    | 0.054    | 0.841    | 0.327    | 0.408  | 0.147    | 0.011  | 0.038    | 6.807              | 7.405               | 0.508 |
| 13345         | 0.978    | 0.045    | 0.886    | 0.402    | 0.420  | 0.264    | 0.021  | 0.116    | 21.472             | 6.240               | 0.491 |
| 13348.2       | 0.884    | 0.046    | 0.825    | 0.291    | 0.428  | 0.127    | 0.012  | 0.037    | 7.143              | 10.013              | 0.534 |
| 13353         | 0.849    | 0.047    | 0.811    | 0.300    | 0.405  | 0.104    | 0.011  | 0.030    | 5.222              | 9.732               | 0.532 |
| 13353.6       | 0.910    | 0.046    | 0.838    | 0.334    | 0.422  | 0.143    | 0.017  | 0.051    | 5.947              | 6.237               | 0.441 |
| 13354         | 0.246    | 0.057    | 0.757    | 0.332    | 0.362  | 0.084    | 0.007  | 0.015    | 0.882              | 26.613              | 1.353 |

| Depth<br>(ft) | Ca/Ca+Al | Ti/Ti+Al | Si/Si+Al | Fe/Fe+Al | K/K+Al | Na/Na+Al | P/P+Al | Sr/Sr+Al | Mn/Mn+Al<br>(x100) | Mn/Mn+Ca<br>(x1000) | Mg/Ca |
|---------------|----------|----------|----------|----------|--------|----------|--------|----------|--------------------|---------------------|-------|
| 13364.5       | 0.897    | 0.054    | 0.848    | 0.271    | 0.419  | 0.153    | 0.011  | 0.051    | 6.050              | 7.318               | 0.542 |
| 13367         | 0.958    | 0.048    | 0.867    | 0.299    | 0.462  | 0.218    | 0.016  | 0.090    | 12.770             | 6.413               | 0.530 |
| 13372.5       | 0.967    | 0.040    | 0.883    | 0.296    | 0.426  | 0.224    | 0.016  | 0.106    | 17.334             | 7.107               | 0.481 |
| 13378.5       | 0.929    | 0.044    | 0.848    | 0.256    | 0.431  | 0.154    | 0.014  | 0.052    | 9.617              | 8.047               | 0.505 |
| 13386.2       | 0.956    | 0.051    | 0.858    | 0.278    | 0.435  | 0.200    | 0.016  | 0.065    | 5.304              | 2.589               | 0.524 |
| 13388.5       | 0.899    | 0.054    | 0.836    | 0.284    | 0.419  | 0.150    | 0.013  | 0.047    | 6.734              | 8.053               | 0.472 |
| 13402.5       | 0.901    | 0.046    | 0.845    | 0.258    | 0.437  | 0.143    | 0.015  | 0.059    | 6.147              | 7.136               | 0.461 |
| 13407         | 0.886    | 0.054    | 0.851    | 0.271    | 0.396  | 0.144    | 0.010  | 0.060    | 5.651              | 7.655               | 0.454 |
| 13410.5       | 0.932    | 0.039    | 0.845    | 0.273    | 0.453  | 0.156    | 0.015  | 0.076    | 8.607              | 6.863               | 0.403 |
| 13417         | 0.903    | 0.052    | 0.832    | 0.268    | 0.436  | 0.115    | 0.012  | 0.071    | 4.492              | 5.015               | 0.142 |
| 13422.5       | 0.920    | 0.054    | 0.855    | 0.326    | 0.446  | 0.144    | 0.012  | 0.065    | 7.518              | 6.976               | 0.237 |
| 13434         | 0.794    | 0.048    | 0.801    | 0.299    | 0.403  | 0.096    | 0.010  | 0.050    | 3.731              | 9.935               | 0.160 |
| 13436         | 0.089    | 0.058    | 0.748    | 0.355    | 0.370  | 0.082    | 0.006  | 0.015    | 0.518              | 50.872              | 2.936 |
| 13436.3       | 0.107    | 0.058    | 0.769    | 0.383    | 0.378  | 0.085    | 0.007  | 0.015    | 0.658              | 52.220              | 2.417 |
| 13436.6       | 0.214    | 0.062    | 0.797    | 0.323    | 0.382  | 0.094    | 0.009  | 0.016    | 0.521              | 18.865              | 1.021 |
| 13437.5       | 0.834    | 0.057    | 0.838    | 0.327    | 0.430  | 0.132    | 0.012  | 0.053    | 8.588              | 18.338              | 0.488 |
| 13443         | 0.844    | 0.059    | 0.850    | 0.273    | 0.405  | 0.138    | 0.011  | 0.062    | 12.605             | 25.884              | 0.445 |
| 13452         | 0.867    | 0.057    | 0.843    | 0.299    | 0.429  | 0.127    | 0.011  | 0.049    | 12.401             | 21.317              | 0.178 |
| 13460         | 0.810    | 0.048    | 0.818    | 0.289    | 0.431  | 0.106    | 0.012  | 0.046    | 7.307              | 18.147              | 0.071 |
| 13461.5       | 0.781    | 0.056    | 0.832    | 0.320    | 0.407  | 0.112    | 0.010  | 0.036    | 11.063             | 33.685              | 0.382 |
| 13472.5       | 0.688    | 0.058    | 0.821    | 0.308    | 0.393  | 0.105    | 0.009  | 0.029    | 8.657              | 41.298              | 0.507 |
| 13480         | 0.834    | 0.056    | 0.844    | 0.263    | 0.428  | 0.124    | 0.010  | 0.044    | 12.869             | 28.603              | 0.216 |
| 13492         | 0.885    | 0.054    | 0.846    | 0.275    | 0.429  | 0.124    | 0.011  | 0.064    | 12.459             | 18.175              | 0.107 |
| 13508.5       | 0.778    | 0.058    | 0.838    | 0.409    | 0.417  | 0.127    | 0.011  | 0.039    | 11.933             | 37.184              | 0.358 |
| 13516         | 0.714    | 0.055    | 0.838    | 0.299    | 0.431  | 0.115    | 0.010  | 0.026    | 10.689             | 45.782              | 0.575 |
| 13522         | 0.820    | 0.055    | 0.845    | 0.297    | 0.441  | 0.113    | 0.010  | 0.048    | 6.114              | 14.136              | 0.147 |
| 13537         | 0.975    | 0.043    | 0.871    | 0.270    | 0.538  | 0.138    | 0.019  | 0.191    | 15.396             | 4.722               | 0.017 |
| 13537.5       | 0.831    | 0.056    | 0.848    | 0.274    | 0.451  | 0.118    | 0.011  | 0.082    | 4.182              | 8.815               | 0.077 |
| 13545.5       | 0.929    | 0.051    | 0.860    | 0.221    | 0.471  | 0.123    | 0.013  | 0.129    | 14.594             | 12.926              | 0.021 |
| 13554         | 0.184    | 0.058    | 0.762    | 0.334    | 0.410  | 0.076    | 0.009  | 0.012    | 0.795              | 34.225              | 1.731 |
| 13554.5       | 0.992    | 0.028    | 0.868    | 0.390    | 0.548  | 0.208    | 0.035  | 0.353    | 48.074             | 7.339               | 0.006 |
| 13557.5       | 0.709    | 0.032    | 0.920    | 0.088    | 0.453  | 0.206    | 0.009  | 0.030    | 3.814              | 16.032              | 0.046 |
| 13568.5       | 0.103    | 0.062    | 0.779    | 0.291    | 0.380  | 0.099    | 0.008  | 0.013    | 0.648              | 53.547              | 4.333 |
| 13586.5       | 0.216    | 0.049    | 0.816    | 0.397    | 0.393  | 0.253    | 0.007  | 0.027    | 0.700              | 24.991              | 1.429 |

**Table 4.** Ca and trace element ratio normalized with respect to Al of the Smackover from the #1 NEAL ET AL UNIT 30-1 of the Manila Embayment.

| Depth<br>(ft) | Ca<br>(%) | Pb/Pb+Al<br>(x1000) | Ba/Ba+Al<br>(x1000) | Zn/Zn+Al<br>(x1000) | Cu/Cu+Al<br>(x1000) | Ni/Ni+Al<br>(x1000) | Cr/Cr+Al<br>(x1000) | V/V+Al<br>(x1000) | V/Cr  |
|---------------|-----------|---------------------|---------------------|---------------------|---------------------|---------------------|---------------------|-------------------|-------|
| 13100         | 70.847    | 0.496*              | 13.494              | 0.991*              | 13.242              | 5.401               | 4.509               | 4.756             | 1.055 |
| 13114.5       | 52.519    | 0.300               | 3.540               | 0.276               | 0.970               | 0.722               | 0.725               | 0.717             | 0.990 |
| 13117.1       | 23.717    | 0.300               | 4.387               | 0.422               | 0.417               | 0.224               | 0.456               | 0.802             | 1.759 |
| 13122         | 33.384    | 0.429               | 3.575               | 0.719               | 0.688               | 0.203               | 0.616               | 0.867             | 1.407 |
| 13130         | 24.885    | 0.370               | 3.954               | 0.473               | 0.434               | 0.307               | 0.555               | 0.948             | 1.709 |
| 13135         | 23.432    | 0.348               | 4.300               | 0.404               | 0.373               | 0.373               | 0.625               | 0.942             | 1.507 |
| 13140         | 22.117    | 0.288               | 3.674               | 0.496               | 0.344               | 0.358               | 0.608               | 1.020             | 1.678 |
| 13140.5       | 6.770     | 0.362               | 4.497               | 0.652               | 0.317               | 0.529               | 0.823               | 1.487             | 1.808 |
| 13143         | 2.464     | 0.149               | 9.468               | 0.104               | 0.095               | 0.016*              | 0.289               | 0.398             | 1.380 |
| 13154         | 18.884    | 0.355               | 4.319               | 0.482               | 0.377               | 0.449               | 0.664               | 1.202             | 1.811 |
| 13159         | 8.608     | 0.342               | 6.772               | 0.339               | 0.304               | 0.233               | 0.601               | 0.728             | 1.210 |
| 13175         | 26.036    | 0.340               | 4.013               | 0.484               | 0.409               | 0.342               | 0.587               | 1.073             | 1.827 |
| 13180.2       | 11.379    | 0.248               | 4.981               | 0.432               | 0.301               | 0.241               | 0.538               | 1.036             | 1.925 |
| 13180.5       | 6.156     | 0.230               | 6.579               | 0.148               | 0.156               | 0.103               | 0.345               | 0.557             | 1.613 |
| 13181         | 16.434    | 0.398               | 4.287               | 0.624               | 0.365               | 0.401               | 0.657               | 1.104             | 1.681 |
| 13187.5       | 34.123    | 0.433               | 4.794               | 0.389               | 0.572               | 0.129               | 0.449               | 1.155             | 2.576 |
| 13191.5       | 36.878    | 0.605               | 4.337               | 0.060*              | 0.852               | 0.400               | 0.554               | 0.746             | 1.346 |
| 13199         | 34.177    | 0.456               | 3.320               | 0.743               | 0.572               | 0.237               | 0.481               | 0.749             | 1.558 |
| 13208         | 25.279    | 0.478               | 4.210               | 0.557               | 0.422               | 0.447               | 0.625               | 1.082             | 1.732 |
| 13214         | 4.843     | 0.338               | 6.919               | 0.194               | 0.158               | 0.016*              | 0.318               | 0.519             | 1.630 |
| 13216.3       | 28.719    | 0.294               | 3.075               | 0.418               | 0.381               | 0.378               | 0.445               | 0.775             | 1.742 |
| 13236.4       | 33.995    | 0.365               | 4.163               | 0.944               | 0.460               | 0.181               | 0.531               | 0.917             | 1.728 |
| 13244.2       | 40.748    | 0.103*              | 6.004               | 0.733               | 1.424               | 0.103*              | 0.491               | 0.773             | 1.575 |
| 13256         | 31.697    | 0.357               | 3.433               | 0.318               | 0.504               | 0.173               | 0.416               | 0.793             | 1.908 |
| 13275         | 34.325    | 0.392               | 4.174               | 0.343               | 0.482               | 0.246               | 0.446               | 1.006             | 2.258 |
| 13280.2       | 36.703    | 0.593               | 7.468               | 0.302               | 0.712               | 0.465               | 0.750               | 1.120             | 1.495 |
| 13298.2       | 33.714    | 0.343               | 4.567               | 0.343               | 0.439               | 0.325               | 0.666               | 0.531             | 0.798 |
| 13295.2       | 26.445    | 0.274               | 2.962               | 0.353               | 0.441               | 0.497               | 0.485               | 1.001             | 2.064 |
| 13297         | 20.439    | 0.226               | 3.285               | 0.505               | 0.433               | 0.383               | 0.570               | 1.033             | 1.812 |
| 13300         | 15.575    | 0.161               | 3.364               | 0.577               | 0.459               | 0.476               | 0.648               | 1.176             | 1.815 |
| 13302         | 29.809    | 0.147               | 4.644               | 0.311               | 0.505               | 0.385               | 0.468               | 1.014             | 2.170 |
| 13305         | 22.885    | 0.169               | 3.579               | 0.409               | 0.315               | 0.311               | 0.552               | 0.793             | 1.436 |
| 13310         | 25.233    | 0.155               | 3.844               | 0.360               | 0.420               | 0.352               | 0.488               | 1.127             | 2.308 |
| 13310.5       | 1.412     | 0.211               | 4.025               | 0.721               | 0.522               | 0.538               | 0.823               | 1.717             | 2.087 |
| 13334.1       | 8.927     | 0.184               | 3.496               | 0.666               | 0.553               | 0.518               | 0.757               | 1.577             | 2.084 |
| 13339         | 26.359    | 0.123               | 3.491               | 0.301               | 0.366               | 0.276               | 0.515               | 0.816             | 1.585 |
| 13345         | 37.022    | 0.245               | 4.625               | 0.182               | 0.873               | 0.059*              | 0.482               | 1.152             | 2.390 |
| 13348.2       | 24.343    | 0.123               | 3.095               | 0.353               | 0.339               | 0.377               | 0.526               | 0.990             | 1.883 |
| 13353         | 21.906    | 0.137               | 2.951               | 0.394               | 0.339               | 0.353               | 0.541               | 0.924             | 1.709 |
| 13353.6       | 27.661    | 0.129               | 3.376               | 0.402               | 0.391               | 0.422               | 0.483               | 0.964             | 1.997 |
| 13354         | 2.861     | 0.207               | 3.864               | 0.733               | 0.549               | 0.607               | 0.849               | 1.644             | 1.938 |
| 13364.5       | 24.432    | 0.133               | 3.039               | 0.409               | 0.301               | 0.215               | 0.518               | 0.714             | 1.379 |
| 13367         | 32.523    | 0.209               | 3.986               | 0.216               | 0.491               | 0.262               | 0.521               | 0.733             | 1.407 |
| 13372.5       | 34.627    | 0.191               | 3.683               | 0.209               | 0.597               | 0.472               | 0.456               | 0.566             | 1.242 |

| Depth   | Ca     | Pb/Pb+Al | Ba/Ba+Al | Zn/Zn+Al | Cu/Cu+Al | Ni/Ni+Al | Cr/Cr+Al | V/V+Al  | V/Cr  |
|---------|--------|----------|----------|----------|----------|----------|----------|---------|-------|
| (ft)    | (%)    | (x1000)  | (x1000)  | (x1000)  | (x1000)  | (x1000)  | (x1000)  | (x1000) |       |
| 13378.5 | 29.146 | 0.181    | 3.264    | 0.221    | 0.405    | 0.298    | 0.459    | 0.801   | 1.744 |
| 13386.2 | 32.816 | 0.360    | 3.600    | 0.308    | 0.561    | 0.186    | 0.481    | 0.633   | 1.316 |
| 13388.5 | 26.093 | 0.185    | 3.548    | 0.366    | 0.417    | 0.460    | 0.524    | 1.010   | 1.929 |
| 13402.5 | 25.978 | 0.162    | 2.975    | 0.323    | 0.397    | 0.362    | 0.539    | 0.728   | 1.350 |
| 13407   | 23.852 | 0.150    | 3.493    | 0.316    | 0.322    | 0.420    | 0.580    | 0.881   | 1.520 |
| 13410.5 | 31.189 | 0.106    | 2.548    | 0.273    | 0.440    | 0.378    | 0.430    | 0.989   | 2.304 |
| 13417   | 31.606 | 0.166    | 3.024    | 0.461    | 0.486    | 0.523    | 0.608    | 0.933   | 1.534 |
| 13422.5 | 30.984 | 0.216    | 2.948    | 0.466    | 0.494    | 0.508    | 0.615    | 0.864   | 1.405 |
| 13434   | 20.722 | 0.247    | 3.289    | 0.473    | 0.580    | 0.663    | 0.754    | 1.534   | 2.035 |
| 13436   | 0.920  | 0.244    | 4.218    | 0.798    | 0.579    | 0.567    | 1.065    | 2.067   | 1.943 |
| 13436.3 | 1.044  | 0.207    | 4.301    | 0.784    | 0.669    | 0.616    | 0.984    | 1.858   | 1.889 |
| 13436.6 | 2.121  | 0.208    | 3.910    | 0.529    | 0.411    | 0.511    | 0.730    | 1.259   | 1.726 |
| 13437.5 | 19.265 | 0.221    | 3.429    | 0.498    | 0.385    | 0.370    | 0.653    | 1.146   | 1.756 |
| 13443   | 19.749 | 0.167    | 3.823    | 0.380    | 0.244    | 0.349    | 0.542    | 0.901   | 1.664 |
| 13452   | 24.644 | 0.195    | 3.220    | 0.466    | 0.422    | 0.616    | 0.673    | 1.123   | 1.670 |
| 13460   | 21.504 | 0.229    | 3.141    | 0.494    | 0.588    | 0.640    | 0.720    | 1.439   | 1.999 |
| 13461.5 | 16.438 | 0.151    | 3.463    | 0.425    | 0.340    | 0.389    | 0.627    | 1.040   | 1.659 |
| 13472.5 | 11.956 | 0.160    | 3.712    | 0.716    | 0.352    | 0.480    | 0.716    | 1.169   | 1.635 |
| 13480   | 20.756 | 0.227    | 3.404    | 0.477    | 0.461    | 0.618    | 0.730    | 1.082   | 1.483 |
| 13492   | 27.742 | 0.202    | 3.575    | 0.482    | 0.478    | 0.654    | 0.749    | 1.217   | 1.625 |
| 13508.5 | 15.771 | 0.357    | 4.985    | 0.531    | 0.640    | 0.725    | 0.712    | 1.464   | 2.058 |
| 13516   | 12.020 | 0.157    | 3.849    | 0.536    | 0.238    | 0.310    | 0.706    | 0.961   | 1.362 |
| 13522   | 19.816 | 0.221    | 3.431    | 0.493    | 0.416    | 0.470    | 0.746    | 1.156   | 1.550 |
| 13537   | 52.157 | 0.347    | 4.770    | 0.390    | 0.908    | 0.695    | 0.865    | 1.088   | 1.258 |
| 13537.5 | 21.186 | 0.269    | 4.410    | 0.471    | 0.397    | 0.395    | 0.696    | 1.120   | 1.611 |
| 13545.5 | 36.521 | 0.429    | 4.204    | 1.018    | 0.565    | 0.648    | 0.834    | 0.686   | 0.822 |
| 13554   | 1.973  | 0.161    | 4.024    | 0.882    | 2.206    | 0.710    | 1.026    | 2.182   | 2.128 |
| 13554.5 | 63.780 | 1.479    | 4.291    | 0.098*   | 4.291    | 1.444    | 0.854    | 1.425   | 1.670 |
| 13557.5 | 7.672  | 0.240    | 6.266    | 0.194    | 0.850    | 0.127    | 0.324    | 0.670   | 2.072 |
| 13568.5 | 0.959  | 0.125    | 4.366    | 0.533    | 6.652    | 0.701    | 0.988    | 1.587   | 1.607 |
| 13586.5 | 1.872  | 0.198    | 4.612    | 0.528    | 0.153    | 0.540    | 0.829    | 1.595   | 1.925 |

**Note:** \* Samples which consist of element concentration smaller than 2 ppm and were assigned value of 0.5 ppm in order to be able to be calculated.

**Table 5.** Carbonate, non-carbonate (residue) components, TOC and isotopic compositions of the Smackover samples from the #1 NEAL ET AL UNIT 30-1 of the Manila Embayment.

| Depth<br>(ft) | CaCO <sub>3</sub> <sup>1</sup><br>(%) | nonCaCO3<br>(%) | TOC <sup>2</sup><br>(%) | TOC* <sup>3</sup><br>(%) | δ <sup>13</sup> C <sub>CaCO3</sub><br>(‰) | δ <sup>18</sup> O <sub>CaCO3</sub><br>(‰) | δ <sup>13</sup> C <sub>Org</sub><br>(‰) |
|---------------|---------------------------------------|-----------------|-------------------------|--------------------------|---|---|---|
| 13100         | 2.03                                  | 97.97           | 0.00                    | 0.00                     | n.a.                                      | n.a.                                      | n.a.                                    |
| 13114.5       | 17.43                                 | 82.57           | 0.03                    | 0.04                     | 4.22                                      | -1.29                                     | n.a.                                    |
| 13117.1       | 66.30                                 | 33.70           | 0.07                    | 0.19                     | n.a.                                      | n.a.                                      | -23.99                                  |
| 13122         | 86.86                                 | 13.14           | 0.09                    | 0.67                     | n.a.                                      | n.a.                                      | n.a.                                    |
| 13130         | 72.58                                 | 27.42           | 0.08                    | 0.29                     | n.a.                                      | n.a.                                      | n.a.                                    |
| 13135         | 68.24                                 | 31.76           | 0.11                    | 0.35                     | n.a.                                      | n.a.                                      | n.a.                                    |
| 13140         | 65.52                                 | 34.48           | 0.18                    | 0.51                     | 4.67                                      | 2.12                                      | n.a.                                    |
| 13140.5       | 34.06                                 | 65.94           | 0.53                    | 0.80                     | 4.86                                      | 2.57                                      | -22.92                                  |
| 13143         | 8.98                                  | 91.02           | 0.00                    | 0.00                     | 4.19                                      | -1.3                                      | n.a.                                    |
| 13154         | 64.21                                 | 35.79           | 0.23                    | 0.65                     | 4.4                                       | 1.7                                       | -23.7                                   |
| 13159         | 36.08                                 | 63.92           | 0.08                    | 0.12                     | n.a.                                      | n.a.                                      | n.a.                                    |
| 13175         | 74.84                                 | 25.16           | 0.17                    | 0.69                     | 4.85                                      | 1.95                                      | -24.66                                  |
| 13180.2       | 32.12                                 | 67.88           | 0.20                    | 0.29                     | n.a.                                      | n.a.                                      | n.a.                                    |
| 13180.5       | 18.18                                 | 81.82           | 0.00                    | 0.00                     | 4.58                                      | -0.11                                     | n.a.                                    |
| 13181         | 53.16                                 | 46.84           | 0.28                    | 0.60                     | n.a.                                      | n.a.                                      | n.a.                                    |
| 13184.5       | 4.06                                  | 95.94           | 0.00                    | 0.00                     | 3.88                                      | -6.95                                     | n.a.                                    |
| 13187.5       | 88.03                                 | 11.97           | 0.11                    | 0.96                     | n.a.                                      | n.a.                                      | n.a.                                    |
| 13191.5       | 90.57                                 | 9.43            | 0.16                    | 1.73                     | n.a.                                      | n.a.                                      | n.a.                                    |
| 13199         | 87.05                                 | 12.95           | 0.32                    | 2.49                     | 5.48                                      | 1.77                                      | -24.77                                  |
| 13208         | 74.97                                 | 25.03           | 0.20                    | 0.79                     | n.a.                                      | n.a.                                      | n.a.                                    |
| 13214         | 11.53                                 | 88.47           | 0.00                    | 0.00                     | 4.94                                      | -3.46                                     | n.a.                                    |
| 13216.3       | 78.86                                 | 21.14           | 0.10                    | 0.49                     | n.a.                                      | n.a.                                      | n.a.                                    |
| 13236.4       | 88.14                                 | 11.86           | 0.14                    | 1.22                     | n.a.                                      | n.a.                                      | n.a.                                    |
| 13244.2       | 94.02                                 | 5.98            | 0.09                    | 1.57                     | 4.93                                      | 0.6                                       | -25.44                                  |
| 13256         | 84.54                                 | 15.46           | 0.15                    | 0.98                     | n.a.                                      | n.a.                                      | -25.35                                  |
| 13275         | 88.66                                 | 11.34           | 0.11                    | 0.95                     | 4.82                                      | 0.71                                      | -25.48                                  |
| 13280.2       | 90.75                                 | 9.25            | 0.18                    | 1.98                     | n.a.                                      | n.a.                                      | n.a.                                    |
| 13298.2       | 82.00                                 | 18.00           | 0.22                    | 1.22                     | 4.46                                      | 0.83                                      | -24.83                                  |
| 13295.2       | 67.85                                 | 32.15           | 1.13                    | 3.50                     | n.a.                                      | n.a.                                      | n.a.                                    |
| 13297         | 66.93                                 | 33.07           | 1.14                    | 3.44                     | 3.28                                      | 1.73                                      | -20.78                                  |
| 13300         | 57.42                                 | 42.58           | 1.02                    | 2.41                     | n.a.                                      | n.a.                                      | n.a.                                    |
| 13302         | 82.01                                 | 17.99           | 0.43                    | 2.36                     | n.a.                                      | n.a.                                      | n.a.                                    |
| 13305         | 69.71                                 | 30.29           | 0.29                    | 0.97                     | 3.58                                      | 1.09                                      | -24.7                                   |
| 13310         | 75.45                                 | 24.55           | 1.43                    | 5.84                     | 2.44                                      | 1.11                                      | -20.87                                  |
| 13310.5       | 9.21                                  | 90.79           | 3.32                    | 3.65                     | 4.25                                      | 1.94                                      | -20.38                                  |
| 13334.1       | 53.08                                 | 46.92           | 0.81                    | 1.72                     | 3.06                                      | 1.15                                      | -22.84                                  |
| 13339         | 75.90                                 | 24.10           | 0.66                    | 2.74                     | n.a.                                      | n.a.                                      | n.a.                                    |
| 13345         | 91.72                                 | 8.28            | 0.08                    | 0.95                     | 3.94                                      | -1.12                                     | -24.37                                  |
| 13348.2       | 72.33                                 | 27.67           | 0.38                    | 1.36                     | n.a.                                      | n.a.                                      | n.a.                                    |
| 13353         | 69.99                                 | 30.01           | 0.31                    | 1.02                     | n.a.                                      | n.a.                                      | n.a.                                    |
| 13353.6       | 77.15                                 | 22.85           | 0.67                    | 2.94                     | 3.14                                      | 0.02                                      | n.a.                                    |
| 13354         | 15.21                                 | 84.79           | 0.99                    | 1.16                     | 3.16                                      | 0.22                                      | -23.59                                  |
| 13356.2       | 86.28                                 | 13.72           | 0.14                    | 1.05                     | n.a.                                      | n.a.                                      | n.a.                                    |
| 13364.5       | 71.53                                 | 28.47           | 0.17                    | 0.60                     | 4.36                                      | -2.41                                     | n.a.                                    |

| Depth<br>(ft) | CaCO <sub>3</sub> <sup>1</sup><br>(%) | nonCaCO <sub>3</sub><br>(%) | TOC <sup>2</sup><br>(%) | TOC* <sup>3</sup><br>(%) | δ <sup>13</sup> C <sub>CaCO<sub>3</sub></sub><br>(‰) | δ <sup>18</sup> O <sub>CaCO<sub>3</sub></sub><br>(‰) | δ <sup>13</sup> C <sub>org</sub><br>(‰) |
|---------------|---------------------------------------|-----------------------------|-------------------------|--------------------------|--|--|---|
| 13367         | 86.03                                 | 13.97                       | 0.09                    | 0.65                     | 4.55   | -2.29  | -24.5                                   |
| 13372.5       | 88.14                                 | 11.86                       | 0.11                    | 0.89                     | n.a.   | n.a.   | n.a.                                    |
| 13378.5       | 82.04                                 | 17.96                       | 0.17                    | 0.97                     | n.a.   | n.a.   | n.a.                                    |
| 13386.2       | 81.19                                 | 18.81                       | 0.20                    | 1.07                     | n.a.   | n.a.   | n.a.                                    |
| 13388.5       | 75.13                                 | 24.87                       | 0.25                    | 1.00                     | 4.46   | -1.52  | -23.8                                   |
| 13393.5       | 81.60                                 | 18.40                       | 0.14                    | 0.75                     | n.a.   | n.a.   | n.a.                                    |
| 13398         | 77.81                                 | 22.19                       | 0.21                    | 0.92                     | n.a.   | n.a.   | n.a.                                    |
| 13402.5       | 74.22                                 | 25.78                       | 0.11                    | 0.44                     | n.a.   | n.a.   | n.a.                                    |
| 13407         | 68.54                                 | 31.46                       | 0.17                    | 0.54                     | n.a.   | n.a.   | n.a.                                    |
| 13410.5       | 81.21                                 | 18.79                       | 0.13                    | 0.70                     | 4.39   | -1.55  | n.a.                                    |
| 13417         | 70.74                                 | 29.26                       | 0.27                    | 0.92                     | n.a.   | n.a.   | n.a.                                    |
| 13422.5       | 72.97                                 | 27.03                       | 0.17                    | 0.64                     | 3.03   | 0.73   | -24.99                                  |
| 13434         | 54.42                                 | 45.58                       | 0.89                    | 1.95                     | n.a.   | n.a.   | n.a.                                    |
| 13436         | 10.18                                 | 89.82                       | 1.09                    | 1.22                     | 4.89   | 0.06   | -23.62                                  |
| 13436.3       | 1.56                                  | 98.44                       | 0.76                    | 0.78                     | n.a.   | n.a.   | n.a.                                    |
| 13436.6       | 10.33                                 | 89.67                       | 0.61                    | 0.68                     | n.a.   | n.a.   | n.a.                                    |
| 13437.5       | 61.88                                 | 38.12                       | 0.28                    | 0.73                     | 4.59   | -0.2   | n.a.                                    |
| 13443         | 62.04                                 | 37.96                       | 0.14                    | 0.38                     | 2.99   | 1.15   | -24.99                                  |
| 13452         | 61.03                                 | 38.97                       | 0.23                    | 0.60                     | n.a.   | n.a.   | n.a.                                    |
| 13460         | 11.51                                 | 88.49                       | 1.96                    | 2.22                     | 1.23   | -5.84  | -23.26                                  |
| 13460.5       | 54.21                                 | 45.79                       | 0.58                    | 1.28                     | n.a.   | n.a.   | n.a.                                    |
| 13461.5       | 55.94                                 | 44.06                       | 0.21                    | 0.47                     | n.a.   | n.a.   | n.a.                                    |
| 13472.5       | 46.40                                 | 53.60                       | 0.36                    | 0.68                     | n.a.   | n.a.   | n.a.                                    |
| 13480         | 56.64                                 | 43.36                       | 0.17                    | 0.40                     | n.a.   | n.a.   | n.a.                                    |
| 13492         | 65.87                                 | 34.13                       | 0.21                    | 0.62                     | 3.05   | 1.52   | n.a.                                    |
| 13508.5       | 50.58                                 | 49.42                       | 0.75                    | 1.51                     | n.a.   | n.a.   | -23.53                                  |
| 13513         | 43.29                                 | 56.71                       | 0.33                    | 0.58                     | 3.63   | -0.53  | n.a.                                    |
| 13516         | 48.5434                               | 51.46                       | 0.20                    | 0.38                     | n.a.   | n.a.   | n.a.                                    |
| 13522         | 51.88536                              | 48.11                       | 0.24                    | 0.50                     | 3.18   | -0.41  | -24.66                                  |
| 13537         | 84.68                                 | 15.32                       | 0.08                    | 0.54                     | 3.34   | 0.39   | -24.52                                  |
| 13537.5       | 50.58084                              | 49.42                       | 0.26                    | 0.52                     | 3.24   | 0.53   | n.a.                                    |
| 13545.5       | 73.16                                 | 26.84                       | 0.14                    | 0.52                     | 3.27   | 0.75   | n.a.                                    |
| 13554         | 16.19                                 | 83.81                       | 0.13                    | 0.15                     | -0.16  | -0.31  | -23.76                                  |
| 13554.5       | 94.76                                 | 5.24                        | 0.04                    | 0.86                     | 2.74   | 0.3  | n.a.                                    |
| 13557.5       | 15.48                                 | 84.52                       | 0.00                    | 0.00                     | -0.71  | -6.55  | n.a.                                    |
| 13565         | 6.39                                  | 93.61                       | 0.00                    | 0.00                     | n.a.   | n.a.   | n.a.                                    |
| 13568.5       | 7.59                                  | 92.41                       | 0.02                    | 0.02                     | n.a.   | n.a.   | n.a.                                    |
| 13586.5       | 8.60                                  | 91.40                       | 0.00                    | 0.00                     | n.a.   | n.a.   | n.a.                                    |
| 13594         | 4.55                                  | 95.45                       | 0.00                    | 0.00                     | n.a.   | n.a.   | n.a.                                    |

**Note:** CaCO<sub>3</sub><sup>1</sup> an average value from two analysis by HCl digestion of the whole rock samples.  
TOC<sup>2</sup> an average content of TOC in the whole rock from two analysis by TOC analyzer.  
TOC<sup>3</sup> a calculated TOC content in the non-carbonate (residue) fraction.